

The copyright of this thesis vests in the author. No quotation from it or information derived from it is to be published without full acknowledgement of the source. The thesis is to be used for private study or non-commercial research purposes only.

Published by the University of Cape Town (UCT) in terms of the non-exclusive license granted to UCT by the author.

A Pharmacokinetic and Efficacy Study of Lumefantrine in Mice; Evaluating the Application of Pheroid™ Technology

Katya Govender



Thesis presented for the degree of

Master of Science in Medicine

In the Division of Pharmacology

UNIVERSITY OF CAPE TOWN

October 2012

Supervisor: Dr L. Wiesner, Division of Pharmacology, UCT

Co-supervisor: Dr L. du Plessis, Department of Pharmaceutics, NWU

Declaration

Title: A Pharmacokinetic and Efficacy Study of Lumefantrine in Mice; Evaluating the Application of Pheroid™ Technology

Candidate: Katya Govender

I, Katya Govender, hereby grant the University of Cape Town free licence to reproduce the above thesis in whole or in part, for the purpose of research. I declare that this thesis represents my own unaided work and that apart from the normal guidance from my supervisor, I have received no assistance (except where acknowledgements indicate otherwise) and that neither the substance nor any part of the above thesis has been submitted in the past, or is being, or is to be submitted for a degree at this University or at any other university

This thesis is presented for examination for the degree of Master of Science in Pharmacology

Signed: _____

Date: _____

Acknowledgments

I would here like to express my gratitude to the many people who have assisted me in completing this thesis. First and foremost I have to give thanks to the Lord our God for blessing me with the opportunity to do what I love, my faith has truly been a source of strength and motivation.

As usual I have to thank my family (love you guys long time!!) for their continued financial and emotional support, however coerced, of cause none of them will ever read or take a second glance at this thesis as its not edible nor does the title promise a ‘Mills and Boon’ type adventure. To my bff (best friend forever-not found in list of abbreviations) Kariema Dhansay, you’ve truly been a rock of support, I’m truly blessed to have you apart of my life.

I would like to specifically thank Sumaya Salie, Ntokozo Dambuza, Dale Taylor, Carmen de Kok, Trevor Finch, Grace Magumbate, Paolo Denti, Wynand Smythe and Prof. Hundt for their contribution in completing this project. Also, a big thank you to Tracy Kellermann for being my editor (pro-bono) and offering continuous encouragement.

I would also like to voice my appreciation to my project supervisors Dr Lubbe Wiesner and Dr Lissinda du Plessis, without whom this project would not have been possible. Thank you for your intellectual and physical contributions as well as invaluable expert advice.

Last but not least I would like to thank Prof. Peter Smith and the Division of Pharmacology, University of Cape Town as well as the National Research Foundation (NRF) for financially supporting this project.

Abstract

Malaria is a mosquito-borne infection caused by *Plasmodium* parasites. This disease occurs predominantly in tropical and sub-tropical regions causing 216 million clinical cases annually and resulting in 655 000 deaths. It is estimated that more than 90% of the deaths due to malaria infection occur in Africa with children younger than 5 years of age and pregnant women being most susceptible to infection, disease progression and death. Due to antimalarial drug resistance and other disease compounding factors such as poor socio-economic conditions and patient compliance, there is a need to discover and develop effective novel antimalarials with a unique mode of action. However the discovery and development of new drugs is an expensive and time consuming venture therefore the use of drug formulation to improve and/or enhance existing antimalarial chemotherapy is a cost-effective and feasible alternative strategy in eradicating malaria.

Artemisinin based combination therapy's (ACTs) are recommended as first line treatment for uncomplicated malaria. ACTs combine a rapid acting antimalarial such as artemisinin or a derivative, to reduce parasite load, with a longer acting partner antimalarial to eliminate residual parasites thus curing infection as well as preventing the selection of drug resistant parasites. Lumefantrine (LF) is a long acting antimalarial; it is co-formulated with artemether and available commercially as the ACT, Coartem[®]. LF is a highly lipophilic drug resulting in poor and variable oral bioavailability. The primary aim of this study is to improve the bioavailability of LF with the application of Pheroid[™] formulation technology. A further intention is to determine if the Pheroid[™] formulated LF eliminates the positive 'food effect' associated with LF and improves *in vivo* antimalarial efficacy.

Using the *in silico* tools, Volsurf[®] and MoKa[®], LF was predicted to have low aqueous solubility (LogP = 9) and good membrane permeability. The oral absorption of compounds with low aqueous solubility is typically limited by the dissolution rate in the GI tract resulting in erratic absorption and variable bioavailability. Pheroid[™] technology was applied to improve the solubility of LF after oral administration. A bioavailability study of LF was conducted in a mouse model to compare LF in Pheroid[™] formulation with LF in reference (aqueous) solution and LF in canola oil. LF was quantitated in mouse whole blood and plasma using high performance liquid chromatographic separation coupled with tandem mass spectrometric detection (LC-MS/MS). The developed LC-MS/MS methods, using a sample

volume of 20 μ l and an isotopic labelled internal standard, for the quantitation of LF over a concentration range of 15.6 – 4000 ng/ml, were validated according to FDA guidelines.

For the bioavailability experiment the mice were divided into treatment groups each receiving LF in one of the three test formulations. The three treatment groups were further divided into the fed group and starved group. LF was tested at a 10 mg/kg dose concentration, administered to the experimental mice by oral gavage. Blood (and plasma) samples were collected via tail bleeding over a 24 hour test period and subsequently extracted using a protein precipitation method and analysed using LC-MS/MS. The concentration-time data was used to develop a population pharmacokinetic (PPK) model to describe and compare the bioavailability of the test group administered LF in Pheroid™ formulation to the reference and canola oil groups. The bioavailability of LF in reference formulation heavily depended on food intake resulting in a 2.7 times higher bioavailability in the fed state when compared to the starved state. The bioavailability of LF, calculated using the PPK model was 3.2 times higher when formulated using the Pheroid™ technology as compared to LF in the reference solution (fasting state). For LF in Pheroid™ formulation, the between subject variability (BSV) for bioavailability was ~15% compared to ~44% for LF in reference solution, under fasting conditions.

In vitro and *in vivo* antimalarial experiments were also performed to determine if LF when formulated using Pheroid™ technology would show enhanced efficacy compared to LF in the reference solution. The antimalarial efficacy of LF in Pheroid™ and reference formulation was tested against a chloroquine sensitive (D10) strain of *Plasmodium falciparum* using a colorimetric pLDH assay. LF in reference and Pheroid™ formulation had an IC₅₀ value of 50.9 and 27.1 nM respectively. The results indicated that LF in Pheroid™ formulation exhibited improved antimalarial activity *in vitro* by 46.8%, when compared to the reference formulation.

A Peters' 4-day suppressive test was conducted to assess and compare the efficacy of LF in Pheroid™ and reference formulation to chloroquine (positive control). LF was tested at 10, 5 and 1 mg/kg dose concentrations. The experimental mice were inoculated intra-peritoneally with parasitized erythrocytes and administered a dose of LF, by oral gavage, for four consecutive days. The results of the experiment indicated no significant difference in the efficacy or mean survival time of the mice in the Pheroid™ formulation and reference formulation test groups when compared to chloroquine.

Thus it may be concluded that using the Pheroid[™] formulation improves the bioavailability of LF, eliminates the food effect associated with LF as well as significantly reducing the between subject variability in bioavailability when compared to the reference formulation. A similar effect can be obtained after the oral administration of LF in canola oil. LF in Pheroid[™] formulation showed improved *in vitro* efficacy when compared to the reference formulation, however the improved bioavailability of LF in Pheroid[™] formulation did not translate into improved antimalarial efficacy *in vivo*.

University of Cape Town

List of Abbreviations

ACT	Artemisinin Based Combination Therapy
ACTG	AIDS Clinical Trial Group
ADME	Absorption, Distribution, Metabolism and Excretion
ADMET	Absorption, Distribution, Metabolism, Excretion and Toxicity
AL	Artemether-Lumefantrine
APAD	3-acetyl pyridine adenine dinucleotide
APCI	Atmospheric Pressure Chemical Ionization
API	Active pharmaceutical ingredient
APPI	Atmospheric Pressure Photo Ionisation
AUC	Area under the curve
BCS	Biopharmaceutics Classification System
BSV	Between subject variability
CE	Capillary Electrophoresis
CI	Confidence interval
CLSM	Confocal Laser Scanning Microscopy
CM	Culture medium
C _{max}	Maximum systemic concentration
CMC	Carboxy methyl cellulose
CQ	Chloroquine
CQ-R	Chloroquine resistant
CQ-S	Chloroquine sensitive
CYP 3A4	Cytochrome P450 3A4
DDS	Drug delivery system
DDT	dichloro-diphenyl-trichloroethane
D-LF	Deuterated internal standard
DMSO	Dimethyl sulfoxide
ED ₅₀	Drug concentration that inhibits 50% parasite growth
ELISA	Enzyme-Linked Immunosorbant Assay
ESI	Electrospray Ionization
FPM	First pass metabolism
GC	Gas Chromatography
GIT	Gastrointestinal tract
HF	Halofantrine
HIV	Human Immunodeficiency Virus
HPLC	High Pressure Liquid Chromatography
HRP2	Histidine rich protein 2
IM	Intestinal membrane
IP	Intraperitoneal
IPTi	Intermittent presumptive antimalarial therapy during infancy
IPTp	Intermittent presumptive antimalarial therapy during pregnancy
IRS	Indoor residual insecticide spraying
ISTD	Internal standard
ITNs	Insecticide-impregnated bed nets
IVM	Integrated Vector Management
LC-MS/MS	Liquid Chromatography and tandem Mass Spectrometry
LDCs	Lipid Drug Conjugates
LF	Lumefantrine
LLINs	Long-lasting insecticidal nets
LLOQ	Lower Limit of Quantification
LogD	Log of Distribution coefficient
LogP	Log of Partition coefficient
MALDI	Matrix Assisted Laser Desorption/Ionization

ME	Matrix effect
MIF	Molecular interaction field
MMV	Medicines for Malaria Venture
MRM	Multiple reaction monitoring
MS	Mass spectrometry
MST	Mean survival time
MTT	Mean transit time
MQ	Mefloquine
NBT	Nitro blue tetrazolium salt
NCs	Nanocapsules
NCA	Non-compartmental analysis
NONMEM	Non-linear mixed effects modelling
PBS	Phosphate buffered saline
PEG	Polyethylene glycol
<i>pfmdr1</i>	<i>Plasmodium falciparum</i> multi-drug resistant gene
PK	Pharmacokinetics
pKa	Acid-base ionization constant
pLDH	Parasite lactate dehydrogenase enzyme
PLS	Partial least-squares
PPB	Plasma protein binding
PPK	Population pharmacokinetic
PPT	Precipitation solution
PQ	Primaquine
QCs	Quality control standards
QSPR	Quantitative Structure-Property Relationship
RBCs	Red blood cells
RBM	Roll Back Malaria
RDTs	Rapid diagnostic tests
RE	Recovery
rhTNF α	Recombinant human tumour necrosis factor
SLNs	Solid lipid nanoparticles
SMEDDS	Self-Microemulsifying Drug Delivery System
SP	Sulfadoxine-pyrimethamine
SRM	Selective reaction monitoring
SS	Stock solute
STDs	Calibration standards
SYS	System performance verification sample
ULOQ	Upper limit of quantification
USFDA	United States Food and Drug Administration
WB	Whole blood
WHO	World Health Organisation

Table of Contents

Declaration.....	ii
Acknowledgements.....	iii
Abstract.....	iv
List of Abbreviations.....	
Table of Contents.....	
List of Figures.....	
List of Tables.....	
 Chapter 1: Introduction.....	 1
1.1 Malaria: cause and effect.....	1
1.2 Life cycle of <i>P. falciparum</i>	2
1.3 Strategies to control malaria.....	4
1.4 Vector control.....	5
1.5 Diagnostic tools.....	5
1.6 Antimalarial chemotherapy.....	6
1.7 Antimalarial drug resistance.....	7
1.8 Artemisinin based Combination Therapy (ACT).....	8
1.9 Lumefantrine.....	9
1.10 Lumefantrine pharmacokinetics and the food effect.....	10
1.11 Clinical evidence.....	12
1.12 Strategies to overcome poor oral bioavailability.....	14
References.....	16
 Chapter 2: Describing the Physicochemical Properties of Lumefantrine using Computational Predictive Models.....	 21
2.1 Introduction.....	21
2.1.1 Physicochemical properties influencing drug bioavailability.....	23
2.2 Experimental.....	26
2.3 Results.....	27
2.4 Discussion.....	30
References.....	33
 Chapter 3: Drug Formulation of Lumefantrine using Pheroid™ Technology.....	 35
3.1 Introduction: drug formulation and delivery systems.....	35
3.2 Colloidal drug delivery systems.....	36
3.2.1 Liposomes.....	36
3.2.2 Emulsions and microemulsions.....	37
3.2.3 Nanoparticles.....	38
3.3 Pheroid™ technology.....	39
3.3.1 Pheroid™ composition and molecular organisation.....	39
3.3.2 Pro-Pheroid™	40
3.3.3 Applications of Pheroid™ technology.....	41
References.....	43

Chapter 4: <i>In vitro</i> Antimalarial Activity of Lumefantrine against <i>P. falciparum</i>	45
4.1 Introduction.....	45
4.2 Materials and Methods.....	48
4.3 Results.....	51
4.4 Discussion.....	53
References.....	54
Chapter 5: Quantitative Bioanalysis of Lumefantrine using LC-MS/MS	56
5.1 Introduction.....	56
5.2 Materials and Methods.....	60
5.3 Results.....	72
5.3.1 Validation of the LC-MS/MS method for the quantitation of lumefantrine in mouse whole blood.....	72
5.3.2 Validation of the LC-MS/MS method for the quantitation of lumefantrine in mouse plasma.....	83
5.4 Discussion.....	95
References.....	97
Chapter 6: A Bioavailability Study of Lumefantrine in Mice; Evaluating the Application of Pheroid™ Technology	99
6.1 Introduction.....	99
6.2 Materials and Methods.....	102
6.3 Results.....	107
6.3.1 Quantitation of lumefantrine in reference formulation.....	107
6.3.2 Quantitation of lumefantrine in canola oil.....	112
6.3.3 Quantitation of lumefantrine in Pheroid™ formulation.....	117
6.3.4 Population pharmacokinetic modeling.....	124
6.4 Discussion.....	132
References.....	134
Chapter 7: <i>In vivo</i> Efficacy Study of Lumefantrine	136
7.1 Introduction.....	136
7.2 Materials and Methods.....	138
7.3 Results.....	142
7.3.1 Lumefantrine in reference formulation.....	142
7.3.2 Lumefantrine in Pheroid™ formulation.....	145
7.4 Discussion.....	148
References.....	150
Chapter 8: Conclusion	151

List of Figures

Figure 1.1	Global distribution of malaria endemic areas	1
Figure 1.2	A diagram depicting the life cycle of the malaria parasite, detailing the A. Exo-erythrocytic cycle, B. Erythrocytic cycle and C. Sporogonic cycle.	3
Figure 1.3	Worldwide malaria transmission areas and antimalarial resistance	7
Figure 1.4	Chemical structure of lumefantrine	9
Figure 1.5	Schematic illustration of the disposition of an orally administered drug within the body and the organs involved in the ADME process	11
Figure 2.1	A flow diagram detailing the pharmacokinetic parameters that are affected by poor drug bioavailability.	21
Figure 2.2	A representative graph depicting the causative factors for, and their contribution to, drug compound failure	22
Figure 2.3	A schematic describing the relationship between pKa, LogP and LogD. 1: the equilibrium is a function of acid/base strength (pKa) and 2: the equilibrium is a function of the compounds lipophilicity (LogP)	23
Figure 2.4	A hypothetical depiction of how lipophilicity can affect the efficient absorption of a drug compound	24
Figure 2.5	Solubility, permeability and metabolism may influence the systemic bioavailability of an orally administered drug	24
Figure 2.6	Diagram showing passive diffusion of a drug molecule through a biological membrane	25
Figure 2.7	Ionization pattern of LF as predicted using MoKa [®] . The structure of the dominant ionized species of LF at physiological pH (pH 7.4) is illustrated on the graph.	27
Figure 2.8	Partial Least Square (PLS) t-t score plots for solubility model for LF.	28
Figure 2.9	Partial Least Squares (PLS) t-t score plots for Caco-2 permeability model for LF	29
Figure 2.10	Description of the Biopharmaceutics Classification System (BCS) Class categories	31
Figure 3.1	A representative example of a surface modified liposome encapsulating hydrophilic drugs in the aqueous interior and hydrophobic drugs in the lipid bi-layer	36
Figure 3.2	A representation of a (micro)emulsion; a system of oil, water and surfactant	37
Figure 3.3	A representation of a nanoparticle, drugs compounds may be encapsulated in a nanocapsule or attached to the surface to the nanoparticle creating a nanosphere	38

Figure 3.4	An illustration of the constituent components of a) Pro-Pheroid™ and b) Pheroid™	40
Figure 3.5	A representative confocal laser scanning micrograph of Pheroid™ vesicles (red) of submicron size with entrapped drug (dark spots)	41
Figure 4.1	An experimental flow diagram for the screening of antimalarial compounds	45
Figure 4.2	A representative 96-well plate detailing <i>in vitro</i> assay sample locations	49
Figure 4.3	A representative 96 well plate after development, the darker the colour in the wells the more parasites have survived the exposed drug concentration	50
Figure 4.4	Dose response curves of LF in Pheroid™ formulation against <i>P. falciparum</i> D10 strain (CQ-S), a. and b. corresponds to experiment 1 and 2 respectively	52
Figure 4.5	Dose response curves of LF in reference formulation against <i>P. falciparum</i> D10 strain (CQ -S), a. and b. corresponds to experiment 1 and 2 respectively	52
Figure 4.6	Dose response curves of CQ, standard control, against <i>P. falciparum</i> D10 strain (CQ-S), a. and b. corresponds to experiment 1 and 2 respectively	52
Figure 5.1	A schematic of the constituent components of a mass spectrometer	56
Figure 5.2	MRM scan mode in a triple quadrupole mass spectrometer	57
Figure 5.3	Chemical structure of the analyte lumefantrine (LF)	60
Figure 5.4	Chemical structure of the internal standard; deuterated lumefantrine (LF-D ₉)	60
Figure 5.5	Product ion spectrum (Q3) of the analyte, showing the [M+H] ⁺ ion at <i>m/z</i> 530.0 and product ion at <i>m/z</i> 347.8	61
Figure 5.6	Product ion spectrum (Q3) of the ISTD, showing the [M+H] ⁺ ion at <i>m/z</i> 539.0 and product ion at <i>m/z</i> 347.8	62
Figure 5.7	Sample extraction procedures for LF whole blood (WB) and plasma samples	64
Figure 5.8	Representative calibration curve for LF	66
Figure 5.9	Chromatogram of a LF in WB sample, at LLOQ level	78
Figure 5.10	A representative chromatogram of a blank extracted WB sample situated after the ULOQ (STD 9), in the analytical batch list. The analyte peak was manually integrated to calculate percentage carryover	79
Figure 5.11	Chromatogram of a double blank (no analyte and no ISTD) WB extract	80
Figure 5.12	Raw chromatogram of LF at LLOQ with calculated analyte signal/noise ratio of 23.7:1	80

Figure 5.13	Slopes of LF/ISTD peak ratios at three concentrations for six different lots of mouse WB	82
Figure 5.14	Representative chromatogram of LF at LLOQ (STD1)	90
Figure 5.15	A representative chromatogram of a blank extracted plasma sample situated after the standard with the highest analyte concentration (STD 9), in the analytical batch list. The analyte peak as manually integrated to calculate percentage carryover	91
Figure 5.16	Representative chromatogram of a double blank extracted plasma sample, with no LF peak at 1.12 min	91
Figure 5.17	Raw chromatogram of LF at LLOQ with calculated analyte signal/noise of 29.5:1	92
Figure 5.18	Slopes of analyte/ISTD peak ratios at three concentrations for six different lots of mouse plasma	94
Figure 6.1	The composition of the rodent feed used during the bioavailability experiments	102
Figure 6.2	Picture of experimental mice in cage with food and water source	103
Figure 6.3	Diagram showing experimental design of the bioavailability study. *Each treatment arm of the experiment had the same experimental design	104
Figure 6.4	Calculation for 10 mg/kg LF dosing solutions	104
Figure 6.5	Average concentration vs. time graph for reference formulated LF in WB, evaluated in the fed (A&B) and starved (C&D) state.	110
Figure 6.6	Average concentration vs. time graph for reference formulated LF in mouse plasma, evaluated in the fed (A&B) and starved (C&D) state.	111
Figure 6.7	Average concentration vs. time graphs of canola oil formulated LF in WB, administered to groups of mice under fed (A&B) and starved (C&D) conditions.	115
Figure 6.8	Average concentration vs. time graphs of canola oil formulated in plasma, administered to groups of mice under fed (A&B) and starved (C&D) conditions	116
Figure 6.9	Average concentration vs. time graphs of Pheroid™ formulated LF in WB, administered to groups of mice under fed (A&B) and starved (C&D) conditions.	120
Figure 6.10	Average concentration vs. time graphs of Pheroid™ formulated LF in plasma, administered to groups of mice under fed (A&B) and starved (C&D) conditions	121

Figure 6.11	Graphs of pooled average concentration vs. time for LF in the three different formulations, a. and b. represents the WB data in starved and fed state respectively, c. and d. represents the plasma data in the starved and fed state respectively	123
Figure 6.12	An illustration of the final LF pharmacokinetic model.	124
Figure 6.13	Visual predictive check diagrams for the LF PPK model in plasma and WB. The open blue circles represent the actual observed LF concentrations. The lower and upper dashed lines represent the 5 th and 95 th percentiles of the observed data, respectively. The middle solid line represents the median of the observed data. The shaded areas represent the 95% confidence intervals for the 5 th , 50 th and 95 th percentiles of the simulated data.	125
Figure 6.14	Goodness of fit plots of LF for the final model. The upper left and right panels show population and individual predicted concentration versus observed concentration. The solid lines are lines of identity. The lower panels are the conditional weighted residual plots for the final model	126
Figure 6.15	Observed and predicted WB LF concentration vs. time profiles for 8 randomly selected experimental mice administered LF in reference solution	127
Figure 6.16	Observed and predicted WB LF concentration vs. time profiles for 8 randomly selected experimental mice administered LF in canola oil.	127
Figure 6.17	Observed and predicted WB LF concentration vs. time profiles for 8 randomly selected experimental mice administered LF in Pheroid TM formulation	128
Figure 6.18	Observed and predicted plasma LF concentration vs. time profiles for 8 randomly selected experimental mice administered LF in reference solution	128
Figure 6.19	Observed and predicted plasma LF concentration vs. time profiles for 8 randomly selected experimental mice administered LF in canola oil	129
Figure 6.20	Observed and predicted plasma LF concentration vs. time profiles for 8 randomly selected experimental mice administered LF in Pheroid TM formulation	129
Figure 7.1	Schematic detailing the experimental procedure for the <i>in vivo</i> 4-day suppressive test	140
Figure 7.2	Images depicting the morphology of <i>P. berghei</i> using light microscopy, the different stages of parasite development shown here are: a. ring-form, b. trophozoite and c. shizont	141
Figure 7.3	Average % parasitemia vs. time graph for the LF in reference formulation treatment groups at concentrations of 10, 5 and 1mg/kg as well as the control groups; CQ (positive control) and DMSO (negative control). The error bars represent the standard deviation in the data	143

Figure 7.4	Kaplan-Meier survival estimate: Proportion surviving (S) vs. Time (days) plot for the LF in reference formulation treatment groups at 10, 5 and 1 mg/kg as well as the control groups. The survival plot for 10 mg/kg dose is identical to the 5 mg/kg plot. CQ; chloroquine, DMSO; 10% DMSO in water solution	144
Figure 7.5	Average % parasitemia vs. time graph for the LF in Pheroid™ formulation treatment groups at concentrations of 10, 5 and 1 mg/kg as well as the control groups; CQ (positive control) and DMSO (negative control).	145
Figure 7.6	Kaplan-Meier survival estimate: Proportion surviving (S) vs. Time (days) plot for the LF in Pheroid™ formulation treatment groups at 10, 5 and 1 mg/kg as well as the control groups. CQ; chloroquine, D; 10% DMSO in water solution	146

University of Cape Town

List of Tables

Table 2.1	<i>in silico</i> predicted lipophilicity values for LF	27
Table 4.1	Results of <i>in vitro</i> drug susceptibility assay against <i>P. falciparum</i> D10 strain detailing the average IC ₅₀ values for LF in Pheroid™, LF in reference formulation and CQ. Reported IC ₅₀ values are the average of two experiments performed in triplicate	47
Table 4.2	Reported <i>in vitro</i> activity (IC ₅₀ values) for lumefantrine/benflumetol tested using isolates of <i>P. falciparum</i>	51
Table 5.1	Summary of published LC-MS/MS methods for LF	58
Table 5.2	ESI settings	62
Table 5.3	MS/MS settings	63
Table 5.4	Preparation of calibration standards for LF	65
Table 5.5	Preparation of quality control standards for LF	65
Table 5.6	A representation of a validation run sample batch list. Abbreviations: DB (double blank); sample containing no analyte or ISTD, SYS; system performance verification standard.	67
Table 5.7	LF calibration curve accuracy and precision for validation 1	72
Table 5.8	Summary of LF inter-validation quality control standards for validation 1	72
Table 5.9	LF calibration curve accuracy and precision for validation 2	73
Table 5.10	Summary of LF inter-validation quality control standards for validation 2	73
Table 5.11	LF calibration curve accuracy and precision for validation 3	73
Table 5.12	Summary of LF inter-validation quality control standards for validation 3	73
Table 5.13	Overall accuracy and precision estimation for the quantification of LF in mouse WB	74
Table 5.14	Stock solution stability at ambient temperature (16°C) and -20°C compared to fresh reference solution at three different concentrations	75
Table 5.15	Freeze and thaw stability of LF	76
Table 5.16	On bench (at room temperature) stability of LF	77
Table 5.17	On-instrument stability for extracted samples: Medium concentration – 800 ng/ml	78
Table 5.18	Calculation of carryover of LF in mouse WB	79
Table 5.19	Recovery calculation results for LF extraction from mouse WB	81

Table 5.20	Mean LF / ISTD peak area ratios and the precision (CV) of slopes of lines fitted through low, medium and high samples of LF in six different lots of WB.	82
Table 5.21	LF calibration curve accuracy and precision for plasma validation 1	83
Table 5.22	Summary of LF intra-validation quality control standards for plasma validation 1	83
Table 5.23	LF calibration curve accuracy and precision for plasma validation run 2	83
Table 5.24	Summary of LF inter-validation quality control standards for plasma validation run 2	84
Table 5.25	LF calibration curve accuracy and precision for plasma validation run 3	84
Table 5.26	Summary of LF inter-validation quality control standards for plasma validation run 3	84
Table 5.27	Summary of combined QC results for the three validation runs	85
Table 5.28	Stock solution stability assessment at 500 ng/ml	86
Table 5.29	Freeze and thaw stability of LF	87
Table 5.30	On bench (at ambient temperature) stability of LF	88
Table 5.31	On-Instrument stability for extracted samples containing LF at a concentration of 800 ng/ml	89
Table 5.32	Calculated carryover of LF in plasma	90
Table 5.33	Recovery data for LF in plasma at low, medium and high concentrations	93
Table 5.34	Mean LF / ISTD peak area ratios and the precision (CV) of slopes of lines fitted through low, medium and high samples of LF in six different lots of mouse plasma.	94
Table 5.35	A comparison between published and currently presented (in blue) LC-MS/MS methods for LF	96
Table 6.1	Reported pre-clinical pharmacokinetic parameters for LF in a rat model after oral dose administration. *Food was returned to experimental rats 3 hours post dose administration.	100
Table 6.2	Dose calculation for LF in Pheroid™ formulation. *Calculated for a mouse of average weight 30 g.	105
Table 6.3	Summary of the calibration standard concentrations for the analytical runs of reference formulated LF in WB	108

Table 6.4	Summary of quality control standard concentrations for the analytical runs of reference formulated LF in WB	108
Table 6.5	Summary of the calibration standard concentrations for reference formulated LF in mouse plasma.	109
Table 6.6	Summary of the quality control standard concentrations for reference formulated LF in mouse plasma.	109
Table 6.7	Concentrations of reference formulated LF in WB, tested in the fed (Groups A and B) and starved (Groups C and D) state.	110
Table 6.8	Concentrations of reference formulated LF in plasma, tested in the fed (Groups A and B) and starved (Groups C and D) state.	111
Table 6.9	Summary of calibration standard concentrations for the analytical runs of canola oil formulated LF in WB	113
Table 6.10	Summary of quality control standard concentrations for the analytical runs of canola oil formulated LF in WB	113
Table 6.11	Summary of calibration standard concentrations for the analytical runs of canola oil formulated LF in plasma	114
Table 6.12	Summary of quality control standards concentrations for the analytical runs of canola oil formulated LF in plasma	114
Table 6.13	Concentrations of canola oil formulated LF in WB, tested in the fed (Groups A and B) and starved (Groups C and D) state.	115
Table 6.14	Concentrations of canola oil formulated LF in plasma, tested in the fed (Groups A and B) and starved (Groups C and D) state.	116
Table 6.15	Summary of calibration standard concentrations for the analytical runs of Pheroid™ formulated LF in WB	118
Table 6.16	Summary of quality control standard concentrations for the analytical runs of Pheroid™ formulated LF in WB	118
Table 6.17	Summary of calibration standard concentrations for the analytical runs of Pheroid™ formulated LF in plasma	119
Table 6.18	Summary of quality control standard concentrations for the analytical runs of Pheroid™ formulated LF in plasma	119
Table 6.19	Concentrations of Pheroid™ formulated LF in WB, tested in the fed (Groups A and B) and starved (Groups C and D) state. BLQ: below limit of quantitation.	120
Table 6.20	Concentrations of Pheroid™ formulated LF in plasma, tested in the fed (Groups A and B) and starved (Groups C and D) state.	121
Table 6.21	The final parameter estimates for the LF pharmacokinetic model. CL and V are reported for a 27 g mouse and allometrically scaled according to Anderson and Holford, 2008.	130

Table 6.22	Simulation based NCA-equivalent PK parameter estimates for LF in the three different formulations. The values stated are the mean values (90% confidence interval [CI])	130
Table 7.1	Dose calculation for LF in reference formulation. *Calculated for an average mouse weight of 25 g	138
Table 7.2	Dose calculation for LF in Pheroid™ formulation. *Calculated for an average mouse weight of 25 g	139
Table 7.3	Average % parasitemia values for the LF in reference formulation group at each treatment dose including the controls	142
Table 7.4	<i>In vivo</i> antimalarial activity (chemosuppression) of LF in reference formulation on day 8 post infection. S.D; standard deviation	143
Table 7.5	Average % parasitemia values for the LF in Pheroid™ formulation group at each treatment dose including the controls	145
Table 7.6	<i>In vivo</i> antimalarial activity (chemosuppression) of LF in Pheroid™ formulation on day 12 post infection.	146

Chapter 1

Introduction

1.1 Malaria: Cause and Effect

Malaria is a dual-host hematoprotzoan parasitic infection, transmitted by certain species of the female anopheline mosquitoes. In humans, malaria is caused by four parasite species; *Plasmodium falciparum*, *Plasmodium vivax*, *Plasmodium ovale* and *Plasmodium malariae* (Hoffman *et al.*, 2012). In recent years, *Plasmodium knowlesi*, a species that causes malaria among monkeys, has also caused human cases of malaria. *P. falciparum* is the most virulent of the species and largely responsible for severe morbidity and mortality (WHO; malaria fact sheet, 2012). The life cycle of the *P. falciparum* parasite will be discussed in detail in Section 1.2.

Malaria is an infectious disease that is preventable and curable yet 216 million clinical cases occur annually with 655 000 people succumbing to infection (WHO; malaria fact sheet, 2012). Approximately half of the world's population live at risk of infection in the 99 countries and territories affected by malaria. The risk of death as a result of *P. falciparum* infection is higher in Africa than other malaria endemic countries (Snow *et al.*, 1997, Prusty and Das, 2001, Snow *et al.*, 2005). Extensive areas of Latin America, Africa and South-East Asia, some of the poorest economies, have high prevalence of malaria infection (WHO; malaria fact sheet, 2012, Snow *et al.*, 2005) as seen in Figure 1.1.

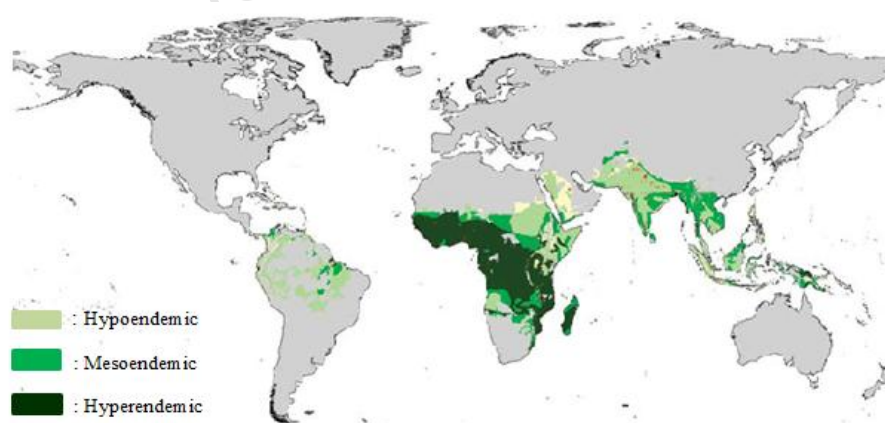


Figure 1.1: Global distribution of malaria endemic areas. The light green shaded areas have low levels of transmission with a childhood infection prevalence of <10%. Medium green shaded areas have an infection prevalence between 11% and 50%. Dark green shaded areas have an infection prevalence $\geq 50\%$ (Figure sourced from Snow *et al.*, 2005)

It is estimated that 90% of deaths caused by malaria occur in Africa, children under the age of 5 years and pregnant women being most susceptible to infection (WHO, world malaria report 2011). Although the malaria mortality rates have been reduced by more than 25%, globally, the burden of malaria extends well beyond morbidity and mortality. Malaria is closely correlated with poor socio-economic conditions. Malaria endemic countries may benefit less from foreign investment, market trade and industrial development due to the excessive cost of infection prevention, treatment and loss of labour (Gallup and Sachs, 2001, Malaney *et al.*, 2004). High child mortality leads to increased fertility rates which affect the demographic structure of a country and discourages investment in education. Malaria in childhood has also been shown to permanently affect development and reduce cognitive performance (Serouri *et al.*, 2000, Holding and Snow, 2001). The magnitude of the disease burden caused by endemic malaria is evident in the prevalence of a potentially fatal genetic modification which causes sickle cell disease in 130 000 infants annually (Malaney *et al.*, 2004, Natarajan *et al.*, 2010). As a result of the protective nature of the sickle cell trait against malaria infection, the disease is still prevalent in malaria endemic areas. Due to the geographical overlap, malaria and Human Immunodeficiency Virus (HIV) co-infection has major public health and economic implications, especially in Sub-Saharan Africa where comorbidity causes increased prevalence of both diseases (Abu-Raddad *et al.*, 2006). In summation, malaria is a global health threat that causes substantial morbidity, mortality, negative socio-economic growth and diminished quality of life for the populations living in endemic regions.

1.2 Life cycle of *P. falciparum*

The life cycle of the malarial parasite incorporates stages in both the mosquito vector and the human host. As depicted in Figure 1.2, the infective sporozoites present in the mosquito's saliva is transferred to the human host during a blood meal. In the human host the sporozoites develop in the parenchymal cells of the liver (exo-erythrocytic cycle) to produce merozoites which are released into the blood stream (erythrocytic cycle) to infect and reproduce in red blood cells (RBCs). Most antimalarials eliminate the parasite from infected red blood cells, as indicated in Figure 1.2, malaria diagnosis also occurs when the parasite is in the blood stage or erythrocytic cycle. The sporogonic, exo-erythrocytic and erythrocytic stages of *P. falciparum* are detailed in this section.

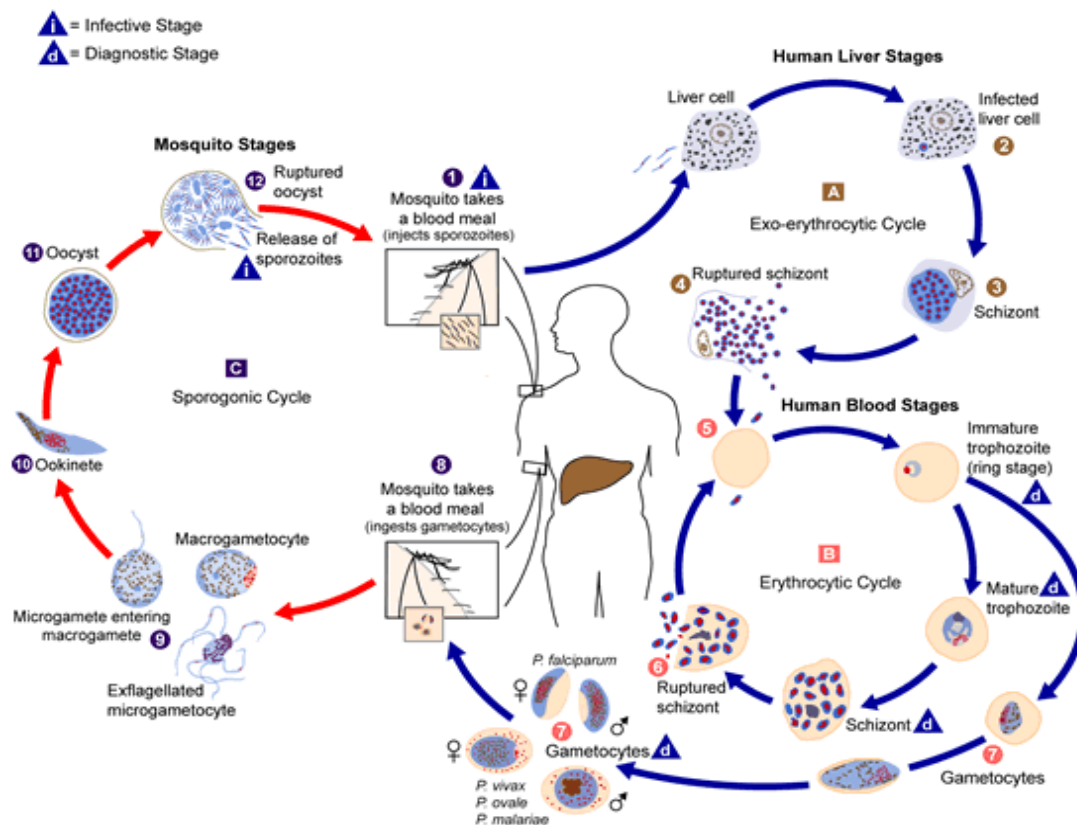


Figure 1.2: A diagram depicting the life cycle of the malaria parasite, detailing the A. Exo-erythrocytic cycle, B. Erythrocytic cycle and C. Sporogonic cycle. (Diagram sourced from: <http://dpd.cdc.gov/dpdx/html/Malaria.htm>)

A. Exo-erythrocytic cycle

Malaria infection is transmitted to a human host when an infectious female *Anopheles* mosquito bites and injects saliva, containing anti-coagulant agents and infective sporozoites, into the blood stream of the human host. The sporozoites circulate in the bloodstream before actively entering the liver of the host. In the liver they invade the hepatocytes and initiate the asexual exo-erythrocytic cycle. The sporozoites transform into mature schizonts that reproduce asexually generating extensive numbers of merozoites. After 5-20 days the merozoites rupture the hepatic cells, enter the blood stream and invade the red blood cells.

Only *P. vivax* and *P. ovale* produce hypnozoites which remain dormant, for varying periods of time, in the liver of human hosts and may cause relapse infections (Hoffman *et al.*, 2012).

B. Erythrocytic cycle

The blood stage cycle of the parasite replication is responsible for the pathology associated with malaria. The merozoites released from the liver into the blood stream recognize, attaches and enters the RBC. The blood stage parasite grows, feeds and undergoes periodic (24-72 hour) cycles of asexual replication; producing and releasing daughter merozoites. Within the RBC, the merozoite matures from a ring-stage trophozoite to a pigmented trophozoite and then undergoes multiple rounds of nuclear division to form a shizont. A mature shizont generates merozoites which rupture the host RBC, enter the blood circulatory system and infect other RBCs. Instead of undergoing cycles of asexual replication, merozoites may also develop into sexual forms of the parasite; male and female gametocytes. These gametocytes are the precursor cells of the male and female gametes, once formed they exit the RBC and circulate in the bloodstream. These gametocytes are ingested by a mosquito when it bites and takes a blood meal from the infected human host (Hoffman *et al.*, 2012).

C. Sporogonic cycle

The female anopheline mosquito serves as a vector for the transmission of *Plasmodium* parasites among human hosts. In the event of a mosquito taking a blood meal from a malaria infected human, it also takes up mature gametocytes, this is the start of the sporogonic cycle. In the midgut of the mosquito, the microgametes (male gametes) fertilize the macrogametes (female gametes) producing zygotes which in turn develop into ookinetes. The ookinete penetrates the epithelium of the midgut, settles beneath the outer gut wall and develops into an oocyst. The oocyst then matures over a period of approximately 14 days and produces sporozoites. The sporozoites are actively mobile; they migrate to the salivary glands and settle in the salivary duct of the mosquito. During subsequent blood meals, the salivary fluid and its content of infective sporozoites are injected into the human host and initiate another asexual replicative stage (Hoffman *et al.*, 2012).

1.3 Strategies to control malaria

The effective control of malaria is threatened by many factors; including drug-resistant parasites, poor patient compliance, counterfeit drugs, poor health care systems, insecticide resistant anopheline mosquitos and inaccurate diagnostic methods. As a result, any successful malaria control program needs to be multi-faceted, incorporating methods for vector control, preventative therapy, accurate diagnosis and treatment of malaria infection.

The current interventions implemented for the control of malaria includes the distribution and use of insecticide-impregnated bed nets (ITNs), particularly long-lasting insecticidal nets (LLINs), indoor residual insecticide spraying (IRS) using dichloro-diphenyl-trichloroethane (DDT), rapid diagnostic tests (RDTs), intermittent preventative antimalarial therapy during pregnancy (IPTp) and infancy (IPTi), and antimalarial chemotherapy (WHO; World Malaria Report, 2011).

1.4 Vector control

Integrated vector management (IVM) is a new ‘adaptive’ and cost-effective strategy for the control and prevention of malaria. IVM incorporates the knowledge of local vector ecology and patterns of disease transmission in selecting the most appropriate method for vector control. IVM attempts to minimize health risks from acute exposure to toxic pesticides and the development of vector resistance to widely-used insecticides by combining environmental management and chemical tools. Environmental management strategies (reducing water logged areas) to reduce mosquito breeding grounds and biological controls (bacterial larvicides and larvivorous fish) to target and eliminate mosquito larvae may be used to replace chemical methods of vector control. The IVM system has been successfully used in Asia and Africa to reduce the transmission and incidence of malaria (WHO; Malaria control, 2011).

1.5 Diagnostic tools

Inaccurate clinical (declared fever) or self-diagnosis of malaria contributes to the misdiagnosis of malaria and the misuse of antimalarial drug resources. The clinical signs and symptoms of malaria are non-specific and resemble many other febrile illnesses (Luxemburger *et al.*, 1998, WHO; Guidelines for the treatment of malaria, 2011). Light microscopy; the direct examination of intracellular parasites on stained blood films, is regarded as the gold standard for diagnosis. It is inexpensive but is time-consuming, requires adequate equipment, maintenance and trained personnel; however it still remains an important diagnostic tool. RDTs are quick and easy to perform, sensitive and specific for *P. falciparum* and have less investigator-related variation than microscopy (Guerin *et al.*, 2002). The drawbacks of RDTs include cost, lack of sensitivity to detect malaria caused by other *Plasmodium* species and heat instability (Guerin *et al.*, 2002, Chiodini *et al.*, 2007). Developing robust, accurate and cost effective diagnostic tools is another challenging

endeavour against the onslaught of malaria that requires financial investment for continuous research and development.

1.6 Antimalarial chemotherapy

Chemotherapy is essentially used for prophylaxis and the effective treatment of malaria in order to prevent disease progression and transmission of infection. The current antimalarials available for clinical use are: the 4-aminoquinolines (e.g. chloroquine, amodiaquine), 8-aminoquinolines (e.g. primaquine), arylaminoalcohols (eg. halofantrine, lumefantrine), artemisinin and its derivatives (e.g. artemether, artesunate, etc.), antifolates (e.g. pyrimethamine, sulfadoxine, etc.), antibiotics (e.g. azithromycin) and combination therapies such as artemisinin based combination therapy (ACT).

ACTs are recommended as first line therapy for uncomplicated malaria and are discussed in detail in this chapter. Parenteral artesunate is recommended as first line treatment for severe malaria caused by *P. falciparum* (WHO; World Malaria Report, 2011). In malaria endemic areas with high transmission, the World Health Organisation (WHO) recommends intermittent preventive treatment with sulfadoxine-pyrimethamine (SP) for pregnant women and infants (WHO; World Malaria Report, 2011). 8-aminoquinolines such as primaquine are the only drugs used for effective elimination of liver stage parasites and dormant stage *P. vivax* and *P. ovale* hypnozoites found in the liver. These dormant hypnozoites may cause recurrent malaria infections (Krotoski *et al.*, 1982, Greenwood *et al.*, 2008). Inhabitants of malaria endemic areas naturally develop immunity (after at least one or two episodes of infection) to blood stage infections; curtailing parasitemia and preventing the development of severe disease (Gupta *et al.*, 1999). Likewise, antimalarial vaccines, which elicit long term immunity, may be imperative to counteract the malaria parasite at all life stages, preventing transmission and facilitating the eradication of malaria (Richie and Saul, 2002).

The concurrent use of vector control measures, accurate diagnosis and chemotherapy has been shown to be effective in reducing malaria morbidity and mortality (Barnes *et al.*, 2005). The WHO global malaria programme, the Roll Back Malaria partnership (RBM) and Medicines for Malaria Venture (MMV) are some examples of initiatives dedicated to the eradication of malaria through research and development (Nabarro and Tayler, 1998, Bathurst and Hentschel, 2006). The discovery and development of antimalarials with a long therapeutic lifespan and the ability to restrict the development of parasite drug resistance is of paramount importance.

1.7 Antimalarial drug resistance

Drug resistance develops when malaria parasites subjected to sub-therapeutic drug levels acquire spontaneous genetic mutations that confer diminished drug susceptibility. The resulting parasite strain, possessing the drug resistant genotype may survive, replicate and cause treatment failure in the host despite optimal dosing (Bloland, 2001, Wilairatana *et al.*, 2001, WHO; malaria fact sheet, 2012). The selection for drug resistant parasites may be compounded by inappropriate antimalarial prescribing, poor patient compliance, counterfeit drugs and variable drug pharmacokinetics (Wilairatana *et al.*, 2001). Understanding the genetic and molecular factors underlying the development of parasite drug resistance is imperative in sustaining the lifespan of the current antimalarials in clinical use, including ACTs (Hyde, 2005, Greenwood *et al.*, 2008). Chloroquine (CQ) was introduced in the 1940's and was considered the 'gold standard' treatment for malaria. Parasite resistance to CQ emerged in South-East Asia during the late 1950's and spread to Africa in the late 1970's (Harinasuta *et al.*, 1965, Campbell *et al.*, 1979, Fogh *et al.*, 1979). Sulfadoxine-pyrimethamine (SP) then replaced CQ as first-line therapy for uncomplicated malaria but drug resistant parasites soon emerged (Mita *et al.*, 2009, Petersen *et al.*, 2011). With reference to Figure 1.3, *P. falciparum* resistant to CQ and SP is now predominant in nearly all malaria endemic areas (Black *et al.*, 1981, Bjorkman *et al.*, 1990, Wongsrichanalai *et al.*, 2002).

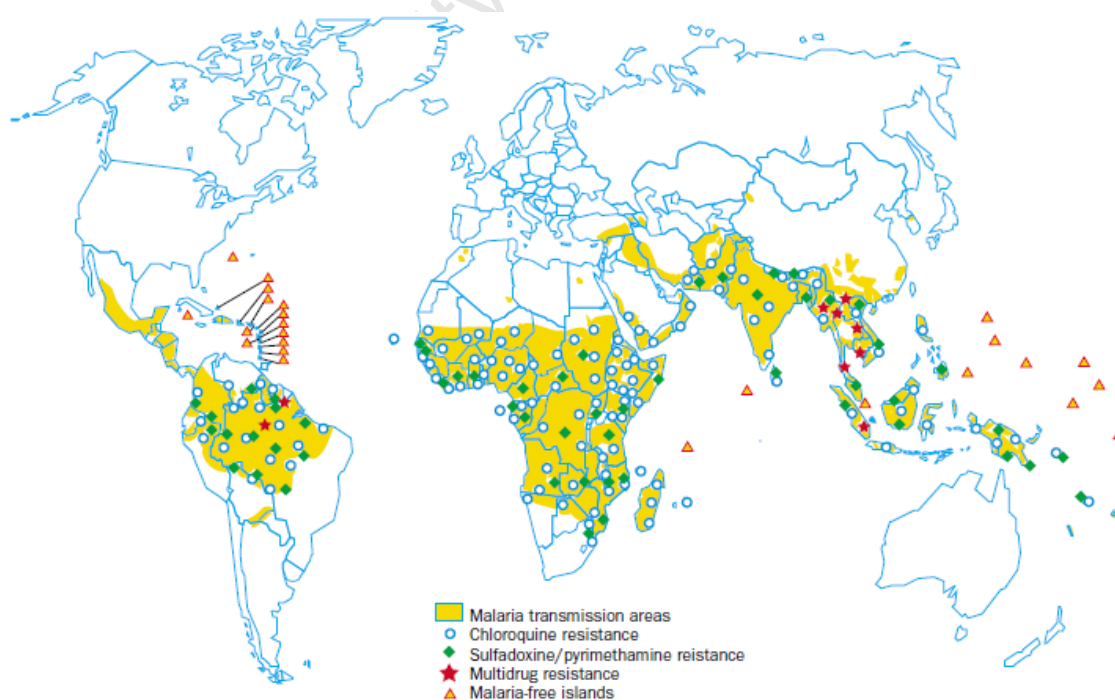


Figure 1.3: Worldwide malaria transmission areas and antimalarial resistance (Wongsrichanalai *et al.*, 2002)

Parasite resistance has however recently emerged to all antimalarials including the artemisinin derivatives and effective treatment policies are necessary to prevent the spread of resistance (Anderson *et al.*, 2010, Dondorp *et al.*, 2010).

Compounds that can reverse resistance to CQ in the parasites, known as chemosensitizers, may be used to improve or reinstate the clinical response to CQ (Zishiri *et al.*, 2011). Many compounds such as imipramine (anti-psychotic) and verapamil (calcium channel blocker), have been shown to reverse CQ resistance (Krogstad *et al.*, 1987, Martin *et al.*, 2009). There are currently no drugs to replace ACTs thus strategies to prevent artemisinin-resistant malaria will depend on optimizing the partner drugs of existing ACTs. For future reference triple therapy, including an artemisinin derivative and two partner drugs may be considered as an alternative treatment strategy (Dondorp *et al.*, 2010). ACTs however are still the most effective antimalarial treatment option in most malaria endemic areas.

1.8 Artemisinin based Combination Therapy (ACT)

During the 1990's *P. falciparum* developed widespread resistance against Chloroquine (CQ) and Sulfadoxine-Pyrimethamine (SP) drug therapies, causing an increase in disease transmission and mortality due to diminished treatment efficacy (Price and Nosten, 2001, Mita *et al.*, 2009, WHO, malaria fact sheet). Effective drug therapy to combat malaria as well as prevent parasite resistance was required. The additional problem of cross-resistance, where the development of parasite resistance to one drug may relay parasite resistance to other antimalarials with similar modes of action, may also be overcome and prevented by using combination therapy instead of monotherapy (WHO, Global report, 2010). The rationale for combining two antimalarials with independent modes of action is that the probability of the parasite developing resistance to two drugs simultaneously is significantly reduced compared to developing resistance to one drug (White and Olliaro, 1996). The WHO recommended the deployment of ACTs for the treatment of uncomplicated malaria in November 2000 (WHO, malaria fact sheet). ACTs combine a rapid acting antimalarial such as artemisinin or a derivative, to reduce parasite load with a partner antimalarial that has a long half-life which eliminates remaining parasites and prevents recrudescence (White *et al.*, 1999, WHO; antimalarial combination therapy, 2001). Recrudescence is a recurrent infection that usually occurs after inadequate treatment due to parasite drug resistance, variable drug pharmacokinetics or incomplete dosage (WHO, Global report, 2010, Hoffman *et al.*, 2012).

The artemisinin derivative and partner antimalarial may offer mutual protection against the development of drug resistant parasites, as resistant parasites to one of the drugs may be eliminated by the partner drug (Nosten *et al.*, 2012). Artemisinin derivatives also eliminate young parasite gametocytes. Combination therapy may thus safeguard the therapeutic longevity of the constituent drugs and decrease parasite transmission (White *et al.*, 1999, Greenwood *et al.*, 2008). The effective ACTs, as recommended by the WHO are Artemether-Lumefantrine (AL, Coartem[®]), Artesunate-Amodiaquine, Artesunate-Mefloquine, Artesunate-Sulfadoxine/Pyrimethamine and Dihydroartemisinin-Piperaquine (WHO; Antimalarial combination therapy, 2001). A more recent combination; Pyronaridine-Artesunate has also demonstrated clinical efficacy when compared to Artemether-Lumefantrine (AL) in a randomized non-inferiority clinical trial (Tshefu *et al.*, 2010). AL is the first and only fixed dose (both active drugs in one tablet) ACT recommended by the WHO and has been adopted as first-line therapy for uncomplicated malaria in more than 20 African countries (Premji *et al.*, 2008, WHO, world malaria report, 2011). ACTs in a fixed dose formulation may facilitate patient adherence to full treatment course (Price *et al.*, 2006).

1.9 Lumefantrine

The chemical structure of lumefantrine (LF), shown in Figure 1.4, is a racemic fluorene derivative originally called benflumetol. It was synthesized in the 1970's by the Academy of Military Medical Sciences in Beijing and registered in China for use as an antimalarial drug in 1987 (White *et al.*, 1999, Ezzet *et al.*, 2000).

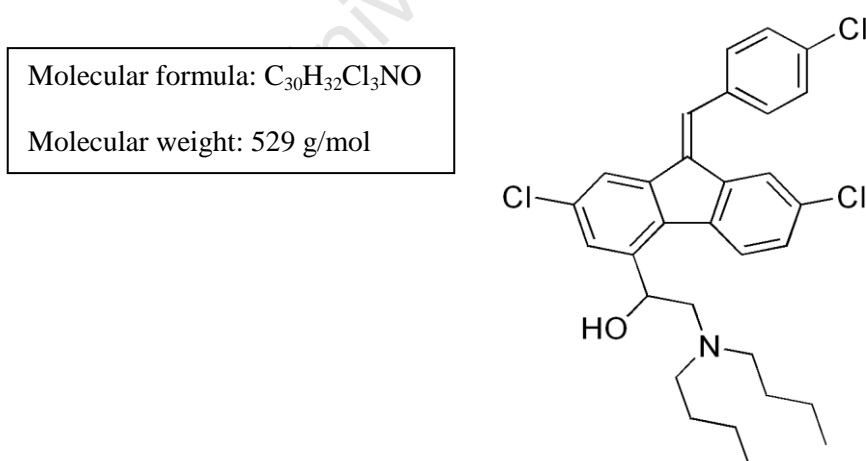


Figure 1.4: Chemical structure of lumefantrine. Chemical name: (1*RS*)-2-(dibutylamino)-1-[(9*Z*)-2,7-dichloro-9-[(4-chlorophenyl)methylidene]-9*H*-fluorene-4-yl]ethanol.

Due to LFs chirality, it occurs in a laevorotatory and dextrorotatory form both of which have similar activity against *P. falciparum* as well as very low toxicity (Zeng *et al.*, 1996, Wernsdorfer *et al.*, 1998). LF is a hydrophobic and highly lipophilic compound with a terminal half-life of 3-4 days in malaria infected patients (White *et al.*, 1999). Absorption of LF is influenced by lipids and food intake. As a result, high variability of therapeutic LF plasma levels has been observed in clinical trials (Wernsdorfer *et al.*, 1998, White *et al.*, 1999, Ezzet *et al.*, 2000). LF is available commercially as part of a co-formulated ACT called Coartem[®] (Artemether + Lumefantrine) manufactured by Novartis Pharma AG, Basel, Switzerland. Coartem[®] is safe, well tolerated and effective for treating multi-drug resistant malaria (Stohrer *et al.*, 2004, Ratcliff *et al.*, 2007). In 2010, Coartem[®] accounted for more than 70% of the overall ACT supplies to the public sector. The price for Coartem[®] ranges between 0.36-1.3 United States dollars (USD) per treatment course and drug accessibility may be increased in poor socio-economic areas due to the efforts of the WHO and the Global Health Fund (WHO, World Malaria Report, 2011).

Coartem[®] needs to be administered with food to ensure adequate oral bioavailability (White *et al.*, 1999, Davis *et al.*, 2005, Lindergardh *et al.*, 2005). Poor drug pharmacokinetics and inefficient parasite elimination can prove to be disadvantageous, leading to the development of parasite drug resistance as a result of sub-therapeutic levels and eventually treatment failure (WHO; Global report 2010). The ideal antimalarial drug should have a rapid onset of the antiparasitic effect and a slow elimination to prevent recrudescence but not encourage the development of parasite resistance due to prolonged exposure to sub-therapeutic drug levels (Winstanly *et al.*, 2002).

1.10 Lumefantrine pharmacokinetics and the food effect

Pharmacokinetics (PK) is a study of what the body does to the drug, after administration, involving the processes of drug absorption, distribution, metabolism and excretion (ADME) (Smith *et al.*, 2001). A drug may be administered orally, parenterally (intravenous, intramuscular, subcutaneous), transdermally, rectally or via nasal spray. The route of drug administration and site (gastrointestinal tract (GIT), nasal cavity, conjunctiva, etc.) of drug absorption has a direct effect on its PK (Benedetti *et al.*, 2009).

Oral administration is the preferred and most frequently used route for drug administration; it is convenient, non-invasive, safe and eases patient compliance (Gomez-Orellana, 2005, Kerns & Di, 2008). As shown in Figure 1.5 below, an orally administered drug is absorbed in the

GIT. In the body, absorption is the process whereby a drug is transported from the site of administration to the systemic blood circulation. Once the orally administered drug is absorbed across the intestinal membrane it enters the blood circulation via the hepatic portal vein, which collects the blood supply from the GIT and passes through the liver, where a portion of the absorbed drug may be extracted and altered by enzymes. A drug may bind to proteins within the blood and only unbound or free drug may impart a therapeutic effect, be metabolised or excreted. Extraction occurs predominantly in the liver or kidneys and refers to the irreversible excretion or metabolism (chemical alteration by enzymes generating metabolites) of the drug. 'First pass metabolism' occurs when the drug passes from the GIT to the liver for the first time after being absorbed and a fraction of the drug is extracted by enzymes in the GI membranes and liver before re-entering the blood circulation system. First pass metabolism may substantially reduce the amount of drug that eventually enters the systemic circulation (Smith *et al.*, 2001, Benedetti *et al.*, 2009).

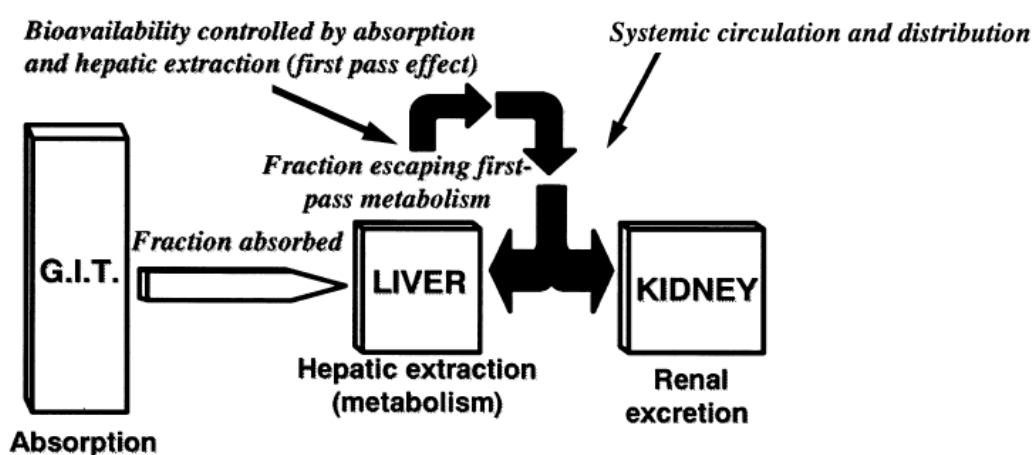


Figure 1.5: Schematic illustration of the disposition of an orally administered drug within the body and the organs involved in the ADME process (Figure sourced from Smith *et al.*, 2001).

The most relevant PK parameter for characterizing drug absorption is bioavailability. Bioavailability describes the fraction of the administered dose that reaches the systemic circulation. A bioavailability study is performed to elucidate the time course of the disposition of a drug within a biological system, by measuring concentration levels in blood or plasma over a period of time (Smith *et al.*, 2001).

Many factors may influence the oral bioavailability of a drug, including aqueous solubility, dissolution rate, membrane permeability and food (Gomez-Orellana, 2005, Kerns & Di, 2008). Orally administered drugs need to dissolve in the gastric fluid before traversing the GI membrane and for lipophilic drugs such as LF, poor aqueous solubility leads to variable oral

bioavailability (Ezzet *et al.*, 2000). LF is also subject to the 'food effect', as detailed in clinical research papers, with a reported 16-fold increase in bioavailability when administered with food compared to administration under fasted conditions (White *et al.*, 1999, Ezzet *et al.*, 2000). A food effect may be defined as an observed relative difference in systemic exposure or bioavailability, of a drug when administered orally in a fed state as compared to when the same drug formulation is administered in a fasted or starved state (Singh, 1999).

It is thought that the fat content in digested food may increase the solubility of the lipophilic drug thereby facilitating its dissolution, absorption and oral bioavailability. Food may decrease a drugs oral bioavailability by delaying absorption due to slow gastric emptying and input into the intestine, where most of the drug absorption takes place. Food may increase the absorption of lipophilic drugs by stimulating bile salt secretion and changing the pH conditions of the gastric fluid. In the presence of food there is less pre-systemic metabolism or loss of drug due to metabolism by gastric enzymes which means that, a larger fraction of the drug is thus absorbed into the blood stream (Kerns & Di 2008).

1.11 Clinical Evidence

The bioavailability of LF is the principal determinant of treatment efficacy of AL (artemether + lumefantrine) (Ezzet *et al.*, 1998, Price *et al.*, 2006). Clinical evidence suggests that variable inter-individual bioavailability can be attributed to the food effect associated with AL, predominantly in the case of LF and to a lesser extent, Artemether (White *et al.*, 1999, Ezzet *et al.*, 2000, Ashley *et al.*, 2007, Premji *et al.*, 2008 and Borrmann *et al.*, 2010). It is thus recommended that AL be administered after meals. This may pose a potential problem as patients with malaria often present with symptoms such as fever, nausea, vomiting and anorexia, and therefore eat very little during the acute phase of the disease. The affected people living in the malaria endemic areas in Africa are also often very poor and may not be able to eat a meal before every dose (White *et al.*, 1999).

A study done by Ashley *et al.* to determine how much ingested fat is necessary to obtain optimum LF exposure found that a meal containing 1.6 g of fat eaten before dose administration of AL would be sufficient (Ashley *et al.*, 2007). The average fat consumption of children living in Sub-Saharan Africa is in the range of 30-60 g/day and the content of African diets is adequate to achieve optimum LF exposure when administered fixed-dose AL (Premji *et al.*, 2008). This finding was reiterated in a study done by Piola *et al.*, in a randomized trial of 957 patients in Mabarara, Uganda. It was concluded that AL has a high

cure rate, >96%, irrespective of supervised food intake or routine outpatient conditions (Piola *et al.*, 2005).

Borrmann *et al.* conducted a randomized, multi-centre study in children in five different African countries to assess the food effect on the bioavailability and efficacy of AL. The study included 621 children and also evaluated the dispersible form of AL compared to the crushed tablet. It was concluded that the consumption of milk or traditional African food was sufficient to achieve adequate LF absorption, from both formulations, in children and that the increase in LF plasma concentration as a result of the 'food effect' had no direct influence on the 28-day cure rate. The cure rate in the study was reported to be 98.2% and treatment failure was not related to food intake (Borrmann *et al.*, 2010).

Price *et al.* performed a clinical trial in Thailand to characterize the molecular and pharmacological determinants of therapeutic failure when using AL to treat multi-drug resistant *P. falciparum* malaria. The study enrolled 1588 patients and evaluated the 4-dose regimen of AL versus the 6-dose regimen in curing malaria and preventing recrudescence. South-East Asia is recognized as the 'hot spot' for the development of drug resistant malaria parasites. Thailand has established *P. falciparum* drug-resistance to CQ, SP and mefloquine (MQ). It has been discovered that the P-glycoprotein pump encoded by the *P. falciparum* multi-drug resistant gene (*pfmdr1*) regulates the *in vitro* and *in vivo* parasite response to mefloquine, halofantrine, quinine and artesunate (Price *et al.*, 2004). Gene amplification of *pfmdr1* is the main molecular determinant of MQ resistance and there is *in vitro* evidence of cross-resistance between LF and MQ (Duraisingh *et al.*, 2000). Results showed that gene amplification of *pfmdr1* in *P. falciparum* isolates from study patients increased the risk of treatment failure in patients treated with the 4-dose regimen but not the 6-dose regimen of AL. The study found that 24% of patients with a LF plasma concentration <175 ng/ml on day 7, post treatment, developed recrudescence as compared to the 1.1% of patients with LF plasma concentrations ≥175 ng/ml. The oral bioavailability of LF is the main pharmacological determinant of efficacy of AL and the 4-day regimen did not provide consistent LF levels to overcome susceptible parasites. The 6-day regimen provided sufficient drug levels to treat multi-drug resistant *P. falciparum* malaria (Price *et al.*, 2006).

Slower acting antimalarials such as LF, which serve as partner drugs to the fast acting artemisinin derivatives, may play an essential role in preventing recrudescence and parasite drug resistance (Ezzet *et al.*, 1998). However for LF to be clinically effective it has to be adequately bioavailable after oral administration. Formulations and other strategies may

be used to improve the solubility of lipophilic drugs and thereby improve the drugs oral bioavailability and clinical efficacy.

1.12 Strategy to overcome poor oral bioavailability and food effect

There are many strategies that may be employed to improve drug absorption and bioavailability including chemical modification (e.g. cyclodextrine inclusion) and drug formulation using colloidal drug delivery systems (e.g. self-emulsifying drug delivery systems). For this study Pheroid™ technology was used to enhance the bioavailability of LF. Pheroid™ technology is a patented, novel fatty-acid based drug delivery system that may enhance drug bioavailability and therapeutic efficacy (Grobler *et al.*, 2008). With the use of Pheroid™ based formulation, we may improve the solubility and subsequently the absorption and bioavailability of LF (du Plessis *et al.*, 2010, Steyn *et al.*, 2011). The formulation may eliminate the ‘food effect’ associated with LF and shorten dosage regimens (White *et al.*, 1999, Ezzet *et al.*, 2000). Pheroid™ technology and its application as a drug delivery system for LF will be discussed in detail in Chapter 3.

Aims

The primary aim of this project is to improve the *in vivo* bioavailability of the antimalarial, LF using novel Pheroid™ drug formulation technology. A further intention is to determine if the Pheroid™ formulated LF eliminates the ‘food effect’ associated with LF and assess *in vitro* and *in vivo* antimalarial efficacy.

Objectives

For the purpose of comparing LF in Pheroid™ formulation to LF in reference formulation (LF dissolved in a DMSO:water (1:9 v/v) solution), pre-clinical antimalarial *in vitro* and *in vivo* assays will be performed.

1. Determine the physicochemical properties of LF using *in silico* (computational) tools.
2. Determine the *in vitro* activity of LF with Pheroid™ formulation as compared to the reference formulation.
3. Develop and validate quantitative methods, using liquid chromatography and tandem mass spectrometry (LC-MS/MS), for the determination of LF in mouse whole blood and plasma.
4. To generate whole blood and plasma concentration-time profiles of LF dissolved in the Pheroid™ formulation, reference solution and canola oil, in a mouse model.
5. Use NONMEM software to generate a population pharmacokinetic (PPK) model and PK parameter estimates, using the bioavailability data.
6. Perform *in vivo* efficacy experiments using Peters’ 4-day test, to compare Pheroid™ formulated LF to the reference formulation at three different dosing concentrations.

References:

1. Abu-Raddad L.J., Patnaik P. and Kublin J.G. Dual infection with HIV and Malaria fuels the spread of both diseases in Sub-Saharan Africa. *Science*, 341 (2006) 1603-1606
2. Anderson T.J.C., Nair S., Nkhoma S., Williams J.T., Imwong M., Yi P., Socheat D., Das D., Chotivanich K., Day N.P.J., White N.J. and Dondorp A.M. High heritability of malaria parasite clearance rate indicates a genetic basis for artemisinin resistance in western Cambodia. *The Journal of Infectious Diseases* 201;9 (2010) 1326-1330
3. Ashley E.A., Stepniewska K., Lindergardh N., Annerberg A., Kham A., Brockman A., Singhasivanon P., White N. and Nosten F. How much fat is necessary to optimize lumefantrine oral bioavailability? *Tropical Medicine and International Health*, 12;2 (2007) 195-200
4. Barnes K.I., Durrheim D.N., Little F., Jackson A., Mehta U., Allen E., Dlamini S.S., Tsoka J., Bredenkamp B., Mtembu D.J., White N.J. and Sharp B.L. Effect of artemether-lumefantrine policy and improved vector control on malaria burden in KwaZulu-Natal, South Africa. *PLOS Medicine*, 2;11 (2005) e330
5. Bathurst I. and Hentschel C. Medicines for Malaria Venture: sustaining antimalarial drug development, a Review. *TRENDS in Parasitology*, 22;7 (2006) 301-307
6. Benedetti M.S., Whomsley R., Poggesi I., Cawello ., Marthy F.X., Delporte M.L., Papeleu P. and Watelet J.B. Drug metabolism and pharmacokinetics. *Drug Metabolism Reviews* 41;3 (2009) 344-390
7. Björkman A. and Phillips-Howard P.A. The epidemiology of drug resistant malaria. *Transactions of the Royal Society of Tropical Medicine and Hygiene* 84;2 (1990) 177-180
8. Black F., Bygbjerg I., Effersoe P., Gromme G., Jepsen S. and Axelgaard Jensen G. Fansidar resistant falciparum malaria acquired in south east Asia. *Transactions of the Royal Society of Tropical Medicine and Hygiene*, 75;5 (1981) 715-716
9. Boland P.B. Drug resistance in malaria. WHO/CDS/CSR/DRS/2001.4 (2001) <http://www.who.int/emc>
10. Borrmann S., Sallas W.M., Machevo S., Gonzalez R., Bjorkman A., Martensson A., Hamel M., Juma E., Peshu J., Ogutu B., Djimede A., D'Alessandro U., Marrest A.C., Lefevre G and Kern S.E. The effect of food consumption on lumefantrine bioavailability in African children receiving artemether-lumefantrine crushed or dispersible tablets (Coartem®) for acute *Plasmodium falciparum* malaria. *Tropical Medicine and International Health*, 15;4 (2010) 434-441
11. Campbell C.C., Collins W.E., Chin W., Teutsch S.M. and Moss D.M. Chloroquine resistant *Plasmodium falciparum* from east Africa: Cultivation and drug sensitivity of the Tanzanian I/CDC strain from American tourist. *The Lancet*, 314;8153 (1979) 1151-1154
12. Chiodini P.L., Bowers K., Jorgensen P., Barnwell J.W., Grady K.K., Luchavez J., Moody A.H., Cenizal A. and Bell D. The heat stability of plasmodium lactate dehydrogenase-based and histidine-rich protein 2-based malaria rapid diagnostic tests. *Royal Society of Tropical Medicine and Hygiene*, 101 (2007) 331-337
13. Davis T.M.E., Karunajeewa H.A., Ilett K.F. Artemisinin-based combination therapies for uncomplicated malaria. *Medical Journal of Australia*, 182; 4 (2005) 181-185
14. Dondorp A.M., Yeung S., White L., Nguon C., Day N.P.J., Socheat D and von Seidlein L. Artemisinin resistance: current status and scenarios for containment. *Nature Reviews* 8 (2010) 272-280

15. Du Plessis L.H., Lubbe J., Strauss T. and Kotze A.F. Enhancement of nasal and intestinal calcitonin delivery by the novel Pheroid™ fatty acid based delivery system, and by *N*-trimethyl chitosan chloride. *International Journal of Pharmaceutics*, 385 (2010) 181-186
16. Duraisingh MT, Roper C, Walliker D, Warhurst DC. Increased sensitivity to the antimalarials mefloquine and artemisinin is conferred by mutations in the *pfmdrl* gene of *Plasmodium falciparum*. *Molecular Microbiology*, 36 (2000) 955-961
17. Ezzet F., Mull R. and Karbwang J. Population pharmacokinetics and therapeutic response of CGP 56697 (artemether+benflumetol) in malaria patients. *British Journal of Clinical Pharmacology*, 46 (1998) 553-561
18. Ezzet F., van Vugt M., Nosten F., Looareesuwan S. and White N.J. Pharmacokinetics and pharmacodynamics of lumefantrine (Benflumetol) in acute falciparum malaria. *Antimicrobial Agents and Chemotherapy*, 44; 3 (2000) 697-704
19. Fogh S., Jepsen S. and Effersoe P. Chloroquine resistant *Plasmodium falciparum* malaria in Kenya. *Transactions of the Royal Society of Tropical Medicine and Hygiene*, 73;2 (1979) 228-229
20. Gallup J.L. and Sachs J.D. The economic burden of malaria. *American Journal of Tropical Medicine and Hygiene* 64 (2001) 85–96.
21. Gomez-Orellana I. Strategies to improve oral drug bioavailability. *Expert Opinion Drug Delivery* 2;3 (2005) 419-433
22. Greenwood B.M., Fidock D.A., Kyle D.E., Kappe S.H.I., Alonso P.L., Collins F.H. and Duffy P.E. Malaria: progress, perils and prospects for eradication. *The Journal of Clinical Investigation*, 118;4 (2008) 1266-1276
23. Grobler A., Kotzé A.F., Du Plessis J. The design of a skin-friendly carrier for cosmetic compounds using Pheroid™ technology. In: Wiechers, J. (Ed.), *Science and Applications of Skin Delivery Systems*. Allured Publishing Corporation (2008)
24. Guerin P.J., Olliaro P., Nosten F., Druilhe P., Laxminarayan R., Binka F., Kilama W.L., Ford N. and White N.J. Malaria: current status of control, diagnosis, treatment and a proposed agenda for research and development. *The Lancet*, 2 (2002) 564-573
25. Gupta S., Snow R.W., Donnelly C.A., Marsh K. and Newbold C. Immunity to non-cerebral severe malaria is acquired after one or two infections. *Nature Medicine*, 5;3 (1999) 340-343
26. Harinasuta T., Suntharasamai P. and Viravan C. Chloroquine resistant falciparum malaria in Thailand. *The Lancet*, 286; 7414 (1965) 657-660
27. Hoffman S.L., Campbell C.C. and White N.J. Malaria (Chapter 96), In: *Tropical Infectious Diseases: Principles, Pathogens and Practice*. Guerrant R.L., Walker D.H. and Weller P.F. 3rd Edition, Elsevier (2010) 646-670
28. Holding P.A. and Snow R.W. Impact of *Plasmodium falciparum* malaria on performance and learning: review of the evidence. *American Journal of Tropical Medicine and Hygiene*, 64 (2001) 68–75
29. Hyde J.E. Drug resistant malaria. Review in *TRENDS in Parasitology*, 21;11 (2005) 494-498
30. Kerns E.H. and Di L. *Drug-like Properties: Concepts, Structure Design and Methods*. (2008) Elsevier.
31. Krogstad D.J., Gluzman I.Y., Kyle D.E., Oduola A.M.J., Martin S.K., Milhous W.K. and Schlesinger P.H. Efflux of Chloroquine from *Plasmodium falciparum*: Mechanism of chloroquine resistance. *Science*, 238;4831 (1987) 1283-1285
32. Krotoski W.A., Collins W.E., Bray R.S., Garnham P.C.C., Cogswell F.B., Gwadz R.W., Killick-Kendrick R., Wolf R., Sinden R., Koontz L.C. and Stanfill P.S. Demonstration of hypnozoites in sporozoites-transmitted *Plasmodium vivax* infection. *American Journal of Tropical Medicine and Hygiene*, 31;6 (1982) 1291-1293

33. Lindergardh N., Annerberg A., Blessborn D., Bergqvist Y., Day N., White N.J. Development and validation of a bioanalytical method using automated solid-phase extraction and LC-UV for the simultaneous determination of lumefantrine and its desbutyl metabolite in plasma. *Journal of Pharmaceutical and Biomedical Analysis*, 37 (2005) 1081-1088
34. Luxemburger C., Nosten F., Kyle D.E., Kiricharoen L., Chongsuphajaisiddhi T., White N.J. Clinical features cannot predict a diagnosis of malaria or differentiate the infecting species in children living in an area of low transmission. *Transactions of the Royal Society of Tropical Medicine and Hygiene*, 92 (1998) 45–49.
35. Malaney P., Spielman A. and Sachs J. The malaria gap. *American Journal of Tropical Medicine and Hygiene*, 71;2 (2004) 141-146
36. Martin R.E., Marchetti R.V., Cowan A.I., Howitt S.M., Broer S. and Kirk K. Chloroquine transport via the malaria parasite's chloroquine resistance transporter. *Science*, 325 (2009) 1680-1682
37. Mita T., Tanabe K. and Kita K. Spread and evolution of *Plasmodium falciparum* drug resistance. *Parasitology International*, 58 (2009) 201-209
38. Nabarro D.N. and Tayler E.M. The “Roll Back Malaria” campaign. *Science*, 280;5372 (1998) 2067-2068
39. Natarajan K, Townes TM, Kutlar A. Chapter 48. Disorders of Hemoglobin Structure: Sick Cell Anemia and Related Abnormalities. In: Williams Hematology. 8th Edition. Prchal JT, Kaushansky K, Lichtman MA, Kipps TJ, Seligsohn U, eds. New York: McGraw-Hill (2010) <http://www.accessmedicine.com/content.aspx?aID=6130552>
40. Nosten F., Phillips-Howard P.A. and ter Kuile F. Other 4-Methanolquinolines, Amyl Alcohols and Phentathrenes: Mefloquine, Lumefantrine and Halofantrine. In: *Staines H.M. and Krishna S. Treatment and Prevention of Malaria; antimalarial drug chemistry, action and use*. 3rd Edition, Springer-Basel (2012) 95-111
41. Petersen I., Eastman R. and Lanzer M. Drug-resistant malaria: Molecular mechanisms and implications for public health, A Review. *FEBS Letters*, 585 (2011) 1551-1562
42. Piola P., Fogg C., Bajunirwe F., Biraro S., Grandesso F., Ruzagira E., Babigumira J., Kigozi I., Kiguli J., Kyomuhendo J., Ferradini L., Taylor W., Checchi F. and Guthmann J.P. Supervised versus unsupervised intake of six-dose artemether-lumefantrine for treatment of acute, uncomplicated *Plasmodium falciparum* malaria in Mbarara, Uganda: a randomized trial. *The Lancet*, 365 (2005) 1467-1473
43. Premji Z.G., Abdulla S., Ogutu B., Ndong A., Falade C.O., Sagara I., Mulure N., Nwaiwu O and Kokwaro G. The content of African diets is adequate to achieve optimal efficacy with fixed-dose artemether-lumefantrine: a review of the evidence. *Malaria Journal*, 7;244 (2008)
44. Price RN, Uhlemann AC, Brockman A, et al. Mefloquine resistance in *Plasmodium falciparum* and increased pfmdrl gene copy number. *Lancet*, 364 (2004) 438-447.
45. Price R.N., Uhlemann A.C., van Vugt M., Brockman A., Hutagalung R., Nair S., Nash D., Singhasivanon P., Anderson T.J.C., Krishna S., White N.J. and Nosten F. Molecular and pharmacological determinants of the therapeutic response to artemether-lumefantrine in multidrug-resistant *Plasmodium falciparum* malaria. *Clinical Infectious Diseases*, 42 (2006) 1570-1577
46. Prusty, S. K. R. and Das, B. S. Low incidence of the severe complications of malaria and absence of malaria-specific mortality, in Tensa, Sundergarh district, Orissa State, India, an area hyper-endemic for malaria. *Annals of Tropical Medicine and Parasitology*, 95 (2001) 133–140
47. Ratcliff A., Siswantor A., Kenangalem E., Manstela R., Wuwung R.M., Laihad F., Ebsworth E.P., Anstey N.M., Tjitra E. and Price R.N. Two fixed-dose artemisinin combinations for

- drug-resistant falciparum and vivax malaria in Papuo, Indonesia, an open-label randomized comparison. *The Lancet*, 369 (2007) 757-765
48. Richie T.L. and Saul A. Progress and challenges for malaria vaccines- Insight Review Articles. *Nature*, 415 (2002) 694-701
 49. Serouri A.W., Grantham-McGregor S.M., Greenwood B., Costello A. Impact of asymptomatic malaria parasitaemia on cognitive function and school achievement of schoolchildren in the Yemen Republic. *Parasitology*, 121 (2000) 337–345.
 50. Singh B.N. Effects of food on clinical pharmacokinetics. *Clinical Pharmacokinetics*, 37;3 (1999) 213-255
 51. Smith D.A., van der Waterbeemd H., Walker D.K., Mannhold R., Kubinyi H. and Timmerman H. *Pharmacokinetics and Metabolism in Drug Design*. Wiley (2001)
 52. Snow, R. W., Omumbo J.A., Lowe B., Molyneux C.S., Obiero J.O., Palmer A., Weber M.W., Pinder M., Nahlen B., Obonyo C., Newbold C., Gupta S. and Marsh K. Relation between severe malaria morbidity in children and level of *Plasmodium falciparum* transmission in Africa. *Lancet*, 349 (1997) 1650–1654
 53. Snow R.W., Guerra C.A., Noor A.M., Myint H.Y. and Hay S.I. The global distribution of clinical episodes of *Plasmodium falciparum* malaria. *Nature*, 434 (2005) 214-217
 54. Steyn D.W., Wiesner L., du Plessis L.H., Grobler A.F., Smith P.J., Chan W.C., Haynes R.K. and Kotze A.F. Absorption of the novel artemisinin derivatives artemisone and artemiside: Potential application of Pheroid™ technology. *International Journal of Pharmaceutics*, 414 (2011) 260-266
 55. Stohrer J.M., Dittrich S., Thongpaseuth V., Vanisaveth V., Phetsouvanh R., Phompida S., Monti F., Christophel E.M., Lindergardh N., Annerberg A. and Jelinek T. Therapeutic efficacy of artemether-lumefantrine and artesunate-mefloquine for the treatment of uncomplicated *Plasmodium falciparum* malaria in Luang Namtha Province, Lao People's Democratic Republic. *Tropical medicine and International Health*, 9;11 (2004) 1175-1183
 56. Tshefu AK, Gaye O, Kayentao K, et al. (2010). Efficacy and safety of a fixed-dose oral combination of pyronaridine-artesunate compared with artemether-lumefantrine in children and adults with uncomplicated *Plasmodium falciparum* malaria: a randomised non-inferiority trial. *Lancet* 375 (9724): 1457–1467.
 57. Wernsdorfer W.H., Landgraf B., Kilimal V.A. and Wernsdorfer G. Activity of benflumetol and its enantiomers in fresh isolates of *Plasmodium falciparum* from East Africa. *Acta Tropica*, 70 (1998) 9-15
 58. Wernsdorfer W.H. Coartemether (artemether and lumefantrine): an oral antimalarial drug. *Expert Review Anti-Infective Therapies*, 2 (2004) 181-196
 59. White N.J. Delaying antimalarial drug resistance with combination chemotherapy. *Parasitologia* 41(1999), 301-308
 60. White N.J. and Olliaro P.L. Strategies for the prevention of antimalarial drug resistance: rationale for combination therapy for malaria. *Parasitology Today*, 12 (1996) 399-401
 61. White N.J., van Vugt M. and Ezzet F. Clinical pharmacokinetics and pharmacodynamics of artemether-lumefantrine. *Clinical Pharmacokinetics*, 37;2 (1999) 105-125
 62. White N.J. How antimalarial drug resistance affects post-treatment prophylaxis. *Malaria Journal*, 7;8 (2008)
 63. WHO; Global report on antimalarial drug efficacy and drug resistance:2000-2010
 64. WHO; Antimalarial combination therapy (2001)
 65. WHO. World Malaria Report (2011). <http://www.who.int>
 66. WHO. Guidelines for the treatment of malaria, 2nd edition (2011) <http://www.who.int/malaria/publications/atoz/9789241547925/en/index.html>

67. WHO, Malaria fact sheet (2012) <http://www.who.int/mediacentre/factsheets>
68. WHO. Global Malaria Programme. (2012) <http://www.who.int>
69. WHO. Malaria control: the power of integrated action. <http://www.who.int>
70. Wilairatana P., Krudsood S., Treeprasertsuk S., Chalermrut K. and Looareesuwan S. The future outlook of antimalarial drugs and recent work on the treatment of malaria. Archives of Medical Research, 33 (2001) 416-421
71. Winstanley P.A., Ward S.A. and Snow R.W. Clinical status and implications of antimalarial drug resistance. Microbes and Infection, 4 (2002) 157-164
72. Wongsrichanalai C., Pickard A.L., Wernsdorfer W.H. and Meshnick S. Epidemiology of drug-resistant malaria. The Lancet Infectious Diseases 2 (2002) 209-218
73. Zeng M-Y., Lu Z-L., Yang S-C., Zhang M., Liao J., Liu S-L. and Teng X-H. Determination of benflumetol in human plasma by reversed-phase high-performance liquid chromatography with ultraviolet detection. Journal of Chromatography B, 681 (1996) 299-306
74. Zishiri V.K., Hunter R., Smith P.J., Taylor D., Summers R., Kirk K., Martin R.E. and Egan T.J. A series of structurally simple chloroquine chemosensitizing dibemethin derivatives that inhibit chloroquine transport by PfCRT. European Journal of Medicinal Chemistry, 46 (2011) 1729-1742

Chapter 2

Computational Predictive Models: Using *in silico* tools to predict the physicochemical properties of lumefantrine

2.1 Introduction

Drug discovery and development is a time consuming and costly process, thus efficient experimental testing is undertaken to minimize the risk of drug failure. A flow diagram illustrating the physiological and physicochemical factors that may influence a drugs oral bioavailability and pharmacokinetics is shown in Figure 2.1.

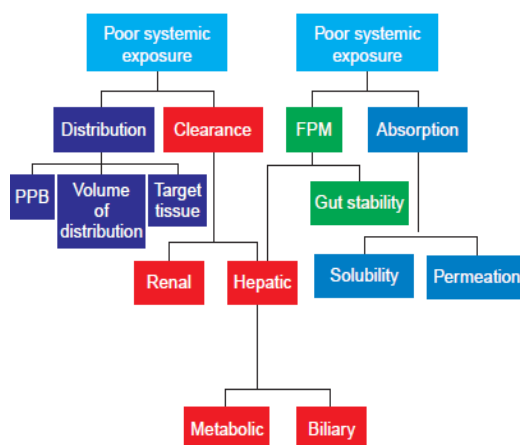


Figure 2.1: A flow diagram detailing the pharmacokinetic parameters that are influenced by poor drug bioavailability. The diagram is colour coded with processes involved in drug absorption being coloured blue, distribution: dark blue, metabolism: green and elimination: red. Abbreviations: FPM, first pass metabolism; PPB, plasma protein binding (Figure adapted from Eddershaw *et al.*, 2000)

Clinical pharmacokinetics involves all the factors that determine or influence the variability in systemic drug concentration. Clearance is a PK parameter that describes the volume of plasma that is cleared of drug per unit time. The rate of drug elimination is proportional to the systemic drug concentration for drugs following first order kinetics. The liver (site of drug metabolism) and kidneys (elimination of unchanged drug) are predominantly responsible for drug clearance. Volume of distribution represents the volume into which the drug appears to be distributed after administration. Once distributed in the blood, drugs may bind (reversibly) to plasma proteins and this may be of importance as only unbound drug is able to act on receptors, confer activity and be eliminated. Plasma drug concentration is therefore

influenced by the rate of drug administration, the volume into which it distributes and its clearance (Makoid *et al.*, 1999, Eddershaw *et al.*, 2000).

It has been estimated that 43% of drug compounds fail during phase III studies and a further 23% fail at registration (Kola, 2008). The paradigm shift in drug discovery and development, to prevent late stage drug failures, involves high-throughput screening of new drug compounds prior to *in vivo* testing for early information on absorption, distribution, metabolism, excretion and toxicity (ADMET) (van der Waterbeemd & Gifford, 2003). Computational predictive tools may be incorporated to streamline the drug development process by relating chemical structure to ADME/PK behaviour. 'Poor pharmacokinetics' is the major underlying cause of compound failure in drug development programmes. A drug with poor PK may be described as having low or variable bioavailability which may result in inefficient activity (Eddershaw *et al.*, 2000). The most common factors responsible for drug development failure are presented in Figure 2.2, the implementation of early PK drug screening resulted in a decrease of drug development failure due to poor PK/bioavailability from 40% to less than 10% over the ten year period 1991-2000 (Kola & Landis, 2004).

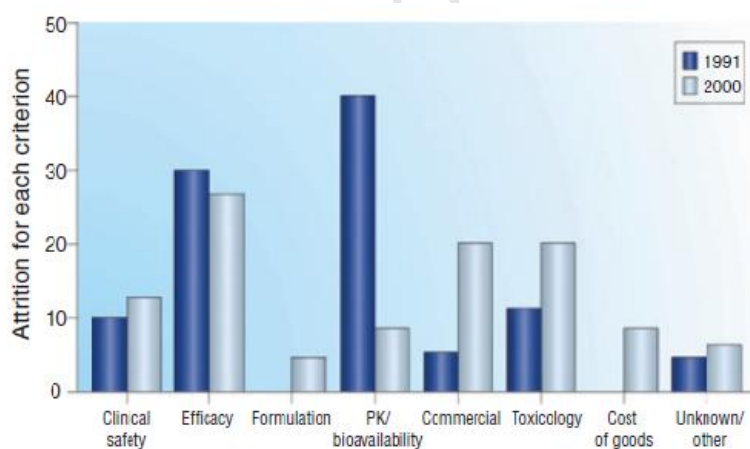


Figure 2.2: A representative graph depicting the causative factors for, and their contribution to, drug compound failure. (Kola & Landis, 2004)

In silico (computational) tools can be used to accelerate and optimize drug discovery and development by predicting ADMET and physicochemical data based on a compound's molecular structure. This information is valuable as the physicochemical properties of a compound may provide relevant insight regarding its pharmacokinetics and efficacy. For the purpose of this study, it is hypothesized that the improvement of LF solubility will improve

its bioavailability and antimalarial efficacy, *in silico* predictions were used to confirm the poor aqueous solubility of LF and corroborate the *in vivo* experimental results.

2.1.1 Physicochemical factors influencing drug bioavailability

Lipophilicity

The lipophilicity of a compound is defined as its intrinsic affinity for a lipidic as opposed to a aqueous environment and is measured by determining the compounds distribution behaviour in a biphasic system i.e. 1-octanol/water (Smith *et al.*, 2001). Lipophilicity, for a neutral compound, is represented by the partition coefficient (LogP). For compounds that are ionisable, lipophilicity is pH dependant and is represented by the distribution coefficient (LogD). The acid-base ionization constant (pKa) of a compound indicates its ionisability at a particular pH. Figure 2.3 details the inter-relationship between the ionization properties of a drug and its lipophilicity, the ionized form of a drug compound is more soluble in the aqueous phase and the unionized form more readily partitions into the lipid phase (biological membrane). Thus, LogP may be described as the log of the partition coefficient of a compound, in neutral (unionized) form, in a biphasic system. LogD may be described as the log of the distribution coefficient of a compound (ionized and unionized) in a biphasic system at a specific pH (Kerns & Di, 2008).

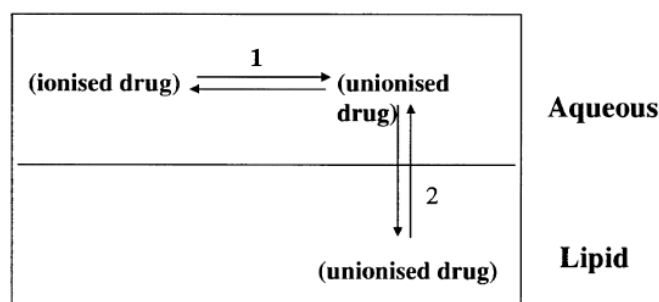


Figure 2.3: A schematic describing the relationship between pKa, LogP and LogD. 1: the equilibrium is a function of acid/base strength (pKa) and 2: the equilibrium is a function of the compounds lipophilicity (LogP). (Smith *et al.*, 2001)

Lipophilicity is an important physicochemical property that influences the pharmacokinetics of an orally administered drug compound. As presented in Figure 2.4, a LogP value between zero and three is considered optimal for permeation of biological membranes (Kerns & Di, 2008).

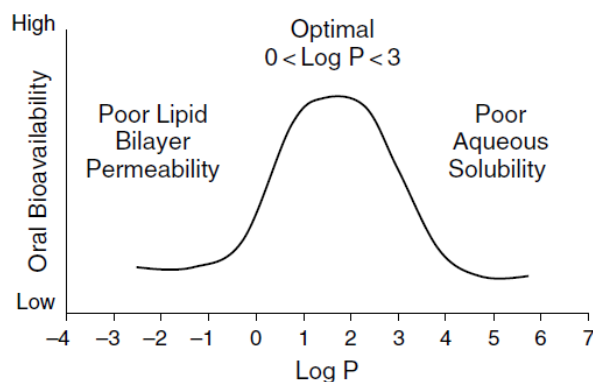


Figure 2.4: A hypothetical depiction of how lipophilicity can affect the efficient absorption of a drug compound (Kerns & Di, 2008).

Solubility and Permeability

Once a drug is orally administered it dissolves in the predominantly aqueous contents of the GI tract prior to absorption across the intestinal membrane (IM) and entry into the blood circulation. The dissolution of the compound in the GI tract and its ability to permeate the IM has a direct effect on its oral bioavailability. Figure 2.5 illustrates the processes that may influence the transport of a drug to the systemic blood circulation after oral administration.

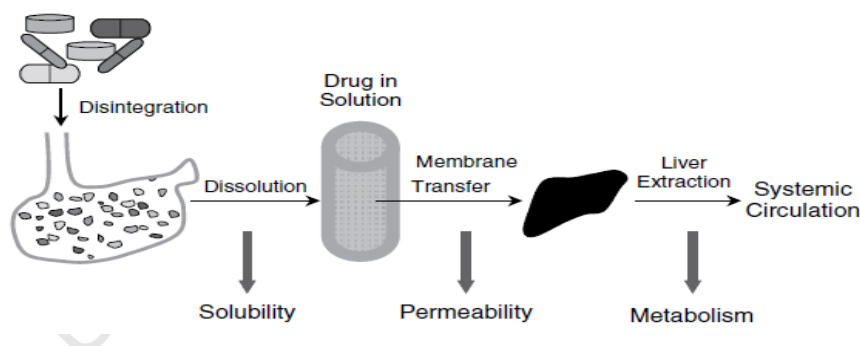


Figure 2.5: Solubility, permeability and metabolism may influence the systemic bioavailability of an orally administered drug (Kerns & Di, 2008).

The speed at which the solid compound dissolves in a solvent is referred to as the dissolution rate (Smith *et al.*, 2001). Solubility of a compound may be described as the degree to which it dissolves, and the maximum concentration attained, in a specific solvent. Permeability describes the ability of the dissolved drug to traverse across a biological membrane as illustrated in Figure 2.6. The solubility and permeability for an orally administered drug are variable and influenced by the physicochemical and structural properties of the drug as well as the physiological conditions (eg. pH) of the GI tract. The degree of ionization (pKa) of a

compound also affects its absorption, as ionized compounds are more soluble than neutral compounds in aqueous medium. However the structural attributes of a compound that favour solubility in an aqueous environment often reduces permeability. Biological membranes are composed of phospholipid molecules, polar head groups and non-polar side chains, that self-assemble forming a lipid bilayer as depicted in Figure 2.6. Lipophilic, neutral compounds permeate more readily than polar molecules as they pass easily through the lipid bilayer membrane.

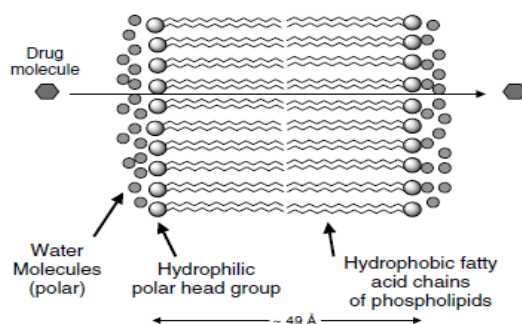


Figure 2.6: Diagram showing passive diffusion of a drug molecule through a biological membrane (Kerns & Di, 2008).

Aim

The aim of the investigation was to determine the physicochemical properties of LF that may influence its oral bioavailability.

Objectives

To predict the lipophilicity (LogP, LogD and pKa), solubility and permeability of lumefantrine using *in silico* tools; Volsurf+[®] and MoKa[®].

2.2 Experimental

There is an interconnection between the molecular structure of a compound and its inherent physicochemical properties (lipophilicity, solubility and permeability.). The surface properties (electrostatic forces, hydrophobicity, potential hydrogen bonding, etc.) of a molecule can be used to calculate potential interaction sites around the molecule thereby producing a 3D molecular interaction field (MIF). *In silico* tools such as Volsurf+[®] and MoKa[®] (available on <http://www.moldiscovery.com>) apply statistical/mathematical algorithms using 3D MIFs to predict physicochemical as well as ADME parameters of compounds (Cruciani *et al.*, 2000). The incorporated computational models were generated from experimental data obtained for a wide range of structurally diverse compounds, referred to as a training set, for ADME predictions (Bohets *et al.*, 2001).

The Volsurf+[®] software was used to predict the lipophilicity (LogP and LogD) of LF and to qualitatively assess its aqueous solubility and permeability (Caco-2 cells). To generate partial least-squares projection (PLS) t-t plots, LF was projected onto in-built solubility (Soly) and Caco-2 models. Caco-2 cells are well-differentiated intestinal cells derived from human colorectal carcinoma and are used for *in vitro* drug absorption assays to assess permeability (Guangli & Yiyu, 2006). Studies have demonstrated a relation between human oral drug absorption and Caco-2 permeability, thus proving it a valuable model for assessing permeability (Stenberg *et al.*, 2001). The Volsurf+[®] software has been used, successfully, for the accurate prediction of Caco-2 permeability of new compounds (Cruciani *et al.*, 2000).

MoKa[®] incorporates a quantitative structure-property relationship (QSPR) pKa prediction method that describes the molecular structure around an ionisable centre using topological distances and it consists of a model based on a training set of over 26 000 unique pKa values (Cruciani *et al.*, 2000, Milletti *et al.*, 2007). The software suite was used to predict the pKa values and ionization pattern (shows the relative abundant ionized species at various pH values) for LF.

2.3 Results

The *in silico* analysis of LF was performed under the direction and supervision of Dr Grace Magumbate, Medicinal Chemistry Research group, UCT.

Lipophilicity

The predicted LogP, LogD and pKa values for LF are detailed in Table 2.1. LF is highly lipophilic as indicated by the reported LogP value for LF (with artemether) which was 8.81 (Kassim *et al.*, 2003), and the predicted value using Volsurf +[®] was 9.

Table 2.1: *in silico* predicted lipophilicity values for LF

LogP	9
LogD at:	
Blood (pH 7.4)	8.74
Intestine (pH 6.5)	5.13
Stomach (pH 3.5)	7.8
pKa values	8.3 and 14.9

The ionization pattern of LF as predicted using MoKa[®] details the species (ionized or neutral) of LF present at any specific pH (Figure 2.7). LF is a weak base with two ionisable sites (shown by red circles); the most abundant ionized form present at physiological pH (7.4) is shown in Figure 2.7.

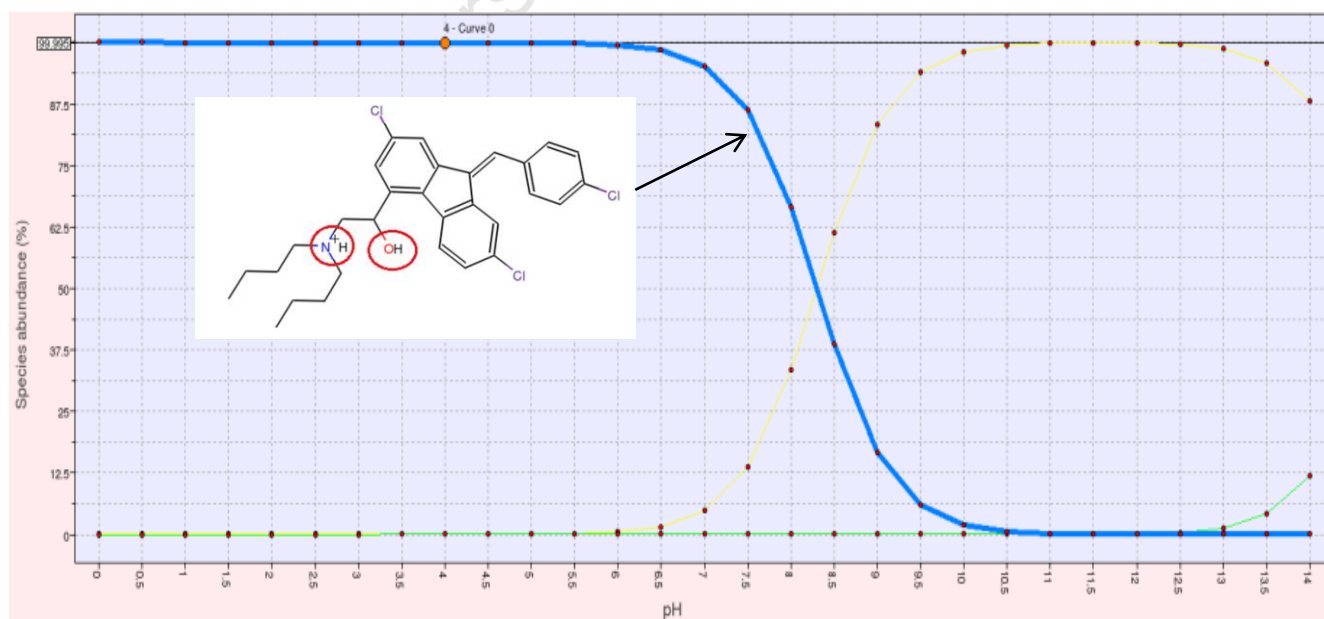


Figure 2.7: Ionization pattern of LF as predicted using MoKa[®]. The structure of the dominant ionized species of LF at physiological pH (pH 7.4) is illustrated on the graph.

Solubility and Permeability

A qualitative assessment of LF and CQ was performed using the Volsurf+[®] software to predict the solubility and membrane permeability. CQ, considered to be the ‘gold standard’ antimalarial for *in vitro* assays, was used as a reference drug. The generated PLS t-t score solubility and permeability plots are shown in Figures 2.8 and 2.9. The pink and blue regions indicate poor and high property regions respectively, and the solid and broken circles show 99% and 95% confidence levels respectively. The black dots are the training set molecules. In both cases, CQ was predicted to have moderate solubility and good permeability. However the solubility of the highly lipophilic LF is very poor hence it appears in the poor solubility region (pink) and outside the 95% confidence level (Figure 2.8). LF was predicted to have good permeability; it is positioned in the blue region of the Caco-2 model generated using Volsurf+[®] (Figure 2.9).

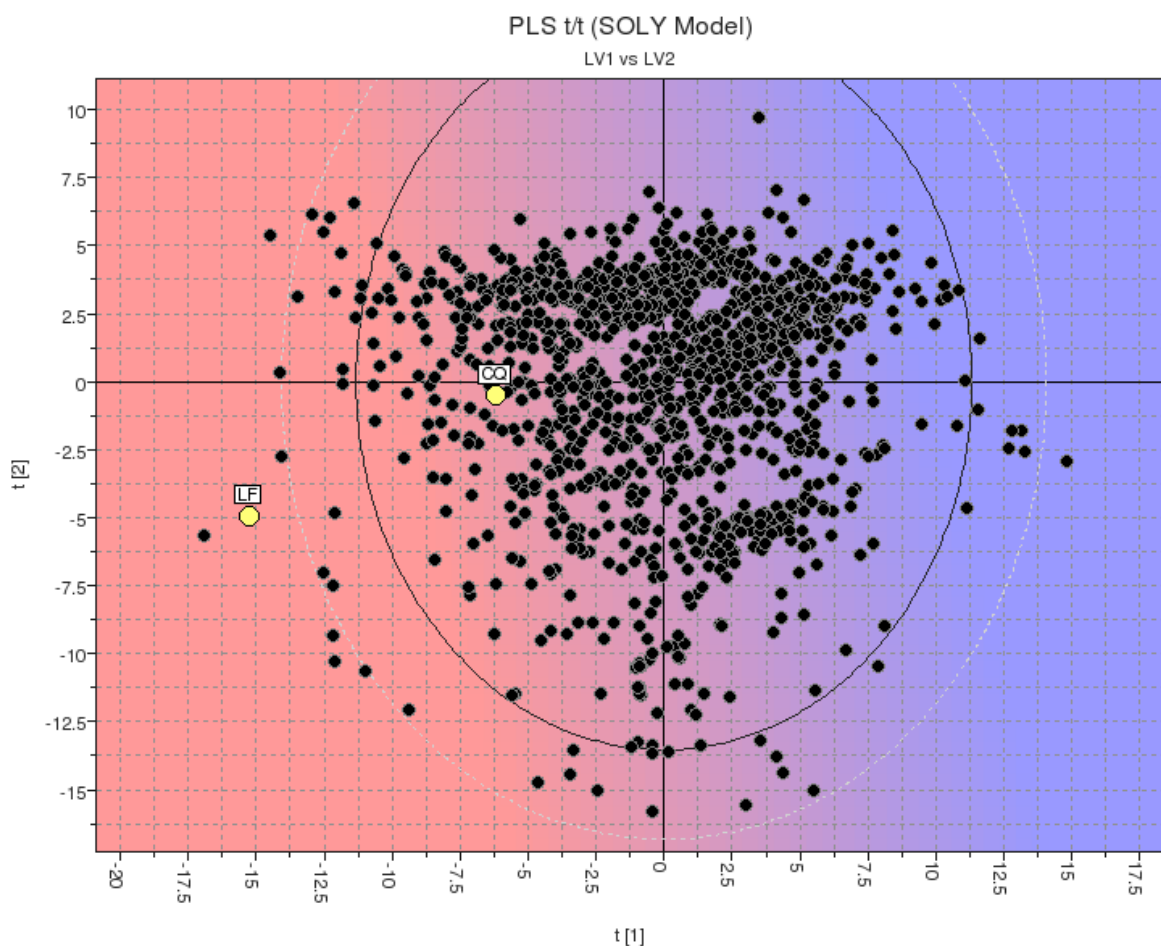


Figure 2.8: Partial Least Square (PLS) t-t score plots for solubility model for LF. Black dots represent the library of known compounds comprising the models data set. Yellow dots represent labelled, LF and CQ. The blue section indicates; good and the pink section poor solubility.

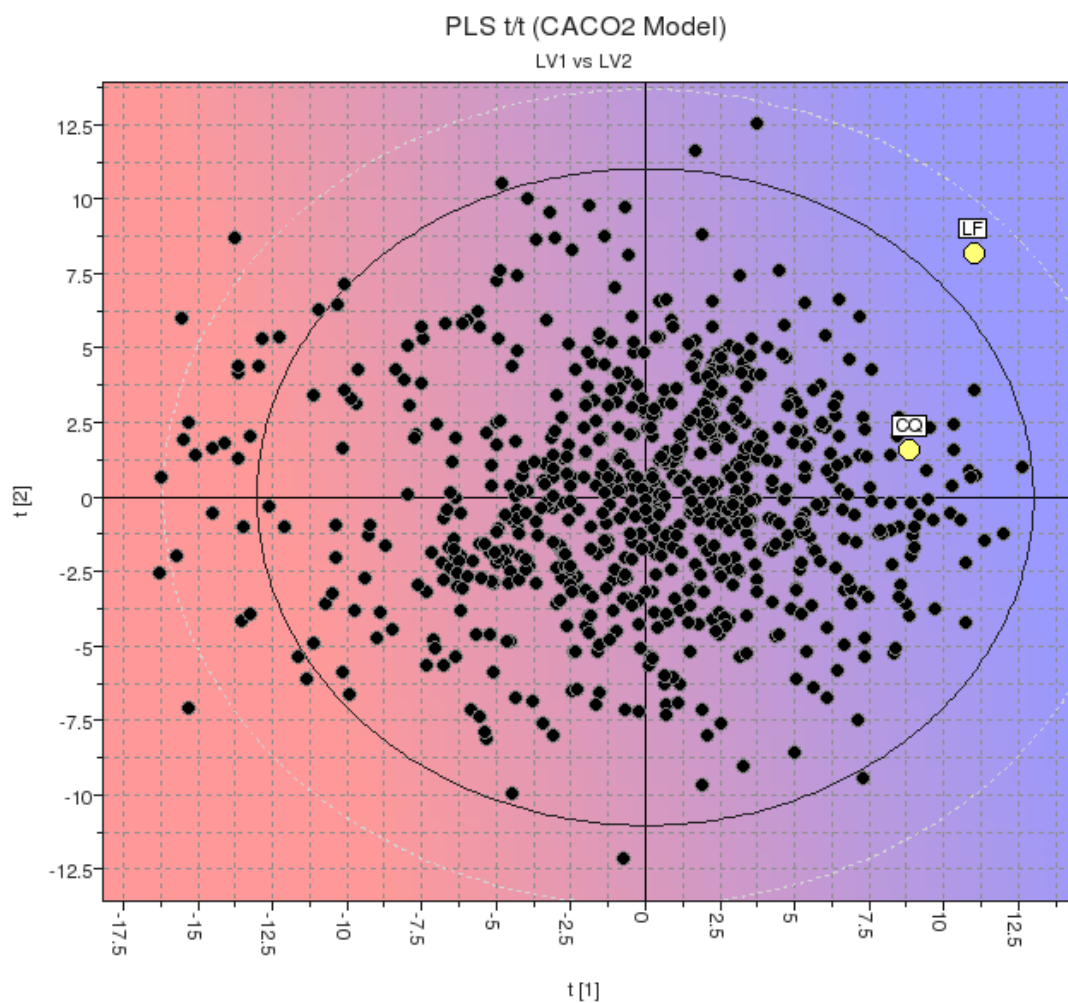


Figure 2.9: Partial Least Squares (PLS) t-t score plots for Caco-2 permeability model for LF. Black dots represent the library of known compounds comprising the models data set. Yellow dots represent projected LF and CQ molecules. The blue section indicates; good and the pink section poor membrane permeability.

2.4 Discussion

For the purpose of this project, the *in silico* tools were used to predict the physicochemical properties of LF that may explain its poor and variable oral absorption. Good absorption is dependent on the orally administered drug dissolving in the gastrointestinal tract, traversing the intestinal epithelium and entering the blood stream (Bohets *et al.*, 2001). As a result drug compounds with low solubility and permeability may have poor absorption, variable bioavailability and lack of efficacy (Kerns and Di, 2008).

The pKa values for LF (8.3 and 14.9) as predicted using MoKa[®], is comparable to the reported values of 8.71 and 13.4, calculated using Advanced Chemistry Development Software V11.02 (Debrus *et al.*, 2011). LF is predicted to be predominantly ionized at physiological pH (Figure 2.7), LF is also described as a weak base and thus ionized in acid environments like the GI tract and effective absorption may therefore be hindered as unionized drugs traverse lipid membranes more efficiently than ionized drugs.

The qualitative assessment of LF using the *in silico* tools predicted that LF has relatively low solubility and good Caco-2 cell permeability. Kassim *et al.* reported the LogP value for LF (with artemether) as 8.81 obtained using ChemDraw Ultra 6.0 (Kassim *et al.*, 2003). Huang *et al.* reported a LogP value of 8.67 and a LogD_{pH7} value of 7 for LF, calculated using Advanced Chemistry Development Software V11.02 (Huang *et al.*, 2012). Debrus *et al.* used the same software as Huang *et al.* and also reported a LogP value of 8.67 for LF. The LogP value predicted for LF using Volsurf+[®] was 9 and LogD_{pH7.4} was 8.74, which appears to be comparable to published results. According to Lipinski's 'rule of 5', a LogP value of less than 5 is considered ideal for good oral drug absorption and permeability (Lipinski *et al.*, 1997). LF's high LogP value indicating poor aqueous solubility may therefore be a contributing factor to its poor absorption and unpredictable oral bioavailability. The predicted LogD values for LF at pH 7.4 (blood pH) is above five. Compounds having Log D values greater than five are postulated to have poor GI absorption and bioavailability due to insolubility (Kerns & Di, 2008). Permeability, volume of distribution and elimination half-life is predicted to be high as these compounds partition into tissues, therefore less bioavailable (Kerns & Di, 2008). In a pharmacokinetic study performed in rats LF displayed low clearance and a large volume of distribution resulting in a long terminal elimination half-life (Wahajuddin *et al.*, 2011). Clinical studies have reported LF to display variable absorption and bioavailability (Ezzet *et al.*, 2000; White *et al.*, 1999).

For correlating *in vitro* drug dissolution and *in vivo* bioavailability, compounds are categorized using the Biopharmaceutics Classification System (BCS). The BCS, provided by the United States Food and Drug Administration (FDA), classifies drugs according to their absorption potential in the GI tract (Amidon *et al.*, 1995). With reference to Figure 2.10, Lindenberg *et al.* categorised Coartem[®] as a Class II or Class IV drug, however the classification was made using inconclusive solubility and permeability data (Lindenberg *et al.*, 2004).

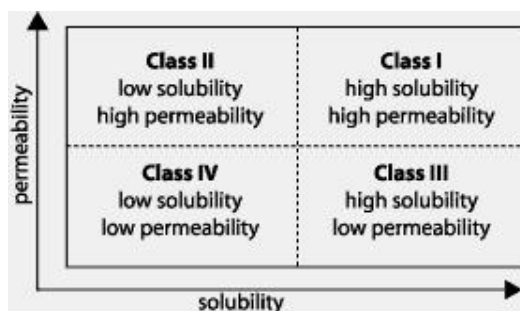


Figure 2.10: Description of the Biopharmaceutics Classification System (BCS) Class categories.

Class II compounds have low solubility and high permeability, indicating poor/slow drug dissolution but good absorption across the intestinal membrane. Class IV drug compounds have low solubility and low permeability indicating poor absorption as well as variable bioavailability (Amidon *et al.*, 1995, Lindenberg *et al.*, 2004). In a review by Kassim *et al.*, the co-formulated artemether and lumefantrine was grouped in the BCS Class I category (Kassim *et al.*, 2003). BCS Class I drugs have high solubility and high permeability which indicates good absorption. An *in-situ* permeability study of LF in rats demonstrated that LF had greater permeability than metoprolol (USFDA approved high permeability marker) (Wahajuddin *et al.*, 2011). According to the BCS, Coartem[®] (Artemether and Lumefantrine) could not be assigned to a specific class due to conflicting or insufficient solubility/permeability data. Considering the literature, categorizing a co-formulated drug such as Coartem[®] would be difficult and vary from one scientific investigation to the next due to the different physicochemical properties of each individual drug. Considering the predictions generated in this investigation of LF, one may conclude that the compound has low solubility and good permeability and therefore comparable to the BCS Class II category however LF is ionized in acidic environments which may contribute to its poor absorption in the GI tract and therefore, LF may be more appropriately classified as a BCS Class IV drug.

The computational predictions of LF with respect to its lipophilicity, low aqueous solubility and good membrane permeability are comparable to reported experimental findings. It is well documented that LF is highly lipophilic and has variable oral bioavailability; which is a result of poor dissolution and erratic absorption in the GI tract (White *et al.*, 1999, Ezzet *et al.*, 2000). Formulation strategies that may be utilised to address the poor aqueous solubility of LF will be discussed in the following chapter.

University of Cape Town

References

1. Amidon G.L., Lennernas H., Shah V.P. and Crison J.R. The theoretical basis for the biopharmaceutic drug classification: the correlation of *in vitro* drug product dissolution and *in vivo* bioavailability. *Pharmaceutical Research*, 12:3 (1995) 413-420
2. Benedetti M.S., Whomsley R., Poggesi I., Cawello W., Mathy F.X., Delporte M.L., Papeleu P. and Watelet J.B. Drug metabolism and pharmacokinetics. *Drug Metabolism Reviews*, 41:3 (2009) 344-390
3. Bohets H., Annaert P., Mannens G., van Beijsterveldt L., Anciaux K., Verboven P., Meuldermans W. and Lavrijsen K. Strategies for absorption screening in drug discovery and development. *Current Topics in Medicinal Chemistry*, (2001) 367-383
4. Cruciani G., Milletti F., Storch L., Sfona G. and Goracci L. In silico pKa prediction and ADME profiling. *Chemistry and Biodiversity*, 6 (2009) 1812-1821
5. Cruciani G., Pastor M. and Guba W. Volsurf: a new tool for the pharmacokinetic optimization of lead compounds. *European Journal of Pharmaceutical Sciences*, 11:2 (2000) S29-S39
6. Debrus B., Lebrun P., Kidenge J.M., Lecomte F., Ceccato A., Caliaro G., Mbay J.M.T., Baulanger B., Marini R.D., Rozet E and Hubert Ph. Innovative high-performance liquid chromatography method development for the screening of 19 antimalarial drugs based on a generic approach, using design of experiments, independent component analysis and design space. *Journal of Chromatography A*, 1218 (2011) 5205-5215
7. Eddershaw P.J., Beresford A.P. and Bayliss M.K. ADME/PK as part of a rational approach to drug discovery, A Review. *Drug Discovery Today*, 5:9 (2000) 409-414
8. Ezzet F., van Vugt M., Nosten F., Looareesuwan S and White N.J. Pharmacokinetics and pharmacodynamics of lumefantrine in acute falciparum malaria. *Antimicrobial Agents and Chemotherapy*, 44:3 (2000) 697-704
9. Guangli M. and Yiyu C. Predicting Caco-2 permeability using support vector machine and chemistry development kit. *Journal of Pharmacy and Pharmaceutical Sciences*, 9:2 (2006) 210-221
10. Huang L., Li X., Marzan F., Lizak P.S. and Aweeka F.T. Determination of lumefantrine in small-volume human plasma by LC-MS/MS: using a deuterated lumefantrine to overcome matrix effect and ionization saturation. *Bioanalysis*, 4:2 (2012) 157-166
11. Kassim N.A., Whitehouse M., Ramachandran C., Bermejo M., Lennernas H., Hussain A.S., Junginger H.E., Stavchansky S.A., Midha K.K., Shah V.P. and Amidon G.L. Molecular properties of WHO essential drugs and provisional biopharmaceutic classification. *Molecular Pharmaceutics*, 1:1 (2003) 85-96
12. Kerns E.K. and Di L. Drug-like properties: Concepts, structure, design and methods. In: *ADME to toxicity optimization* (2008) 1st Edition, Academic Press/Elsevier
13. Kola I. The state of innovation in drug development. *Clinical Pharmacology and Therapeutics*, 83:2 (2008) 227-230
14. Kola I. and Landis J. Can the pharmaceutical industry reduce attrition rates? *Nature Reviews Drug Discovery*, 3 (2004) 711-715
15. Lindenberg M., Kopp S. and Dressman J.B. Classification of orally administered drugs on the World Health Organization Model list of Essential Medicines according to the Biopharmaceutics classification system. Review article in *European Journal of Pharmaceutics and Biopharmaceutics*, 8 (2004) 265-278

16. Lipinski C.A., Lombardo F., Dominy B.W. and Feeney P.J. Experimental and computational approaches to estimate solubility and permeability in drug discovery and development settings. *Advanced Drug Delivery Reviews*, 23 (1997) 3-25
17. Makoid M.C., Vuchetich P.J. and Banakar U.V. Bioavailability, bioequivalence and drug selection in *Basic Pharmacokinetics*, 1st Edition (1999) <http://kiwi.creighton.edu/pkinbook/>
18. Milletti F., Storchi L., Sforza G. and Cruciani G. New and original pK_a prediction method using grid molecular interaction fields. *Journal of Chemical Information and Modeling*, 47 (2007) 2172-2181
19. Smith D.A., van de Waterbeemd H., Walker D.K., Mannhold R., Kubiyni H. and Timmerman H. *Pharmacokinetics and Metabolism in Drug Design* (2001) Wiley
20. Stenberg P., Norinder U., Luthman K and Artursson P. Experimental and computational screening models for the prediction of intestinal drug absorption. *Journal of Medicinal Chemistry*, 44 (2001) 1927-1937
21. White N.J., van Vugt M. and Ezzet F. Clinical pharmacokinetics and pharmacodynamics of artemether-lumefantrine. Drug disposition, *Clinical Pharmacokinetics*, 37;2 (1999) 105-125
22. Wahajuddin, Singh S.P., Raju K.S.R., Nafis A., Puri S.K. and Jain G.K. Intravenous pharmacokinetics, oral bioavailability, dose proportionality and in situ permeability of anti-malarial lumefantrine in rats. *Malaria Journal* (2011) www.malariajournal.com/content/10/1/293
23. van de Waterbeemd H and Gifford E. ADMET *in silico* modelling: Towards predicting paradise? *Nature Reviews*, 2 (2003) 192-204

Chapter 3

Drug formulation of lumefantrine using Pheroid™ technology

3.1. Introduction: Drug formulation and delivery systems

Malaria is an infective disease that affects some of the poorest countries in the world, with the majority of malaria endemic areas located in Africa. Most of the drugs that form part of modern day antimalarial treatment regimens have been in circulation for decades. One such antimalarial is LF, which has poor aqueous solubility, variable bioavailability and is considered to have poor ‘drug like’ properties. The efficacy of conventional antimalarial chemotherapy is threatened by the development of drug resistance, poor socio-economic conditions and patient compliance. Using drug formulation to improve and/or enhance existing antimalarial chemotherapy is a cost-effective and feasible strategy in eradicating malaria (Bagwe *et al.*, 2001).

The discovery and development of novel compounds is a time consuming and expensive process and many potential drugs are rejected due to poor oral bioavailability, toxicity or lack of efficacy. A drug delivery system (DDS) may be defined as a formulation or device that may improve a drug’s therapeutic efficacy, safety and tolerability by facilitating its passage from administration to the target site (Jain, 2008). A suitable drug delivery system may serve as a ‘rescue’ for drugs with poor ‘drug like’ properties and improve the number of drug compounds that reach clinical trials. Drug delivery systems may also increase the longevity and improve the pharmacokinetics of well-established drugs like LF.

An ideal DDS should be composed of biocompatible and/or biodegradable constituents that have the ability to easily entrap or adsorb a drug compound. The DDS should protect the entrapped drug from physical, chemical and enzymatic degradation before it reaches the target site; this is of particular importance for drugs administered via oral route. The DDS should be pliable and modifiable with regards to size, shape and functionality. It should lack immunogenicity and be able to traverse cell membranes. The production and manufacturing process of the drug and carrier (DDS) formulation should be cost-effective, consistent and reproducible (Jain, 2008). Pheroid™ technology is a patented novel colloidal drug delivery system that was used in this research study and will be discussed in detail.

3.2 Colloidal drug delivery systems

Colloidal drug delivery systems include liposomes, emulsions and lipid or polymer based nanoparticles. A colloidal system refers to chemical systems that consist of a continuous phase or medium (e.g. water) in which small particles (colloids), typically sized 1-1000 nm, and are dispersed forming an emulsion or suspension. The advantages of using colloidal carriers as DDSs include; optimising oral drug administration, decreasing toxicity, protecting the drug from extracellular degradation, assisting selective transport across cell membranes, drug targeting and improving drug pharmacokinetics as well as efficacy (Bagwa *et al.*, 2001, Grobler *et al.*, 2008). Liposomes, emulsions and nano-particulate drug delivery systems as well as examples of their application in the treatment of malaria will be subsequently discussed.

3.2.1. Liposomes

Liposomes as carriers may be used to entrap hydrophilic and hydrophobic drugs. These lipid molecules arrange into vesicles, in an aqueous solution and range in size from 25 nm to 50 nm (Grobler *et al.*, 2008, Jain 2008). As presented in Figure 3.1, they are composed of phospholipids, other amphipathic lipids and cholesterol arranged in one or more lipid bi-layers separated by aqueous compartments (Grobler *et al.*, 2008). Liposomes may be modified with respect to lipid composition, size, surface charge and method of preparation (Jain 2008).

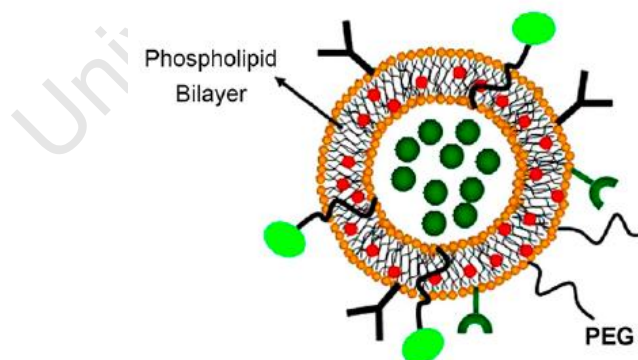


Figure 3.1: A representative example of a surface modified liposome encapsulating hydrophilic drugs in the aqueous interior and hydrophobic drugs in the lipid bi-layer (picture sourced from Fahmy *et al.*, 2007).

Studies performed using a murine model, demonstrated that liposome encapsulated β -artemether, administered intravenously, was effective for the treatment of recrudescence

malaria (Chimanuka *et al.*, 2002, Date *et al.*, 2007). Liposomes also allow for surface modification and attachments of ligands (Grobler *et al.*, 2008, Date *et al.*, 2007). In a study done by Postma *et al.*, liposome bound recombinant human tumour necrosis factor (rhTNF α), administered intravenously, was found to suppress parasitemia and protect against induced experimental cerebral malaria in mice (Postma *et al.*, 1999, Date *et al.*, 2007). However liposomes are not stable in the GI tract and require optimization of liposome composition and surface modification to effectively deliver drugs via oral administration (Woodley, 1985).

3.2.2. Emulsions and Microemulsions

Emulsions consist of two or more immiscible, typically, liquid phases (oil and water) and a surfactant and are used to solubilize hydrophobic drugs (Grobler *et al.*, 2008). As shown in Figure 3.2, the droplets that assemble spontaneously may form water-in-oil or oil-in-water emulsions and are generally $\geq 1\ \mu\text{m}$ in size. Emulsions are optically turbid dispersions and may separate, over time, to form a two-phase system however microemulsions are optically isotropic and thermodynamically stable (Bagwe *et al.*, 2001, Lawrence & Rees, 2000). The droplet sizes of a microemulsion range from 20 to 200 nm. Microemulsions require surfactants (lecithin, sodium palmitate, Tween80, cremophore EL) as well as co-surfactants (ethanol, glycerol and PEG) to stabilize the interfacial area and maintain droplet formation (Gelderblom *et al.*, 2001). Self-microemulsifying drug delivery system (SMEDDS) is a type of emulsion, consisting of an oil component and surfactant, used to improve the oral bioavailability of hydrophobic drugs. The SMEDDS formulation is transformed into an oil-in-water microemulsion in GI fluids after *in vivo* oral administration (Mandawgade *et al.*, 2008, Gursoy & Benita, 2001). Large amounts of hydrophobic and hydrophilic drugs may be solubilized using microemulsions allowing for improved drug absorption after oral administration, improved efficacy and minimized toxicity (Bagwe *et al.*, 2001).

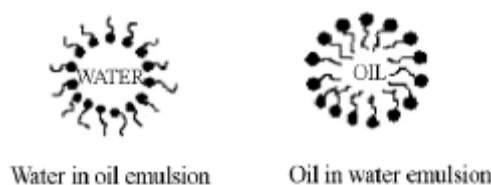


Figure 3.2: A representation of a (micro)emulsion; a system of oil, water and surfactant (picture sourced from Sahoo *et al.*, 2008).

Primaquine (PQ) is the only antimalarial used to eradicate asexual hepatic stages and latent tissue forms (in liver) of *P. vivax* and *P. ovale*. A study done by Dierling *et al.*, prepared an artificial chylomicron emulsion incorporating PQ to enhance the uptake and accumulation of PQ in mouse liver for treatment of resurgent *P. vivax* malaria. The incorporation of PQ into the emulsion significantly enhanced its accumulation in the mouse liver and prevented enzymatic degradation *in vivo* (Dierling & Cui, 2005).

3.2.3. Nanoparticles

Nanoparticulate delivery systems encompass solid lipid nanoparticles (SLN), lipid drug conjugates (LDCs), nanosuspensions, dendrimers, nanocapsules, inorganic and polymeric nanocapsules (Date *et al.*, 2007). Nanoparticles are composed of biodegradable polymers such as polylactides (PLAs) as well as natural polymers such as albumin and chitosan. These carrier particles range in size from 1 to 1000 nm, an active pharmaceutical ingredient (API) may be entrapped, adsorbed or covalently attached to the particle, as shown in Figure 3.3. The miniscule size of these drug carriers allow for efficient transport across biological membranes and delivery to target sites. Nanoparticles are biologically stable and suitable for drug delivery using oral administration (Date *et al.*, 2007).

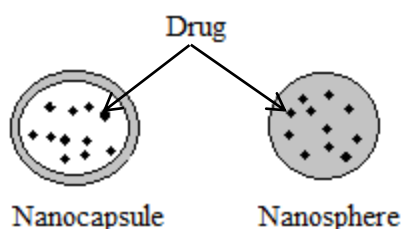


Figure 3.3: A representation of a nanoparticle, drugs compounds may be encapsulated in a nanocapsule or attached to the surface to the nanoparticle creating a nanosphere.

Mosqueira *et al.* prepared PLA nanocapsules (NCs) containing the antimalarial halofantrine (HF) and assessed the improved efficacy in mice infected with *Plasmodium berghei*. PLA nanocapsules containing HF with surface attached polyethylene glycol (PEG) was also prepared. PEG may enhance the circulation life span of the NCs, and other drug carriers, as it functions to prevent interactions with plasma proteins and hinder enzymatic degradation (Mosqueira *et al.*, 2004). The NCs loaded with HF reduced the parasite development more rapidly when compared to the prepared HF intravenous solution. The NCs containing PEG

had a more sustained effect *in vivo*. The study concluded that using the NCs as a carrier also reduced the toxicity of HF.

3.3 Pheroid™ technology

Pheroid™ technology originated from Emzaloid™ technology which was a product initially used for the treatment of psoriasis, formulated by MeyerZall Laboratories. It was discovered that the Emzaloid™ formulation contained micro and nano-sized vesicles that could entrap the active component (coal tar for psoriasis). Further research proved that the vesicles could be used to entrap active drug compounds as well as assist its delivery to the target site. The intellectual property of Emzaloid™ technology was purchased by the North West University, South Africa from MeyerZall (Pty) (ltd) in 2003 where, after further development, the term Pheroid™ was coined. The Pheroid™ formulation differs from Emzaloid™ with respect to the constituent components of the formulation as well as the manufacturing processes (Grobler *et al.*, 2008).

Pheroid™ technology can be described as a colloidal drug delivery system that contains stable lipid-based vesicular structures called Pheroids™. These Pheroid™ vesicles range in size from 200-400 nm and have porous membranes. Like liposomes, Pheroids™ contain a lipid bi-layer but do not contain phospholipid or cholesterol. Pheroid™ vesicles form by a self-assembly process and are dispersed within a dispersion medium, similar to microemulsions. The morphology, structure, size and function of the Pheroid™ vesicles may be modified specifically for the active drug compound of interest as well as the intended route of administration (Grobler *et al.*, 2008).

3.3.1 Pheroid™ composition and molecular organisation

Pheroid™ formulations consist of ethylated and PEGylated polyunsaturated fatty acids in the cis-configuration including Omega 3 and 6 fatty acids but excluding arachidonic, oleic, linoleic and linolenic fatty acids. Like other drug colloidal carriers, Pheroids™ are composed of biocompatible constituents. Pheroids™ also contain vitamin E (tocopherol) which serves as an anti-oxidant and PEG which has been shown to contribute to extending the circulating life of the drug formulation (Grobler *et al.*, 2008).

The Pheroid™ consists of an oil, water and gas phase. Nitrous oxide (N₂O) gas is water and fat soluble and is dispersed within the oil and water phases, adding another dimension to the basic Pheroid™ formulation. The N₂O gas is a unique component of the system and has been

shown to contribute to the self-assembly process and the physical stability of the Pheroids™ as well as to facilitate the formation of a homogeneous solution. Due to its unique inter-dispersed phases the Pheroid™ delivery system is able to entrap and transport hydrophobic and hydrophilic drugs to target sites (Grobler *et al.*, 2008).

3.3.2. Pro-Pheroid™

Different types of Pheroid™ formulations such as lipid-bilayer vesicles, Pheroid™ microsponges and Pro-Pheroids™ may be prepared by varying the composition or ratio of the fatty acids and manufacturing method. Pro-Pheroid™ formulation differs from a Pheroid™ formulation as it contains no water phase as shown in Figure 3.4.

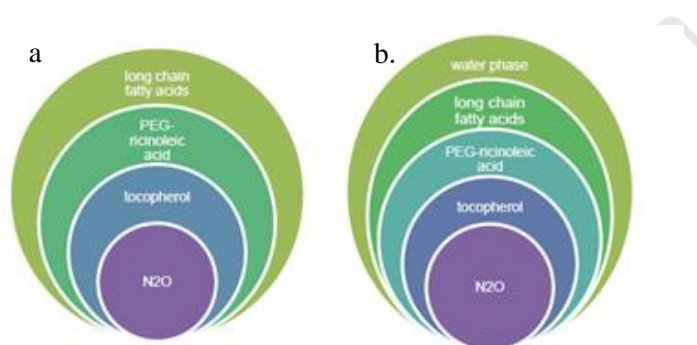


Figure 3.4: An illustration of the constituent components of a) Pro-Pheroid™ and b) Pheroid™ (figure sourced from Grobler *et al.*, 2008)

The Pro-Pheroid™ consists of an oil based liquid phase with an interdispersed gas phase. The APIs suspended in a Pro-Pheroid™ formulation may be included into Pheroid™ vesicles upon the addition of water or aqueous medium. A Pro-Pheroid™ formulation may be likened to a SMEDDS formulation as it is hypothesized that the Pheroid™ vesicles spontaneously form in aqueous GI fluids after *in vivo* oral administration (Grobler *et al.*, 2008).

Confocal laser scanning microscopy (CLSM) is used to visualize the Pheroids™ and determine the structural characteristics and morphology of the particles. Confocal microscopy is a technique used for high-resolution three dimensional imaging of fluorescently labelled biological samples, as shown in Figure 3.5; the Pheroid™ is labelled with the fluorophore Nile red, allowing for the visualisation of the Pro-Pheroid™ with entrapped drug (Paddock, 1999).

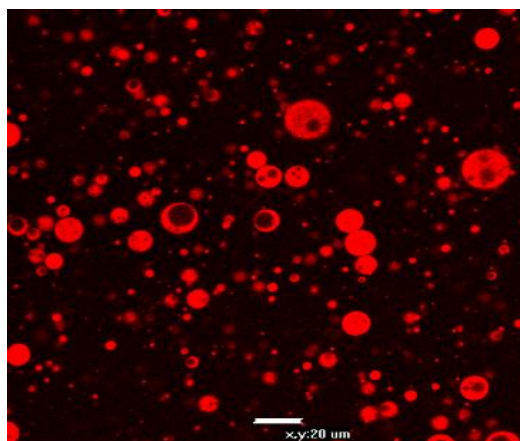


Figure 3.5: A representative confocal laser scanning micrograph of Pheroid™ vesicles (red) of submicron size with entrapped drug (dark spots). *Image obtained from a spectrophotometric method report for lumefantrine, courtesy of Dr.Lissinda du Plessis, North-West University.*

CLSM is used for the qualitative control monitoring of manufactured Pheroid™ formulations. CLSM is also used to determine the entrapment efficacy of drug in Pheroid™ formulations. The size, charge, solubility and concentration of the drug or API influences the amount of molecules entrapped within the Pheroids™. Pheroid™ formulations are reproducible and have an entrapment efficacy of 85-100% with all compounds tested (Grobler *et al.*, 2008).

3.3.3. Applications of Pheroid™ technology

Pheroid™ technology has been used for various applications to enhance or improve existing and novel drug therapy. The application of Pheroid™ technology to enhance the oral absorption of novel artemisinin derivatives, for the treatment of malaria, was investigated by Steyn *et al.* and the concentration of artemisone in blood was reported to be 4.57 times higher when the drug was entrapped in the Pheroid™ vesicles as compared to artemisone in reference (aqueous) formulation (Steyn *et al.*, 2011). Pheroid™ technology has also been successfully used for nasal peptide delivery, transdermal drug delivery and cosmetic applications (Saunders *et al.*, 1999, Grobler *et al.*, 2008, Gerber *et al.*, 2008, du Plessis *et al.*, 2009).

Literature Review

One scientific publication was found, detailing the use of drug formulation to enhance the antimalarial efficacy of LF. Gahoi *et al.* prepared a LF nanopowder using a wet milling DYNO MILL technique to improve drug dissolution rate and therapeutic efficacy. Wet milling is a nanonization technique used to mechanically reduce drug particle size thereby generating nano-sized drug crystals. LF was first dispersed uniformly in an aqueous medium containing dispersing agents (HPMC E3, PVP and Tween 80), these components are used to facilitate reduction in particle size, before being milled for 6 hours with 0.4-0.6 mm yttrium-stabilized zirconium beads. Unmilled LF was found to have a particle size of 75.24 μm and the mean particle size of the LF nanopowder was 0.251 μm . It was reported that the nano-sized LF had an enhanced dissolution rate compared to unmilled LF. *In vitro* antimalarial activity was assayed using a chloroquine (CQ) sensitive *P. falciparum* 3D7 strain, the IC_{50} value of nano-sized LF was 0.1 ng/ml which was considerably lower than the IC_{50} for unmilled LF and CQ which was 17.5 ng/ml and 4.2 ng/ml respectively. The *in vivo* antimalarial experiment was performed in mice inoculated with *P. Yeolii nigeriensis* (rodent malaria parasite). The drug was tested at three different dose concentrations; 60, 30 and 15 mg/kg and the mice were monitored for 28 days. The test groups that received the LF nanopowder had a mean survival time (MST) of ≥ 28 days at all examined dose strengths and the groups that received the unmilled LF had a MST of ≥ 28 days at the 60 and 30 mg/kg dose and a MST of 23.8 days at the 15 mg/kg dose (Gahoi *et al.*, 2012). The results of the study demonstrated the efficiency of wet milling using DYNO MILL to produce stable LF nanopowder. The LF nanopowder enhanced *in vitro* antimalarial efficacy however bioavailability studies need to be performed to gain greater insight into the pharmacokinetics of this drug formulation (Gahoi *et al.*, 2012).

Aim and Objective

For this 'proof of concept' study LF was entrapped in a Pro-PheroidTM formulation, to evaluate an improvement in *in vitro* efficacy and *in vivo* bioavailability and efficacy, compared to a reference formulation. The LF in Pro-PheroidTM used in this study was a preliminary formulation that may be optimized for further investigation. The *in vitro* and *in vivo* bioavailability experiments will be detailed in Chapters 4, 6 and 7.

References

1. Bagwe R.P., Kanicky J.R., Palla B.J., Patanjali P.K. and Shah D.O. Improved drug delivery using microemulsions: Rationale, recent progress and new horizons. *Critical Reviews in Therapeutic Drug Carrier Systems*, 18;1 (2001) 77-140
2. Chimanuka B., Gabriels M., Detaevernier M.R. and Plaizier-Vercammen J.A. Preparation of β -artemether liposomes, their HPLC-UV evaluation and relevance for clearing recrudescence parasitemia in *Plasmodium chabaudi* malaria-infected mice. *Journal of Pharmaceutical and Biomedical Analysis*, 28 (2002) 13-22
3. Date A.A., Joshi M.D. and Patravale V.B. Parasitic diseases: Liposomes and polymeric nanoparticles versus lipid nanoparticles. *Advanced Drug Delivery Reviews*, 59 (2007) 505-521
4. Du Plessis L.H., Lubbe J. and Kotze A.F. Enhancement of nasal and intestinal calcitonin delivery by the novel Pheroid™ fatty acid based delivery system, and by N-trimethyl chitosan chloride. *International Journal of Pharmaceutics* (2009)
5. Dierling A.M. and Cui Z. Targeting primaquine into the liver using chylomicron emulsions for the potential *vivax* malaria therapy. *International Journal of Pharmaceutics*, 303 (2005) 143-152
6. Fahmy T.M., Fong P.M., Park J., Constable T. and Saltzman W.M. Nanosystems for the simultaneous imaging and drug delivery to T cells. *The AAPS Journal*, 9;2 (2007) E171-E180
7. Gahoi S., Jain G.K., Tripathi R., Pandey S.K., Anwar M., Warsi M.H., Singhal M., Khar R.K. and Ahmad F.J. Enhanced antimalarial activity of lumefantrine nanopowder prepared by wet-milling DYNO MILL technique. *Colloids and Surfaces B: Biointerfaces* (2012)
8. Gelderblom H., Verweij J., Nooter K. and Sparreboom A. Cremophor EL: the drawbacks and advantages of vehicle selection for drug formulation. *European Journal of Cancer*, 37 (2001) 1590-1598
9. Gerber M., Breytenbach J.C. and du Plessis J. Transdermal penetration of zalcitabine, lamivudine and synthesized N-acyl lamivudine esters. *International Journal of Pharmaceutics*, 351 (2008) 186-193
10. Gursoy R.N. and Benita S. Self-emulsifying drug delivery systems (SEDDS) for improved oral delivery of lipophilic drugs. *Biomedicine and Pharmacotherapy*, 58 (2004) 173-182
11. Grobler A.F., Kotze A. and du Plessis J. The design of a skin-friendly carrier for cosmetic compounds using Pheroid™ technology. In: Wiechers J. (Ed.) *Science and Applications of Skin Delivery Systems*. Allured Publishing Corporation, Wheaton, IL (2008)
12. Jain K.K. (Ed.) *Drug Delivery Systems*, In: *Methods in Molecular Biology*, 437 (2008) Humana Press, Totowa, NJ
13. Lawrence M.J. and Rees G.D. Microemulsion-based media as a novel drug delivery system. *Advanced Drug Delivery Reviews*, 45 (2000) 89-121
14. Mandawgade S.D., Shobhona S., Pathak S. and Partavale V.B. Development of SMEDDS using natural lipophile: Application to β -artemether delivery. *International Journal of Pharmaceutics*, 362 (2008) 179-183
15. Muller R.H. and Keck C.M. Challenges and solutions for the delivery of biotech drugs- a review of drug nanocrystal technology and lipid nanoparticles. *Journal of Biotechnology*; 113 (2004) 151-170
16. Mosqueira V.C.F., Loiseau P.M., Bories C., Legrand P., Devissaguet J.P. and Barrat G. Efficacy and pharmacokinetic study of intravenous nanocapsule formulations of halofantrine in *Plasmodium berghei*-infected mice. *Antimicrobial Agents and Chemotherapy*, 48;4 (2004) 1222-1228
17. Paddock S.W. Confocal laser scanning microscopy. *BioTechniques*, 27 (1999) 992-1004
18. Porter C.J.H., Trevaskis N.L. and Charman W.N. Lipids and lipid-based formulations: optimizing the oral delivery of lipophilic drugs. *Nature Reviews; Drug Discovery*, 6 (2007) 231-248

19. Postma N.S., Crommelin D.J.A., Eling W.M.C and Zuidema J. Treatment with liposome-bound recombinant human tumor necrosis factor- α suppresses parasitemia and protects against *Plasmodium berghei* k173-induced experimental cerebral malaria in mice. *The Journal of Pharmacology and Experimental Therapeutics*, 288;1 (1999) 114-120
20. Pouton C.W. and Porter C.J.H. Formulation of lipid-based delivery systems for oral administration: Materials, methods and strategies. *Advanced Drug Delivery Reviews*, 60 (2008) 625-637
21. Sahoo S.K., Dilnawaz F. and Krishnakumar S. Nanotechnology in ocular drug delivery. *Drug Discovery Today*, 13;3 (2008) 144-151
22. Santos-Magalhães N.S. and Mosqueira V.C.F. Nanotechnology applied to the treatment of malaria. *Advanced Drug Delivery Reviews*, 62 (2010) 560-575
23. Saunders J.C.J., Davis H.J., Coetzee L., Botha S., Kruger A.E. and Grobler A. A novel skin penetration enhancer: elevation by membrane diffusion and confocal microscopy. *Journal of Pharmacy and Pharmaceutical Science*, 2 (1999) 99-107
24. Slabbert C., du Plessis L.H. and Kotze A.F. Evaluation of the physical properties and stability of two lipid drug delivery systems containing mefloquine. *International Journal of Pharmaceutics*, 409 (2011) 209-215
25. Steyn J.D., Wiesner L., du Plessis L.H., Grobler A.F., Smith P.J., Chan W, Haynes R.K and Kotze A. Absorption of the novel artemisinin derivatives artemisone and atremiside: Potential application of Pheroid™ technology. *International Journal of Pharmaceutics*, 414 (2011) 260-266.
26. Wissing S.A., Kayser O. and Muller R.H. Solid lipid nanoparticles for parenteral drug delivery. *Advanced Drug Delivery Reviews*, 56 (2004) 1257-1272
27. Woodley J.F. Liposomes for oral administration of drugs. *Critical Reviews in Therapeutic Drug Carrier Systems*, 2;1 (1985) 1-18

Chapter 4

In vitro antimalarial activity against *P. falciparum*

4.1 Introduction

A typical screening program, as detailed in Figure 4.1, consisting of pre-clinical *in vitro* and *in vivo* assays, was followed for the purpose of comparing the antimalarial activity of the Pheroid™ formulated LF with LF suspended in reference solution (LF in reference formulation). This chapter will elaborate on the antimalarial activity of LF in the two different formulations against a chloroquine sensitive (CQ-S) *P. falciparum* strain using an *in vitro* drug susceptibility assay.

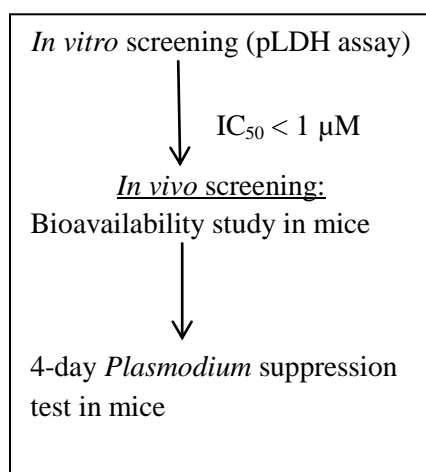


Figure 4.1: An experimental flow diagram for the screening of antimalarial compounds

The activity or effect of the test drug is quantified as inhibition of parasite growth; an IC₅₀ is the concentration of the test drug that inhibits parasite growth by 50%. When screening novel compounds for *in vitro* antimalarial activity, compounds exhibiting an IC₅₀ < 1 μM with equivalent activity against CQ-S and CQ-R strains warrants further development and *in vivo* activity testing (Fidock *et al.*, 2004). Routine *in vitro* antimalarial assays are also performed, using fresh parasite isolates from malaria infected individuals, to monitor the activity of drugs in clinical use and predict the emergence of drug resistant parasites.

Several *in vitro* assays have been developed to measure antimalarial activity against malaria parasites and these may be categorised as isotopic (using radioactive material) or non-isotopic. [³H]-hypoxanthine is an isotopic *in vitro* assay which uses radioactive tritium labelled hypoxanthine that may be incorporated into parasite DNA as the parasite propagates. This assay measures how much an antimalarial drug inhibits parasite growth (drug activity) by quantitating the uptake of [³H]-hypoxanthine using a liquid scintillation spectrometer.

A fluorimetric test is a non-radioactive DNA based assay which uses a fluorescent nucleic acid stain (PicoGreen[®] or Sybr Green) to measure parasite growth and drug activity. Immunoenzymatic assays are also non-isotopic and may utilise monoclonal antibodies specific for parasite lactate dehydrogenase enzyme (pLDH activity is correlated to parasite growth) to quantify drug activity by measuring the inhibition of enzyme activity (Co *et al.* 2010). Another example of an immunoenzymatic antimalarial assay is the highly sensitive enzyme-linked immunosorbant (ELISA) test kits, it allows for the measurement of histidine rich protein 2 (HRP2) which is produced by the parasite as it grows. The Giemsa stained slide method is low cost but not suitable for high throughput *in vitro* antimalarial drug screening. The parasites are incubated with the test compounds and the parasitemia is determined by preparing blood films and counting Giemsa stained parasites using light microscopy (Kalra *et al.*, 2006, Co *et al.*, 2010). The WHO *in vitro* micro test kit consists of plates pre-dosed with antimalarial drug compounds, parasites are added to the plates followed by an incubation period of 24 hours. Thereafter thick blood films are prepared and parasite drug susceptibility is determined microscopically by counting the amount of Giemsa stained parasites that have developed into shizonts (WHO, Mark III test kit instructions, 2001).

The colorimetric pLDH assay was used for quantifying the antimalarial activity of the test formulations in this study. This *in vitro* assay described by Makler *et al.* was developed to detect *P. falciparum* by measuring the enzymatic activity of pLDH in clinical samples. pLDH is differentiated from human red blood cell LDH as it rapidly uses 3-acetyl pyridine NAD (APAD) as a coenzyme in the reaction leading to the formation of pyruvate from lactate. This reaction produces a reduced APAD which in turn reduces tetrazolium (colour changing substrate) forming a blue formazan product that can be measured using a spectrophotometric plate reader (Makler and Hinrichs, 1993).

There are many factors such as initial haematocrit and parasitemia which may influence the *in vitro* drug sensitivity of the parasite and lead to variable results. Using synchronous parasite cultures for the *in vitro* assays ensures more consistent results (Kalra *et al.*, 2006, Co *et al.*, 2010). As detailed in Table 4.1, the IC₅₀ values reported for LF ranges from 1.91 to 90.1 nM. This high variability may be due to the lipophilicity of LF, the type of *in vitro* assay used as well as the strain of *Plasmodium* isolates used.

Table 4.1: Reported *in vitro* activity (IC₅₀ values) for lumefantrine/benflumetol tested using isolates of *P. falciparum*

Author	Year	<i>P. falciparum</i>	Origin	LF IC ₅₀ (nM)	<i>In vitro</i> assay system	Details
Basco <i>et al.</i>	1998	fresh isolates (CQ-S) fresh isolates (CQ-R)	Yaounde, Cameroon	12.4 10.2	isotopic microtest [³ H]hypoxanthine	No significant difference in activity in CQ-S and CQ-R strains
van Vugt <i>et al.</i>	1998	fresh isolates (PI) fresh isolates (RI)	Thailand	54 42	isotopic microtest [³ H]hypoxanthine	Isolates from a primary infection Isolates from recrudescence infection
Wernsdorfer <i>et al.</i>	1998	fresh isolates (CQ-R)	Tanzania	12.4	WHO microtest	No significant difference in activity between LF and respective enantiomers
Hassan-Alin <i>et al.</i>	1999	T-996, multiresistant strain LS-21, CQ-R	Thailand India	2.3 1.91	Giemsa stained thin blood films	Laboratory adapted strains
Pradines <i>et al.</i>	1999	fresh isolates	Senegal	55	isotopic microtest, [³ H]hypoxanthine	
Brockman <i>et al.</i>	2000	fresh isolates (PI) fresh isolates (RI)	Thailand Thailand	61.1 78.5	isotopic microtest [³ H]hypoxanthine	Isolates from a primary infection Isolates from recrudescence infection
Tanariya <i>et al.</i>	2000	fresh isolates (PI) fresh isolates (RI)	Thailand Thailand	18.1 14.9	Giemsa stained thin blood films	Isolates from a primary infection Isolates from recrudescence infection
Denis <i>et al.</i>	2006	fresh isolates (ATR) fresh isolates (LTF)	NW Cambodia NW Cambodia	18.8 28.9	isotopic microtest [³ H]hypoxanthine	Tested using isolates from patients with adequate treatment response and treatment failure
Nkhoma <i>et al.</i>	2007	fresh isolates	Blantyre, Malawi	90.1	WHO microtest	
Starzengruber <i>et al.</i>	2007	fresh isolates	Thailand	27.3	WHO microtest	
Kaddouri <i>et al.</i>	2008	fresh isolates	Bamako, Mali	11.2	(pLDH) ELISA	
Mwai <i>et al.</i>	2009	fresh isolates	Kenya	50	isotopic microtest, [³ H]hypoxanthine	
Wong <i>et al.</i>	2011	3D7 (CQ-S) W2mef (CQ-R)	Laboratory adapted strains	65.2 55.5	isotopic microtest [³ H]hypoxanthine	Laboratory adapted strains

Abbreviations: CQ-S; chloroquine sensitive, CQ-R; chloroquine resistant, PI; primary infection, RI; recrudescence infection, ATR; adequate treatment results, LTF; late treatment failure.

Aim and Objective

To determine and compare the *in vitro* activity (IC₅₀ value) of LF in Pheroid™ formulation and LF in reference formulation against a CQ-S strain of *P. falciparum* using the pLDH assay.

4.2 Materials and Methods

Chemicals & Reagents

Acetonitrile, methanol and water of HPLC grade, LiChrosolv[®] was purchased from Merck (Darmstadt, Germany). Formic acid and Dimethyl sulfoxide (DMSO) was purchased from Merck (Darmstadt, Germany). Acetic acid purchased from Sigma-Aldrich (Germany). N₂O water was supplied by Dr. Lissinda Du Plessis, University of North West (Potchefstroom). Lumefantrine (LF) was donated by Novartis (Basel, Switzerland). Chloroquine diphosphate (CQ) was purchased from Sigma.

Sample preparation for antimalarial assay

LF in 10% DMSO sample (reference)

The reference stock sample of LF was prepared at a concentration of 2 µg/ml in a DMSO:water (1:9 v/v) solution. The sample was mixed using a vortex mixer (Scientific Industries, Vortex Genie 2) and then sonicated for 10 minutes at 100% power and 18°C (Labcon, ultra-sonic). LF dissolved poorly in the reference solution and was tested as a suspension. The 2 µg/ml reference sample was diluted 10-fold using culture medium (CM) to a concentration of 200 ng/ml.

LF in Pro-Pheroid[™] formulation sample (test)

The Pro-Pheroid[™] stock sample of LF was prepared by Dr L. du Plessis (University of North West, Potchefstroom) at a concentration of 5 mg/ml. Due to the high lipid content of the Pro-Pheroid[™] formulation, the samples have a milky appearance which may cause interference with absorption reading and variability in the results. The Pro-Pheroid[™] formulation was diluted, using a drug free Pro-Pheroid[™] solution, for the pLDH assay to ensure accurate results. The diluent; a blank Pro-Pheroid[™] and N₂O water solution was used for dilutions. The test sample was prepared at a concentration of 2 µg/ml. The 2 µg/ml (2000 ng/ml) test sample was then serially diluted 2-fold using diluent, producing ten concentrations ranging from 2000-4 ng/ml. The ten test samples were then further diluted 10-fold, using aseptic technique, with CM resulting in a concentration range of 200-0.4 ng/ml.

Antimalarial *in vitro* assay

The assay was performed by Mrs Sumaya Salie and Ms Ntokozo Dambuza, at the Division of Pharmacology, UCT. Continuous *in vitro* cultures of asexual blood stages of *P. falciparum* were maintained using a modified method described by Trager and Jensen (Trager and Jensen, 1976). Using a modified pLDH assay, the antiplasmodial activity of LF in a reference and Pheroid™ formulation was quantitatively determined as inhibition of parasite growth.

The drug samples were evaluated in triplicate, on two different occasions, against a chloroquine (CQ) sensitive strain of *P. falciparum* (D10). Chloroquine diphosphate was used as the reference control drug in the pLDH assay. The diluent was used as a negative control for the test sample and DMSO:water (1:9 v/v) solution was used as a negative control for the reference sample.. As shown in Figure 4.2, negative (non-infected RBC at 1% hematocrit) and positive (drug-free RBC at 1% parasitemia) assay controls were added in column one and two respectively.

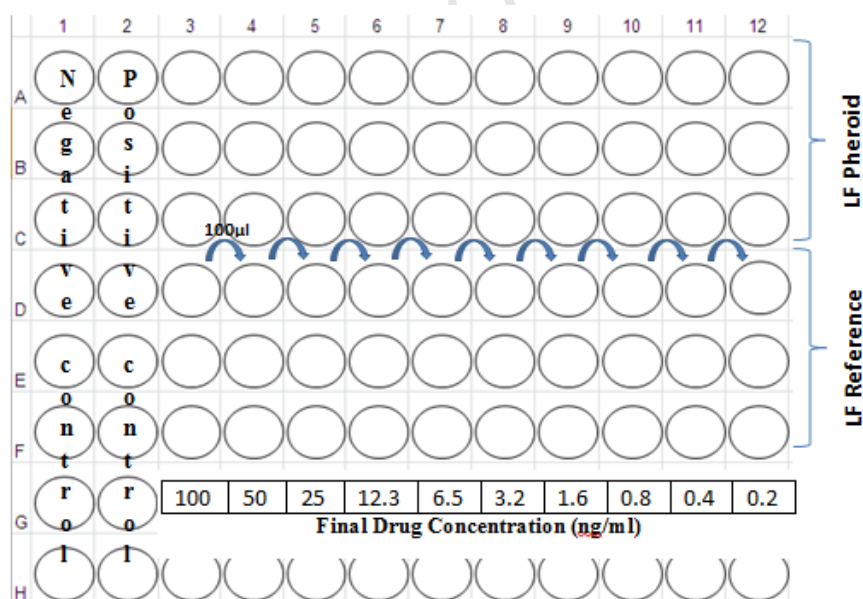


Figure 4.2: A representative 96-well plate detailing the *in vitro* assay sample locations and the final drug concentration range after the addition of RBCs.

As detailed in Figure 4.2, 100µl of the test samples at each concentration was added directly to the wells in columns 3 to 12 in rows A, B and C followed by the addition of 100 µl of parasitized red blood cells. Two hundred microliters of the reference sample was then

transferred to the well in column 3 in rows D, E and F at a starting concentration of 200 ng/ml and thereafter serially diluted 2-fold using CM producing ten concentrations ranging from 200-0.4 ng/ml. The reference samples were then further diluted 2-fold with the addition of 100 μ l parasitized red blood cells yielding a final concentration range of 100-0.2 ng/ml. The same dilution technique was used for the control samples with a total volume of 200 μ l in each well of the 96-well assay plate. All drug samples were tested for their antimalarial activity at ten different concentrations; ranging from 100-0.2 ng/ml to determine the concentration inhibiting 50% of parasite growth.

The assay plates were incubated (Prolab incubator) at 37°C in a gas chamber with a controlled environment of 3% O₂, 4% CO₂ and 93% N₂ for 48 hours. The plates were then removed from the incubator and stored at -20°C until analysis. The plates were thawed, the contents of each well was re-suspended using a pipette and then 15 μ l of the cell suspension was transferred to a corresponding well in a separate plate containing 100 μ l of Malstat reagent (Sigma-Aldrich). The cell suspension and Malstat reagent were mixed thoroughly and air bubbles were removed. Subsequently 25 μ l of nitro blue tetrazolium salt (NBT) (Sigma-Aldrich) was added to each well and the plate was placed in a dark cupboard to develop, the result can be seen in Figure 4.3. Thereafter the absorbance was measured using a Midas microplate reader at 600 nm; the growth in drug-exposed cultures was determined relative to that of positive control.

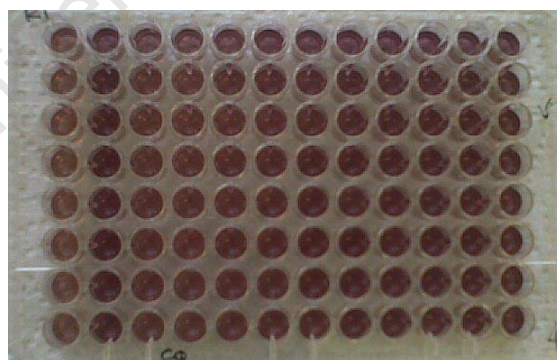


Figure 4.3: A representative 96 well plate after development, the darker the colour in the wells the more parasites have survived the exposed drug concentration.

4.3 Results

The *in vitro* antimalarial assays were performed on two separate occasions and the average calculated IC₅₀ values (average of six replicates) are reported in Table 4.2 below. Using the average IC₅₀ values, LF in the Pheroid™ formulation was 1.87 times more active against the CQ-S *P. falciparum*, D10 strain than LF in the reference formulation.

Table 4.2: Results of *in vitro* drug susceptibility assay against *P. falciparum* D10 strain detailing the average IC₅₀ values for LF in Pheroid™, LF in reference formulation and CQ. Reported IC₅₀ values are the average of two experiments performed in triplicate

Assay	IC ₅₀ (nM)		
	Pheroid™	Reference	CQ
Experiment 1	33.1	73.4	18.5
Experiment 2	21.1	28.4	9.45
Ave.	27.1	50.9	14.0
STDEV	8.5	31.8	6.4
CV (%)	31.3	62.6	45.7

With respect to the calculated CV (%), which is an indication of the precision of the assay, there is less variability in the results when LF is formulated with the Pheroid™ than when dissolved in the reference solution. This may be as result of LF's aqueous insolubility, the reference solution is a mostly aqueous solution and LF did not dissolve appropriately however LF was completely dissolved in the Pheroid™ formulation.

The dose-response curves generated using GraphPad Prism 4.0, for the test formulations and CQ are illustrated in Figures 4.4 to 4.6. These graphs are plotted using the Log concentration values of the test compounds and the corresponding % parasite survival for the purpose of determining IC₅₀ values. In Figure 4.5, the test formulations exhibit variable results which may be as result of the poor solubility of the reference formulation.

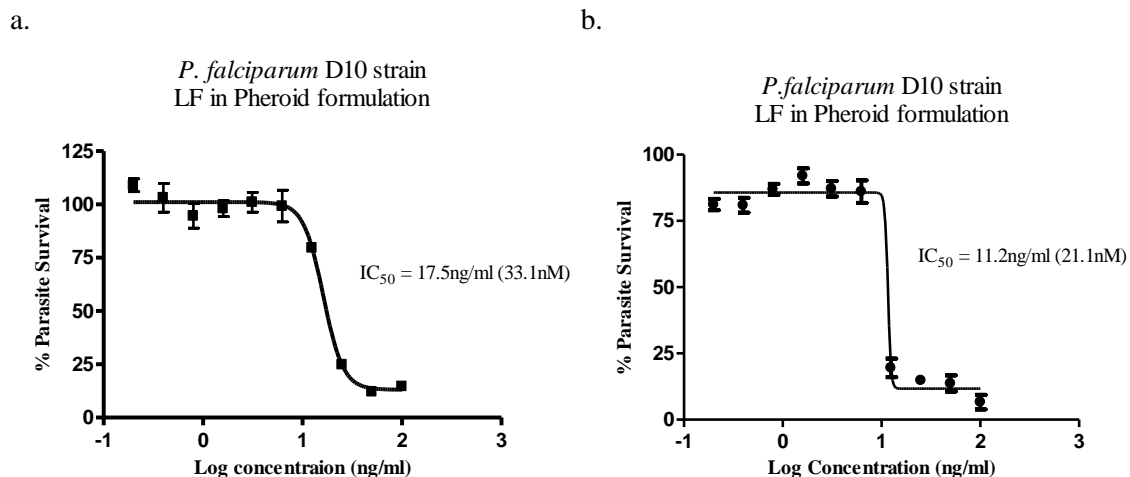


Figure 4.4: Dose response curves of LF in Pheroid™ formulation against *P. falciparum* D10 strain (CQ-S), a. and b. corresponds to experiment 1 and 2 respectively.

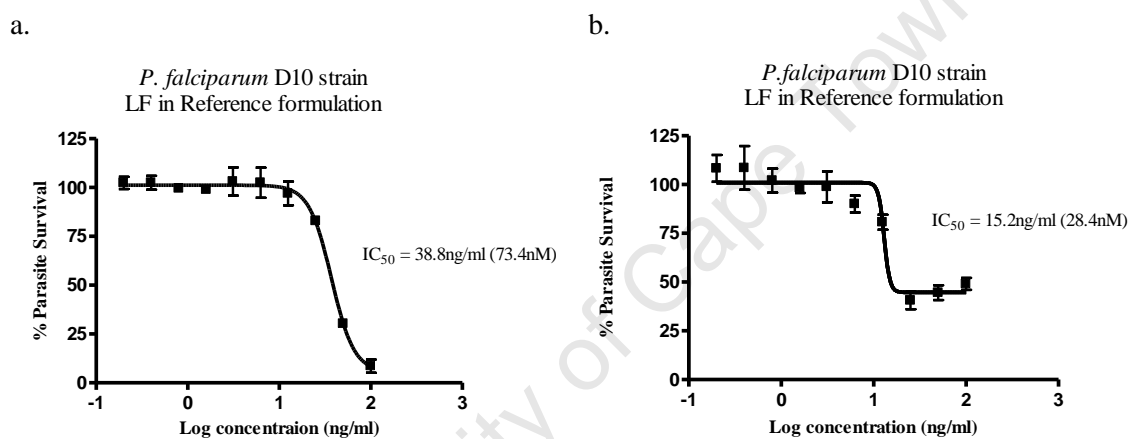


Figure 4.5: Dose response curves of LF in reference formulation against *P. falciparum* D10 strain (CQ-S), a. and b. corresponds to experiment 1 and 2 respectively.

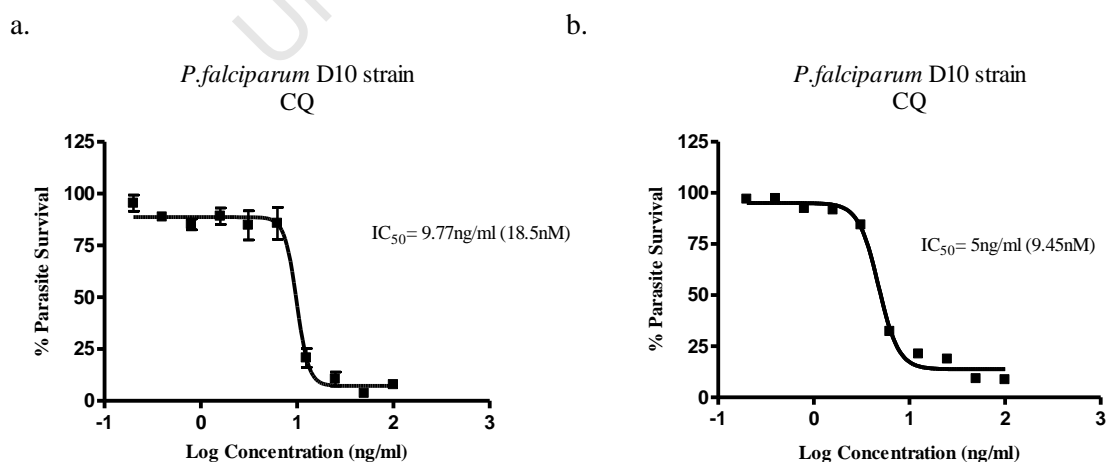


Figure 4.6: Dose response curves of CQ, standard control, against *P. falciparum* D10 strain (CQ-S), a. and b. corresponds to experiment 1 and 2 respectively.

4.4 Discussion

This *in vitro* antimalarial assay was performed to determine if the improved solubility of LF in the Pheroid™ formulation would result in lower IC₅₀ values when compared to LF in an aqueous reference solution. The results indicate that the LF in Pheroid™ formulation has improved antimalarial activity *in vitro* by 47%, when compared to the reference formulation, however the large variation in the data may render this conclusion unreliable.

The reported IC₅₀ values for LF against *P. falciparum*, determined using *in vitro* assays are detailed in Table 4.1 (refer to page 47). LF in reference and Pheroid™ formulation had an IC₅₀ value of 50.9 and 27.1 nM respectively. These values fall within the reported range of 1.91 to 90.1 nM, determined from the studies presented in Table 4.1.

There are various reasons for the wide range of reported IC₅₀ values for LF. Most of the *in vitro* assays, as shown in Table 4.1, were performed using fresh *P. falciparum* isolates from malaria infected individuals and parasite drug susceptibility may vary from one geographical area to another. Also the different *in vitro* assays are not standardized or comparable with respect to the calculated IC₅₀ values. The study performed by Wong *et al.* was the only one to use laboratory adapted parasite strains, and they reported an IC₅₀ value of 65.2 nM for LF against a CQ-S strain which is comparable to the reported value of 50.9 nM in this study (Wong *et al.*, 2011). The *in vitro* antimalarial assay, using fresh parasite isolates, allows for the determination of the intrinsic drug-susceptibility of the parasite however no deductions can be made regarding the effect of pharmacokinetic or immunological variations (Kalra *et al.*, 2005, Nkhoma *et al.*, 2007). As a result, *in vitro* drug susceptibility assays are performed using clinical isolates from a primary infection and then performed again using isolates from subjects with recrudescence infections or experiencing late treatment failure to confirm the presence of drug resistant parasites (van Vugt *et al.*, 1998, Brockman *et al.*, 2000, Tanariya *et al.*, 2000, Denis *et al.*, 2006).

Despite the limitations, *in vitro* drug susceptibility assays are fast, efficient and allow for high through-put screening of antimalarial compounds. For this study the *in vitro* results were used to corroborate the *in vivo* efficacy results when comparing LF in Pheroid™ formulation to LF in reference formulation.

References

1. Basco L.K., Bickii J. and Ringwald P. In vitro activity of lumefantrine (benflumetol) against clinical isolates of *Plasmodium falciparum* in Yaounde', Cameroon. *Antimicrobial Agents and Chemotherapy*, 42;9 (1998) 2347–2351
2. Brockman A., Price R.N., van Vugt M., Heppner D.G., Walsh D., Sookto P., Wimonwattrawatee T., Looreesuwat S., White N.J. and Nosten F. Plasmodium falciparum antimalarial drug susceptibility on the north-western border of Thailand during five years of extensive use of artesunate-mefloquine. *Transactions of The Royal Society of Tropical Medicine and Hygiene*, 94 (2000) 537-544
3. Co E.M.A. Johnson S.M., Murthy T., Talwar T., Hickman M.R. and Johnson J.D. Recent methods in antimalarial susceptibility testing. *Ant-Infective Agents in Medicinal Chemistry*, 9 (2010) 148-160
4. Denis M.B., Tsuyuoka R., Lim P., Lindergardh N., Yi P., Top S.N., Socheat D., Fandeur T., Annerberg A., Christophel E.M. and Ringwald P. Efficacy of artemether-lumefantrine for the treatment of uncomplicated falciparum malaria in the northwest Cambodia. *Tropical Medicine and International Health*, 11;12 (2006) 1800-1807
5. Fidock D.A., Rosenthal P.J., Croft S.L., Brun R. and Nwaka S. Antimalarial drug discovery: Efficacy models for compound screening. *Nature Reviews*, 3 (2004) 509-520
6. Hassan-Alin M., Bjorkman A. and Wernsdorfer W.H. Synergism of benflumetol and artemether in *Plasmodium falciparum*. *American journal of Tropical Medicine and Hygiene*, 61;3 (1999) 439-435
7. Kaddouri H., Djimde A., Dama S., Kodio A., Tekete M., Hubert V., Kone A, Maiga H., Yattara O., Fofana B., Sidibe B., Sangare C.P.O., Doumbo O. and Le Bras J. Baseline in vitro efficacy of ACT component drugs on *Plasmodium falciparum* clinical isolates from Mali. *International journal for Parasitology*, 38 (2008) 791-798
8. Kalra B.S., Chawla S., Gupta P. and Valecha N. Screening of antimalarial drugs: An overview. *Indian Journal of Pharmacology*, 38;1 (2006) 5-12
9. Makler M.T. and Hinrichs D.J. Measurement of the lactate dehydrogenase activity of Plasmodium falciparum as an assessment of parasitemia. *American Journal of Tropical Medicine and Hygiene*, 48;2 (1993) 205-210
10. Mwai L., Kiara S.M., Abdirahman A., Pole L., Rippert A., Dirye A., Bull P., Marsh K., Borrmann S. and Nzila A. In vitro activities of Piperaquine, Lumefantrine and Dihydroartemisinin in Kenyan *Plasmodium falciparum* isolates and polymorphisms in *pfprt* and *pfmdr1*. *Antimicrobial Agents and Chemotherapy*, 53;12 (2009) 5069-5073
11. Nkohoma S., Molyneux M. and Ward S. In vitro antimalarial susceptibility profile and *prcrt*/*pfmdr1* genotypes of Plasmodium falciparum field isolates from Malawi. *American Journal of Tropical Medicine and Hygiene*, 76;6 (2007) 1107-1112
12. Pradines B., Tall A., Fusai T., Spiegel A., Hienne R., Rogier C., Trape J.F., Le Bras J and Parzy D. In vitro activities of benflumetol against 158 Senegalese isolates of *Plasmodium falciparum* in comparison with those of standard antimalarial drugs. *Antimicrobial Agents and Chemotherapy*, 43;2 (1999) 418-420
13. Starzengruber P., Wernsdorfer G., Parizek M., Rojanawatsirivet C., Kollaritsch H. and Wernsdorfer W.H. Specific pharmacokinetic interaction between lumefantrine and monodesbutyl-benflumetol in *Plasmodium falciparum*. *The Middle European Journal of Medicine*, 119;3 (2007) 60–66
14. Tanariya P., Tippawangkoson P., Karbwang J., Na-Bangchang K. and Wernsdorfer W.H. In vitro sensitivity of *Plasmodium falciparum* and clinical response to lumefantrine (benflumetol) and artemether. *British Journal of Clinical Pharmacology*, 49 (2000) 437-444
15. Trager W. and Jensen J.B. Human malaria parasites in continuous culture. *Science*, 193;4254 (1976) 673-675

16. Van Vugt M., Brockman B., Gemperli B., Luxemburger C., Gathmann I., Royce C., Thra Slight S., Looreesuwan S., White N.J. and Nosten F. Randomized comparison of artemether-benflumetol and artesunate-mefloquine in the treatment of multidrug-resistant falciparum malaria. *Antimicrobial Agents and Chemotherapy*, 42;1 (1998) 135-139
17. Wernsdorfer W.H., Landgraf B., Kilimali V.A.E.B. and Wernsdorfer G. Activity of benflumetol and its enantiomers in fresh isolates of *Plasmodium falciparum* from East Africa. *Acta Tropica* 70 (1998) 9-15
18. WHO (2001). Instructions for the use of the in vitro micro test kit (Mark III) for the assessment of the response of *Plasmodium falciparum* to Chloroquine, Mefloquine, Quinine, Amodiaquine, Sulfadoxine/Pyrimethamine and Artemisinin.
19. Wong R.P.M., Salman S., Ilett K.F., Siba P.M., Mueller I. and Davis T.M.E. Desbutyl-lumefantrine is a metabolite of lumefantrine with potent in vitro antimalarial activity that may influence artemether-lumefantrine treatment outcome. *Antimicrobial Agents and Chemotherapy*, 55;3 (2011) 1194-1198

University of Cape Town

Chapter 5

Quantitative bioanalysis of lumefantrine

5.1 Introduction

Developing sensitive and selective analytical methods for analyte and/or metabolite quantification is imperative for any pharmacokinetic study. When developing a bioanalytical method there are many techniques which can be employed in order to produce an efficient, accurate and reliable method. For this study high pressure liquid chromatography and tandem mass spectrometry (LC-MS/MS) was chosen for sample analysis. A LC-MS/MS bioanalytical method consists of four procedures, namely sample extraction, chromatography, detection and quantification. High performance liquid chromatography (HPLC) is a technique used for the chromatographical separation of the analyte(s) of interest, based on physicochemical properties or size, prior to detection and quantification using mass spectrometry (MS). Mass spectrometry may be coupled to other separation techniques including gas chromatography (GC) or capillary electrophoresis (CE) (de Hoffmann & Stoobant, 2007). Samples may also be introduced directly into the ion source of the mass spectrometer, bypassing elution chromatography, and analysed by flow-injection-MS/MS (Niessan, 2006).

A mass spectrometer is an analytical tool, for quantitative and qualitative analysis, with increasing scientific application including high throughput bioanalysis, structure elucidation of unknown compounds, metabolite identification, to name a few examples. A mass spectrometer is a computerized system and consists of essentially five parts: a sample inlet, an ion source interface, mass analyser, ion detector and data processor as shown in Figure 5.1 below.

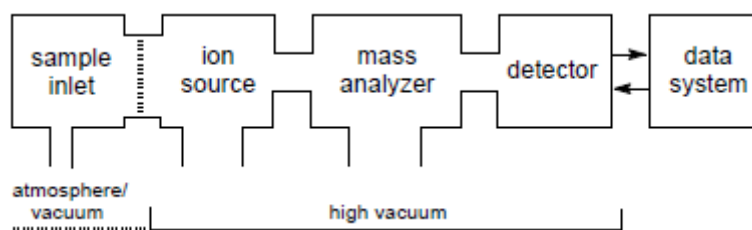


Figure 5.1: A schematic of the constituent components of a mass spectrometer (Gross, 2011)

The liquid chromatography coupled to tandem mass spectrometry process involves the separation of an analyte using a chromatographic column. The analyte is then delivered in

solution to an ion source for the production of molecular ions, for example via electrospray ionization (ESI), atmospheric pressure chemical ionization (APCI) or atmospheric pressure photo ionisation (APPI). The ions then pass through a Curtain GasTM interface between atmospheric pressure and high vacuum. Ion separation occurs in the mass analyser; according to specific mass-to-charge (m/z) ratio values (Q1), fragmentation in a collision cell (Q2) and selection of product ion (Q3) as shown in Figure 5.2. The charged ions are detected using an electron multiplier and signals are then transferred to a computer and data analysis is performed using analytical software.

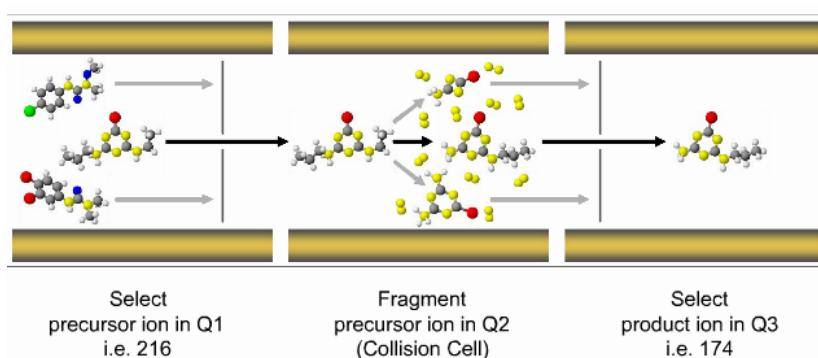


Figure 5.2: MRM scan mode in a triple quadrupole mass spectrometer (Picture sourced from AB Sciex)

When a sample is introduced, depending on the specific ion source utilized, molecular ions may be produced by electron ejection, electron capture, protonation, deprotonation or adduct formation. Sample ionization is necessary as a mass spectrometer only detects charged species and separates ions according to their mass-to-charge (m/z) ratio (de Hoffmann & Stroobant, 2007, Gross, 2011). Multiple reaction monitoring (MRM) or selective reaction monitoring (SRM) has become the mode of choice in quantitative mass spectrometric bioanalysis (Niessan, 2006). As illustrated in Figure 5.2, SRM allows for the selection of a specific precursor or molecular ion (e.g. m/z 216) in the first quadrupole (Q1) then controlled fragmentation of the selected precursor ion in the collision cell (Q2) and selection of a specific product or fragment ion (e.g. m/z 174), for detection, in the third quadrupole (Q3) (Gross, 2011). Ions exiting the quadrupoles are detected, transformed into a digital signal and relayed to the computer for data processing and interpretation using Analyst[®] software.

LC-MS/MS is an analytical technique utilized in the drug development process, allowing fast and efficient sample analysis.

LC-MS/MS method validation

The purpose of validating bioanalytical methods for analyte quantification in a specific biological matrix (blood, plasma, urine, etc.), is to ensure that the method is robust and reproducible for analysing samples of unknown concentrations. A LC-MS/MS method validation, involving specific laboratory investigations, was performed according to the guidelines for bioanalytical method validation, developed by the USFDA (FDA; Guidelines for Industry, 2001). These procedures are undertaken to ensure a complete system of quality control and assurance. A LC-MS/MS method validation is performed to objectively demonstrate and document the accuracy, precision, selectivity, sensitivity and reproducibility of the developed method. The stability of the analyte is also investigated to ensure that the analyte concentration is not affected by the assay procedure or associated storage conditions.

Literature Review

Published LC-MS/MS methods for the quantification of LF in biological matrix are detailed in Table 5.1. One method was developed for the determination of LF in rat plasma while the other five were developed for human plasma. All the methods were developed and validated according to FDA or the AIDS Clinical Trial Group (ACTG) guidelines. There are no published LC-MS/MS methods for the determination of LF in mouse whole blood (WB) and/or plasma (refer to Table 5.1).

Table 5.1: Summary of published LC-MS/MS methods for LF

Reference	Year	Extraction Method	Conc. range (ng/ml)	Sample vol (ul)	Injection vol (ul)	LC Analytical Column	Flow rate (ml/min)	Sample run time (min)	Biological Matrix
Wahajuddin <i>et al.</i>	2009	Liquid-Liquid	2-500	100	10	C ₁₈	0.5	5	rat plasma
Hodel <i>et al.</i>	2009	Protein prec.	4-4000	200	10	C ₁₈	0.3	17	human plasma
Munjal <i>et al.</i>	2010	Protein prec.	210-25050	100	5	C8	0.6	2.9	human plasma
Cesar <i>et al.</i>	2011	Protein prec.	10-18000	250	50	Zorbax SB-Cyano	1	9	human plasma
Sethi <i>et al.</i>	2011	SPE	2-2000	100	10	Xterra RP18	0.5	15	human plasma
Huang <i>et al.</i>	2012	Liquid-Liquid	50-20000	25	10	Zorbax C ₁₈	0.4	8	human plasma
Present study	2012	Protein prec.	15.6-4000	20	2	PFP (2)	0.5	3	mouse plasma and WB

Liquid chromatography coupled to tandem mass spectrometry allows for the development of sensitive and selective quantitative methods, using low sample volumes and run time, which may be utilised for high throughput sample analysis (Jemal 2000). The methods for the detection of LF developed by Sethi *et al.*, Hodel *et al.*, Cesar *et al.* and Huang *et al.*, each have long sample run times (≥ 5 min) which may not be feasible for high throughput sample analysis (i.e. process ≥ 100 samples/day) (Lee1999). Sethi *et al.* used a solid phase extraction method which is time consuming and expensive. Wahajuddin *et al.* and Huang *et*

al. used a liquid-liquid sample extraction method which is more labour intensive and time consuming than protein precipitation sample extraction. A plasma volume of ≥ 100 μl would be considered a large volume, using the mouse as an experimental animal but the sensitivity of mass spectrometry allows for the reduction of the biological sample volume required. Huang *et al.* developed the only LC-MS/MS method for the quantitation of LF using a stable isotope labelled analyte as internal standard (ISTD) to eliminate matrix effects and ionization saturation. All the published methods have shortcomings regarding their use for pre-clinical high throughput analysis in mouse blood or plasma.

Aim and Objective

To develop and validate a LC-MS/MS method for the quantification of LF in mouse plasma and WB, using 20 μl of biological matrix.

5.2 Materials and Methods

Solvents and chemicals

Analytical grade, LiChrosolv[®] water, acetonitrile and methanol were purchased from Merck (Darmstadt, Germany). Formic acid was purchased from Merck (Darmstadt, Germany). Acetic acid was purchased from Sigma-Aldrich (Germany). LF (Figure 5.3) was donated by Novartis (Basel, Switzerland) and the deuterated internal standard, D₉-LF (Figure 5.4) was purchased from Toronto Research Chemicals Inc. (Ontario, Canada).

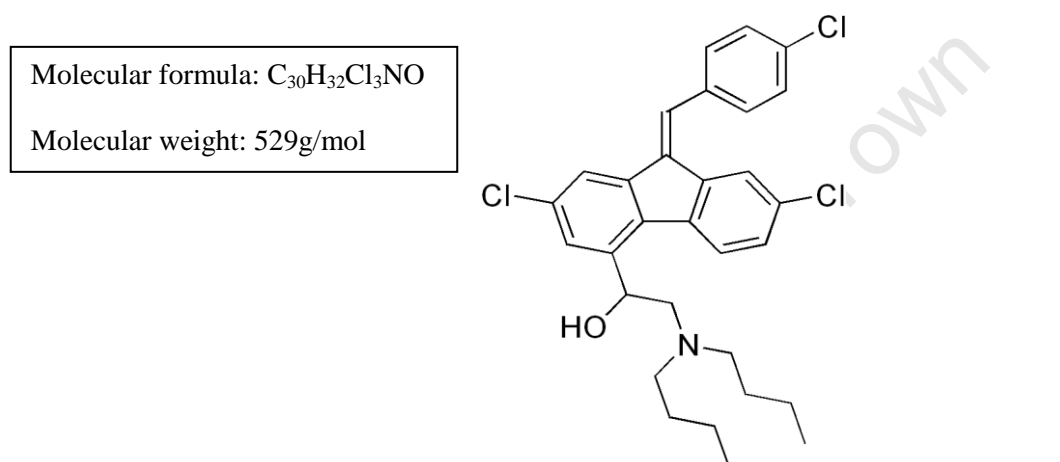


Figure 5.3: Chemical structure of the analyte lumefantrine (LF)

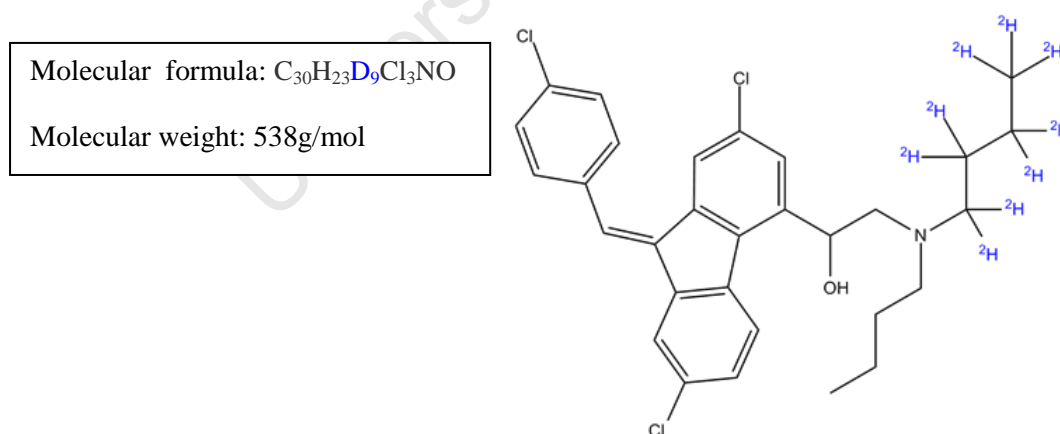


Figure 5.4: Chemical structure of the internal standard; deuterated lumefantrine (D₉-LF)

Biological matrix

Blood from C57/BL6 mice was collected by cardiac puncture in Lithium Heparin (anti-coagulant) vacuum tubes. The mice, sacrificed for blood collection, were obtained from the Animal Unit, University of Cape Town. The pooled mouse blood was used for the

preparation of the calibration standards and quality control standards. The fresh mouse blood was centrifuged at 2300 G for 10 minutes (Eppendorf 5415D) to obtain mouse plasma.

Instrumentation

The LC-MS/MS method was developed and validated on an Agilent 1200 series HPLC system coupled with an AB Sciex API 3200 triple quadrupole mass spectrometer (AB Sciex). The mass spectrometer is equipped with a Turbo VTM ion source and patented LINAC[®] collision cell. Bioanalysis was performed using ESI in the positive ion mode. For the quantitation of LF the LC-MS/MS system was operated at unit resolution in MRM mode, monitoring the transition of the precursor ion m/z 530.1 to the product ion m/z 347.9 for LF and the transition of precursor ion m/z 539.1 for D-LF (ISTD), to product ion m/z 347.9 as presented in Figure 5.5 and Figure 5.6 respectively. The LC-MS/MS system was interfaced with a DELL[®] Windows[®] XP computer running Analyst[®] software version 1.5.1. Analyst[®] software was used for LF chromatographic data acquisition, peak integration and quantification.

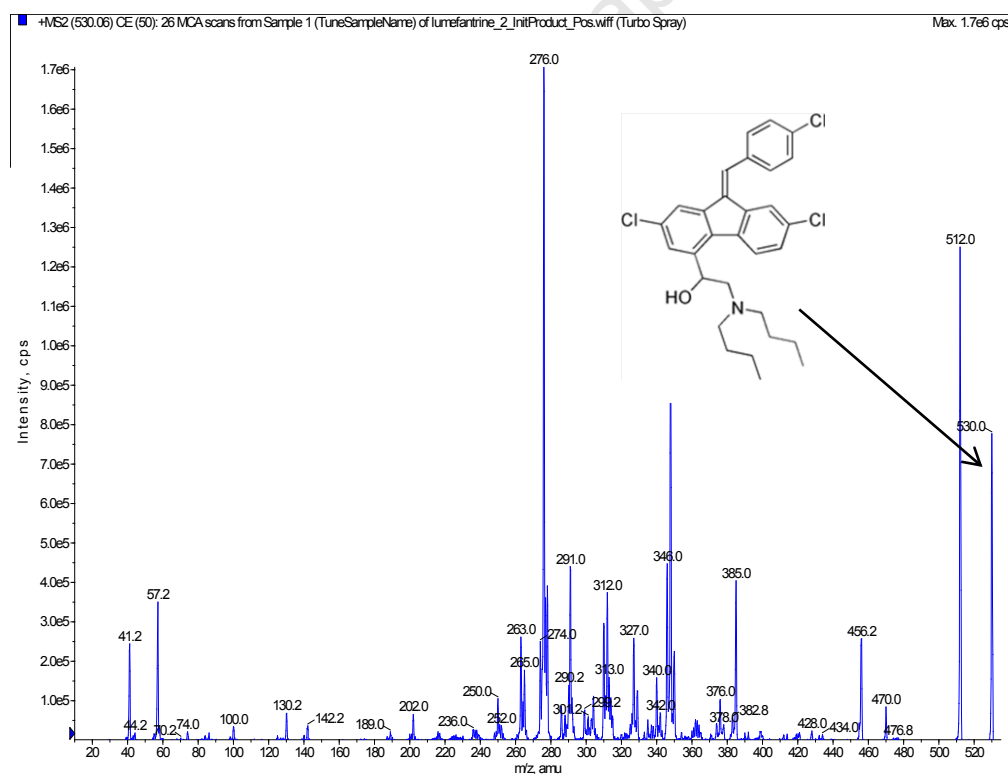


Figure 5.5: Product ion spectrum (Q3) of the analyte, showing the $[M+H]^+$ ion at m/z 530.0

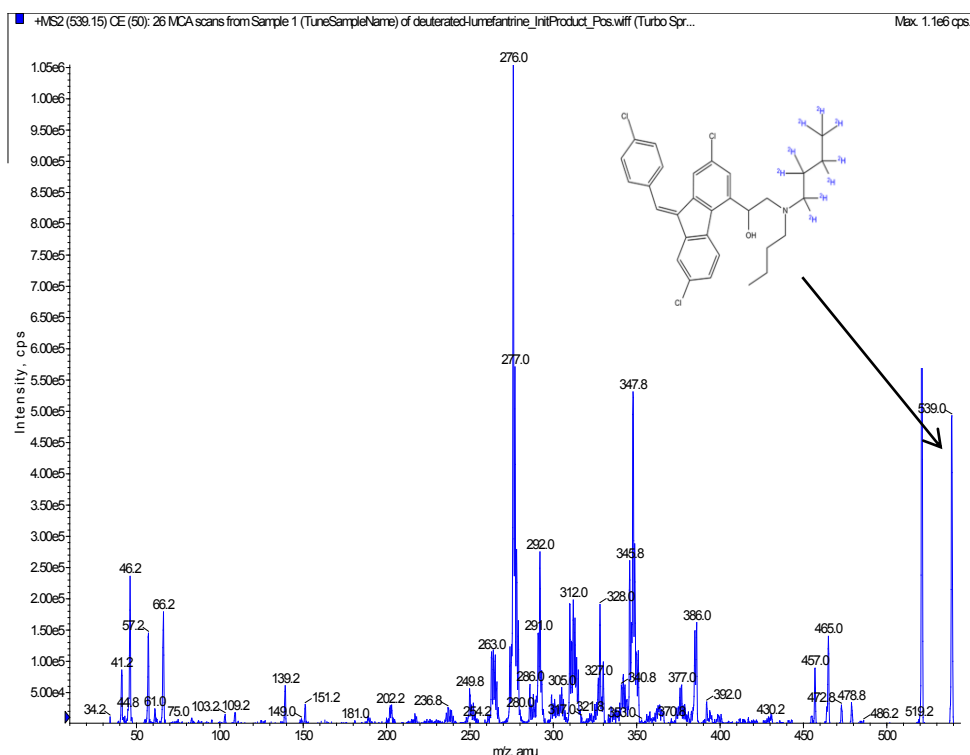


Figure 5.6: Product ion spectrum (Q3) of the ISTD, showing the $[M+H]^+$ ion at m/z 539.0

Chromatography and Mass Spectrometry

Chromatography was performed on a Phenomenex Luna, PFP 2 (50 x 2.0 mm, 5 μ m) analytical column (Separations, South Africa). The sample injection volume was 2 μ l and the mobile phase consisting of acetonitrile and 0.1% formic acid (formic acid: water, 1:1000 v/v) at a ratio of 3:7 (v/v) was delivered at a constant flow rate of 0.5 ml/min. The analyte eluted at 1.3 min for WB samples and 1.12 min for plasma samples. Detection was performed on an AB Sciex 3200 mass spectrometer and the optimised settings are summarised in Tables 5.2 and 5.3. The total LC-MS/MS run time was 3 minutes per sample analysed.

Table 5.2: ESI settings

Curtain gas (CUR)	20
Collision gas (CAD)	5
Ion spray voltage (V)	4500
Source temperature ($^{\circ}$C)	500
Gas 1 (psi)	50
Gas 2 (psi)	60

Table 5.3: MS/MS settings

	LF	D-LF
Q1 mass [M+H]⁺	530.1	539.1
Q3 mass	347.9	347.9
Declustering potential (V)	66	71
Entrance potential (V)	4.5	8.5
Collision energy (V)	59	59
Collision cell exit potential (V)	6	6
Scan type	MRM	MRM
Polarity	positive	positive
Pause time (ms)	5	5

Sample Extraction Procedure

A protein precipitation extraction procedure was developed using 20 µl of mouse WB or plasma sample (Figure 5.7). The extraction procedure was performed in 1.5 ml polypropylene Eppendorf tubes. The precipitation solution (PPT) consisted of 0.1% formic acid and acetonitrile (1:3, v/v). 5 µl of a 1 mg/ml ISTD stock solution (methanol:acetic acid (99.8:0.2, v/v)) was spiked into 30 ml of PPT to yield an final ISTD concentration of 166 ng/ml (PPT+ISTD). The extraction procedures are detailed in Figure 5.7, 200 µl of the PPT+ISTD solution was added to 20 µl of sample and mixed using a vortex mixer (Scientific Industries, Vortex Genie 2), sonicated (Labcon, ultra-sonic) and then centrifuged (Eppendorf 5415D) to yield the analyte containing supernatant. 100 µl of the supernatant was transferred to a polypropylene 96 well plate (Axygen Scientific; California, USA) and analysed using LC-MS/MS.

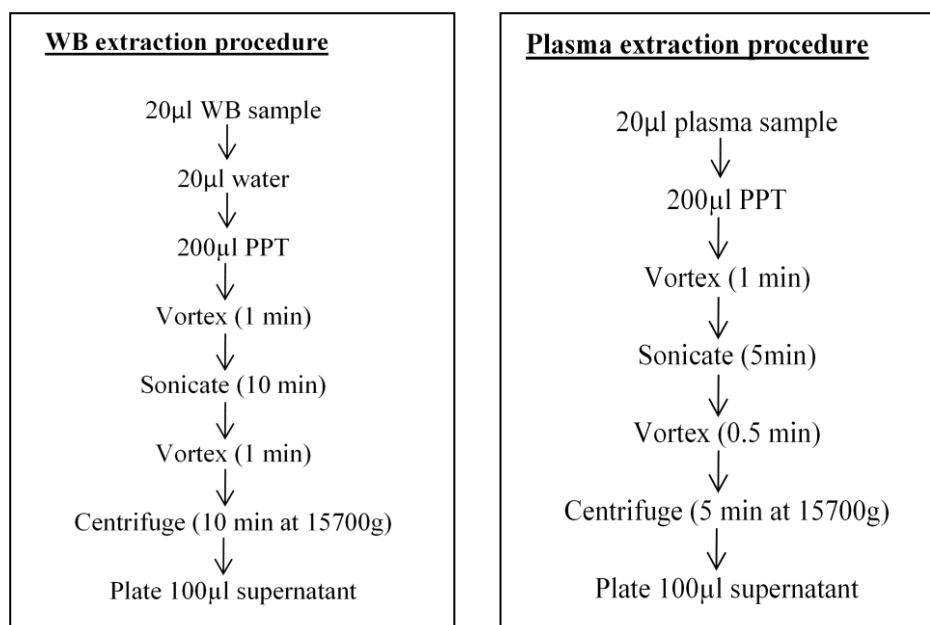


Figure 5.7: Sample extraction procedures for LF whole blood (WB) and plasma samples.

Preparation of ISTD solution

For quantitation accuracy and precision a deuterated internal standard (ISTD) with near identical physicochemical properties was used, namely D₉-LF. One milligram of D₉-LF was weighed accurately using a microbalance scale (Satorius) and subsequently dissolved in 1 ml of stock solution (SS), namely; methanol:acetic acid (99.8:0.2, v/v). Five microliters of 1 mg/ml ISTD stock solution (ISS1) was spiked into 30 ml of the precipitation solution (PPT) resulting in a final concentration of 166.67 ng/ml. ISS1 was stored at -80°C.

Preparation of LF stock solutions

Stock solutions of LF (SS1) were prepared at a concentration of 1 mg/ml. A mass of 1 mg of LF was accurately weighed, using a microbalance scale (Satorius) and dissolved in 1 ml of stock solute (SS), methanol:acetic acid (99.8:0.2 v/v). As stated in an earlier scientific publication, LF dissolves optimally at a lower pH and acetic acid was therefore added to the organic solvent, methanol and found to be efficient (Zeng *et al* 1996). These stock solutions were used to prepare working solutions to spike blank mouse plasma and whole blood as required. All stock solutions were stored at -80°C.

Preparation of calibration standards and quality control standards

A set of calibration standards (STDs) and quality control standards (QCs) were prepared volumetrically in mouse whole blood and plasma, applying the same dilution technique and using the same stock solutions. A working stock solution was prepared at a concentration of 100 µg/ml (SS2) by diluting 100 µl of SS1 with 900 µl SS. 40 µl of SS2 was spiked into 960 µl of blank plasma/WB which was then serially diluted with blank plasma/WB to attain the desired STD concentration range of 15.6 – 4000 ng/ml as presented in Table 5.4. STD 9 at 4000 ng/ml is the upper limit of quantification (ULOQ) and STD 1 at 15.6 ng/ml is the lower limit of quantification (LLOQ).

For the quality control standards, 64 µl of SS2 was spiked into 1936 ml of plasma/WB which was then serially diluted with blank plasma/WB to attain the desired QC concentration range of 25-3200 ng/ml as presented in Table 5.5.

Table 5.4: Preparation of calibration standards for LF

Standard	Blank plasma/wb volume (µl)	Volume SS2 spiked (µl)	Dilution source	Dilution source volume (µl)	Total volume of dilution (µl)	Concentration (ng/ml)
ULOQ - STD 9	960	40			1000	4000
STD 8	500		STD 9	500	1000	2000
STD 7	500		STD 8	500	1000	1000
STD 6	500		STD 7	500	1000	500
STD 5	500		STD 6	500	1000	250
STD 4	500		STD 5	500	1000	125
STD 3	500		STD 4	500	1000	62.5
STD 2	500		STD 3	500	1000	31.3
LLOQ - STD 1	500		STD 2	500	1000	15.6

Table 5.5: Preparation of quality control standards for LF

QC standard	Blank plasma/wb volume (µl)	Volume SS2 spiked (µl)	Dilution source	Dilution source volume (µl)	Total volume of dilution (µl)	Concentration (ng/ml)
QC 1 (High)	1936	64			2000	3200
QC 2 (Medium)	1000		QC 1	1000	2000	1600
QC 3	1000		QC 2	1000	2000	800
QC 4	1000		QC 3	1000	2000	400
QC 5	1000		QC 4	1000	2000	200
QC 6	1000		QC 5	1000	2000	100
QC 7 (Low 1)	1000		QC 6	1000	2000	50
QC 8 (Low 2)	1000		QC 7	1000	2000	25

Calibration standard curve

Aliquots of the full sets of calibration STDs and QCs were made and stored frozen at -80°C. On the day of analysis, the required aliquots were thawed, extracted and analysed for each validation run. Using Analyst[®] software standard curve fitting was determined by applying the simplest model that adequately describes the concentration vs response relationship using appropriate weighting. The calibration curve is comprised of eight different STDs at concentrations ranging from 15.6 ng/ml (LLOQ) to 4000 ng/ml (ULOQ). For LF quantitation the eight-point calibration standard curves were calculated based on peak area ratios of analyte to ISTD and fitted using 1/x (1/concentration) weighted quadratic regression. 1/x weighted quadratic regression was found to be the simplest regression model for LF quantification. A representative calibration curve from the first validation run is presented in Figure 5.8.

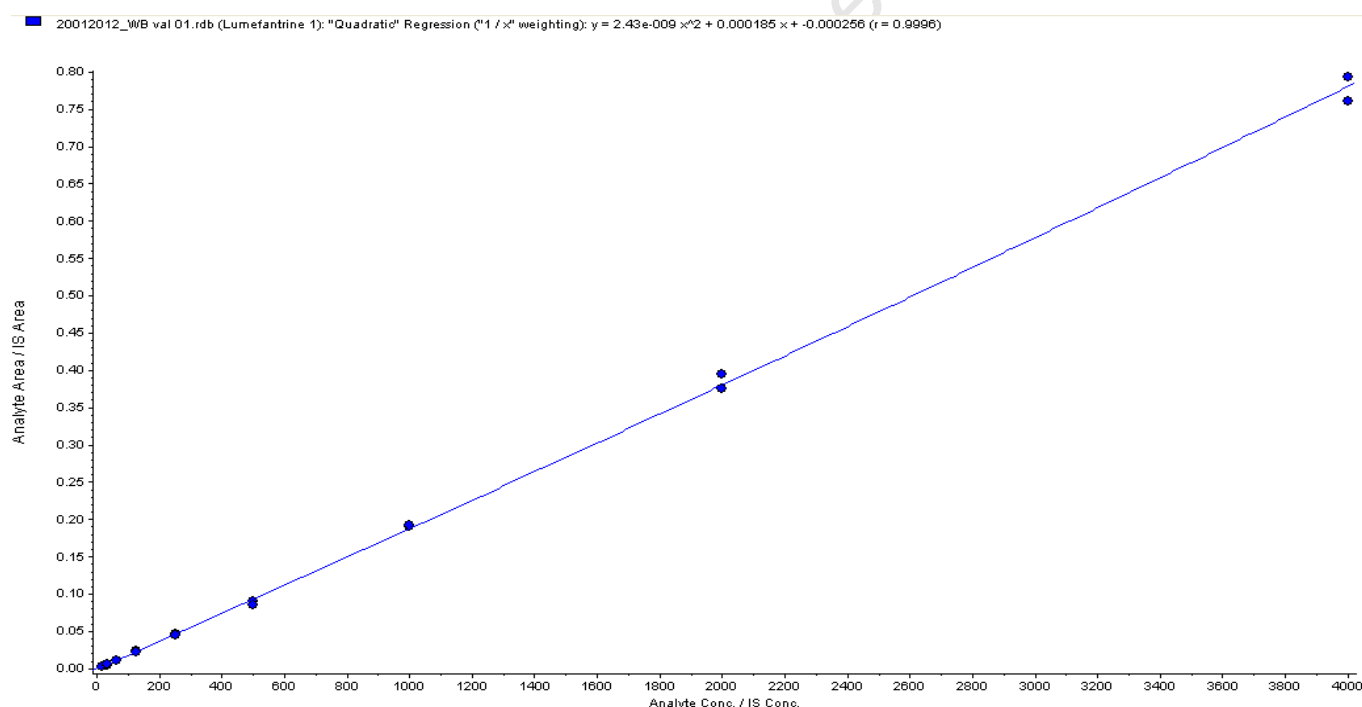


Figure 5.8: Representative calibration curve for LF

LC/MS/MS method validation

A complete method validation consists of three validation batches, analysed on three different occasions as well as a stability assessment of the analyte to ascertain that the method is accurate, precise and reproducible. An example of a typical validation sample batch list is shown in Table 5.6, calibration standards are analysed in duplicate and QC samples in six fold. The QC samples are monitored over the three validation batches performed on three different occasions to demonstrate intra-batch and inter-batch accuracy and precision.

Table 5.6: A representation of a validation run sample batch list. Abbreviations: DB (double blank); sample containing no analyte or ISTD, SYS; system performance verification standard.

Sample no.	Sample ID	Sample no.	Sample ID
1	SYS	25	STD 5
2	Blank	26	QC L2
3	DB	27	QC L1
4	STD 1	28	QC M
5	STD 1	29	QC H
6	STD 2	30	STD 6
7	STD 2	31	STD 6
8	QC L2	32	QC L2
9	QC L1	33	QC L1
10	QC M	34	QC M
11	QC H	35	QC H
12	STD3	36	STD 7
13	STD3	37	STD7
14	QC L2	38	QC L2
15	QC L1	39	QC L1
16	QC M	40	QC M
17	QC H	41	QC H
18	STD 4	42	STD 8
19	STD 4	43	STD 8
20	QC L2	44	STD 9
21	QC L1	45	STD 9
22	QC M	46	Blank
23	QC H	47	DB
24	STD 5	48	SYS

Intra-batch accuracy and precision

As detailed in Table 5.6, a typical validation batch is comprised primarily of a set of calibration standards, analysed in duplicate and the QC standards, analysed in six fold. The system performance verification sample (SYS) is a QC standard that is extracted and injected in triplicate at the beginning and end of every analytical run to monitor the consistency of instrument performance throughout the analytical run. A validation batch also includes a Blank (blank matrix) sample which is an extracted sample containing no analyte as well as a DB (double blank) sample which is an extracted sample containing no analyte and no ISTD.

Inter-batch accuracy and precision

The QC samples are monitored over three successive validation batches performed on different occasions to ascertain between-batch accuracy and precision.

Stability Assessment

For method validation one needs to demonstrate that the analyte is stable (does not degrade) throughout the sample preparation, extraction and analytical procedure including associated conditions such as temperature variations.

Stock solution stability

Stock solutions of LF were prepared in methanol:acetic acid (9.98:0.2 v/v) solution at a concentration of 1 mg/ml and aliquoted. A test sample was left at room temperature for 6 hours and a control sample was kept at -80°C for the same length of time. A fresh reference stock solution was prepared after the storage period of the test and control samples. The reference, test and control samples were subsequently diluted with mobile phase to a concentration of 62.5 ng/ml (low), 800 ng/ml (medium) and 3200 ng/ml (high) then analysed according to the method procedure. Peak areas of the test and control samples were compared to the reference samples. The stability of the ISTD stock solution was not investigated as fresh solutions were prepared for each batch of sample analysis.

Freeze and thaw stability in matrix

To determine the freeze and thaw stability of LF, sample aliquots of quality control standards at low (62.5 ng/ml), medium (800 ng/ml) and high concentrations (3200 ng/ml) were stored frozen at -80°C and put through three freeze and thaw cycles. Each cycle consisted of a thaw session of at least one hour at room temperature followed by a twenty four hours freezing

time. These samples were analysed against a valid calibration curve and compared to controls from the batch, analysed at the same concentration. A precision of more than 15% and an accuracy deviating more than 15% of the observed mean QC concentration could indicate freeze and thaw instability of LF in matrix.

On-bench stability

To determine on-bench stability, sample aliquots at three different concentrations were stored frozen at -80°C then thawed and left on the bench (at room temperature) for six hours. These samples were analysed against a valid calibration curve and compared to QC samples from the batch, analysed at the same concentration.

On-Instrument stability

The on-instrument (sample inlet) stability experiment is performed to ensure analyte reinjection reproducibility and analyte stability, if an analytical run has to be reanalysed in case of instrument failure. Six aliquots of a QC standard at a mid-concentration of 800 ng/ml were extracted and pooled. The samples were analysed as part of a validation batch. These samples were injected six fold over two consecutive days to evaluate the stability of the analyte in extracted samples when kept in the sample inlet compartment at 5°C, throughout the specified 24 hour period. The analyte/ISTD peak area ratios of the '24hr' injections were compared to the ratios of the initial set of injections.

Specificity

A method should be selective for a specific analyte and not be affected by interfering or co-eluting components in the biological matrix. Any interference would be most apparent at low analyte concentration levels. The selection of a specific precursor ion followed by the formation and detection of a specific product ion renders quantitative mass spectrometry highly specific.

Carry-over

Carry-over occurs when traces of analyte are transferred forward to the next chromatographic injection affecting peak intensity (Morin *et al.*, 2012). Carry-over may occur due to analyte adsorption on the chromatographic column or sample residue on the sampling needle. After the sample is taken up, the autosampler needle is washed with needle rinsing solution (acetonitrile:0.1%formic acid, 1:1 v/v) in the flush port for (5 seconds) to prevent carry over.

A blank and a double blank were positioned in the injection sequence directly after the highest calibration standard (ULOQ) to assess possible carry-over effects. A peak that is observed as a result of carry-over should not be $\geq 20\%$ of the area or height of the peak obtained at LLOQ and is calculated using Equation 5.1 (Morin *et al.*, 2012).

$$\% \text{ carry-over} = \left[\frac{\text{peak area of analyte in blank after ULOQ}}{\text{peak area of analyte in LLOQ}} \right] \times 100$$

Equation 5.1: Calculation of percentage analyte carry-over

Sensitivity

The sensitivity of the mass spectrometer and the robustness of the LS-MS/MS quantification method at low analyte concentration levels may be evaluated by determining the analyte signal/noise ratio at LLOQ. The analyte signal/noise ratio calculated from the LLOQ chromatogram should be larger than 5:1 and better than 15% variability.

Matrix effects (ME)

The basis of matrix effect is the modification of the ionization of the drug analyte by endogenous biological matrix background components. The evaluation of ME was performed based on strategies proposed by Matuszewski *et al.* (Matuszewski *et al.*, 2003, Matuszewski, 2006). To evaluate ME, 20 μl aliquots of blank mouse matrix (WB/plasma) from six different sources were processed using the protein precipitation method detailed previously, to yield post-extraction supernatant. Pooled aliquots of post-extraction supernatant from each of the six different lots of matrix were then spiked, using LF stock solutions, to yield post-extraction ME samples containing LF at low, medium or high concentrations. The post-extraction ME samples were added to a 96-well plate and analysed as part of a validation batch.

The average ratio of LF/ISTD peak areas at low, medium and high concentration of the ME samples was used to plot a line graph for each lot of matrix tested. The variability of the slopes of the lines fitted through low, medium and high concentrations of LF samples from the six different lots of matrix (WB/plasma) may be used as a good indicator of relative ME. The precision (CV) of the slopes should not exceed 5%.

Recovery (RE)

The analyte recovery of the extraction procedure was determined by comparing the responses measured for pre-extraction spiked quality control samples with responses measured for post-extraction spiked samples of LF at specified concentrations. To evaluate absolute recovery two sets of samples were prepared. The pre-extraction spiked quality control samples (test samples) were prepared and extracted as detailed previously. For the post-extraction spiked samples (reference samples), 20 µl aliquots of blank mouse matrix (WB/plasma) were processed using the protein precipitation method detailed previously, to yield post-extraction supernatant. Pooled aliquots of post-extraction supernatant was then spiked, using LF stock solutions, to yield post-extraction samples containing LF at low, medium or high concentrations. All samples were analysed in six fold and analyte RE was determined at low, medium and high concentration levels. The ratio of the analyte peak areas of the test and reference samples is expressed as a percentage recovery, calculated using Equation 5.2.

$$\% \text{ RE} = (\text{Peak area of test sample} / \text{Peak area of reference sample}) \times 100$$

Equation 5.2: Calculation to determine percentage analyte recovery

The mean RE of the quantitative drug assay method should be consistent and the precision of the measured RE (CV) should not exceed 15% for any particular concentration of the analyte at which it is determined.

5.3 Results

A validation batch consists of all the STDs analysed in duplicate to produce one calibration curve and six replicates of each QC standard. In order to demonstrate acceptable within- and between day accuracy and precision of the method, the STDs and QCs were extracted and analysed in three consecutive runs.

Accuracy (%) of an analytical method refers to the calculated mean test results relative to the nominal or true concentration of the analyte. The precision of an analytical method describes the closeness of individual measures of an analyte, at a specific concentration, when a procedure is applied repeatedly and is expressed as the coefficient of variation (CV). The acceptance criteria for a valid method require the within- and between-batch accuracy to be within 15% of the nominal concentration for the entire calibration range except for the LLOQ where accuracy within 20% of the nominal concentration is allowed.

5.3.1 Validation of the LC-MS/MS method for the quantitation of LF in mouse WB

Intra-batch accuracy and precision

From the data shown in Tables 5.7 and 5.8 below, it is evident that all the STDs and QCs for the first validation run have demonstrated acceptable accuracy and precision. This indicates that the method is accurate, precise and sensitive for the duration of one validation run.

Table 5.7: Accuracy and precision of LF calibration standards for WB validation 1

Sample ID	Nominal Conc. (ng/ml)	Mean observed conc. (ng/ml)	Standard Deviation	Accuracy (%)	CV (%)	n
S1	15.6	17.3	0.544	110.7	3.2	2
S2	31.3	30.8	1.47	98.5	4.8	2
S3	62.5	59.0	0.859	94.4	1.5	2
S4	125	126.0	5.95	100.8	4.7	2
S5	250	243.9	5.57	97.5	2.3	2
S6	500	473.0	22.2	94.6	4.7	2
S7	1000	1022.1	8.54	102.2	0.8	2
S8	2000	2026.1	72.6	101.3	3.6	2
S9	4000	3985.8	108.8	99.6	2.7	2

Table 5.8: Summary of LF inter-validation quality control standards for WB validation 1

Sample ID	Nominal Conc. (ng/ml)	Mean observed conc. (ng/ml)	Standard Deviation	Accuracy (%)	CV (%)	n
QC L2	25	27.9	2.04	111.7	7.3	6
QC L1	50	47.8	2.82	95.6	5.9	6
QC M	1600	1621.1	106.4	101.3	2.3	6
QC H	3200	3378.4	70.7	105.6	6.6	6
SYS	200	193.6	4.37	96.8	2.1	6

Inter-batch accuracy and precision

From the results presented in Tables 5.9 to 5.12, it may be concluded that the method has performed adequately over three validation runs; all the STDs and QCs have a calculated % CV of less than 15%. The calculated accuracy, for all STDs and QCs are within 15% of the nominal concentration values. The bioanalytical method has demonstrated reproducible precision, accuracy and sensitivity.

Table 5.9: Accuracy and precision of LF calibration standards for WB validation 2

Sample ID	Nominal Conc. (ng/ml)	Mean observed conc. (ng/ml)	Standard Deviation	Accuracy (%)	CV (%)	n
S1	15.6	18	0.011	115.4	0.1	2
S2	31.3	32.79	0.017	104.8	0.1	2
S3	62.5	60.71	1.68	97.1	2.8	2
S4	125	115.8	5.29	92.6	4.6	2
S5	250	228.8	1.49	91.5	0.7	2
S6	500	462.3	16.1	92.5	3.5	2
S7	1000	1018.9	25.7	101.9	2.5	2
S8	2000	2135.3	47.6	106.8	2.2	2
S9	4000	3876.5	16.4	96.9	0.4	2

Table 5.10: Summary of LF inter-validation quality control standards for WB validation 2

Sample ID	Nominal Conc. (ng/ml)	Mean observed conc. (ng/ml)	Standard Deviation	Accuracy (%)	CV(%)	n
QC L2	25	27.2	0.924	108.6	3.4	6
QC L1	50	49.4	1.11	98.8	2.2	6
QC M	1600	1595.9	123.2	99.7	7.7	6
QC H	3200	3236.6	225.5	101.1	7.0	6
SYS	200	176.4	3.63	88.2	2.1	6

Table 5.11: Accuracy and precision of LF calibration standards for WB validation 3

Sample ID	Nominal Conc. (ng/ml)	Mean observed conc. (ng/ml)	Standard Deviation	Accuracy (%)	CV (%)	n
S1	15.6	18.3	1.50	117.5	8.2	2
S2	31.3	33.3	3.30	106.4	9.9	2
S3	62.5	56.8	0.078	90.9	0.1	2
S4	125	117.5	2.60	94.0	2.2	2
S5	250	230.6	6.87	92.2	3.0	2
S6	500	480.8	5.73	96.2	1.2	2
S7	1000	964.7	21.0	96.5	2.2	2
S8	2000	2205.8	11.3	110.3	0.5	2
S9	4000	3814.4	211.6	95.4	5.5	2

Table 5.12: Summary of LF inter-validation quality control standards for WB validation 3

Sample ID	Nominal Conc. (ng/ml)	Mean observed conc. (ng/ml)	Standard Deviation	Accuracy (%)	CV (%)	n
QC L2	25	27.4	0.974	109.5	3.6	6
QC L1	50	44.6	1.68	89.2	3.8	6
QC M	1600	1471.6	51.2	92.0	3.5	6
QC H	3200	3166.8	103.0	99.0	3.3	6
SYS	200	173.2	1.73	86.6	1.0	6

Summary of combined calibration standard quality control results

A summarised analysis of the QC standards for the three validation runs are presented in Table 5.13.

Table 5.13: Overall accuracy and precision estimation for the quality control standards of LF in mouse WB

Validation Batch	Nominal Replicates	QC L2 (25ng/ml)	QC L1 (50ng/ml)	QC M (1600ng/ml)	QC H (3200ng/ml)
		Observed Concentration (ng/ml)			
Validation 1	1	26	50.4	1530	3410
	2	28.5	50.5	1560	3330
	3	31	48.5	1610	3420
	4	27.6	48.6	1620	3400
	5	29	45.2	1580	3260
	6	25.5	43.5	1830	3460
Validation 2	1	27.3	49.9	1540	3590
	2	28.3	50.5	1580	3310
	3	26.9	50.6	1550	3290
	4	27.6	48.9	1480	3160
	5	*	48.4	1580	3170
	6	25.8	48	1840	2900
Validation 3	1	27.9	47.2	1500	3260
	2	27.8	43.1	1540	3230
	3	26.3	44.3	1500	2970
	4	28.8	45.6	1440	3210
	5	27.1	44.7	1390	3140
	6	26.5	42.6	1460	3200
Average		27.6	47.3	1562.8	3261.7
STDEV		1.36	2.76	118.9	168.6
CV (%)		4.9	5.8	7.6	5.2
Accuracy (%)		110.5	94.5	97.7	101.9

*no value due to sample aliquot error

Results from the validation assays indicate that the method is accurate and precise for LF quantification with a valid calibration range of 15.6 – 4000 ng/ml.

Stock solution stability

Stock solution stability was assessed at low, medium and high concentrations namely 62.5, 800 and 3200 ng/ml respectively. The peak areas of the test and control samples were compared to the reference samples, results are presented in Table 5.14.

The % CV calculated for the control samples at low, medium and high concentration were less than 15% which indicates good analyte stability. The % CV calculated for the test samples at medium and high concentration were less than 15% which indicates good analyte stability, when left at ambient temperature for 6 hours. However the accuracy calculated for the analyte at the low concentration under test conditions was 119% which was more than 15% greater than the reference sample peak area. The analyte is more likely to degrade at room temperature and as a result a decrease in accuracy would be expected, thus the discrepancy may be due to matrix effects or a dilution error instead. This discrepancy was not observed during the LF in plasma validation (where a matrix effect evaluation was performed) therefore it more likely occurred as a result of human error than analyte instability. This should not affect the validity of the method as stock solutions are only used for spiking calibration STDs and QCs, during which the stocks are kept on ice and returned to -80°C storage promptly.

Table 5.14: Stock solution stability at ambient temperature (16°C) and -20°C compared to fresh reference solution at three different concentrations

		Reference	Test (16°C)	Controls (-20°C)
Low conc.	Peak area 1	26500	32200	25200
	Peak area 2	26700	31100	24700
	Average	26600	31650	24950
	STDEV	141.4	777.8	353.6
	CV (%)	0.5	2.5	1.4
	Accuracy (%)		119.0	93.8
Medium conc.	Peak area 1	367000	369000	363000
	Peak area 2	360000	361000	371000
	Average	363500	365000	367000
	STDEV	4949.7	5656.9	5656.9
	CV (%)	1.4	1.5	1.5
	Accuracy (%)		100.4	101.0
High conc.	Peak area 1	1020000	1070000	957000
	Peak area 2	1020000	1040000	949000
	Average	1020000	1055000	953000
	STDEV	0.000	21213.2	5656.9
	CV (%)	0	2.0	0.6
	Accuracy (%)		103.4	93.4

Freeze and thaw stability in matrix

Freeze and thaw stability of the analyte in WB was assessed at low, medium and high concentrations, namely 62.5, 800 and 3200 ng/ml respectively. The measured concentrations and calculated accuracy for the test samples, after three freeze and thaw cycles, are presented in Table 5.15. The precision and accuracy for LF tested at the three different concentrations are acceptable, which indicates that LF is stable for at least three freeze and thaw cycles.

Table 5.15: Freeze and thaw stability of LF in mouse WB

Low concentration (62.5ng/ml)		Medium concentration (800ng/ml)		High concentration (3200ng/ml)	
Observed mean QC conc. (ng/ml)	Observed F/T conc. (ng/ml)	Observed mean QC conc. (ng/ml)	Observed F/T conc. (ng/ml)	Observed mean QC conc. (ng/ml)	Observed F/T conc. (ng/ml)
49.4		800		3236.6	
Sample 1	52.5		729		3230
Sample 2	50.4		744		3280
Sample 3	48.4		803		3300
Sample 4	49.2		779		3380
Sample 5	49.3		765		2950
Average	50	Average	764.2	Average	3181.7
STDEV	1.43	STDEV	26.0	STDEV	185.8
CV (%)	2.9	CV (%)	3.4	CV (%)	5.8
Accuracy (%)	101.3	Accuracy (%)	95.5	Accuracy (%)	98.3

On-bench stability

The measured concentrations and calculated accuracies for the test samples are presented in Table 5.16. A % CV of more than 15% and an accuracy deviating more than 15% of the observed mean QC concentration could indicate on-bench instability of LF in mouse WB. The analyte in mouse WB at low, medium and high concentrations was found to be stable at room temperature for six hours.

Table 5.16: On bench (at room temperature) stability of LF in mouse WB

	Low (62.5ng/ml)		Medium (800ng/ml)		High (3200ng/ml)	
	Observed mean QC conc. (ng/ml)	Observed B/T conc. (ng/ml)	Observed mean QC conc. (ng/ml)	Observed B/T conc. (ng/ml)	Observed mean QC conc. (ng/ml)	Observed B/T conc. (ng/ml)
	62.09		800		3228.16	
Sample 1		59		817		3220
Sample 2		59.3		814		3160
Sample 3		59.9		827		3160
Sample 4		62		808		3160
Sample 5		66.1		824		3150
	Average	61.3	Average	818	Average	3170
	STDEV	2.95	STDEV	7.65	STDEV	28.3
	CV (%)	4.8	CV (%)	0.9	CV (%)	0.9
	Accuracy (%)	98.7	Accuracy (%)	102.3	Accuracy (%)	98.2

On-Instrument stability

A % CV and accuracy deviation higher than 15% of the measured ratio values could indicate on-instrument instability. As seen in Table 5.17, extracted WB samples containing the analyte is stable on instrument for 24 hours, with acceptable precision and a calculated 5.2% difference to initial measured concentrations.

Table 5.17: On-instrument stability for extracted samples: Medium concentration - 800ng/ml

	Peak area	ISTD peak area	Ratio		Peak area	ISTD peak area	Ratio
Sample 1	52700	284000	0.186	Sample 1	40200	211000	0.191
Sample 2	50900	285000	0.179	Sample 2	39900	215000	0.186
Sample 3	50800	285000	0.178	Sample 3	39500	207000	0.191
Sample 4	51600	285000	0.181	Sample 4	40100	209000	0.192
Sample 5	49300	281000	0.175	Sample 5	38800	208000	0.187
Average	51060	284000	0.180	Average	39700	210000	0.189
STDEV	1242.2	1732.1	0.004	STDEV	570.1	3162.3	0.003
CV (%)	2.4	0.6	2.1	CV (%)	1.4	1.5	1.5
Accuracy after 24 hrs (%)							105.2
Difference (%)							5.2

Specificity

A representative chromatogram of STD 1 (LLOQ) is presented in Figure 5.9, indicating no interfering peaks. The method is specific for the quantitation of LF from mouse WB samples.

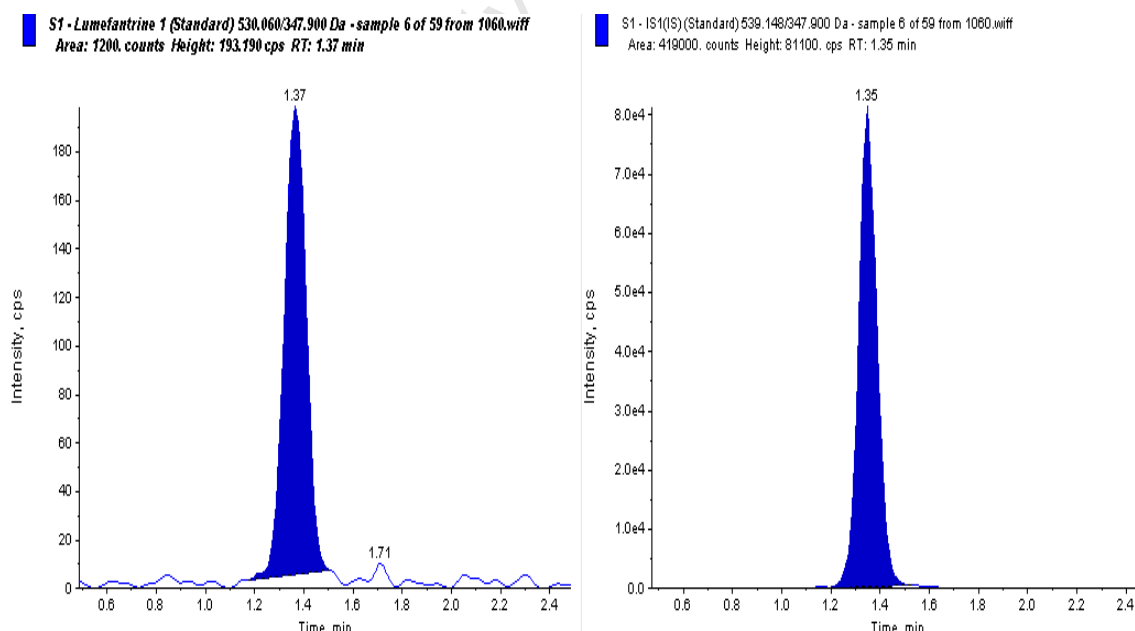


Figure 5.9: Chromatogram of a LF in WB sample, at LLOQ level

Carry-over

As shown in Table 5.18, a 9.3% carryover was calculated using equation 5.1 (refer to page 70) and is within the acceptable limit ($\leq 20\%$). As presented in Figure 5.10 and 5.11, no significant carryover or contamination was observed in the extracted double blank (no analyte and no ISTD) or blank (no analyte) WB samples.

Table 5.18: Calculation of carryover of LF in mouse WB

	Analyte peak area counts
Blank	115
LLOQ (STD 1)	1235
% Carryover	9.31

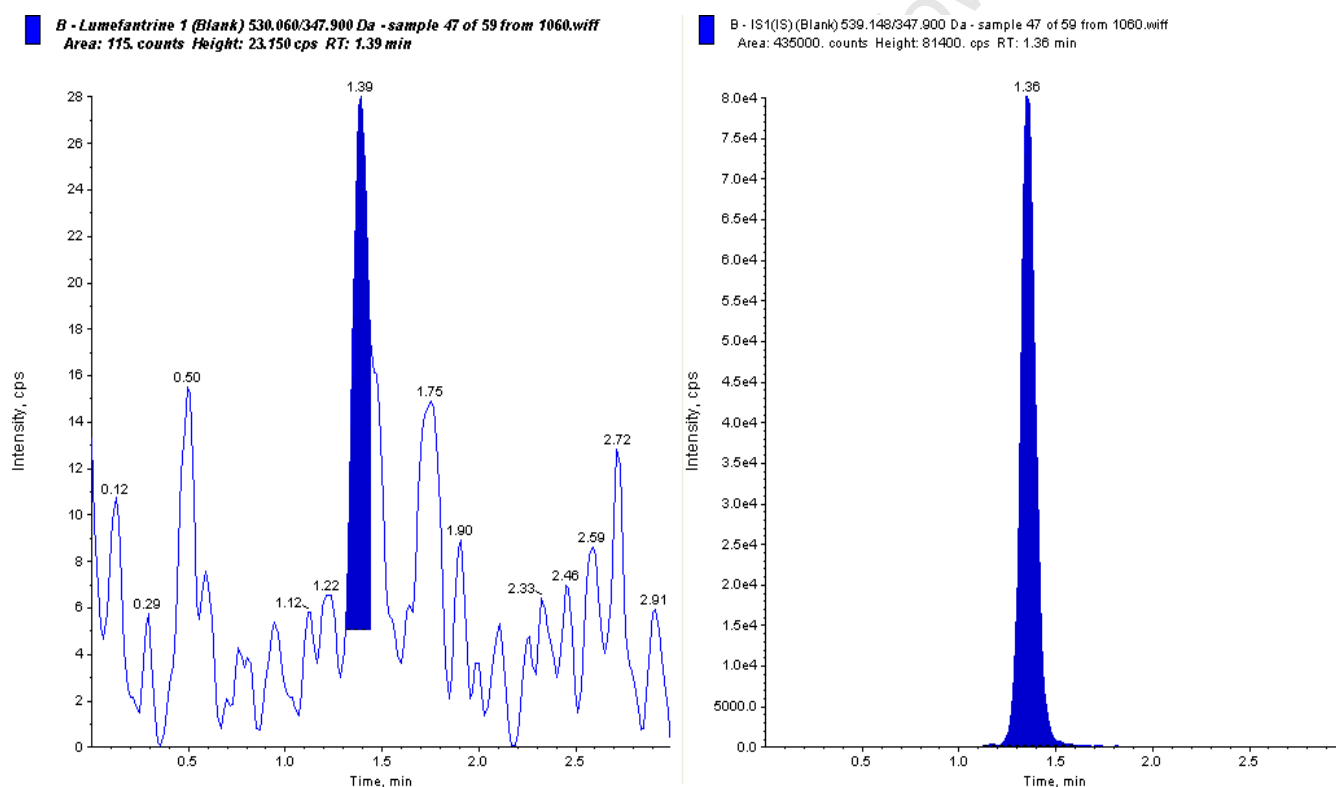


Figure 5.10: A representative chromatogram of a blank extracted WB sample situated after the ULOQ (STD 9), in the analytical batch list. The analyte peak was manually integrated to calculate percentage carryover.

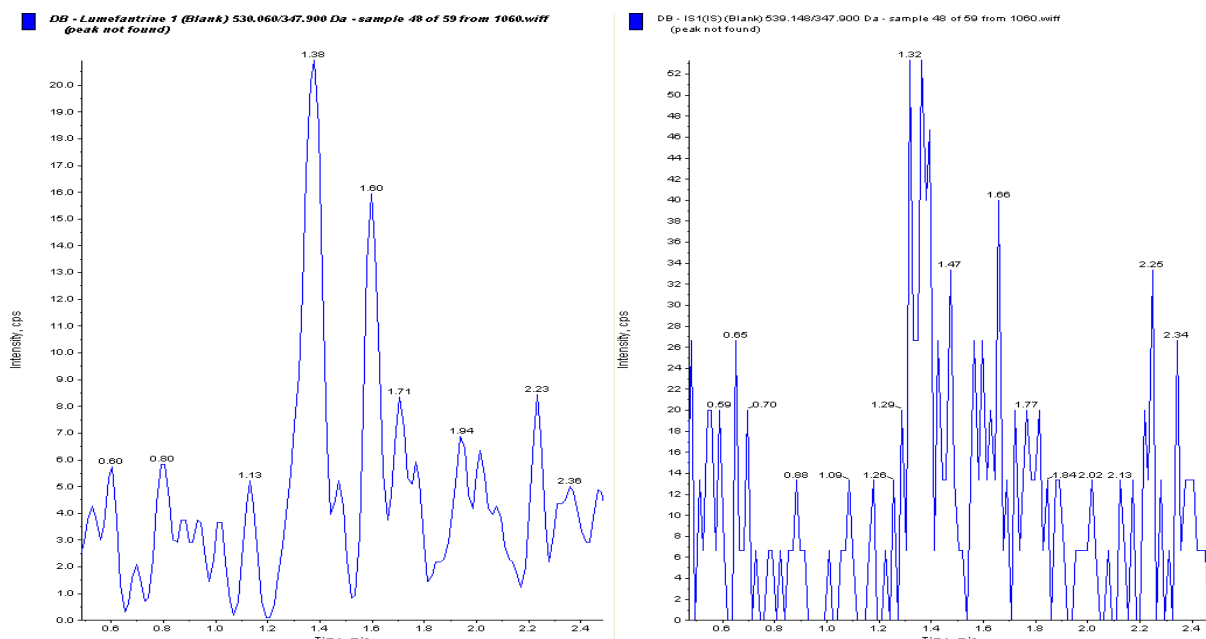


Figure 5.11: Chromatogram of a double blank (no analyte and no ISTD) WB extract

Sensitivity

As presented in Figure 5.12, the calculated analyte signal/noise ratio for LF at LLOQ is 23.7, which indicates that the method is sensitive for LF quantification and not affected by interference at low analyte concentrations.

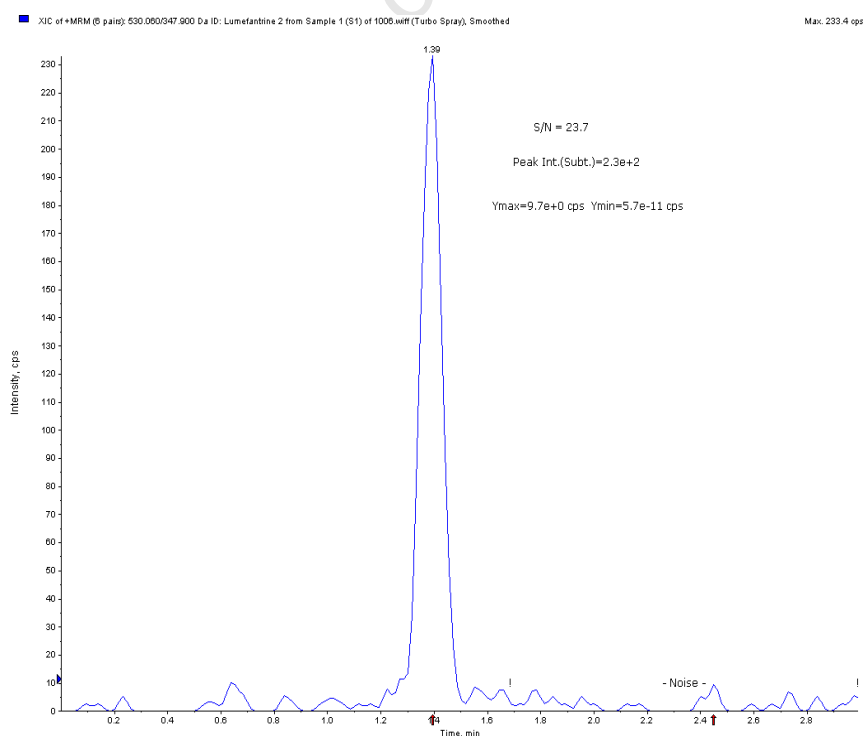


Figure 5.12: Raw chromatogram of LF at LLOQ with calculated analyte signal/noise ratio of 23.7:1

Recovery (RE)

The analyte RE was calculated and expressed as a percentage using Equation 5.2 (refer to page 71). As presented in Table 5.19, the mean recovery of LF from mouse WB over the calibration range, 15.6-4000 ng/ml is 95% with a % CV of 12%. The extraction method has demonstrated acceptable recovery.

Table 5.19: Recovery calculation results for LF extraction from mouse WB

	Low concentration		Medium Concentration		High Concentration		
	Reference peak area	Test peak area (50ng/ml)	Reference peak area	Test peak area (800ng/ml)	Reference peak area	Test peak area (3200ng/ml)	
Sample 1	6575	5880	79875	85800	243750	204000	
Sample 2	6275	6240	79125	86000	241250	190000	
Sample 3	6375	6590	82375	87900	246250	203000	
Sample 4	6350	5610	78875	81800	243750	203000	
Sample 5	6225	6010	81500	86300	236250	207000	
Sample 6	6325	5870	81500	86900	232500	200000	
Average	6354.2	6033.3	80541.7	85783.3	240625	201166.7	
STDEV	120.8	341.3	1444.1	2093.2	5229.1	5913.3	
CV (%)	1.9	5.7	1.8	2.4	2.2	2.9	
Recovery (%)	95.0		106.5			83.6	
						Mean Recovery (%)	95.0
						STDEV	11.5
						CV (%)	12.1

Matrix effects

The analysis was performed using Microsoft Excel 2010, the results are presented in Table 5.20 and the overall % CV of the slopes is calculated and presented graphically in Figure 5.13. The quantity r is known as the correlation coefficient and the value range is $-1 \leq r \leq 1$. In this case r describes the strength of the linear association between the nominal LF concentration and the calculated LF/ISTD ratios. As shown in Table 5.20, the r values for the six different lots of matrix is equal to or close to 1, indicating a strong positive linear relationship between the two variables and it may be deduced that any variance in the LF/ISTD ratio values may be related to analyte concentration and not ME. The calculated precision of the slopes for six different WB (matrix) sources is expressed as a % CV of 3.9%, which indicates that LF quantification from different sources is precise and reproducible with no significant ME on the quantitation of LF.

Table 5.20: Mean LF / ISTD peak area ratios and the precision (expressed as % CV) of slopes of lines fitted through low, medium and high samples of LF in six different lots of WB.

	Concentration (ng/ml)			Slope	r
	62.5	800	3200		
Matrix 1	0.129	1.98	9.07	0.0029	0.9996
Matrix 2	0.132	2.12	8.70	0.0027	1.0000
Matrix 3	0.132	2.07	8.27	0.0026	1.0000
Matrix 4	0.127	2.00	8.31	0.0026	1.0000
Matrix 5	0.130	2.04	8.40	0.0026	1.0000
Matrix 6	0.131	1.98	8.45	0.0027	0.9999
Average	0.13	2.03	8.53	0.0027	
STDEV	0.00	0.057	0.301	0.0001	
CV (%)	1.4	2.8	3.5	3.9	

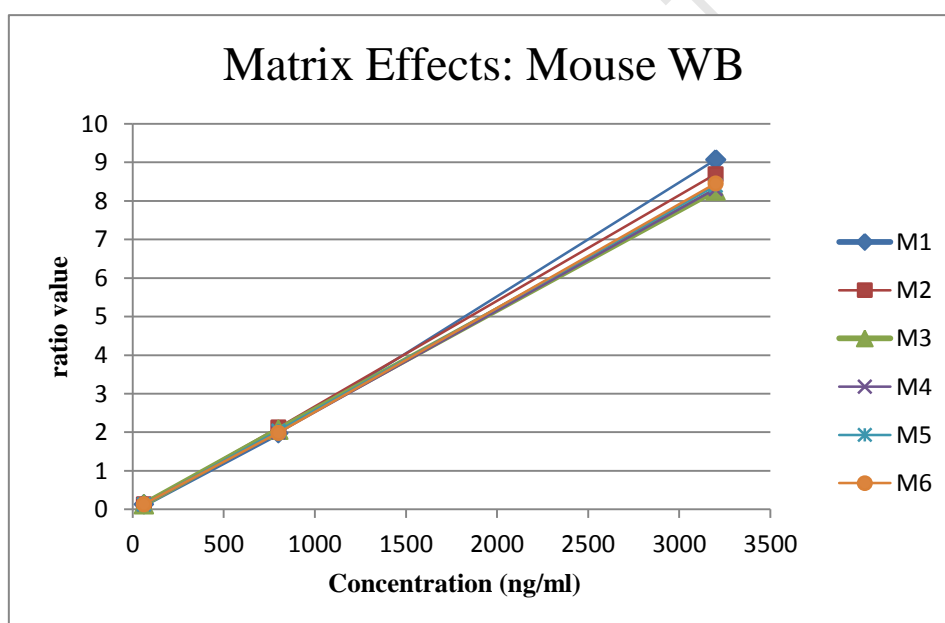


Figure 5.13: Slopes of LF/ISTD peak ratios at three concentrations for six different lots of mouse WB.

5.3.2 Validation of the LC-MS/MS method for the quantitation of LF in mouse plasma

Intra-batch accuracy and precision

As seen in Table 5.21 and Table 5.22, all the STDs and QCs for the first validation run have acceptable precision and accuracy measures. This indicates that the method is accurate, precise and sensitive for the duration of one validation run.

Table 5.21: Accuracy and precision of LF calibration standards for plasma validation 1

Sample ID	Nominal Conc. (ng/ml)	Mean observed conc. (ng/ml)	Standard Deviation	Accuracy (%)	CV (%)	n
S1	15.6	13.9	0.855	89.2	6.1	2
S2	31.3	30.4	0.763	97.3	2.5	2
S3	62.5	67.0	1.74	107.2	2.6	2
S4	125	129.6	0.767	103.7	0.6	2
S5	250	257.7	1.04	103.1	0.4	2
S6	500	508.2	2.65	101.6	0.5	2
S7	1000	988.8	35.3	98.9	3.6	2
S8	2000	1974.4	88.8	98.7	4.5	2
S9	4000	4014.5	44.8	100.4	1.1	2

Table 5.22: Summary of LF intra-validation quality control standards for plasma validation 1

Sample ID	Nominal Conc. (ng/ml)	Mean observed conc. (ng/ml)	Standard Deviation	Accuracy (%)	CV (%)	n
QC L2	25	22.0	1.32	88.0	6.0	6
QC L1	50	46.1	1.85	92.2	4.0	6
QC M	1600	1548.8	20.0	96.8	1.3	6
QC H	3200	3126.3	81.7	97.7	2.6	6
SYS	200	181.4	6.23	90.7	3.4	6

Inter-batch accuracy and precision

As seen in Tables 5.23 to 5.26, the method has performed adequately as all the STDs and QCs have a calculated % CV of less than 15%. The calculated accuracy, for all STDs and QCs including the LLOQ, is within 15% of the nominal concentration values. The bioanalytical method has demonstrated reproducible precision, accuracy and sensitivity.

Table 5.23: Accuracy and precision of LF calibration standards for plasma validation 2

Sample ID	Nominal Conc. (ng/ml)	Mean observed conc. (ng/ml)	Standard Deviation	Accuracy (%)	CV (%)	n
S1	15.6	14.2	1.28	91.0	9.0	2
S2	31.3	32.5	0.539	103.8	1.7	2
S3	62.5	63.4	4.49	101.4	7.1	2
S4	125	134.5	11.9	107.6	8.8	2
S5	250	243.9	6.31	97.6	2.6	2
S6	500	504.7	18.8	100.9	3.7	2
S7	1000	949	5.67	94.9	0.6	2
S8	2000	2059.8	52.0	103.0	2.5	2
S9	4000	3982.0	150.5	99.6	3.8	2

Table 5.24: Summary of LF inter-validation quality control standards for plasma validation 2

Sample ID	Nominal Conc. (ng/ml)	Mean observed conc. (ng/ml)	Standard Deviation	Accuracy (%)	CV (%)	n
QC L2	25	23.4	2.32	93.8	9.9	6
QC L1	50	47.2	3.84	94.3	8.1	6
QC M	1600	1459.5	46.1	91.2	3.2	6
QC H	3200	3047.1	97.2	95.2	3.2	6
SYS	200	186.2	6.32	93.1	3.4	6

Table 5.25: Accuracy and precision of LF calibration standards for plasma validation 3

Sample ID	Nominal Conc. (ng/ml)	Mean observed conc. (ng/ml)	Standard Deviation	Accuracy (%)	CV (%)	n
S1	15.6	16.1	0.432	103.3	2.7	2
S2	31.3	30.1	3.80	96.3	12.6	2
S3	62.5	64.0	2.49	102.3	3.9	2
S4	125	125.8	4.36	100.6	3.5	2
S5	250	250.5	8.03	100.2	3.2	2
S6	500	486.6	19.8	97.3	4.1	2
S7	1000	976.9	78.5	97.7	8.0	2
S8	2000	2054.4	77.2	102.7	3.8	2
S9	4000	3980.1	178.0	99.5	4.5	2

Table 5.26: Summary of LF inter-validation quality control standards for plasma validation 3

Sample ID	Nominal Conc. (ng/ml)	Mean observed conc. (ng/ml)	Standard Deviation	Accuracy (%)	CV (%)	n
QC L2	25	23.3	1.17	93.1	5.0	6
QC L1	50	48.0	3.38	96.0	7.0	6
QC M	1600	1477.3	78.4	92.3	5.3	6
QC H	3200	3042.6	91.7	95.1	3.0	6
SYS	200	185.7	17.2	92.9	9.3	6

Summary of combined quality control results

A summarised analysis of the QC standards for the three validation runs is presented in Table 5.27. Results from the validation assays indicate that the method is accurate and precise for LF quantification with a valid calibration range of 15.6 – 4000 ng/ml.

Table 5.27: Summary of combined QC results for the three validation runs

Validation Batch	Nominal Replicates	QC L2 (25ng/ml)	QC L1 (50ng/ml)	QC M (1600ng/ml)	QC H (3200ng/ml)
		Observed Concentration (ng/ml)			
Validation 1	1	21.7	45.8	1590	3220
	2	21.6	47.4	1550	3120
	3	22.1	47.7	1530	2990
	4	20.4	47.9	1540	3190
	5	24.4	43.6	1530	3150
	6	21.8	44.2	1550	3090
Validation 2	1	21.3	44.9	1500	3120
	2	23.1	44.1	1520	3000
	3	22.7	45.9	1420	2910
	4	22.7	44	1410	3190
	5	22.9	51.2	1480	3040
	6	28	52.8	1430	3020
Validation 3	1	22.9	52.6	1480	2880
	2	24	46.8	1370	3110
	3	21.5	42.9	1550	3050
	4	24.2	46.4	1570	3140
	5	22.4	50.2	1410	3020
	6	24.5	49	1480	3050
Average		23.0	47.1	1495.0	3071.7
STDEV		1.74	3.14	61.2	88.7
CV (%)		7.6	6.7	4.1	2.9
Accuracy (%)		91.9	94.2	93.4	96.0

Stock solution stability

The stability of the analyte in solution was tested at a concentration of 500 ng/ml at ambient temperature (16°C) and control (-20°C) conditions and compared to freshly prepared stock solutions. The peak areas of the test and control samples compared to the reference samples are presented in Table 5.28. Under test (ambient temperature) conditions, the % CV and accuracy for the analyte was 3.25% and 99.6% respectively. Under control conditions; analyte stock solution stored at -20°C, the % CV and accuracy was 3.82% and 99.6%, respectively. These results indicate that the analyte is stable in stock solution when stored at room temperature and -20°C for 6 hours.

Table 5.28: Stock solution stability assessment at 500 ng/ml

		Reference	Test (16°C)	Controls (-20°C)
Medium conc.	Peak area 1	199000	190000	201000
	Peak area 2	196000	184000	180000
	Peak area 3	189000	180000	191000
	Peak area 4	196000	194000	185000
	Peak area 5	166000	186000	185000
	Peak area 6	189000	196000	188000
	Average	189166.7	188333.3	188333.3
	STDEV	12056.8	6121.0	7201.9
	CV (%)	6.4	3.3	3.8
	Accuracy (%)		99.6	99.6

Freeze-Thaw stability

The test results are presented in Table 5.29. The precision and accuracy for LF tested at the three different concentrations are acceptable, which indicates the analyte is stable in plasma for at least three freeze and thaw cycles.

Table 5.29: Freeze and thaw stability of LF

	Low concentration (50ng/ml)		Medium concentration (800ng/ml)		High concentration (3200ng/ml)	
	Observed mean QC conc. (ng/ml)	Observed F/T conc. (ng/ml)	Observed mean QC conc. (ng/ml)	Observed F/T conc. (ng/ml)	Observed mean QC conc. (ng/ml)	Observed F/T conc. (ng/ml)
	47.2		760.0		3047.1	
Sample 1		46.6		683		3000
Sample 2		47.8		664		2880
Sample 3		54.7		746		3010
Sample 4		45.9		710		3020
Sample 5		51.2		709		3060
Sample 6		45.4		751		2720
	Average	48.6	Average	710.5	Average	2948.3
	STDEV	3.64	STDEV	34.1	STDEV	127.2
	CV (%)	7.5	CV (%)	4.8	CV (%)	4.3
	Accuracy (%)	103.0	Accuracy (%)	93.5	Accuracy (%)	96.8

On-bench stability

The test results are presented in Table 5.30. The analyte in mouse plasma at low, medium and high concentrations was found to be stable at ambient temperature (16°C) for 6 hours.

Table 5.30: On bench (at ambient temperature) stability of LF

	Low concentration (50ng/ml)		Medium concentration (800ng/ml)		High concentration (3200ng/ml)	
	Observed mean QC conc. (ng/ml)	Observed B/T conc. (ng/ml)	Observed mean QC conc. (ng/ml)	Observed B/T conc. (ng/ml)	Observed mean QC conc. (ng/ml)	Observed B/T conc. (ng/ml)
	47.2		782.7		3047.1	
Sample 1		48.4		838		3080
Sample 2		49.7		746		2910
Sample 3		46.5		714		2910
Sample 4		45.2		738		2830
Sample 5		44.6		753		2980
Sample 6		46.8		694		2720
	Average	46.9	Average	747.2	Average	2905
	STDEV	1.92	STDEV	49.6	STDEV	123.4
	CV (%)	4.1	CV (%)	6.6	CV (%)	4.2
	Accuracy (%)	99.3	Accuracy (%)	95.5	Accuracy (%)	95.3

On-Instrument stability

A % CV and difference higher than 15% of the measured ratio values could indicate on-instrument instability. The results are presented in Table 5.31. The reported peak area values for both the analyte and ISTD were reduced by approximately 50% over the 24 hour test period. This occurrence was not observed for LF in WB and was therefore most likely due to a drop in instrument sensitivity rather than analyte instability. The extracted plasma samples containing the analyte LF at a medium concentration of 800 ng/ml, are stable on instrument (in the sample inlet compartment) for 24 hours, the % CV is 3.61% and there is a 1.74% difference to the analyte concentrations measured initially.

Table 5.31: On-Instrument stability for extracted samples containing LF at a concentration of 800 ng/ml

	Peak area	ISTD peak area	Ratio		Peak area	ISTD peak area	Ratio
Sample 1	77300	611000	0.127	Sample 1	36100	289000	0.125
Sample 2	74200	610000	0.122	Sample 2	35600	284000	0.125
Sample 3	75100	610000	0.123	Sample 3	36000	302000	0.119
Sample 4	74700	597000	0.125	Sample 4	41100	312000	0.132
Sample 5	74700	599000	0.125	Sample 5	41100	315000	0.130
Sample 6	74900	593000	0.126	Sample 6	42600	331000	0.129
Average	75150	603333.3	0.125	Average	38750	305500	0.127
STDEV	1095	7916.2	0.002	STDEV	3174.1	17490	0.005
CV (%)	1.5	1.3	1.5	CV (%)	8.2	5.7	3.6
Accuracy after 24 hrs (%)							101.7
Difference (%)							1.7

Specificity

A representative chromatogram of STD 1 (LLOQ) is presented in Figure 5.14, indicating no interfering peaks. The method is specific for the quantitation of LF.

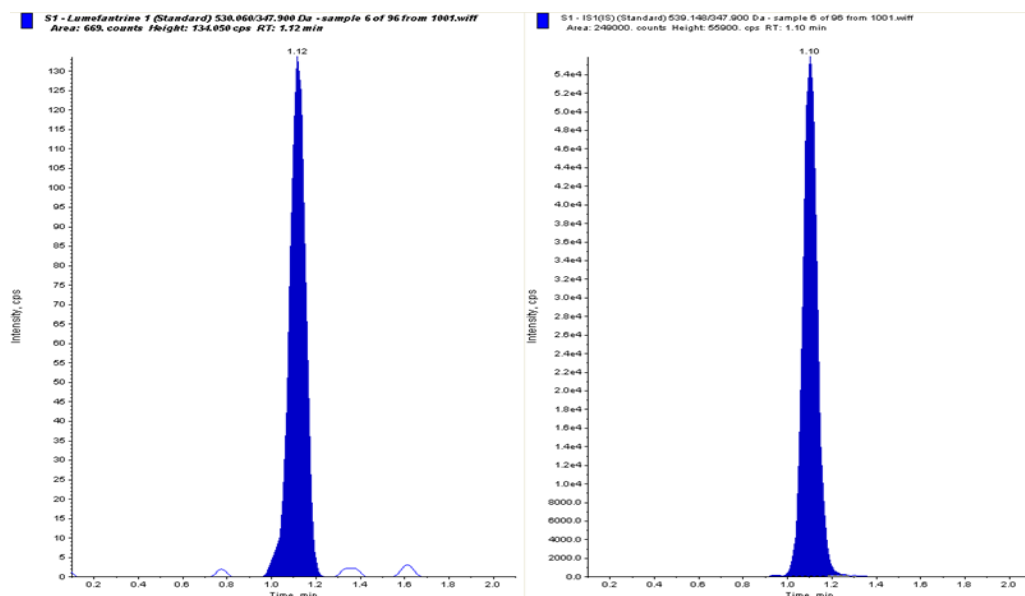


Figure 5.14: Representative chromatogram of LF at LLOQ (STD1)

Carry over

As shown in Table 5.32, the calculated carryover, using equation 5.1 (refer to page 70), is 6.4%. As presented in Figure 5.15 and 5.16, no significant carryover or contamination was observed in the double blank (no analyte and no ISTD) or blank (no analyte) samples.

Table 5.32: Calculated carryover of LF in plasma

	Analyte peak area counts
Blank	40.9
LLOQ (STD 1)	644
% Carryover	6.35

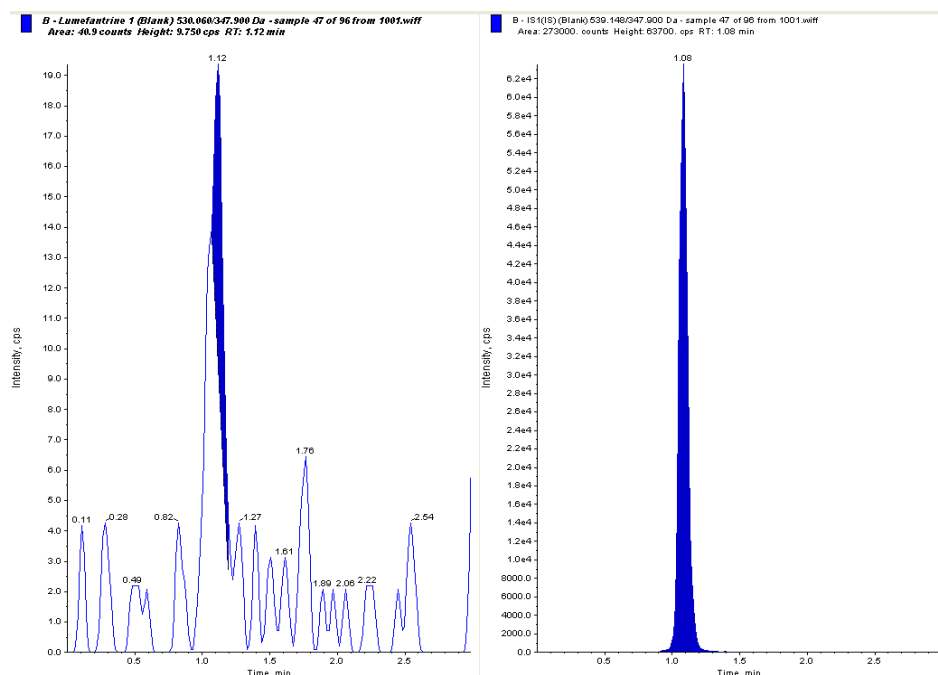


Figure 5.15: A representative chromatogram of a blank extracted plasma sample situated after the standard with the highest analyte concentration (STD 9), in the analytical batch list. The analyte peak was manually integrated to calculate percentage carryover.

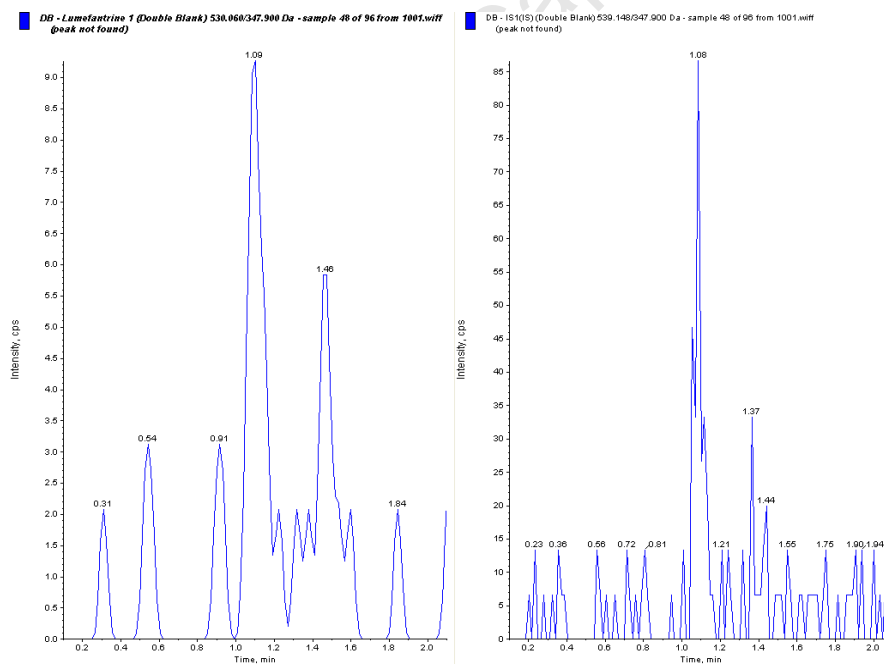


Figure 5.16: Representative chromatogram of a double blank extracted plasma sample, with no LF peak at 1.12 min.

Sensitivity

The method is sensitive for the quantitation of LF, with no interference at the lowest level of quantitation; 15.6 ng/ml. The analyte signal/noise ratio calculated from the LLOQ chromatogram should be larger than 5:1. The calculated analyte signal/noise ratio for LF at LLOQ is 29.5:1 as presented in Figure 5.17.

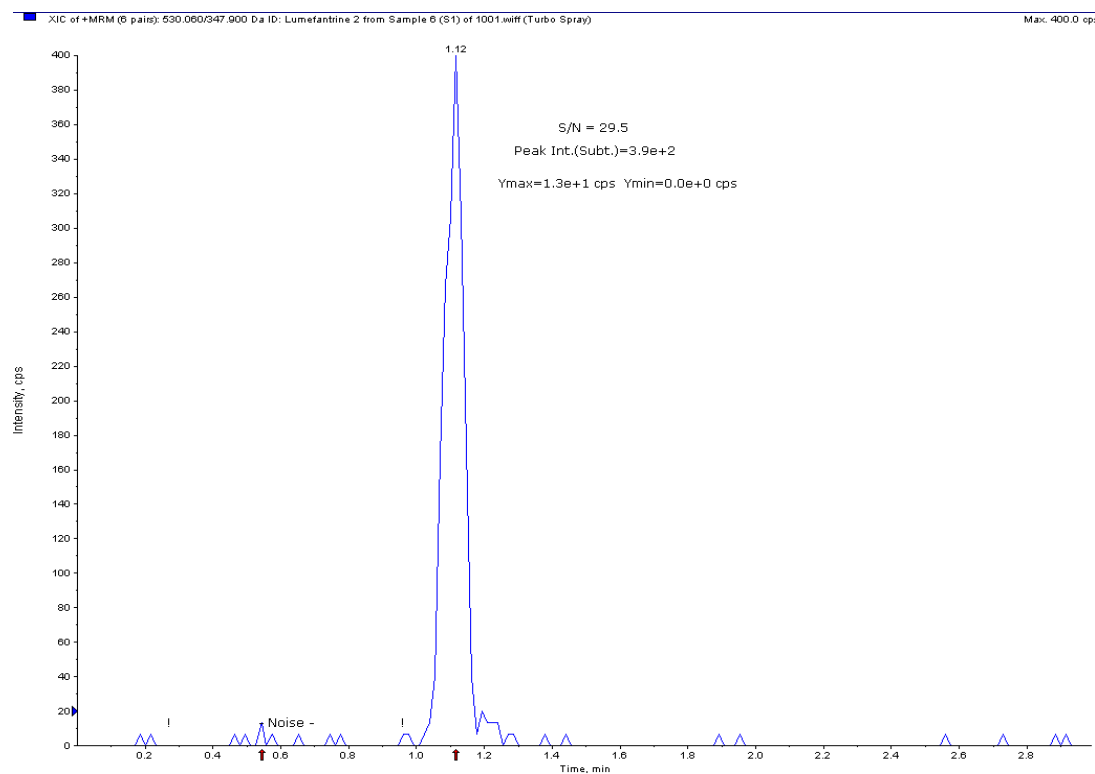


Figure 5.17: Raw chromatogram of LF at LLOQ with calculated analyte signal/noise of 29.5:1

Recovery (RE)

The analyte RE was calculated and expressed as a percentage using Equation 5.2 (refer to page 71). Presented in Table 5.33 are the peak area values for the reference and test samples at low, medium and high analyte concentrations. The extraction method has demonstrated acceptable precision and analyte recovery from mouse plasma with a calculated mean recovery of 108.2% and % CV of 6.5%.

Table 5.33: Recovery data for LF in plasma at low, medium and high concentrations

	Low Concentration		Medium Concentration		High Concentration	
	Corrected Ref. Peak Area	Test Peak Area (50ng/ml)	Corrected Ref. Peak Area	Test Peak Area (800ng/ml)	Corrected Ref. Peak Area	Test Peak Area (3200ng/ml)
	2060	1920	28700	29400	96600	110000
	1970	1960	28600	31600	98200	116000
	2030	2080	28700	33300	96900	109000
	1670	1700	29900	33700	97200	107000
	1800	1920	30300	32500	97100	113000
Average	1906.0	1916.0	29240.0	32100	97200	111000
STDEV	165.9	137.4	798.7	1710.3	604.2	3535.5
CV (%)	8.71	7.17	2.73	5.33	0.622	3.19
Recovery (%)	100.5		109.8		114.2	
					Mean Recovery (%)	108.2
					STDEV	6.98
					CV (%)	6.5

Matrix effects (ME)

The analysis was performed using Microsoft Excel 2010. The results are presented in Table 5.34 and the overall CV (%) of the slopes is calculated and presented in Figure 5.18, the variability or coefficient of variation (CV) of the slopes should not exceed 5%. The calculated variability of the slopes for six different plasma sources is 3.75%, which indicates that LF quantification from different mouse plasma sources is reproducible. As shown in Table 4.33, the correlation coefficient (r) values for the six different lots of matrix is equal to or close to 1, indicating a strong linear relationship between the two variables and it may be deduced that any variance in the LF/ISTD ratio values may be related to analyte concentration and not ME.

Table 5.34: Mean LF / ISTD peak area ratios and the precision (expressed as % CV) of slopes of lines fitted through low, medium and high samples of LF in six different lots of mouse plasma.

	Concentration (ng/ml)			Slope	r
	50	800	3200		
Matrix 1	0.177	3.07	10.7	0.0033	0.999
Matrix 2	0.196	2.95	10.3	0.0032	0.999
Matrix 3	0.173	2.73	10.8	0.0034	1.00
Matrix 4	0.191	2.73	11.3	0.0035	1.00
Matrix 5	0.171	2.87	10.7	0.0033	1.00
Matrix 6	0.177	2.79	10.5	0.0033	1.00
Average	0.181	2.86	10.7	0.0033	
STDEV	0.010	0.134	0.345	0.0001	
CV (%)	5.8	4.7	3.2	3.8	

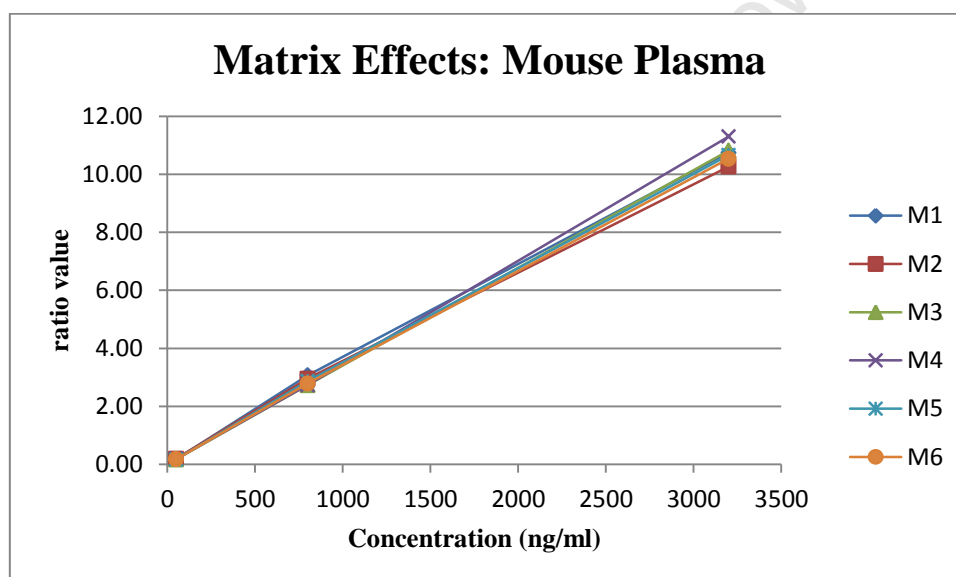


Figure 5.18: Slopes of analyte/ISTD peak ratios at three concentrations for six different lots of mouse plasma.

5.4 Discussion

The accuracy and precision of the developed LC-MS/MS method for quantitating LF in mouse WB and plasma was assessed over three consecutive, independent validation runs and the method was found to be acceptable and reproducible, according to FDA guidelines. A concentration range of 15.6 - 4000 ng/ml was validated for the quantitation of LF in mouse WB and plasma. Stable isotope labelled LF was used as the ISTD and the calibration curve was constructed based on the calculated ratio of the signal intensities of the analyte, LF and the ISTD, D₉-LF. The stable isotope-labelled ISTD compensates for variations that occur during analysis, such as variations in sample injection volume and fluctuations in detector sensitivity (de Hoffmann and Stroobant, 2007). This was amply demonstrated in the present work as variations in LF and D₉-LF concentrations were comparable throughout the analysis. No substantial matrix effects influencing LF quantitation was found, however the detection signal did vary from day to day as demonstrated with the on-instrument analysis. This may be due to matrix components, thus the use of a stable isotope labelled ISTD may prove invaluable to overcome ion suppression and ensure the reproducibility of this quantitative method. The use of a stable isotope labelled LF as the ISTD was shown to eliminate the influence of matrix effects and ionization saturation when quantitating LF in human plasma (Huang *et al.*, 2012).

The mean recovery for LF was 95 and 108.2% for WB and plasma, respectively which is encouraging considering the simple protein precipitation extraction method used. Cesar *et al.* used a protein precipitation extraction method and reported recovery values for LF ranging from 81.4 to 83.2% (Cesar *et al.*, 2011). Munjal *et al.* also used a protein precipitation extraction method and reported a mean LF recovery of 58.8% (Munjal *et al.*, 2010). The longer sample mixing and sonication times incorporated in the developed extraction method may be responsible for the higher analyte recoveries achieved when compared to the extraction method used by Munjal *et al.*.

The developed LC-MS/MS methods, using a stable isotope labelled LF as ISTD, are sensitive and selective for the quantitation of LF. The analyte, LF was shown to be stable in mouse WB and plasma and the quantitation of LF was proven to be reproducible throughout the validation process as well as the stability assessments.

Long term stability of frozen stored WB/plasma samples was not assessed in this validation, primarily due to the fact that a small amount of biological matrix was sampled and repeat

analysis was not a feasible option. Also the samples were only stored at -80°C for a short period of time before analysis. The long term stability of LF has however been assessed and published in other scientific articles. Wahajuddin *et al.* reported that LF was stable in rat plasma, when stored in a freezer at -80°C \pm 10°C for 15 days (Wahajuddin *et al.*, 2009). Lindergardh *et al.* reported no significant loss of LF after storage in plasma at -80°C and -20°C for 4 months (Lindergardh *et al.*, 2005).

There are currently no published LC-MS/MS methods for the quantitation of LF in mouse WB or plasma. As presented in Table 5.35, the developed and validated methods, reported here, are accurate and precise for the quantitation of LF using lower sample volumes, simpler and more cost effective sample extraction procedures, and a minimal run time of 3 minutes when compared to the published LC-MS/MS methods.

Table 5.35: A comparison between published and currently presented (in blue) LC-MS/MS methods for LF

Reference	Year	Extraction Method	Conc. range (ng/ml)	Sample Vol. (µl)	Injection Vol. (µl)	LC Analytical Column	Flow rate (ml/min)	Sample run time (min)	Biological Matrix
Wahajuddin <i>et al.</i>	2009	Liquid-Liquid	2-500	100	10	C ₁₈	0.5	5	rat plasma
Hodel <i>et al.</i>	2009	Protein prec.	4-4000	200	10	C ₁₈	0.3	17	human plasma
Munjal <i>et al.</i>	2010	Protein prec.	210-25050	100	5	C8	0.6	2.9	human plasma
Cesar <i>et al.</i>	2011	Protein prec.	10-18000	250	50	Zorbax SB-Cyano	1	9	human plasma
Sethi <i>et al.</i>	2011	SPE	2-2000	100	10	Xterra RP18	0.5	15	human plasma
Huang <i>et al.</i>	2012	Liquid-Liquid	50-20000	25	10	Zorbax C ₁₈	0.4	8	human plasma
Present study	2012	Protein prec.	15.6-4000	20	2	PFP (2)	0.5	3	mouse plasma and WB

Most methods for the quantification of drugs are developed and validated in plasma; however drug levels may differ with different biological matrices and anticoagulants. Drug analysis should thus be performed using methods that have been validated in the same biological matrix as the test samples. In the following chapter the developed LC-MS/MS methods have been applied in a bioavailability study in mice to quantitate LF in mouse WB and plasma.

References

1. Cesar I.C., de Aquino Ribeiro J.A., de Souza Teixeira L., Bellorio K.B., de Abreu F.C., Moreira J.M., Chellini P.R. and Pianetti G.A. Liquid-chromatography-tandem mass spectrometry for the simultaneous quantitation of artemether and lumefantrine in human plasma: Application for a pharmacokinetic study. *Journal of Pharmaceutical and Biomedical Analysis*, 54 (2011) 114-120
2. Gross J. *Mass Spectrometry* (2011). 2nd Edition. Springer-Verlag, Berlin Heidelberg
3. Guidance for Industry: Bioanalytical Method Validation (2001) <http://www.fda.gov/downloads/Drugs/GuidanceComplianceRegulatoryInformation/Guidances/ucm070107.pdf>
4. Hodel E.M., Zanolari B., Mercier T., Biollaz J., Keiser J., Olliaro P., Genton B. and Decosterd L.A. A single LC-tandem mass spectrometry method for the simultaneous determination of 14 antimalarial drugs and their metabolites in human plasma. *Journal of Chromatography B*, 877 (2009) 867-886
5. de Hoffmann E. and Stroobant V. *Mass Spectrometry Principles and Applications* (2007). 3rd Edition. Wiley
6. Huang L., Li X., Marzan F., Lizak P.S. and Aweeka F.T. Determination of lumefantrine in small-volume human plasma by LC-MS/MS: using a deuterated lumefantrine to overcome matrix effect and ionization saturation. *Bioanalysis*, 4:2 (2012) 157-166
7. Jemal M. High throughput quantitative bioanalysis by LC/MS/MS. *Biomedical Chromatography*, 14 (2000) 422-429
8. Lindergardh N., Annerberg A., Blessborn D., Bergqvist Y., Day N. and White N.J. Development and validation of a bioanalytical method using automated solid-phase extraction and LC-UV for the simultaneous determination of lumefantrine and its desbutyl metabolite in plasma. *Journal of Pharmaceutical and Biomedical Analysis*, 37 (2005) 1081-1088
9. Matuszewski B.K., Constanzer M.L. and Chavez-Eng C.M. Strategies for the assessment of matrix effect in quantitative bioanalytical methods based on HPLC-MS/MS. *Analytical Chemistry*, 71:13 (2003) 3019-3030
10. Matuszewski B.K. Standard line slopes as a measure of a relative matrix effect in quantitative HPLC-MS bioanalysis. *Journal of Chromatography B*, 830 (2006) 293-300
11. Morin L.P., Taillon M.P., Furtado M. and Garafolo F. An alternative solution to overcome carryover issues in bioanalysis. *Bioanalysis*, 4:2 (2012) 133-141
12. Munjal V., Paliwal N., Chaurasia B.K., Varshney B., Ahmed T. and Paliwal J. LC-tandem mass spectrometry method for quantification of lumefantrine in human plasma and its application to bioequivalence study. *Chromatographia*, 71:5/6 (2010) 505-510
13. Niessan W.M.A. *Liquid Chromatography-Mass Spectrometry* (2006). 3rd Edition. Taylor & Francis Group
14. Sethi P., Dua V.K. and Jain R. A LC-MS/MS method for the determination of lumefantrine and its metabolite desbutyl-lumefantrine in plasma from patients infected with *Plasmodium falciparum* malaria. *Journal of Liquid Chromatography & Related Technologies*, 34:20 (2011) 2674-2688
15. Viswanathan C.T., Bansal S., Booth B., DeStefano A.J., Rose M.J., Sailstad J., Shah V.P., Skelly J.P., Swann P.G. and Weiner R. Quantitative bioanalytical methods validation and implementation: best practices for chromatographic and ligand binding assays. *Pharmaceutical Research*, 24:10 (2007) 1962-1972
16. Wahajuddin, Singh S.P. and Jain G.K. Determination of lumefantrine in rat plasma by liquid-liquid extraction using LC-MS/MS with electrospray ionisation: Assay development, validation and application to a pharmacokinetic study. *Journal of Chromatography B*, 877 (2009) 1133-1139

17. Wahajuddin, Singh P.S., Raju K.S.R., Nafis A., Puri S.K. and Jain G.K. Intravenous pharmacokinetics, oral bioavailability, dose proportionality and in situ permeability of anti-malarial lumefantrine in rats. *Malaria Journal*, 10:293 (2011)
18. Wieling J. LC-MS-MS experiences with internal standards. *Chromatographia Supplement*, 55 (2002) 107-113
19. Zeng M.Y., Lu Z.L., Yang S.C., Zang M., Liao J., Liu S.L and Teng X.H. Determination of benflumetol in human plasma by reversed-phase high-performance liquid chromatography with ultraviolet detection. *Journal of Chromatography B*, 618 (1996) 299-396

University of Cape Town

Chapter 6

A bioavailability study of lumefantrine in mice; evaluating the application of Pheroid™ formulation

6.1 Introduction

As detailed previously, pharmacokinetics (PK) is the study of the concentration vs. time course of a drug, in the body, following drug administration. PK studies (pre-clinical and clinical) are essential for drug development and pharmaceutical research as elucidating the *in vivo* disposition of a drug after administration is necessary for optimum therapeutic drug use (Benedetti *et al.*, 2009).

Many factors affect the bioavailability of a drug. Variability in bioavailability may be attributed to the physicochemical properties of the drug compound or dosage form or it may be patient related. The myriad of physiological factors that influence drug bioavailability includes variation in absorption rate across the GI tract, variation of the pH of gastric fluids and gastric emptying rate, all of which may be affected by food (Makoid *et al.*, 1999). Lumefantrine is a hydrophobic and highly lipophilic drug compound displaying variable bioavailability and is associated with a positive food effect (White *et al.*, 1999, Ezzet *et.al.*, 1998, Ashley *et al.*, 2007). As stated in a review by Wernsdorfer, the erratic and potentially inadequate absorption of LF during a fasting state is detrimental for effective antimalarial treatment in acutely ill malaria patients. This would necessitate the need for appropriate dose adjustment of AL as acutely ill malaria patients have a diminished appetite and are often anorexic (Wernsdorfer, 2004). Using formulation technology to address the poor water solubility and variable bioavailability of LF, after oral administration, may eliminate the need for any dose adjustment. The primary objective of this study was to improve the *in vivo* bioavailability of LF by using Pheroid™ formulation to address its aqueous insolubility. Improving the solubility of LF was achieved using the patented Pheroid™ formulation technology. LF was also found to dissolve sufficiently in canola oil. The improvement in bioavailability was determined by comparing groups of mice dosed with LF dissolved in a reference (aqueous) solution to the groups dosed with Pheroid™ formulated LF and LF dissolved in canola oil.

It has been clinically reported that the bioavailability of LF is increased when administered after a meal; this is referred to as the ‘food effect’. The second objective of this study was to determine if the improvement of LF’s solubility could eliminate the food effect. Groups of mice in each of the three treatment arms of the experiment were divided into two groups; one group receiving food throughout the experiment (fed) and the other group had the food removed twelve hours before dose administration and then replaced one hour after dose administration (starved). The mice were fed a standard rodent maintenance feed which contained sufficient fats to render a positive food effect.

LF was quantitated in mouse WB and plasma to investigate any disparities in drug concentration levels between red blood cells and plasma. Determining the blood to plasma ratio may prove valuable when evaluating novel antimalarial compounds. Malaria parasites infect red blood cells specifically therefore a drug that has a higher concentration in WB than plasma, due to the drug distributing to the erythrocyte, may be more effective as an antimalarial (Yu *et al.*, 2005).

LF is absorbed and eliminated slowly, with a terminal elimination half-life of 2-3 days in healthy volunteers and 4-6 days in malaria infected patients (Ezzet *et al.* 1998, White *et al.*, 1999, Ezzet *et al.*, 2000). LF is highly protein bound (>99%) and is predominantly metabolized by cytochrome P450 3A4 (CYP 3A4) (Coloussi *et al.*, 1999, White *et al.*, 1999).

Table 6.1: Reported pre-clinical pharmacokinetic parameters for LF in a rat model after oral dose administration. *Food was returned to experimental rats 3 hours post dose administration.

LF treatment dose (mg/kg)	Duration of sampling time (h)	Fed/Staved state at dose administration	Matrix	PK modelling	AUC _{0-inf} (ng.h/ml)	C _{max} (ng/ml)	t _{max} (h)	t _{1/2} (h)	Reference
20	72	ns	rat plasma	NCA	6579.8	590.6	3	16.8	Wahajuddin <i>et al.</i> , 2009
10 20 40	120	Starved*	rat plasma	NCA	22025.3 18281.1 39958.7	1488 939.8 2280	8 3.5 5	36.1 25.7 38.2	Wahajuddin <i>et al.</i> , 2011
20	120	Starved*	rat plasma	NCA	18281.1	938.8	4.25	ns	Wahajuddin <i>et al.</i> , 2012

Abbreviations: ns; not specified, NCA; non-compartmental analysis was performed using WinNonlin version 5.1

Previous preclinical studies of LF have been performed in rats, as shown in Table 6.1. Wahajuddin *et al.* performed PK studies in male rats, weighing 200-220 g. The animals were fasted for 12-14 hours before the oral administration of LF and food returned 3 hours after

dose administration. In this study LF was dissolved in a 25% carboxy methyl cellulose (CMC) suspension and evaluated at three different concentrations; 10, 20 and 40 mg/kg. Blood samples were collected over a time period of 72-120 hours and the concentration of LF in rat plasma was determined using LC-MS/MS. The study reported a T_{max} range of 2-8 hours for LF after oral administration and the C_{max} and AUC_{0-inf} values did not increase proportionally with the increase of dose. The calculated percentage bioavailability for LF was 11.6, 4.8 and 5.3 for the 10, 20 and 40 mg/kg treatment groups respectively, indicating a non-linear relationship between dose and bioavailability (Wahajuddin *et al.*, 2011).

In this study, the bioavailability of LF was only evaluated at a 10 mg/kg dose over a 24 hour sampling time period. During the bioavailability experiment whole blood and plasma samples were collected and analysed using LC-MS/MS to obtain concentration-time data. The bioavailability data was then modelled, by Dr Paolo Denti (Pharmacometrics, Division of Pharmacology, UCT) using population pharmacokinetic (PPK) compartmental analysis. PPK allows for the identification and quantification of stochastic between-subject variability in PK parameters and deterministic factors that cause changes in a drugs dose-concentration relationship and the extent of the variability of those changes in a representative study population. This analytical approach uses concentration-time data to estimate the PK parameters and explain their variability in the study population using non-linear mixed-effects (NONMEM) modelling (Guidance for industry: population pharmacokinetics, 1999). The PPK analytical approach was thus appropriate for this study as the aim was to improve LF bioavailability with the application of Pheroid™ formulation technology and assess the elimination of the associated food effect and between-subject variability in bioavailability.

Aim

To determine if the bioavailability of LF is improved when formulated using Pheroid™ technology or canola oil as compared to LF in reference solution.

Objectives

Bioavailability experiments will be performed in mice, to test and compare three different formulations of LF namely: reference, canola oil and Pro-Pheroid™ formulations. The concentration-time data from the experiments will be used to generate PK profiles for each formulation to determine any improvement in the bioavailability of LF, when compared to the reference formulation. It will then be determined if LF, formulated using Pheroid™

technology improves the bioavailability of LF and eliminates the clinically associated ‘food effect’ using PPK.

6.2 Materials and Methods

Solvents and solutions

Analytical grade LiChrosolv[®] water and dimethyl sulfoxide (DMSO) was purchased from Merck (Darmstadt, Germany). The retail brand of canola oil used in this project was B-Well, produced by Southern Oil Ltd. (South Africa).

Contents of Mice Food

The rodent feed was supplied by the Faculty of Health Sciences, Animal Unit (UCT). The list of contents of the food is detailed in Figure 6.1, as underlined in red; most of the components contain fat. Soya oil (fat) comprises 5% of the total nutritional composition of the rodent feed. The amount of food each experimental mouse consumed was not monitored or recorded. Food stock per cage, as seen in Figure 6.2, was replenished every 5 days.

LP code: 1016 Description: Rat Cube Maintenance

RM code	Description	Kgs	%	Min.	Max.	RMcost	LOcost	HCcost
36	<u>Wheat chocked flour</u>	600.0	30.0		30.0			
2	<u>Fine Yellow Maize</u>	248.57	12.429					
213	<u>Full Fat Soya</u>	200.0	10.0		10.0			
243	<u>Sunflower O/C 38 %</u>	200.0	10.0		10.0			
331	<u>Local Fish 63%</u>	200.0	10.0		10.0			
184	<u>Oats SGO</u>	153.31	7.6657		10.0			
10	Prime Gluten 60	100.0	5.0		5.0			
399	<u>Soya Oil</u>	100.0	5.0		5.0			
482	Molasses	100.0	5.0	5.0	8.0			
192	<u>Oaten Bran Mix</u>	48.282	2.4141					
700	Monocalcium Phos	20.12	1.006					
703	Limestone	12.508	.62542					
1006	Rat Maintenance Pre-	12.0	0.6	0.6				
705	Salt	4.9237	.24619					
8043	Magnesium Oxide	.27741	.01387					
Total:		2000.0	100.0					
								Batch cost:

Figure 6.1: The composition of the rodent feed used during the bioavailability experiments.



Figure 6.2 Picture of experimental mice in cage with food and water source.

Pro-Pheroid™ Formulation:

For this study LF was entrapped in a Pro-Pheroid™ formulation, prepared by Dr Lissinda Du Plessis (Pheroid™ formulation facility, North-West University). Pro-Pheroids™ are prepared by mixing vitamin F ethyl ester, cremaphor EL and PEG400 (60:30:5) together with preservatives and heating it to 70°C. The dl- α -Tocopherol (1%) is added and the mixture is gassed for four days with N₂O (Steyn *et al.*, 2011). LF was incorporated in the oil phase during manufacturing. The LF in Pro-Pheroid™ formulation was diluted using a drug free Pro-Pheroid™ in N₂O water solution (diluent) to prepare the 10 mg/kg dose for oral administration.

Experimental mice

C57/BL6 male mice, 8-10 weeks old, were used for the bioavailability studies. The mice were sourced from the Animal Unit, University of Cape Town (UCT) Medical School, Chris Barnard building. The mice were housed at the Animal Laboratory Unit, Old main building, Groote Schuur hospital, in open cages with food and water available *ad libitum*. The mice were weighed and randomly grouped (forty mice per experimental group) prior to the bioavailability experiment. As shown in Figure 6.3, the forty mice were then divided into two groups, fed and starved each consisting of twenty mice. The fed and starved groups were further divided into two groups of ten mice each. The bioavailability study was approved by the Research Animal Committee of UCT, *ethical clearance number*: 010/027. All animals were treated humanely and the *in vivo* experiments were planned based on the guidelines for the ethical use of animals in research (Austin *et al.*, 2004).

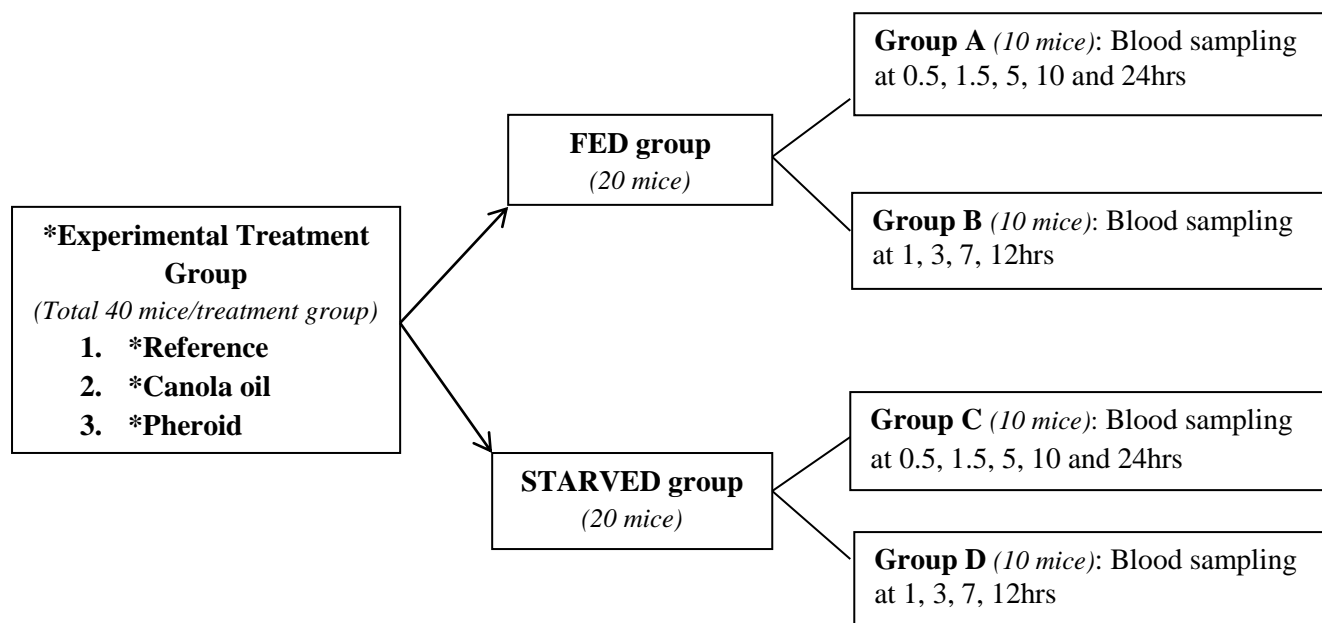


Figure 6.3: Diagram showing experimental design of the bioavailability study. *Each treatment arm of the experiment had the same experimental design.

LF dosage formulations

The reference treatment group received LF dissolved in a DMSO:water (1:9 v/v) solution and the canola group received LF dissolved in canola oil. For the reference and canola oil groups, LF was weighed and dissolved in each respective solution to a concentration calculated according to the average weight of the mice in the treatment group. The 10 mg/kg dosing concentrations were calculated as shown in Figure 6.4; for an average mouse mass of 30 g, 200 µl dose volume per mouse and a total volume of 6ml requires 9 mg of LF to be dissolved in 6 mls of solute.

10 mg per 1000 g	
10 mg/33.3 ↓ 0.3 mg/0.2 ml ↓ 1.5 mg/ml	1000 g / 33.3 ↓ 30 g (ave. mouse mass)
For 6 ml of dosing solution at 10 mg/kg: $1.5 \text{ mg/ml} \times 6 \text{ ml} = 9 \text{ mg of LF}$	

Figure 6.4: Calculation for 10 mg/kg LF dosing solutions.

The Pheroid™ treatment group received LF in Pro-Pheroid™ formulation prepared by Dr L Du Plessis (University of North West, Potchefstroom). As detailed in Table 6.2, the LF in Pro-Pheroid™ formulation was prepared at a concentration of 5 mg/ml and then diluted using a drug free Pro-Pheroid™ solution (Pro-Pheroid™ and N₂O water) to obtain the exact dosage concentrations. The dosage concentrations were calculated based on the average weight of the mice in the treatment group.

Table 6.2 Dose calculation for LF in Pheroid™ formulation. *Calculated for a mouse of average weight 30 g.

Dose (mg/kg)	*Final Concentration (mg/ml)	Pheroid™ Diluent volume (µl)	5 mg/ml Stock spiked volume (µl)	Total volume of dosing solution (µl)
10	1.5	4200	1800	6000

Dose administration and blood sample collection

Mr Trevor Finch (scientific officer) performed the dose administration and blood sample collections. The mice were dosed via oral gavage. The 10 mg/kg dose was calculated and prepared according to the average weight of each experimental group of mice. All the mice received a 10 mg/kg dose of LF dissolved in reference solution, canola oil or Pro-Pheroid™. For the mice in the starved group, food was removed 12 hours before dose administration and returned one hour after. The fed and starved groups were further divided into two subgroups for the purpose of alternating blood sample collection (refer to Figure 6.3). Thus reducing blood sample collections to a maximum of five per mouse and allowing sufficient recovery time. Blood was sampled via tail bleeding at 0.5, 1, 1.5, 3, 5, 7, 10, 12 and 24 hours post dosage. Fifty to sixty microliters of blood was collected per sampling time point in 0.8 ml Lithium Heparin (LiHep) tubes (MiniCollect, greiner bio-one). WB samples (20 µl) were immediately aliquoted into 1.5 ml polypropylene Eppendorf tubes and stored at -80°C. The remaining blood in the LiHep tubes was centrifuged at 2300 G for ten minutes to obtain the plasma samples. The plasma samples were then aliquoted into 1.5 ml polypropylene Eppendorf tubes and stored at -80°C.

Sample Analysis

The WB and plasma samples were analysed using the validated LC-MS/MS methods detailed in Chapter 5.

Population PK

A nonlinear mixed-effects model (Beal & Sheiner, 1982) has been developed for lumefantrine PK. The software NONMEM version 7.2 (Beal *et al.*, 2009) was used for the implementation of the model, while Perl Speaks NONMEM (Lindbom *et al.*, 2004), Xpose (Jonsson & Karlsson, 1999) and Pirana (Keizer *et al.*, 2010) were employed for model diagnostic and to facilitate the modeling process. Model development was guided by the NONMEM objective function value (assumed to be χ^2 -distributed), goodness of fit plots and visual predictive checks (Holford, 2005).

First-order and transit compartment absorption and one- and two-compartment disposition models were tested. Allometric scaling, based on the mouse weight, was used to adjust clearance and volume parameters for the (albeit small) difference in size between mice (Anderson and Holford, 2008). Between-subject variability was tested on the PK parameters using a log-normal distribution, with the exception of bioavailability for which a logit transformation was used, similarly to what was done in Bouzom *et al.* (Bouzom *et al.*, 2000). The effect of fed/starved status and formulation on the PK parameters was investigated, in particular on bioavailability and absorption parameters.

6.3 Results

The developed and validated LC-MS/MS method for the quantitation of LF in mouse WB and plasma was used for the analysis of the bioavailability study samples. The accuracy and precision of the calibration standards and quality control samples of all the analytical runs will be subsequently detailed. The experimental analysis of the fed group was comprised of group A and B samples and the starved group was comprised of group C and D samples.

6.3.1 Quantitation of reference formulated lumefantrine in mouse WB and plasma

A summary of the calibration STDs and QCs used for the WB test sample analysis is shown in Tables 6.3 and 6.4. A summary of the calibration STDs and QCs used for the plasma test sample analysis is shown in Tables 6.5 and 6.6. Each analytical run included all the test samples from a specific group, namely A, B, C or D. The test samples in groups A and B comprised the fed group and the mice in groups C and D comprised the starved group.

All the analytical runs performed well, the precision and accuracy for the calibration STDs and QCs were acceptable and the LF concentrations of the WB and plasma test samples may be deemed accurate.

Animal test samples

LF in reference formulation was administered to the experimental mice in groups of 10. The formulation was evaluated in the fed and starved states. The concentration-time data including the average concentration of LF at each sampling time point is detailed in Tables 6.7 and 6.8 for WB and plasma respectively. The average concentration-time data for LF is illustrated in Figures 6.5 and 6.6 for WB and plasma respectively.

Calibration STD and QC data for reference formulated LF in mouse whole blood

6.3: Summary of calibration standard concentrations for the analytical runs of reference formulated LF in WB

Group Fed/Starved	S1 (15.6 ng/ml) n=8	S2 (31.3 ng/ml) n=8	S3 (62.5 ng/ml) n=8	S4 (125 ng/ml) n=8	S5 (250 ng/ml) n=8	S6 (500 ng/ml) n=8	S7 (1000 µg/ml) n=8	S8 (2000 µg/ml) n=8	S9 (4000 µg/ml) n=8
A-Fed	16.5	30.8	61.9	123.0	253.4	473.7	1022.6	2009.4	3993.0
B-Fed	16.9	29.8	56.3	130.3	257.0	498.1	1001.1	1990.3	4004.8
C-Starved	16.1	30.0	54.2	133.0	273.2	508.4	972.6	1984.4	4021.6
D-Starved	16.5	29.3	55.0	135.4	256.2	494.1	999.5	1993.9	4003.6
Ave	16.5	30.0	56.8	130.4	259.9	493.6	998.9	1994.5	4005.8
STDEV	0.322	0.651	3.46	5.40	8.97	14.6	20.5	10.7	11.8
CV (%)	2.0	2.2	6.1	4.1	3.5	2.9	2.1	0.5	0.3
Accuracy (%)	105.7	95.8	90.9	104.4	104.0	98.7	99.9	99.7	100.1

Table 6.4: Summary of quality control standard concentrations for the analytical runs of reference formulated LF in WB

Group Fed/Starved	QC L2 (25 ng/ml) n=8	QC L1 (50 ng/ml) n=8	QC M (1600 ng/ml) n=7	QC H (3200 ng/ml) n=7	SYS (160 ng/ml) n=24
A-Fed	27.1	51.1	1398.1	2730.5	178.0
B-Fed	25.6	47.4	1377.6	2771.2	165.4
C-Starved	22.3	45.7	1370.0	2730.0	155.0
D-Starved	21.8	43.1	1387.8	2770.0	150.3
Ave	24.2	46.8	1383.4	2750.4	162.2
STDEV	2.56	3.34	12.2	23.3	12.3
CV (%)	10.6	7.1	0.9	0.8	7.6
Accuracy (%)	96.8	93.6	86.5	86.0	101.4

Calibration STD and QC data for reference formulated LF in mouse plasma

Table 6.5: Summary of the calibration standard concentrations for reference formulated LF in mouse plasma.

Group Fed/Starved	S1 (15.6 ng/ml) <i>n</i> =8	S2 (31.3 ng/ml) <i>n</i> =8	S3 (62.5 ng/ml) <i>n</i> =8	S4 (125 ng/ml) <i>n</i> =8	S5 (250 ng/ml) <i>n</i> =8	S6 (500 ng/ml) <i>n</i> =8	S7 (1000 ng/ml) <i>n</i> =8	S8 (2000 ng/ml) <i>n</i> =8	S9 (4000 ng/ml) <i>n</i> =8
A-Fed	14.6	32.0	64.5	127.7	254.1	489.4	981.0	2032.6	3989.2
B-Fed	15.3	30.8	60.8	129.5	261.2	491.6	1007.3	1976.9	4012.8
C-Starved	15.2	32.4	61.2	127.8	252.2	496.6	967.2	2051.0	3980.2
D-Starved	13.5	33.1	65.6	133.9	250.0	495.8	976.5	2023.8	3994.5
Ave	14.7	32.0	63.0	129.8	254.4	493.4	983.0	2021.1	3994.2
STDEV	0.814	0.982	2.38	2.91	4.87	3.41	17.2	31.6	13.8
CV (%)	5.6	3.1	3.8	2.2	1.9	0.7	1.8	1.6	0.3
Accuracy (%)	94.0	102.4	100.8	103.8	101.8	98.7	98.3	101.1	99.9

Table 6.6: Summary of the quality control standard concentrations for reference formulated LF in mouse plasma.

Group Fed/Starved	QC L2 (25 ng/ml) <i>n</i> =8	QC L1 (50 ng/ml) <i>n</i> =8	QC M (1600 ng/ml) <i>n</i> =8	QC H (3200 ng/ml) <i>n</i> =8	SYS (200 ng/ml) <i>n</i> =24
A-Fed	28.6	57.5	1738.9	3375.8	222.7
B-Fed	28.5	56.7	1733.3	3416.4	222.2
C-Starved	30.0	53.4	1763.1	3521.8	219.9
D-Starved	28.6	56.9	1687.8	3632.9	219.9
Ave	28.9	56.2	1730.8	3486.7	221.2
STDEV	0.720	1.87	31.4	115.2	1.51
CV (%)	2.5	3.3	1.8	3.3	0.7
Accuracy (%)	115.6	112.3	108.2	109.0	110.6

Reference formulated LF in WB: Bioavailability Data

Table 6.7: Concentrations of reference formulated LF in WB, tested in the fed (Groups A and B) and starved (Groups C and D) state.

Time (hour)	Mice in Group A (ng/ml)										Ave (ng/ml)	STDEV
	A1	A2	A3	A4	A5	A6	A7	A8	A9	A10		
0.5	45.8	92	142	28	192	234	328	509	199	118	188.8	144.1
1.5	1080	1200	1310	1226	1060	1568	1600	1010	1260	1250	1256.4	197.9
5	1140	1070	1210	1070	623	687	1190	688	965	834	947.7	223.2
10	383	578	610	610	342	332	737	278	474	377	472.1	153.0
24	96.5	91.2	106	178	69.7	83.8	132	64.9	90.4	80.6	99.3	33.5

Time (hour)	Mice in Group B (ng/ml)										Ave (ng/ml)	STDEV
	B1	B2	B3	B4	B5	B6	B7	B8	B9	B10		
1	371	789	301	438	548	71.6	93.3	106	70.1	40.2	282.8	252.7
3	1070	1820	1020	987	1590	149	199	145	143	112	723.5	656.7
7	549	968	644	489	812	90.9	177	166	75.9	68.9	404.1	332.8
12	240	434	314	293	381	53.5	104	166	44	40.9	207.0	146.0

Time (hour)	Mice in Group C (ng/ml)										Ave (ng/ml)	STDEV
	C1	C2	C3	C4	C5	C6	C7	C8	C9	C10		
0.5	104	23.8	24.5	105	0	85.2	139	63.1	311	23.5	87.9	90.4
1.5	476	642	584	991	146	1010	496	514	1090	290	623.9	315.0
5	326	458	278	634	97.9	408	381	373	637	226	381.9	168.0
10	176	247	189	407	55.8	246	252	271	432	175	245.1	110.8
24	62.3	37.2	68.2	126	65.2	79.3	220	69.2	400	71.2	119.9	111.0

Time (hour)	Mice in Group D (ng/ml)										Ave (ng/ml)	STDEV
	D1	D2	D3	D4	D5	D6	D7	D8	D9	D10		
1	88.8	91.3	50	48	545	23.1	39.8	38.6	43	57.9	102.6	156.9
3	302	534	168	575	111	106	149	125	124	127	232.1	179.3
7	206	109	219	130	342	86.4	183	90.7	123	98.6	158.8	80.3
12	83.4	48.8	145	77.9	219	83.7	98.5	35.1	58.4	56.6	90.6	54.6

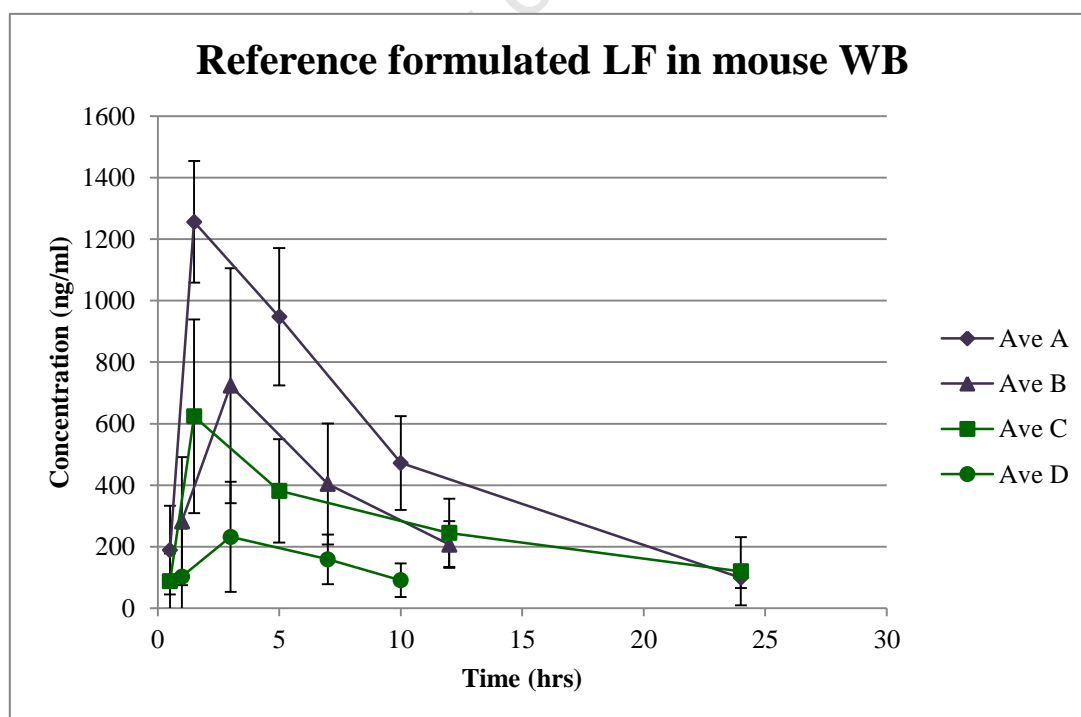


Figure 6.5: Average concentration vs. time graph for reference formulated LF in WB, evaluated in the fed (A&B) and starved (C&D) state.

Reference formulated LF in plasma: Bioavailability Data

Table 6.8: Concentrations of reference formulated LF in plasma, tested in the fed (Groups A and B) and starved (Groups C and D) state.

Time (hour)	Mice in Group A (ng/ml)										Ave (ng/ml)	STDEV
	A1	A2	A3	A4	A5	A6	A7	A8	A9	A10		
0.5	50.6	112	173	25.4	208	290	375	184	229	135	178.2	105.7
1.5	1200	1230	2470	1266	1130	1550	1500	859	1240	1550	1399.5	431.8
5	1050	1090	939	1130	699	768	1010	767	846	819	911.8	152.3
10	405	498	605	625	287	316	702	327	411	292	446.8	152.2
24	102	96	89.1	168	62.6	65.2	91.2	58.1	59.5	60.5	85.2	33.7

Time (hour)	Mice in Group B (ng/ml)										Ave (ng/ml)	STDEV
	B1	B2	B3	B4	B5	B6	B7	B8	B9	B10		
1	435	1020	330	541	672	59.9	106	93.2	88.1	43.5	338.9	327.9
3	511	828	607	451	879	94.2	167	187	75.8	57.7	385.77	313.4
7	263	438	262	226	351	46.7	98.3	120	41.1	34.3	188.0	141.2

Time (hour)	Mice in Group C (ng/ml)										Ave (ng/ml)	STDEV
	C1	C2	C3	C4	C5	C6	C7	C8	C9	C10		
0.5	28.4	26.6	23	84.7	0	107	147	64.9	255	21.5	75.8	77.8
1.5	414	617	584	985	124	821	367	482	876	297	556.7	274.1
5	299	405	215	492	58.2	406	272	289	428	185	304.9	131.3
12	155	201	143	280	37.5	188	170	222	292	136	182.5	73.9
24	50.2	34.9	52.2	71.7	49.5	61.4	185	48.9	280	58.5	89.2	79.3

Time (hour)	Mice in Group D (ng/ml)										Ave (ng/ml)	STDEV
	D1	D2	D3	D4	D5	D6	D7	D8	D9	D10		
1	82.5	78.9	50	47.4	381	0	39	35.5	39	60.4	81.4	107.8
3	277	239	144	460	118	120	126	105	129	105	182.3	113.9
7	176	95	159	114	303	55.4	158	51	108	79.1	129.9	74.6
10	70.8	43	102	68.2	169	41	81.7	33.7	40.7	45.7	69.6	41.2

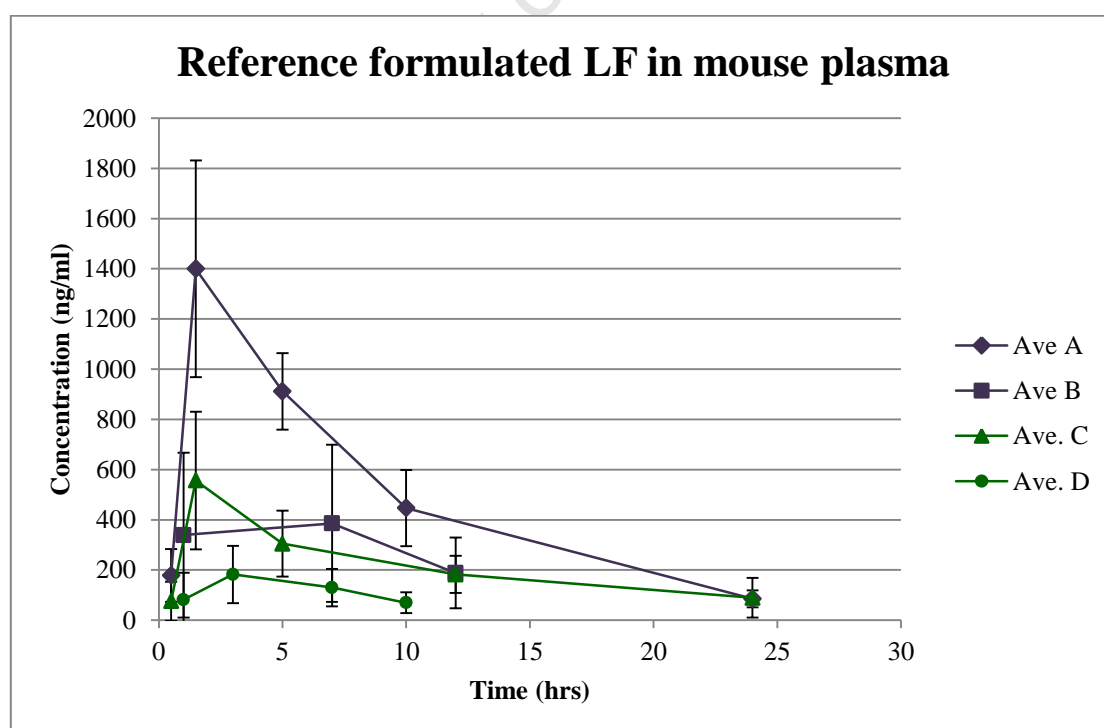


Figure 6.6: Average concentration vs. time graph for reference formulated LF in mouse plasma, evaluated in the fed (A&B) and starved (C&D) state.

Based on the concentration-time data for the reference formulated LF, there is no clearly visible difference in blood and plasma LF concentrations. There is a marked difference in LF concentrations between the fed and starved states, with measured LF concentrations more than 2 times higher in the fed state. The highest measured LF concentration occurred at 1.5 hr sampling time point irrespective of biological matrix or fed state.

6.3.2 Quantitation of canola oil formulated LF in mouse WB and plasma

A summary of the calibration STDs and QCs used for the WB test sample analysis is shown in Tables 6.9 and 6.10. A summary of the calibration STDs and QCs used for the plasma test sample analysis is shown in Tables 6.11 and 6.12. Each analytical run included all the test samples from a specific group, namely A, B, C and D. All the analytical runs performed well, the precision and accuracy for the calibration STDs and QCs were acceptable and the LF concentrations of the WB and plasma test samples may be deemed accurate.

Animal test samples

LF in canola oil was administered to the experimental mice in groups of 10. The formulation was evaluated in the fed and starved states. The concentration-time data including the average concentration of LF at each sampling time point is detailed in Tables 6.13 and 6.14 for WB and plasma respectively. In Table 6.14, there are zero reported values for mouse A10 for time points 5, 10 and 24 hours, as not enough plasma was available for analysis. The average concentration-time data for LF is illustrated in Figures 6.7 and 6.8 for WB and plasma respectively.

Calibration STD and QC data for canola oil formulated LF in mouse WB

Table 6.9: Summary of calibration standard concentrations for the analytical runs of canola oil formulated LF in WB

Group Fed/Starved	S1 (15.6 ng/ml) <i>n</i> =8	S2 (31.3 ng/ml) <i>n</i> =8	S3 (62.5 ng/ml) <i>n</i> =6	S4 (125 ng/ml) <i>n</i> =8	S5 (250 ng/ml) <i>n</i> =8	S6 (500 ng/ml) <i>n</i> =8	S7 (1000 ng/ml) <i>n</i> =8	S8 (2000 ng/ml) <i>n</i> =8	S9 (4000 ng/ml) <i>n</i> =8
A-Fed	13.8	30.3	65.9	132.7	257.7	511.1	1009.0	1929.2	4036.8
B-Fed	13.8	29.6	63.9	147.4	255.2	478.1	989.0	2004.9	4003.0
C-Starved	13.9	33.2	no value	127.6	268.9	485.0	972.2	2028.0	3993.8
D-Starved	15.1	30.8	66.0	133.2	224.3	508.1	1011.0	1996.9	3999.1
Ave	14.1	31.0	65.3	135.2	251.5	495.6	995.3	1989.7	4008.2
STDEV	0.665	1.58	1.15	8.50	19.1	16.5	18.3	42.5	19.5
CV (%)	4.7	5.1	1.8	6.3	7.6	3.3	1.8	2.1	0.5
Accuracy (%)	90.7	98.9	104.4	108.2	100.6	99.1	99.5	99.5	100.2

Table 6.10: Summary of quality control standard concentrations for the analytical runs of canola oil formulated LF in WB

Group Fed/Starved	QC L2 (25 ng/ml) <i>n</i> =8	QC L1 (50 ng/ml) <i>n</i> =8	QC M (1600 ng/ml) <i>n</i> =8	QC H (3200 ng/ml) <i>n</i> =8	SYS (200 ng/ml) <i>n</i> =24
A-Fed	23.6	53.0	1706.8	3253.3	219.4
B-Fed	28.8	54.6	1839.4	3313.9	220.7
C-Starved	25.0	55.0	1758.2	3308.6	230.7
D-Starved	26.2	62.5	1607.6	2836.9	197.4
Ave	25.9	56.3	1728.0	3178.2	217.1
STDEV	2.19	4.23	97.1	229.1	14.0
CV (%)	8.5	7.5	5.6	7.2	6.5
Accuracy (%)	103.6	112.6	108.0	99.3	108.5

Calibration STD and QC data for canola oil formulated LF in mouse plasma

Table 6.11: Summary of calibration standard concentrations for the analytical runs of canola oil formulated LF in plasma

Group Fed/Starved	S1 (15.6 ng/ml) n=8	S2 (31.3 ng/ml) n=8	S3 (62.5 ng/ml) n=8	S4 (125 ng/ml) n=8	S5 (250 ng/ml) n=8	S6 (500 ng/ml) n=8	S7 (1000 ng/ml) n=8	S8 (2000 ng/ml) n=8	S9 (4000 ng/ml) n=8
A-Fed	14.8	28.1	67.2	133.2	256.8	507.7	971.8	2000.3	4004.6
B-Fed	14.7	30.5	68.0	127.1	251.2	484.8	993.2	2021.8	3992.9
C-Starved	17.7	31.0	62.6	123.5	243.4	483.9	987.3	2073.8	3957.8
D-Starved	16.2	31.2	63.2	123.7	243.2	491.5	993.6	2045.7	3975.6
Ave	15.8	30.2	65.3	126.9	248.6	492.0	986.5	2035.4	3982.7
STDEV	1.43	1.45	2.74	4.56	6.58	11.0	10.2	31.6	20.4
CV (%)	9.0	4.8	4.2	3.6	2.6	2.2	1.0	1.6	0.5
Accuracy (%)	101.6	96.5	104.4	101.5	99.5	98.4	98.6	101.8	99.6

Table 6.12: Summary of quality control standards concentrations for the analytical runs of canola oil formulated LF in plasma

Group Fed/Starved	QC L2 (25 ng/ml) n=8	QC L1 (50 ng/ml) n=8	QC M (1600 ng/ml) n=8	QC H (3200 ng/ml) n=8	SYS (200 ng/ml) n=24
A-Fed	24.0	52.8	1673.7	3283.6	191.5
B-Fed	27.9	52.8	1608.3	3249.5	197.4
C-Starved	24.3	49.2	1612.6	3533.0	184.3
D-Starved	23.9	49.0	1709.3	3555.7	199.6
Ave	25.0	51.0	1651.0	3405.4	193.2
STDEV	1.94	2.16	49.0	161.3	6.86
CV (%)	7.8	4.2	3.0	4.7	3.5
Accuracy (%)	100.1	101.9	103.2	106.4	96.6

Canola oil formulated LF in WB: Bioavailability Data

Table 6.13: Concentrations of canola oil formulated LF in WB, tested in the fed (Groups A and B) and starved (Groups C and D) state.

Time (hour)	Mice in Group A (ng/ml)										Ave (ng/ml)	STDEV
	A1	A2	A3	A4	A5	A6	A7	A8	A9	A10		
1.5	163	353	189	381	326	137	224	370	387	271	280.1	95.9
5	535	909	627	705	622	356	831	670	622	685	656.2	151.2
10	679	987	509	1120	474	471	682	712	517	NS	683.4	232.0
24	134	254	108	181	162	247	218	191	191	NS	187.3	48.5

Time (hour)	Mice in Group B (ng/ml)										Ave (ng/ml)	STDEV
	B1	B2	B3	B4	B5	B6	B7	B8	B9	B10		
3	735	839	549	525	632	496	830	319	480	953	635.8	198.2
7	728	961	651	1010	631	851	831	1000	725	810	819.8	138.0
12	740	464	557	785	561	789	967	930	541	326	666.0	208.2
48	27.9	17.3	31.1	38.2	33.4	31.8	46	72.7	36.8	42.4	37.8	14.6

Time (hour)	Mice in Group C (ng/ml)										Ave (ng/ml)	STDEV
	C1	C2	C3	C4	C5	C6	C7	C8	C9	C10		
0.5	BLQ	BLQ	BLQ	BLQ	BLQ	BLQ	BLQ	BLQ	BLQ	21.8	2.18	6.89
1.5	364	68	333	240	68.5	957	341	281	253	624	353.0	264.4
5	788	641	645	329	1330	859	780	832	562	823	758.9	257.6
10	408	402	254	153	707	538	397	540	363	562	432.4	160.7
24	198	135	93.6	51.3	217	195	159	206	74.1	180	150.9	59.5

Time (hour)	Mice in Group D (ng/ml)										Ave (ng/ml)	STDEV
	D1	D2	D3	D4	D5	D6	D7	D8	D9	D10		
1	BLQ	166	79.9	80.8	BLQ	85.4	139	140	96.7	201	98.9	65.5
3	BLQ	967	613	615	422	633	1380	1060	390	1020	710.0	401.0
7	1230	567	397	560	627	825	852	666	236	847	680.7	276.6
12	NS	394	302	377	409	483	425	479	141	436	382.9	105.9

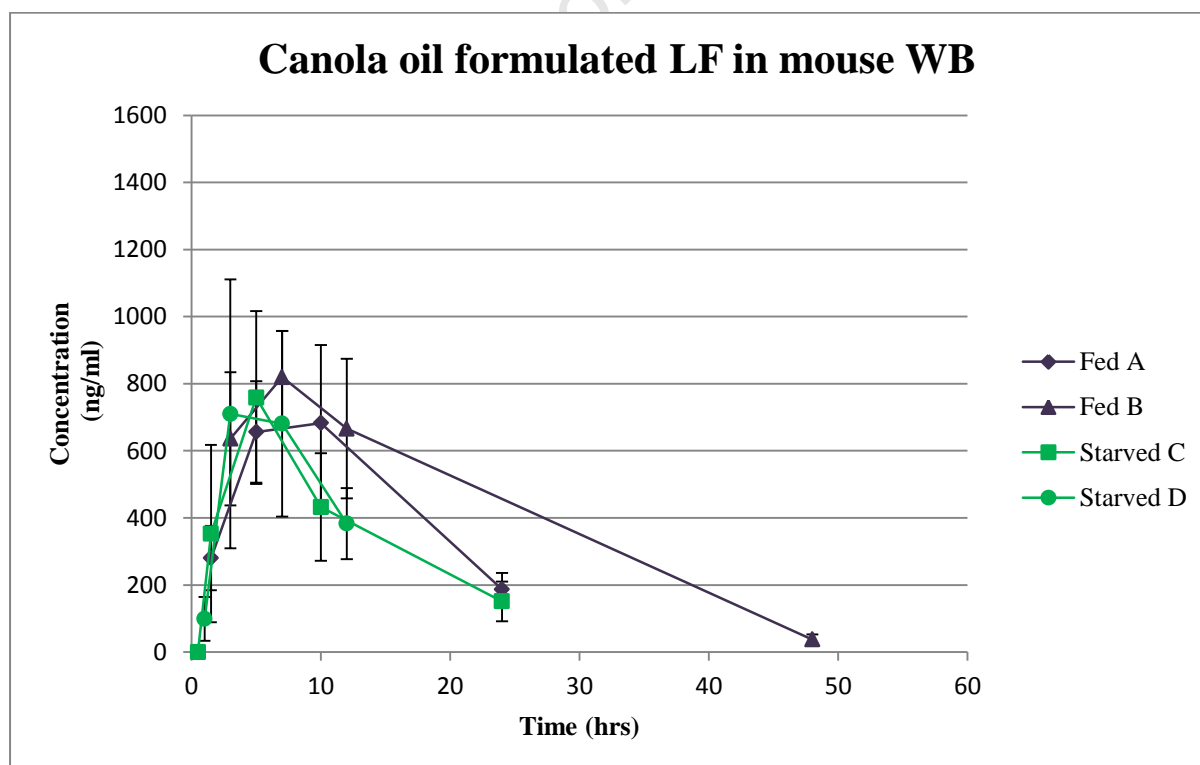


Figure 6.7: Average concentration vs. time graphs of canola oil formulated LF in WB, administered to groups of mice under fed (A&B) and starved (C&D) conditions.

Canola oil formulated LF in plasma: Bioavailability Data

Table 6.14: Plasma concentrations of canola oil formulated LF, tested in the fed (Groups A and B) and starved (Groups C and D) state.

Time (hour)	Mice in Group A (ng/ml)										Ave (ng/ml)	STDEV
	A1	A2	A3	A4	A5	A6	A7	A8	A9	A10		
1.5	267	401	314	444	407	235	308	657	560	453	404.6	132.1
5	773	1290	994	1040	966	557	1110	987	975	0	869.2	361.6
10	916	763	671	1510	616	621	912	950	668	0	762.7	377.1
24	184	338	155	252	241	318	286	242	247	0	226.3	96.7

Time (hour)	Mice in Group B (ng/ml)										Ave (ng/ml)	STDEV
	B1	B2	B3	B4	B5	B6	B7	B8	B9	B10		
3	1210	1340	907	836	1110	784	1280	570	756	1440	1023.3	291.5
7	1080	1450	1050	1570	1300	1280	1140	1560	1130	1280	1284	190.5
12	935	563	833	1140	852	1110	1350	1400	753	754	969	273.1
48	49.5	28.4	54.1	54.6	53.9	58.3	76.8	112	77	85.6	65.02	23.3

Time (hour)	Mice in Group C (ng/ml)										Ave (ng/ml)	STDEV
	C1	C2	C3	C4	C5	C6	C7	C8	C9	C10		
0.5	BLQ	BLQ	BLQ	BLQ	BLQ	BLQ	BLQ	20.2	BLQ	34.3	5.45	12.0
1.5	346	94.1	391	291	84.6	889	447	301	287	795	392.6	264.0
5	1260	844	928	384	1480	989	888	1130	832	1050	978.5	291.1
10	584	731	214	237	995	615	442	642	462	653	557.5	232.1
24	201	180	118	60.3	210	226	197	250	92	215	174.9	62.8

Time (hour)	Mice in Group D (ng/ml)										Ave (ng/ml)	STDEV
	D1	D2	D3	D4	D5	D6	D7	D8	D9	D10		
1	BLQ	212	118	74.3	29.2	157	183	152	98	162	118.6	68.1
3	NS	1230	788	814	470	847	1580	1320	484	1240	877.3	477.1
7	344	639	543	615	606	1060	899	893	302	869	677	249.3
12	NS	441	390	456	420	268	467	501	555	181	367.9	169.7

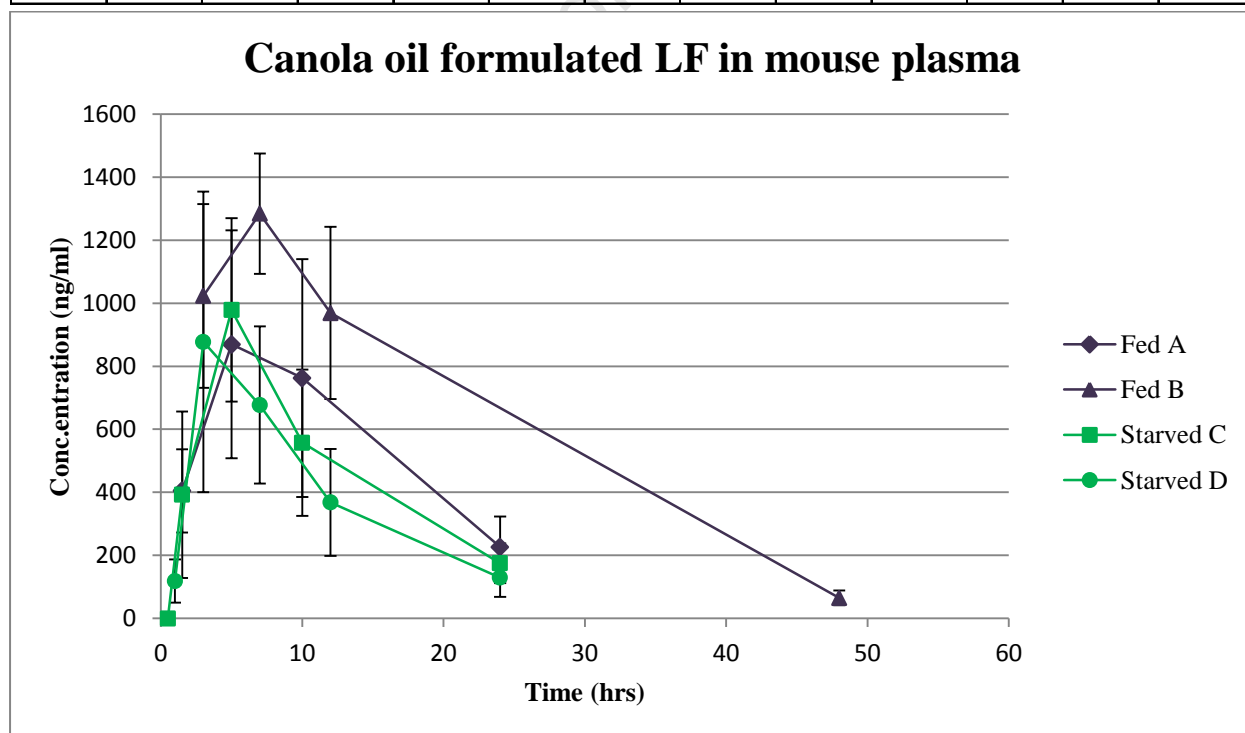


Figure 6.8: Average concentration vs. time graphs of canola oil formulated in plasma, administered to groups of mice under fed (A&B) and starved (C&D) conditions

LF dissolved adequately in canola oil and the evident positive food effect seen with LF in reference solution has been resolved by improving the solubility of LF. When formulated with canola oil, the measured LF concentrations seem to be higher in plasma than WB. In plasma, the measured peak concentrations of LF in the fed and starved state are 1284 ng/ml and 978 ng/ml, respectively. The concentrations of LF are still higher in the fed state. Also in the fed state the maximum measured LF concentration occurred at the 7 hour time point whereas in the starved state the maximum measured LF concentration occurred at the 5 hour time point. The presence of food as well as the formulation may have played a role in delaying the absorption of LF.

6.3.3 Quantitation of Pheroid™ formulated LF in mouse WB and plasma

A summary of the calibration STDs and QCs used for the WB test sample analysis is shown in Tables 6.15 and 6.16. A summary of the calibration STDs and QCs used for the plasma test sample analysis is shown in Tables 6.17 and 6.18. Each analytical run included all the test samples from a specific group, namely A, B, C and D. All the analytical runs performed well, the precision and accuracy for the calibration STDs and QCs were acceptable and the LF concentrations of the WB and plasma test samples may be deemed accurate.

Animal test samples

LF in Pro-Pheroid™ formulation was administered to the experimental mice in groups of 10. The formulation was evaluated in the fed and starved states. The concentration-time data including the average concentration of LF at each sampling time point is detailed in Tables 6.19 and 6.20 for WB and plasma respectively. The average concentration-time data for LF is illustrated in Figures 6.9 and 6.10 for WB and plasma respectively.

Calibration STD and QC data for Pheroid™ formulated LF in mouse WB

Table 6.15: Summary of calibration standard concentrations for the analytical runs of Pheroid™ formulated LF in WB

Group Fed/Starved	S1 (15.6 ng/ml) <i>n</i> =8	S2 (31.3 ng/ml) <i>n</i> =8	S3 (62.5 ng/ml) <i>n</i> =8	S4 (125 ng/ml) <i>n</i> =8	S5 (250 ng/ml) <i>n</i> =8	S6 (500 ng/ml) <i>n</i> =8	S7 (1000 ng/ml) <i>n</i> =8	S8 (2000 ng/ml) <i>n</i> =8	S9 (4000 ng/ml) <i>n</i> =8
A-Fed	13.5	30.7	69.2	129.6	260.1	528.6	1001.5	1914.9	4040.4
B-Fed	14.5	32.5	61.5	134.9	241.0	502.2	981.8	2022.4	3993.1
C-Starved	13.5	27.6	69.1	128.6	261.5	498.1	1056.5	1877.1	4054.2
D-Starved	15.5	31.8	57.8	126.2	267.6	501.2	983.9	1995.2	4005.2
Ave	14.2	30.6	64.4	129.8	257.5	507.5	1005.9	1952.4	4023.2
STDEV	0.963	2.15	5.68	3.66	11.5	14.2	34.9	67.9	28.8
CV (%)	6.8	7.0	8.8	2.8	4.5	2.8	3.5	3.5	0.7
Accuracy (%)	91.3	97.9	103.1	103.8	103.0	101.5	100.6	97.6	100.6

Table 6.16: Summary of quality control standard concentrations for the analytical runs of Pheroid™ formulated LF in WB

Group Fed/Starved	QC L2 (25 ng/ml) <i>n</i> =8	QC L1 (50 ng/ml) <i>n</i> =8	QC M (1600 ng/ml) <i>n</i> =8	QC H (3200 ng/ml) <i>n</i> =8	SYS (200 ng/ml) <i>n</i> =24
A-Fed	21.8	53.9	1817.7	3584.9	226.2
B-Fed	21.8	43.8	1391.9	2758.3	*
C-Starved	22.6	48.6	1789.3	3673.3	*
D-Starved	24.3	55.7	1697.4	3562.3	222.1
Ave	22.6	50.5	1674.1	3394.7	224.2
STDEV	1.19	5.40	195.0	427.0	2.90
CV (%)	5.3	10.7	11.6	12.6	1.3
Accuracy (%)	90.5	101.0	104.6	106.1	112.1

*SYS sample was analysed at a different concentration, therefore excluded

Calibration STD and QC data for Pheroid™ formulated LF in mouse plasma

Table 6.17: Summary of calibration standard concentrations for the analytical runs of Pheroid™ formulated LF in plasma

Group Fed/Starved	S1 (15.6 ng/ml) <i>n</i> =8	S2 (31.3 ng/ml) <i>n</i> =8	S3 (62.5 ng/ml) <i>n</i> =8	S4 (125 ng/ml) <i>n</i> =8	S5 (250 ng/ml) <i>n</i> =8	S6 (500 ng/ml) <i>n</i> =8	S7 (1000 ng/ml) <i>n</i> =8	S8 (2000 ng/ml) <i>n</i> =8	S9 (4000 ng/ml) <i>n</i> =8
A-Fed	16.3	27.0	65.4	123.2	255.0	517.4	1047.6	1893.5	4039.2
B-Fed	13.4	28.4	67.8	147.5	247.6	505.4	969.8	1996.5	4008.1
C-Starved	14.5	29.8	67.6	127.7	256.4	512.7	943.3	2040.4	3991.9
D-Starved	13.5	29.9	70.4	131.1	254.8	501.9	983.6	1992.2	4007.0
Ave	14.4	28.8	67.8	132.4	253.4	509.4	986.1	1980.6	4011.6
STDEV	1.38	1.38	2.04	10.6	3.97	7.00	44.3	62.0	19.9
CV (%)	9.5	4.8	3.0	8.0	1.6	1.4	4.5	3.1	0.5
Accuracy (%)	92.5	92.0	108.5	105.9	101.4	101.9	98.6	99.0	100.3

Table 6.18: Summary of quality control standard concentrations for the analytical runs of Pheroid™ formulated LF in plasma

Group Fed/Starved	QC L2 (25 ng/ml) <i>n</i> =8	QC L1 (50 ng/ml) <i>n</i> =8	QC M (1600 ng/ml) <i>n</i> =8	QC H (3200 ng/ml) <i>n</i> =8	SYS (200 ng/ml) <i>n</i> =27
A-Fed	25.4	47.8	1589.7	3389.4	190.0
B-Fed	24.1	48.4	1586.7	3414.6	206.5
C-Starved	27.1	55.6	1640.2	3375.5	204.8
D-Starved	25.3	51.6	1687.0	3350.4	191.2
Ave	25.5	50.9	1625.9	3382.5	198.1
STDEV	1.23	3.62	47.6	26.8	8.73
CV (%)	4.8	7.1	2.9	0.8	4.4
Accuracy (%)	101.8	101.7	101.6	105.7	99.1

Pheroid™ formulated LF in WB: Bioavailability Data

Table 6.19: Concentrations of Pheroid™ formulated LF in WB, tested in the fed (Groups A and B) and starved (Groups C and D) state. BLQ: below limit of quantitation.

Time (hour)	Mice in Group A (ng/ml)										Ave (ng/ml)	STDEV
	A1	A2	A3	A4	A5	A6	A7	A8	A9	A10		
0.5	26.7	BLQ	BLQ	BLQ	52.2	BLQ	BLQ	BLQ	360	BLQ	43.9	112.4
1.5	137	173	156	167	167	166	367	94.2	1040	122	258.9	284.0
5	984	684	1180	1040	926	1190	954	709	426	928	902.1	236.0
10	1640	741	1550	1370	1070	1420	829	796	0	1270	1187.3	340.1
24	384	232	385	458	398	293	142	573	0	877.0	415.8	213.7

Time (hour)	Mice in Group B (ng/ml)										Ave (ng/ml)	STDEV
	B1	B2	B3	B4	B5	B6	B7	B8	B9	B10		
1	13.9	13.3	43.6	41.6	25.9	26.4	45.1	31.2	57.6	47.5	34.6	14.8
3	296	375	452	301	308	336	503	384	626	443	402.4	105.5
7	911	697	855	822	788	539	670	479	1090	830	768.1	179.3
12	765	538	613	713	811	472	855	700	936	672	707.5	142.4

Time (hour)	Mice in Group C (ng/ml)										Ave (ng/ml)	STDEV
	C1	C2	C3	C4	C5	C6	C7	C8	C9	C10		
0.5	20.7	8	19.4	12	12	15.9	39.9	40	33.3	7.87	20.9	12.5
1.5	263	143	357	218	192	368	257	348	293	128	256.7	86.5
5	1070	857	1460	923	1420	1660	855	767	926	542	1048	353.1
10	1020	687	1290	715	1120	1120	1140	886	1150	909	1003.7	198.8
24	243	102	179	317	416	119	133	406	496	233	264.4	138.6

Time (hour)	Mice in Group D (ng/ml)										Ave (ng/ml)	STDEV
	D1	D2	D3	D4	D5	D6	D7	D8	D9	D10		
1	68.2	30	40	NS	52	69.6	102	43.5	114	56.6	64.0	28.2
3	550	588	293	NS	561	697	912	534	1120	659	657.1	238.2
7	436	486	404	NS	478	672	920	569	737	531	581.4	166.6
12	654	620	453	NS	530	762	768	657	561	481	609.6	113.1

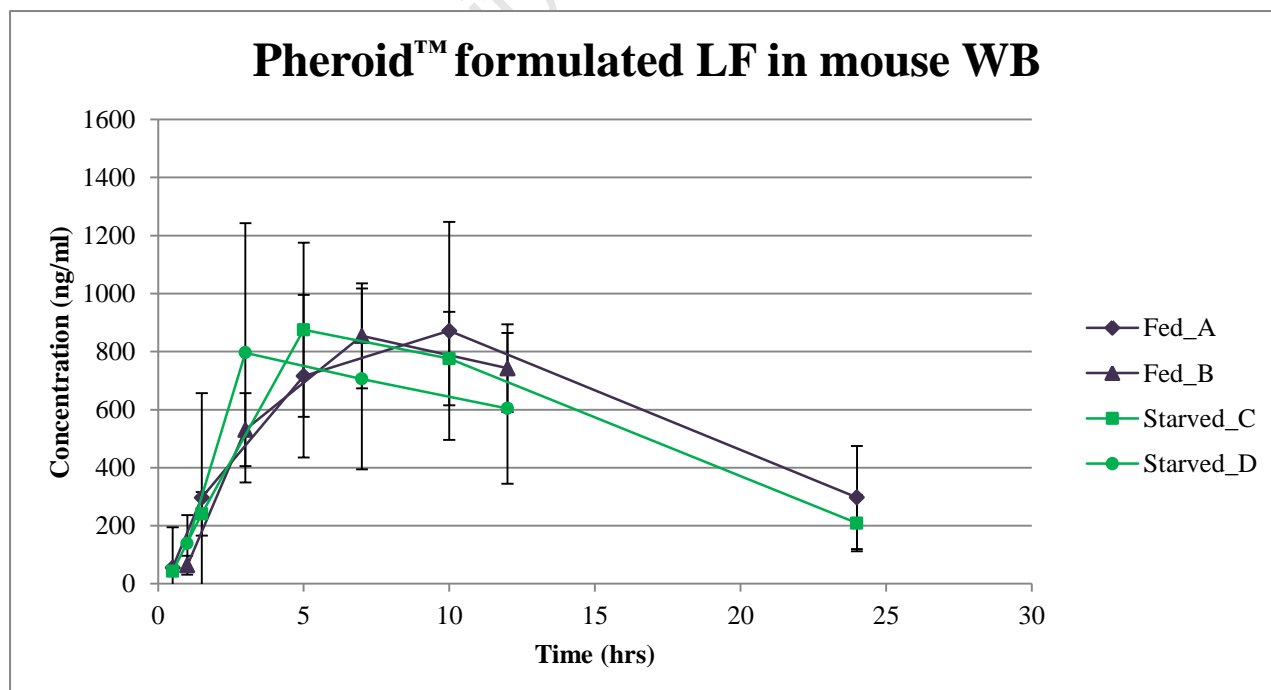


Figure 6.9: Average concentration vs. time graphs of Pheroid™ formulated LF in WB, administered to groups of mice under fed (A&B) and starved (C&D) conditions

Pheroid™ formulated LF in plasma: Bioavailability Data

Table 6.20: Concentrations of Pheroid™ formulated LF in plasma, tested in the fed (Groups A and B) and starved (Groups C and D) state.

Time (hour)	Mice in Group A (ng/ml)										Ave (ng/ml)	STDEV
	A1	A2	A3	A4	A5	A6	A7	A8	A9	A10		
0.5	31.8	BLQ	BLQ	BLQ	78.5	BLQ	BLQ	BLQ	444	BLQ	55.4	138.9
1.5	126	182	165	203	172	164	316	193	1310	137	296.8	359.8
5	873	636	872	879	746	1030	798	652	NS	672	715.8	280.3
10	1250	642	1110	1120	955	1260	738	734	NS	911	872	375.7
24	231	182	271	442	350	319	126	432	NS	623	297.6	177.8

Time (hour)	Mice in Group B (ng/ml)										Ave (ng/ml)	STDEV
	B1	B2	B3	B4	B5	B6	B7	B8	B9	B10		
1	16.9	28.9	60.8	123	54.3	52.1	81.8	42.5	96	82.3	63.9	32.2
3	360	453	559	534	421	412	619	520	763	667	530.8	125.9
7	913	839	920	1040	883	546	745	619	1150	887	854.2	180.8
12	627	655	700	835	829	452	857	773	1000	700	742.8	151.1

Time (hour)	Mice in Group C (ng/ml)										Ave (ng/ml)	STDEV
	C1	C2	C3	C4	C5	C6	C7	C8	C9	C10		
0.5	32.6	19.6	43.5	34.1	41.4	57.9	57.8	54.2	57.2	30.4	42.9	13.6
1.5	249	152	307	199	224	355	260	306	250	106	240.8	74.7
5	857	692	1210	771	1240	1400	716	632	732	501	875.1	300.1
10	726	551	1060	562	857	893	892	673	840	703	775.7	161.0
24	212	97	132	220	307	123	107	282	392	216	208.8	97.1

Time (hour)	Mice in Group D (ng/ml)										Ave (ng/ml)	STDEV
	D1	D2	D3	D4	D5	D6	D7	D8	D9	D10		
1	124	50.4	57.6	386	100	118	170	81.1	189	112	138.8	97.3
3	683	800	390	NS	664	852	1210	774	1680	909	796.2	447.0
7	586	689	565	NS	661	851	1170	738	1020	780	706	312.1
12	404	733	565	NS	532	845	922	688	680	676	604.5	259.4

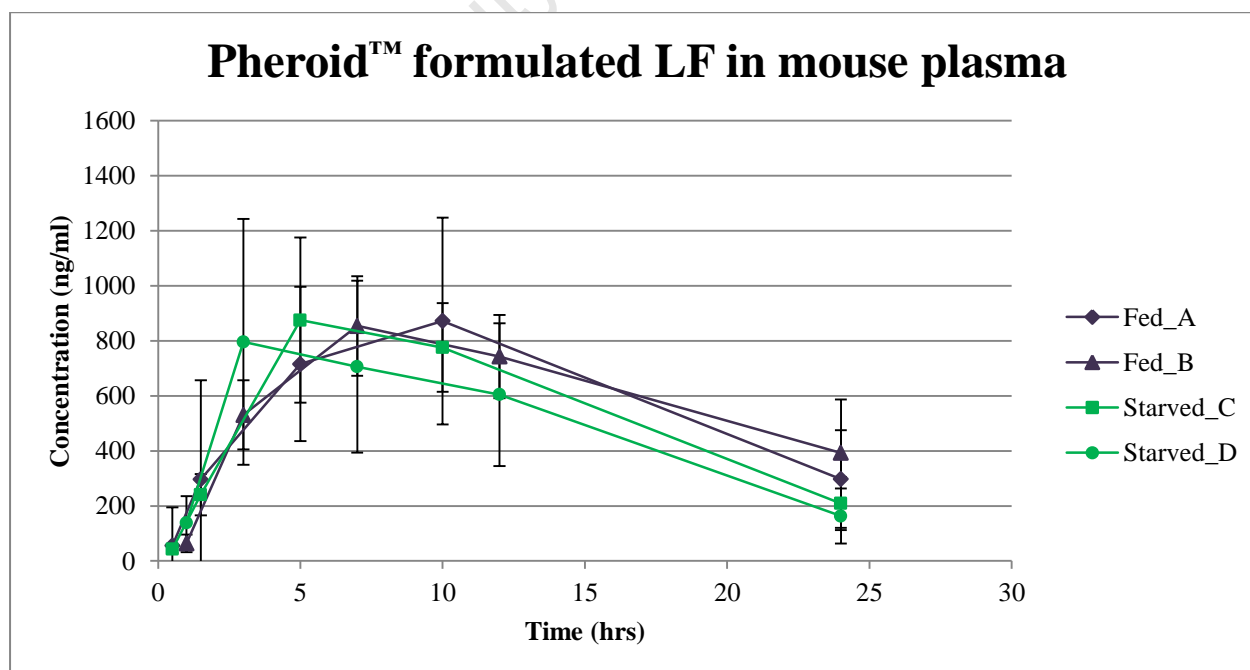


Figure 6.10: Average concentration vs. time graphs of Pheroid™ formulated LF in plasma, administered to groups of mice under fed (A&B) and starved (C&D) conditions

The shape of the concentration-time profile for LF in Pheroid™ formulation differs from the profiles for LF in reference solution or canola oil. The difference in LF concentration-time profile between the fed and starved state seems negligible. The highest measured WB LF concentrations in the fed and starved state were 1187.3 ng/ml and 1048 ng/ml respectively. The highest measured plasma LF concentrations in the fed and starved states were 872 ng/ml and 875 ng/ml respectively. Similar to LF in canola oil, the highest measured LF concentration occurred later in the fed state than the starved state. The presence of food in the GI tract at the time of dose administration may delay LF absorption. As seen with the canola oil formulation, the Pheroid™ formulation may also contribute to delaying the absorption of LF in the GI tract.

The pooled concentration-time data for LF in WB and plasma, in the fed and starved state are graphically presented in Figure 6.11. For LF in the reference solution, in plasma, the concentration-time profile seems to be more erratic in the starved state compared to the fed state. For LF in the Pheroid™ formulation the measured level of LF peaks at 5 hours, then drops at the 7 hour time point before peaking again at the 10hr time point. This occurred for Pheroid™ formulated LF in the WB profile only. LF concentration levels at the 24 hour time point was higher for LF in the Pheroid™ formulation than for LF in canola oil or reference solution.

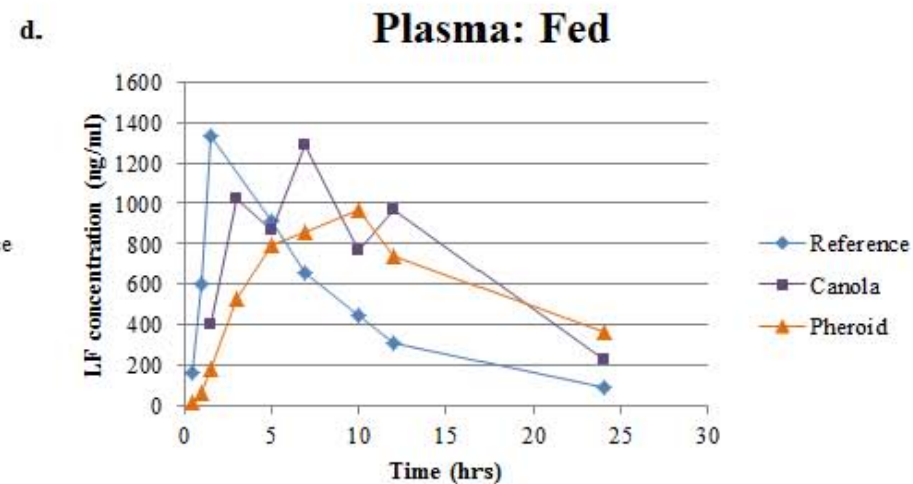
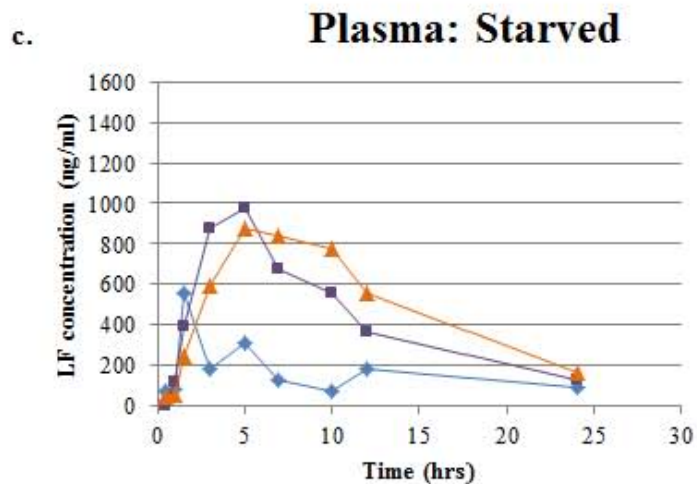
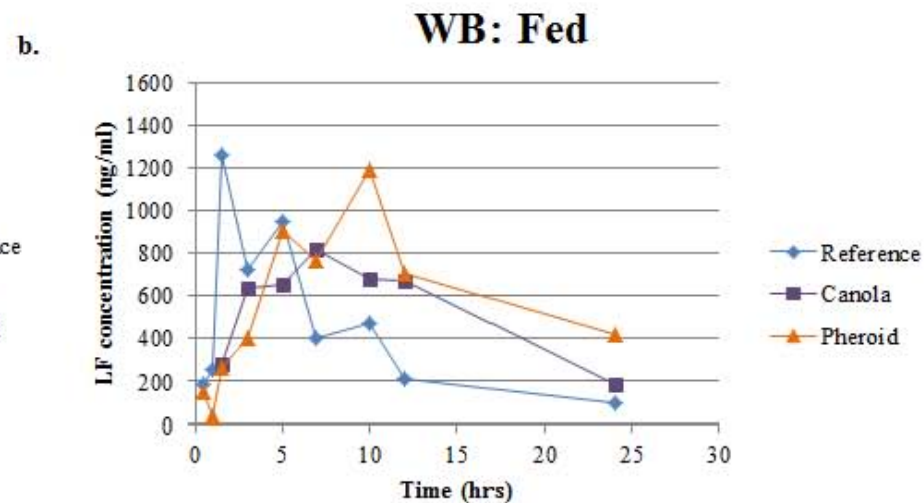
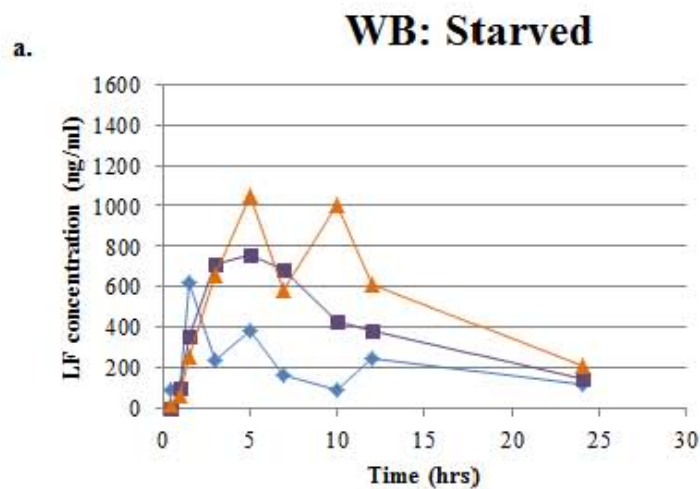


Figure 6.11: Graphs of pooled average concentration vs. time for LF in the three different formulations, a. and b. represents the WB data in starved and fed state respectively, c. and d. represents the plasma data in the starved and fed state respectively.

6.3.4 Population Pharmacokinetics (PPK)

A PPK model was constructed using the collective concentration-time data for all the formulations for each biological matrix; 1113 observations from 123 concentration-time profiles were included.

Lumefantrine PK is best described by a 1-compartment model, with first-order elimination and transit compartment absorption (Savic *et al.*, 2007). A structural representation of the PPK model for LF is shown in Figure 6.12. The final model parameter estimates are reported in Table 6.21, and a VPC is displayed in Figure 6.13.

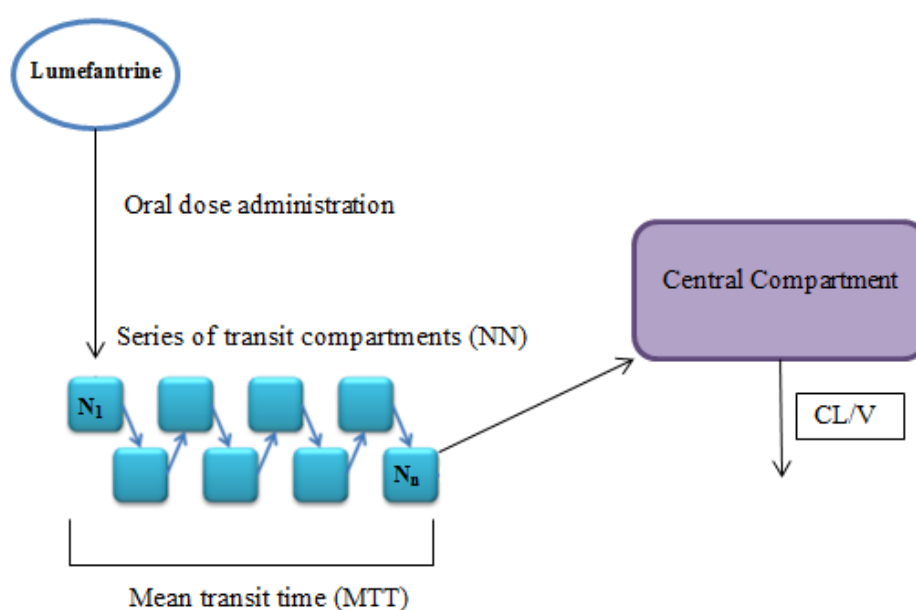


Figure 6.12: An illustration of the final LF pharmacokinetic model. CL; clearance and V; volume.

Model evaluation

The final PPK model for LF was evaluated using a visual predictive check (VPC). VPC was performed to assess the ability of the final model to correctly describe the variability in the data. In the VPC graphs in Figure 6.13, the shaded areas are what the model predicts the 5th, 50th and 95th percentile to be (based on a 1000 simulations), while the solid and dashed lines represent the same percentiles that are observed in this experiment. There is good agreement between the experimental data and model prediction as the percentiles of the observations are consistent with the respective predicted regions. The final model is robust and adequately describes the pharmacokinetics of LF in mice, in plasma and WB.

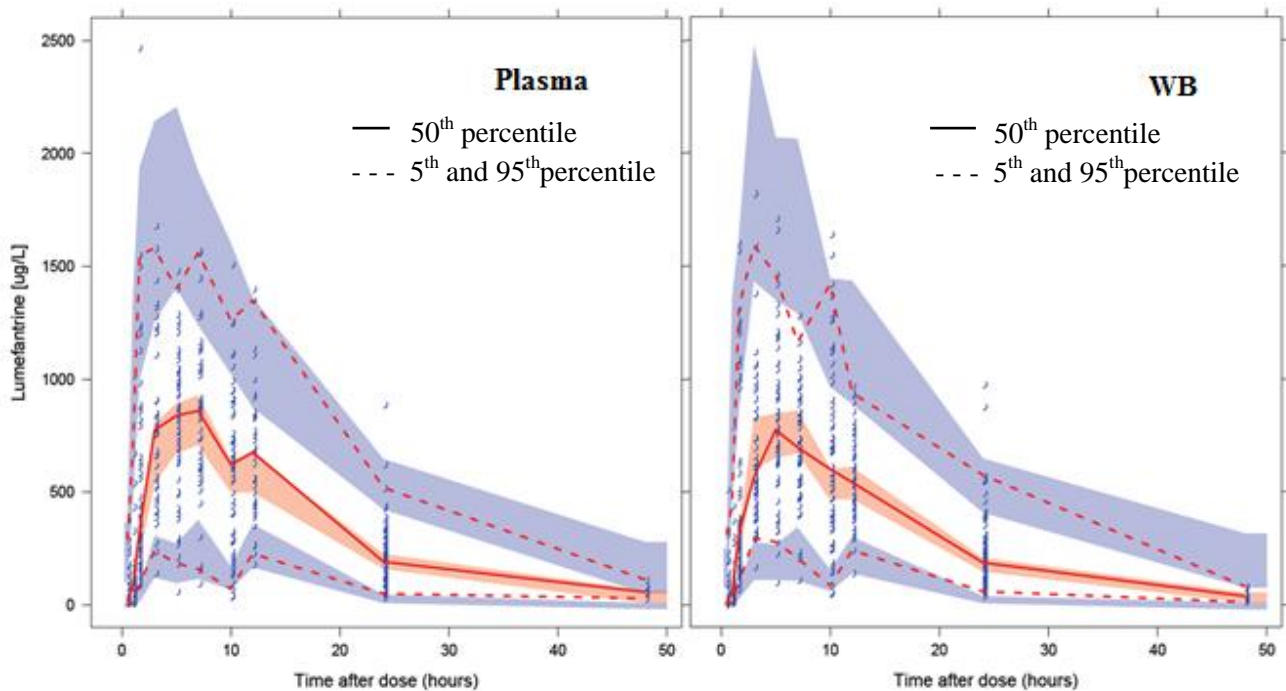


Figure 6.13: Visual predictive check diagrams for the LF PPK model in plasma and WB. The open blue circles represent the actual observed LF concentrations. The lower and upper dashed lines represent the 5th and 95th percentiles of the observed data, respectively. The middle solid line represents the median of the observed data. The shaded areas represent the 95% confidence intervals for the 5th, 50th and 95th percentiles of the simulated data.

Diagnostic plots used to assess the model also included goodness-of-fit plots including observed concentration versus individual and population predictions (Figure 6.14).

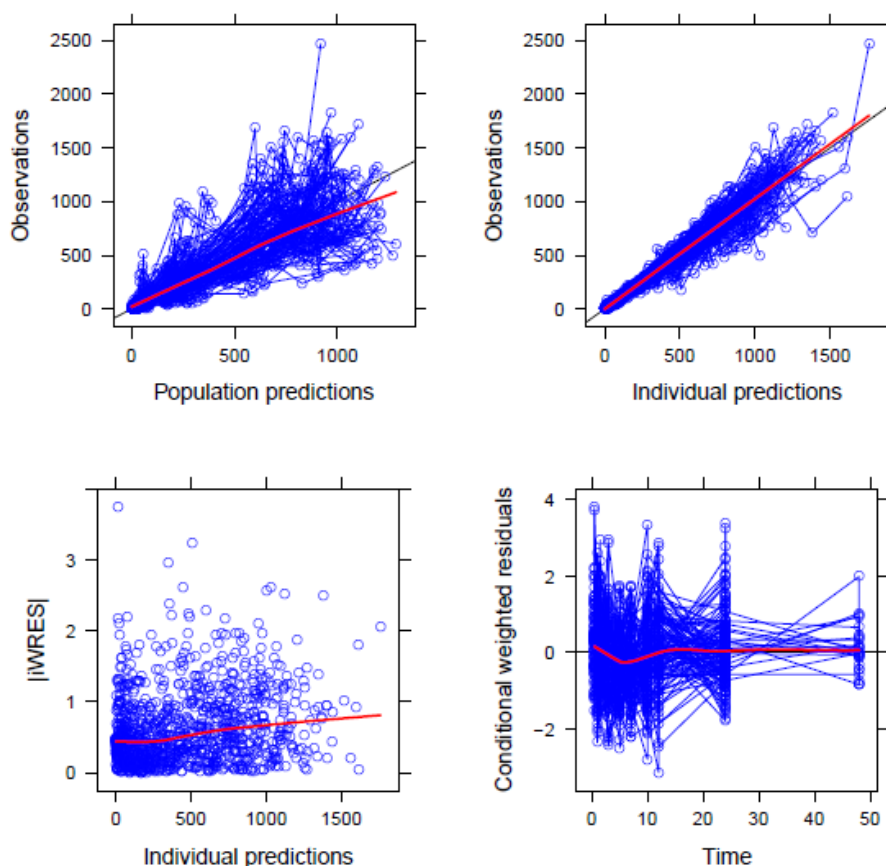


Figure 6.14: Goodness of fit plots of LF for the final model. The upper left and right panels show population and individual predicted concentration versus observed concentration. The solid lines are lines of identity. The lower panels are the conditional weighted residual plots for the final model.

For Figures 6.15 to 6.20, where the open circles represent the observed concentrations, the dotted and solid lines represent the population and individual prediction-time profiles, respectively. The population prediction is the behaviour of the typical subject, i.e. the model prediction obtained considering the deterministic dose and covariate effects, but not the random individual effects specific to that particular subject. From the charts it can be seen that the individual predictions fit the data well, while the discrepancy between population and individual predictions shows the large extent of between-subjects variability not explainable with observed covariates.

Lumefantrine in WB

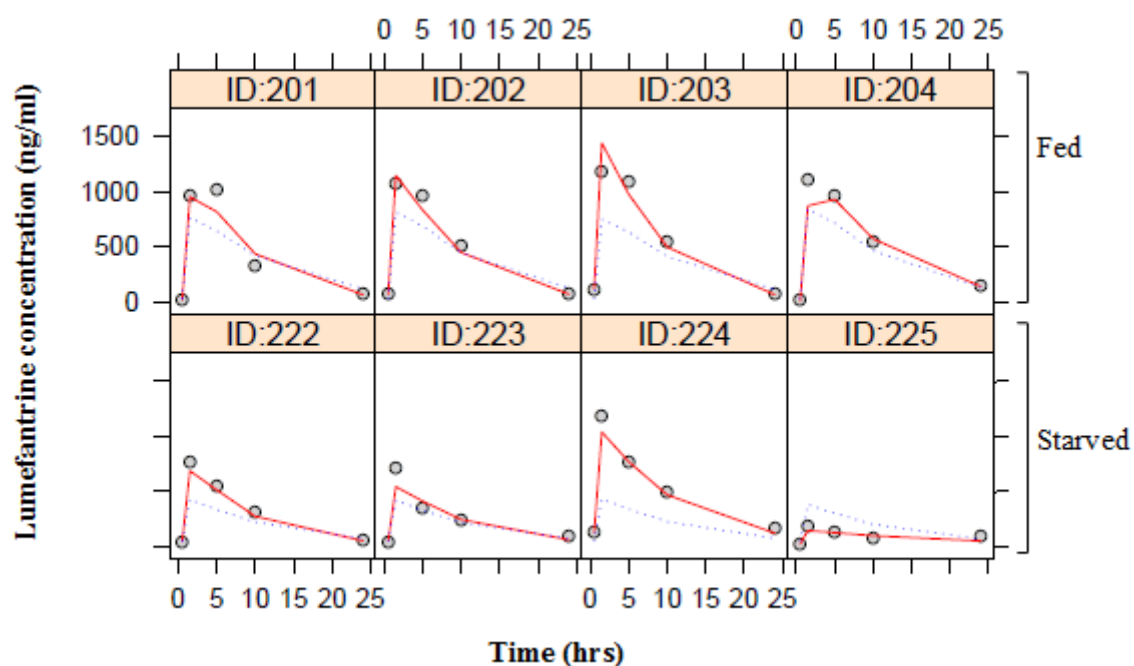


Figure 6.15: Observed and predicted WB LF concentration vs. time profiles for 8 randomly selected experimental mice administered LF in reference solution.

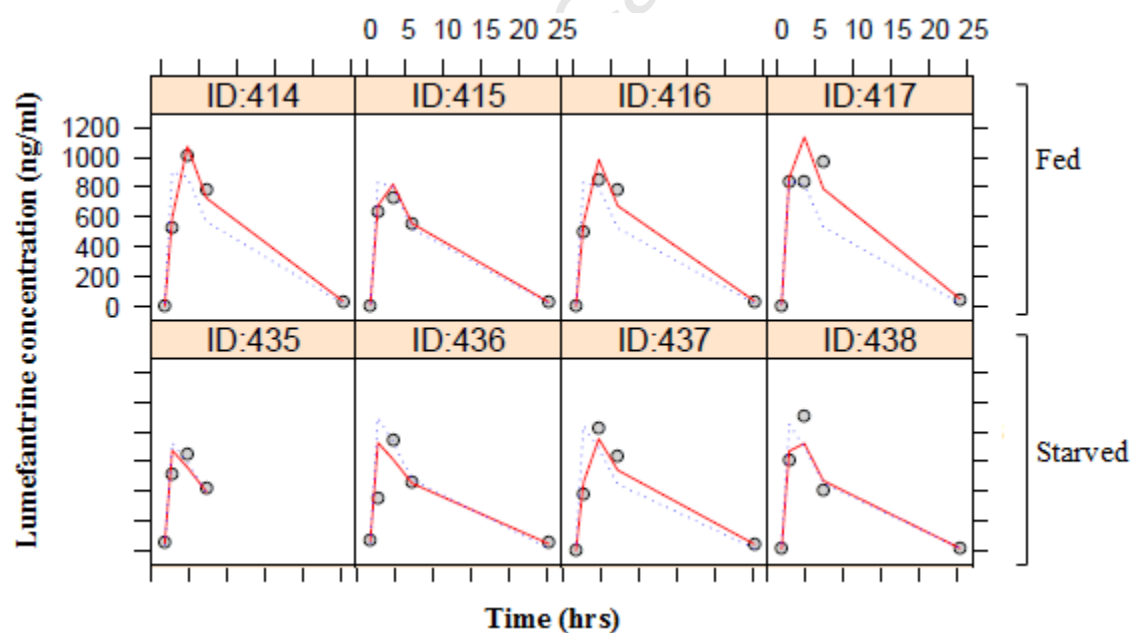


Figure 6.16: Observed and predicted WB LF concentration vs. time profiles for 8 randomly selected experimental mice administered LF in canola oil.

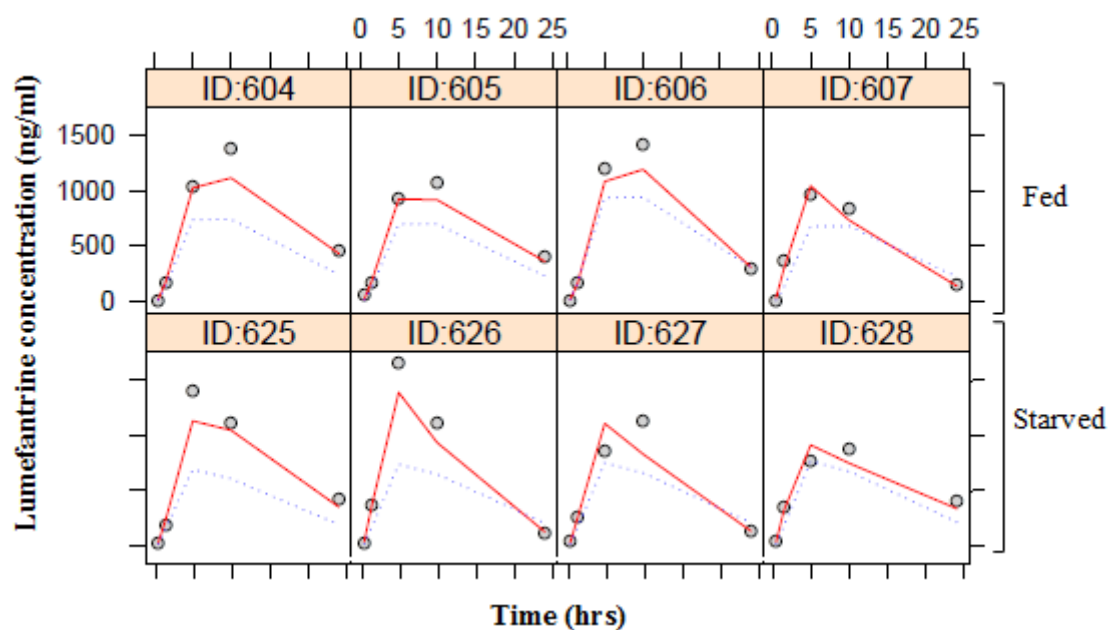


Figure 6.17: Observed and predicted WB LF concentration vs. time profiles for 8 randomly selected experimental mice administered LF in Pheroid™ formulation.

Lumefantrine in plasma

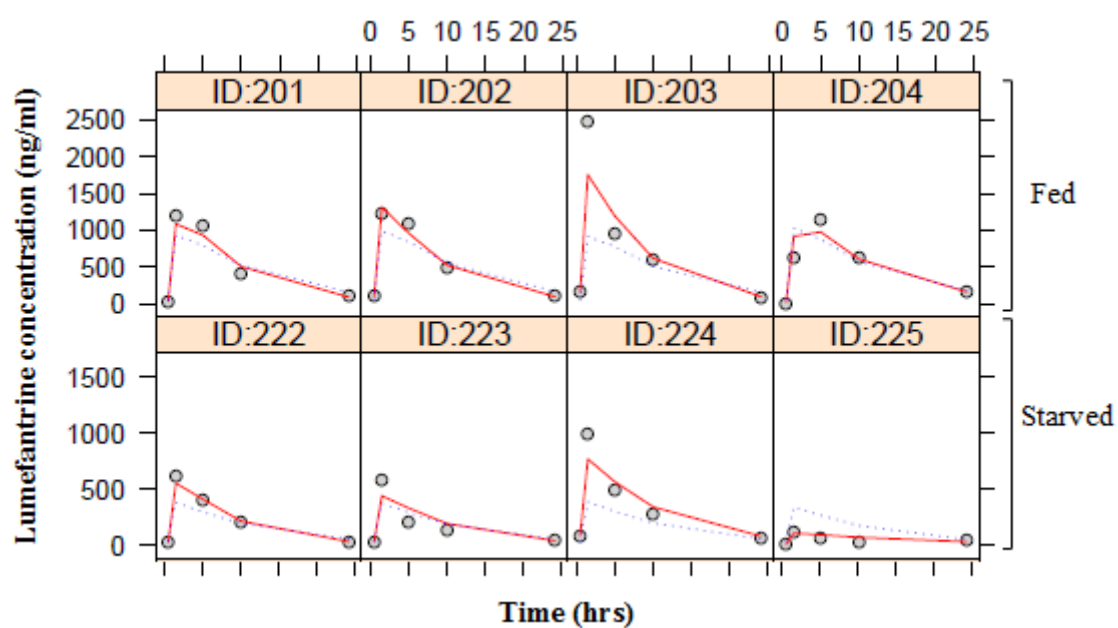


Figure 6.18: Observed and predicted plasma LF concentration vs. time profiles for 8 randomly selected experimental mice administered LF in reference solution.

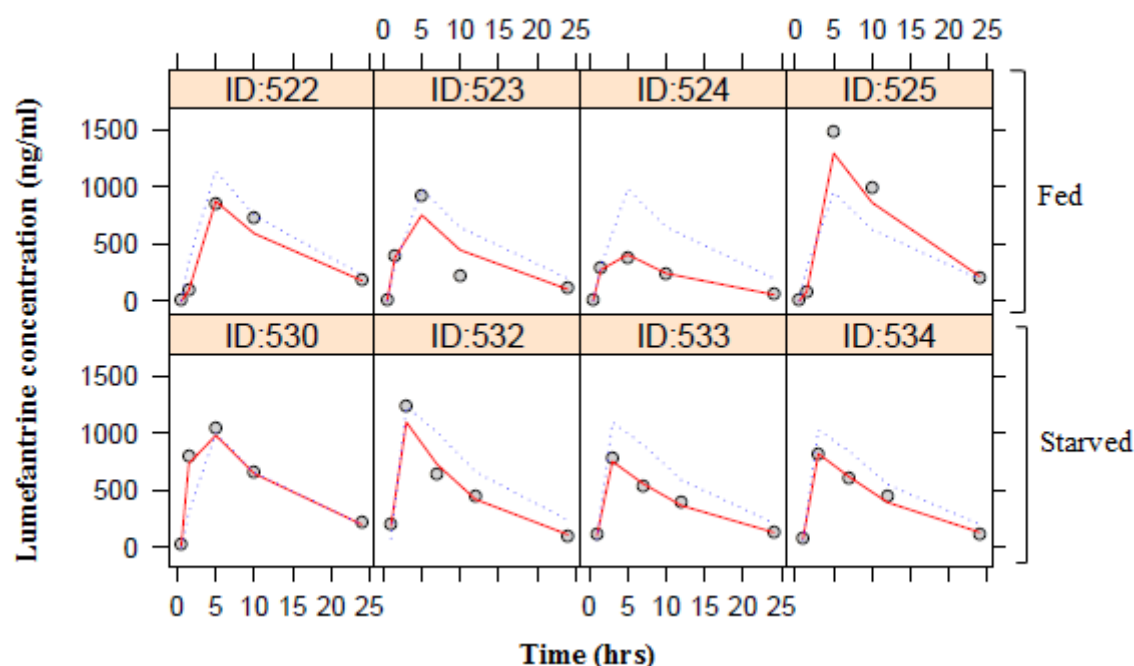


Figure 6.19: Observed and predicted plasma LF concentration vs. time profiles for 8 randomly selected experimental mice administered LF in canola oil.

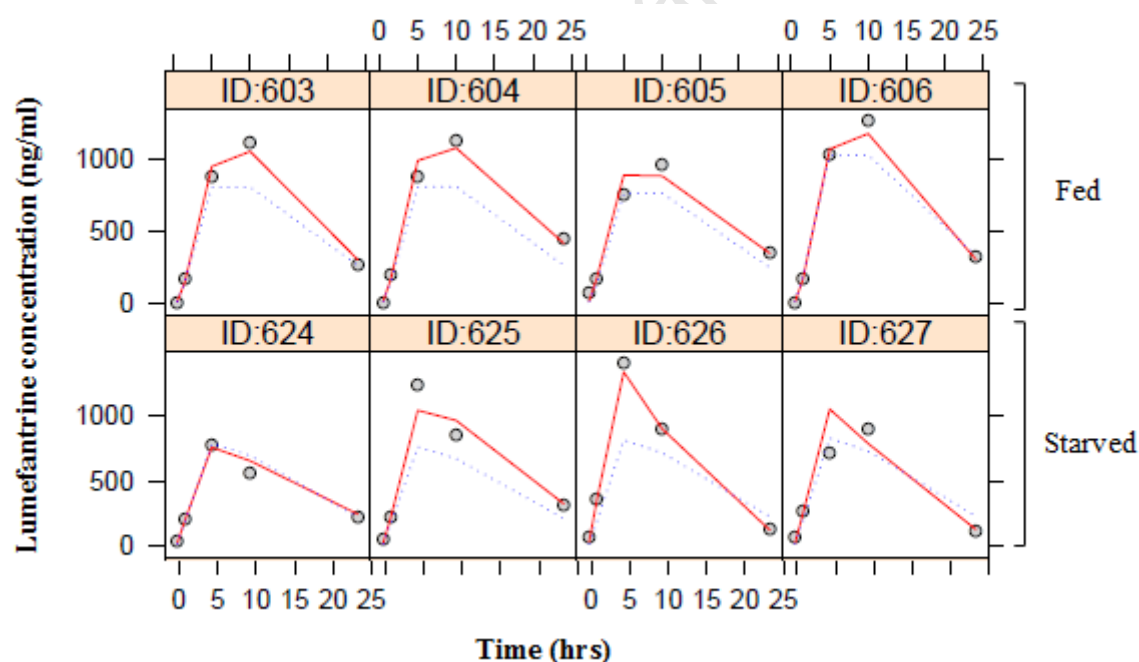


Figure 6.20: Observed and predicted plasma LF concentration vs. time profiles for 8 randomly selected experimental mice administered LF in Pheroid™ formulation.

The plasma and WB data were modelled jointly by introducing a scaling factor, refer to table 6.21. The model based WB/plasma scaling factor or ratio was 0.913 (which is close to 1) and a calculated between-subject variability of 16.7%, which indicates that there is no clinically significant difference in the concentration of LF in WB and plasma. Due to the absence of IV

data for LF, the estimation of the absolute bioavailability of LF was not possible. As a result of the logit transformation, used for bioavailability, NONMEM proposes the most likely bioavailability value for each combination of formulation and fed/starved state, but those values are an approximation. Only the ratios between the estimated bioavailability values are reliable and can be used for comparison. The final PPK parameter estimates are detailed in Table 6.21. A simulation using the final PPK model was used to estimate the NCA-equivalent parameters, shown in Table 6.22.

Table 6.21: The final parameter estimates for the LF pharmacokinetic model. CL and V are reported for a 27g mouse and allometrically scaled according to Anderson and Holford, 2008.

Parameter	Formulation (Fed/Starved)	Typical value (RSE[%])	%BSV (RSE[%])
CL (mL/h)		15.5 (20.1)	26.4 (10.3)
V (mL)		138 (19.5)	28.5 (12.3)
MTT (h)	Reference	0.881 (5.2)	21.4 (8.9)
	Canola oil	2.06 (3.7)	
	Pheroid™	3.51 (6.6)	
Effect of food on MTT (h)		+ 17.3% (32.7)	
NN	Reference & Canola oil	6.33 (5.1)	
	Pheroid™	1.74 (4.8)	
Bioavailability	Reference (Starved)	0.219 (24.2)	44
	Reference (Fed)	0.584 (22.8)	21
	Pheroid™ or Canola oil	0.705 (19.9)	15
Scaling WB/Plasma		0.913 (2.4)	16.7 (19.1)
Additive residual error (mg/L)		16.8 (6.6)	
Proportional residual error (%)		19.7 (2.7)	

Abbreviations: RSE; residual standard error, BSV; between-subject variability, CL; Clearance, V; volume of central compartment, MTT; mean transit time (for absorption) and NN; number of transit compartments.

Table 6.22: Simulation based NCA-equivalent PK parameter estimates for LF in the three different formulations. The values stated are the mean values (90% confidence interval [CI])

LF Formulation:	Reference		Canola oil		Pheroid™	
Starved/Fed	Starved	Fed	Starved	Fed	Starved	Fed
C _{max} (ng/mL)	382 (163-846)	994 (532-1680)	1118 (652-1798)	1088 (635-1742)	916 (545-1422)	866 (528-1331)
T _{max} (h)	1.7 (1.2-3.1)	2.0 (1.4-3.4)	3.7 (2.7-5.2)	4.2 (3.1-6.0)	6.2 (4.6-8.5)	7.2 (5.4-9.6)
AUC _{inf} (ng.h/mL)	5066 (2219-11106)	13229 (7248-22782)	16151 (9177-26427)	15975 (9160-26065)	16050 (9451-26758)	16013 (9457-25992)
T _{1/2} (h)	8.3 (4.3-15.7)	8.2 (4.4-15.2)	8.2 (4.4-15.8)	8.3 (4.3-15.7)	8.3 (4.5-15.8)	8.2 (4.4-15.4)
Bioavailability	0.22 (0.1-0.4)	0.57 (0.36-0.76)	0.69 (0.48-0.84)	0.69 (0.47-0.84)	0.69 (0.48-0.85)	0.69 (0.48-0.84)

The presence of food increased the absorption mean transit time (MTT), calculated for all formulations, by 17.3%. LF in Pheroid™ formulation had the highest MTT of 3.51 hours, which was 75% longer than the MTT for LF in reference solution. The typical value for LF bioavailability was 3.2 times higher when formulated with the Pheroid™ (or canola oil) as compared to LF in the reference solution in the starved state. The bioavailability of LF in reference formulation heavily depended on food intake resulting in a 2.7 times higher

bioavailability in the fed state. The between-subject variability in bioavailability was less for the PheroidTM formulation making the achievement of similar exposure in different subjects more feasible as compared to LF in reference solution, especially in the starved state.

Non compartmental analysis (NCA) was not performed during this study and the NCA PK parameter estimates, detailed in Table 6.22, were generated using model simulation. For the purpose of this study the pharmacokinetic parameters AUC, C_{max} and T_{max} can be used to qualitatively compare the different formulations of LF. AUC is defined as the area under the plasma/WB concentration-time curve; it is directly proportional to the amount of drug that is in systemic circulation and thus proportional to bioavailability and inversely proportional to CL. C_{max} is the highest systemic drug concentration predicted by the model and may serve as an indication of the rate and extent of drug absorption. T_{max} is the time at which C_{max} occurs and reflects the rate of drug absorption.

6.4 Discussion

Using the Pheroid™ formulation to improve the solubility and bioavailability of LF, eliminates the food effect associated with LF as well as significantly reducing the between subject variability in bioavailability. A similar effect can be obtained after the oral administration of LF in canola oil. The bioavailability of LF, calculated using the PPK model was 3.2 higher when formulated using the Pheroid™ technology as compared to LF in the reference solution (fasting state). Food may continue to affect the bioavailability of LF even when formulated using Pheroid™ technology, however the effect detected using the PPK model, was not significant. Food was found to slow down absorption, possibly as result of slower gastric emptying. For LF in Pheroid™ formulation, the between subject variability (BSV) for bioavailability was ~15% compared to ~44% for LF in reference solution, under fasting conditions. The BSV for LF in reference solution in the fed state is approximately half of the BSV in the fasted state.

It has been clinically established that LF exposure (normally quantified using AUC) is associated with its antimalarial efficacy and that the function of LF when co-administered with artemether is to remove residual parasites and prevent recrudescence (Ezzet *et al.*, 1998). A higher LF AUC was also found to significantly increase the antimalarial treatment efficacy or cure rate of AL (Ezzet *et al.*, 1998). The AUC of LF when administered in Pheroid™ formulation (16 013 ng.h/ml) was higher than LF in reference solution (13 229 ng.h/ml) in the fed state. Based on the model predictions, there was no significant difference in bioavailability between LF in Pheroid™ formulation and LF in canola oil. Using the Pheroid™ formulation did improve the solubility, absorption and bioavailability of LF following oral administration. This may indicate that Pheroid™ formulation technology can be applied as a versatile drug delivery system for lipophilic drugs.

The Pheroid™ delivery system has been used in other studies to improve drug pharmacokinetics. A study done by Steyn *et al.*, performed in a mouse model, involved evaluating the potential application of Pheroid™ technology in enhancing the absorption of novel artemisinin derivatives. Steyn *et al.* reported a 4.57 fold increase in AUC of Pheroid™ formulated artemisone, when orally administered compared to the reference formulation (Steyn *et al.*, 2011). In a study done by du Plessis *et al.*, Pheroid™ technology used as a drug delivery system, significantly improved the nasal and intestinal absorption of calcitonin, a polypeptide used for the treatment of osteoporosis (du Plessis *et al.*, 2010).

Despite the enhancement of LF bioavailability when formulated with PheroidTM formulation, the C_{\max} values are comparable to LF in reference solution in the fed state, with LF in canola oil reaching slightly higher concentrations. The LF in PheroidTM formulation used for this study was a preliminary formulation and optimization of drug inclusion into the PheroidTM vesicles was not performed. Other studies using an optimized drug in PheroidTM formulation reported enhanced C_{\max} as well as higher AUC values (Steyn *et al.*, 2011, du Plessis *et al.*, 2010).

When formulated with the PheroidTM, LF had a much longer MTT and took longer to reach C_{\max} than the other formulations. The increase in MTT indicates a delay in absorption rate, due to the composition of the PheroidTM formulation it may form a protective lipid barrier around the drug and this could have delayed the release and metabolism of the entrapped LF (Chigutsa *et al.*, 2011, Velcov *et al.*, 2005, Steyn *et al.*, 2011). The increase in T_{\max} of a PheroidTM formulated drug has been previously reported in a study done by Steyn *et al.* Artemisone in the PheroidTM vesicle formulation took longer to reach its C_{\max} in comparison to artemisone in the reference formulation (Steyn *et al.*, 2011).

The other preclinical studies investigating the pharmacokinetics of LF were performed in a rat model and using NCA analysis, reported LF to have variable oral absorption, low clearance, a large volume of distribution and long elimination half-life which concurs with clinical findings (Wahajuddin *et al.*, 2011). The sensitive LC-MS/MS quantification method developed in this study allowed for the PK investigation of LF in a mouse model, sampling significantly lower blood volumes than previous preclinical studies. PPK can be performed using sparse sampling data therefore the combined use of LC-MS/MS and PPK may reduce the number of experimental animals sacrificed for the pharmacokinetic investigation of drugs with long elimination half lives, saving time and cost.

This study was intended as a ‘proof of concept’ study for the determination of enhanced LF bioavailability, LF was only evaluated over a 24 hour time period which is not sufficient to conclusively describe the elimination phase of LF and effectively measure clearance, volume of distribution and elimination half-life. It is thus difficult to compare this study to previous studies however it can be concluded that the application of PheroidTM formulation technology significantly improves the bioavailability of LF.

References

1. Anderson B.J. and Holford N.H.G. Mechanism-based concepts of size and maturity in pharmacokinetics. *Annual Review of Pharmacology and Toxicology*, 48 (2008) 303-332
2. Ashley E.A., Stepniewska K., Lindergardh N., Annerberg A., Kham A., Brockman A.I., Singhasivanon P., White N.J. and Nosten F. Ho much fat is necessary to optimize lumefantrine oral bioavailability? *Tropical Medicine and International Health*, 12;2 (2007) 195-200
3. Austin JC, du Toit D, Fraser N, Lloyd P, Mansfield D, Macleod A, Odendaal JSJ and Seier J Guidelines on Ethics for Medical Research: Use of Animals in Research and Training South African Medical Research Council (2004)
4. Beal S.L. and Sheiner L.B. Estimating population kinetics. *Critical Reviews in Biomedical Engineering*, 8;3 (1982) 195-222
5. Beal S.L., Sheiner L.B., Boeckmann A. and Bauer R. NONMEM users guide. ICON Development Solutions, Ellicott City, MD, USA (1989-2009)
6. Benedetti M.S., Whomsley R., Poggesi I., Cawello W., Mathy F-X., Delporte M-L., Papeleu P and Watelet J-B. Drug metabolism and pharmacokinetics. *Drug Metabolism Reviews*, 41;3 (2009) 344-390
7. Bouzom F., Laveille C., Merdjan H. and Jochemsen R. Use of nonlinear mixed-effect modelling for the meta-analysis of preclinical pharmacokinetic data: application to S 20342 in the rat. *Journal of Pharmaceutical Sciences*, 89;5 (2000) 603-613
8. Chigutsa E., Visser M.E., Swart E.C., Denti P., Pushpakom S., Egan D., Holford N.H.G., Smith P.J., Maartens G., Owen A. and McIlleron H. The SLCO1B1 rs4149032 polymorphism is highly prevalent in South Africans and is associated with reduced rifampicin concentrations: dosing implications. *Antimicrobial Agents and Chemotherapy*, 55;9 (2011) 4122-4127
9. Coloussi D., Parisot C., Legay F. and Lefevre G. Binding of artemether and lumefantrine to plasma proteins and erythrocytes. *European Journal of Pharmaceutical Sciences*, 9 (1999) 9-16
10. Du Plessis L.H., Lubbe J. and Kotze A.F. Enhancement of nasal and intestinal calcitonin delivery by the novel Pheroid™ fatty acid based delivery system, and by N-trimethyl chitosan chloride. *International Journal of Pharmaceutics* (2009)
11. Ezzet F., Mull R. and Karbwang J. Population pharmacokinetics and therapeutic response of CGP 56697 (artemether+benflumetol) in malaria patients. *British Journal of Clinical Pharmacology*, 46 (1998) 553-561
12. Ezzet F., van Vugt M., Nosten F., Looareesuwan S and White N.J. Pharmacokinetics and pharmacodynamics of lumefantrine in acute falciparum malaria. *Antimicrobial Agents and Chemotherapy*, 44;3 (2000) 697-704
13. Holford N.H.G. The visual predictive check superiority to standard diagnostic (Rorschach) plots. In PAGE: Abstracts of the Annual Meeting of the Population Approach Group in Europe. ISSN 1871-6032 (2005) 14
14. Jonsson E.N. and Karlsson M.O. Xpose – a S-PLUS based population pharmacokinetic/pharmacodynamics model building aid for NONMEM. *Computer Methods and Programs in Biomedicine*, 58;1 (1999) 51-64
15. Keizer R.J., van Benten M., Beijnen J.H., Schellens J.H.M. and Huitema A.D.R. Piraña and PCluster: A modelling environment and cluster infrastructure for NONMEM. *Computer Methods and Programs in Biomedicine* (2010) 1-8
16. Lindbom L., Ribbing J. and Jonsson E.N. Perl-speaks-NONMEM (PsN) – a Perl module for NONMEM related programming. *Computer Methods and Programs in Biomedicine*, 72;2 (2004) 85-94

17. Makoid M.C., Vuchetich P.J. and Banakar U.V. Bioavailability, bioequivalence and drug selection in Basic Pharmacokinetics, 1st Edition (1999) <http://kiwi.creighton.edu/pkinbook/>
18. Savic R.M., Jonker D.M., Kerbusch T. and Karlsson M.O. Implementation of a transit compartment model for describing drug absorption in pharmacokinetic studies. *Journal of Pharmacokinetics and Pharmacodynamics*, 34;5 (2007) 711-726
19. Steyn J.D., Wiesner L., du Plessis L.H., Grobler A.F., Smith P.J., Chan W, Haynes R.K and Kotze A. Absorption of the novel artemisinin derivatives artemisone and atremiside: Potential application of Pheroid™ technology. *International Journal of Pharmaceutics* 414 (2011) 260-266.
20. Velkov T., Chuang S., Wielens J., Sakkellaris H., Charman W.N., Porter C.J.H. and Scanlon M.J. The interaction of lipophilic drugs with intestinal fatty acid binding protein. *Journal of Biological Chemistry*, 280 (2005) 17769–17776
21. Wahajuddin, Singh S.P. and Jain G.K. Determination of lumefantrine in rat plasma by liquid-liquid extraction using LC-MS/MS with electrospray ionization: assay development, validation and application to a pharmacokinetic study. *Journal of Chromatography B*, 877 (2009) 1133-1139
22. Wahajuddin, Singh S.P., Raju K.S.R., Nafis A., Puri S.K. and Jain G.K. Intravenous pharmacokinetics, oral bioavailability, dose proportionality and in situ permeability of anti-malarial lumefantrine in rats. *Malaria Journal* (2011)
23. Wahajuddin, Singh S.P. and Jain G.K. Gender differences in pharmacokinetics of lumefantrine and its metabolite desbutyl-umefantrine in rats. 'Accepted article' (2012)
24. Wernsdorfer W.H. Coartemether (artemether and lumefantrine): an oral antimalarial drug. *Expert Reviews, Anti-Infective Therapy*, 2;2 (2004) 181-196
25. White N.J., van Vugt M. and Ezzet F. Clinical pharmacokinetics and pharmacodynamics of artemether-lumefantrine. *Drug disposition, Clinical Pharmacokinetics*, 37;2 (1999) 105-125
26. Yu S., Li S., Yang H., Lee F., Wu J-T. and Qian M.G. *Rapid Communication in Mass Spectrometry* (2005) 250-254

Chapter 7

Antimalarial efficacy study of lumefantrine in mice

7.1 Introduction

The pre-clinical evaluation of test compounds culminates in determining the efficacy of the drug in treating an active infection in a suitable animal model. *Aotus* and *Saimiri* monkeys may be infected with *P. falciparum* and may be the best animal model for predicting antimalarial efficacy in humans however it's not a cost effective animal model and the mouse malaria model is more suited for preliminary studies. As human malaria parasites are unable to infect non-primate animals, antimalarial efficacy is routinely evaluated using a mouse malaria model. Rodent malaria parasites serve as good experimental models, *in vivo*, for the study of human malaria. *Plasmodium vinckei*, *Plasmodium chabaudi*, *Plasmodium yoelli* and *Plasmodium berghei* are the four malaria parasites that infect rodents and are used for the investigative study of the developmental biology of the malaria parasite, drug resistance, parasite–host interactions and drug efficacy (Fidock *et al.*, 2004, Pink *et al.*, 2005). Rodent malaria parasites exhibit analogous structure, physiology and life cycle when compared to human malaria parasites and are therefore reliable models for predicting treatment efficacy. The rodent parasites also have comparable genetics to human parasites, thus a viable model for genetic modification studies. In previous pre-clinical studies, rodent malaria models have been used to demonstrate the antimalarial efficacy of mefloquine, halofantrine and the artemisinin derivatives (Peters *et al.*, 1977, Peters *et al.*, 1987, Posner *et al.*, 2003 and Fidock *et al.*, 2004). There are, however differences between human and rodent plasmodia and careful assessments need to be considered when making predictions of human treatment outcomes based on efficacy studies in mice.

The rodent plasmodia differ in virulence, pathology, synchronicity and some may be more sensitive to specific antimalarials. *P. chabaudi* and *P. vinckei* generate high parasitemia's and produce synchronous infections; all the parasites exist at the same stage of intracellular development. The *P. yoelli* 17X strain is intrinsically partially resistant to CQ and *P. chabaudi* and *P. vinckei* are sensitive to ion chelators and lipid biosynthesis inhibitors (Carter and Diggs 1977, Fidock *et al.*, 2004). *P. berghei* produces rapidly fulminating, asynchronous infections in mice and has a parasite multiplication rate of 10x every 24 hour period. *P.*

berghei is primarily used in drug screening assays (Carter and Diggs, 1977, Kalra *et al.*, 2006)

There are few publications detailing pre-clinical efficacy studies on LF, Kiboi *et al.* used the *P. berghei* ANKA strain to select for resistance to LF and Piperaquine (PQ) by continuous drug pressure *in vivo*. The effective dose of drug which reduces parasitemia by 50% (ED₅₀) and 90% (ED₉₀) for LF and PQ were measured in a quantitative standard 4-day suppressive test, in which the parasites are exposed to four, daily, drug doses. The reported ED₉₀ for LF using the parent *P. berghei* strain was 3.93 mg/kg, however when using the resistant strain the ED₉₀ increased more than 50 times (Kiboi *et al.*, 2009). The drug resistant parasite strains may be used in future to study and understand the mechanisms of LF and PQ resistance, provided the mechanism of resistance in *P. berghei* is similar to *P. falciparum*. For the purpose of this study, the *P. berghei* ANKA strain was chosen for infection of the experimental mice. It is a CQ sensitive parasite strain and ideal for a preliminary antimalarial efficacy study. A modified Peters' 4-day suppressive test was performed to compare the efficacy of the test formulations, administered in four daily doses, to the standard drug CQ in prolonging the survival of the infected mice.

Aim

This efficacy study was performed to test the hypothesis that an improved oral bioavailability of LF when formulated using Pheroid™ technology, would result in improved antimalarial efficacy. The specific aim was to determine if LF in Pheroid™ formulation, administered orally, was more effective than LF in reference formulation, in increasing the survival time of *P. berghei* infected mice when compared to CQ.

Objectives

Perform Peters' 4-day test to compare the efficacy (suppression of parasitemia) of LF in the reference and Pheroid™ formulations to the standard drug CQ.

Test each formulation at three different concentrations to estimate an effective dose range.

Compare the survival times and chemosuppression of the treatment groups for each formulation, at each dose concentration to CQ.

Determine, using survival analysis, which of the formulations is more effective or comparable to CQ.

7.2 Materials and Methods

Solvents and chemicals

Analytical grade LiChrosolv[®] water and methanol was purchased from Merck (Darmstadt, Germany). Dimethyl sulfoxide (DMSO) was purchased from Merck (Darmstadt, Germany). Chloroquine diphosphate (CQ) was purchased from Sigma.

LF dose formulations

The reference treatment group received LF dissolved in a DMSO:water (1:9 v/v) solution. The 10, 5 and 1 mg/kg dosing concentrations were calculated as shown in Chapter 6, Figure 6.4 (refer to page 104), for an average mouse mass of 25 g and 200 µl dose volume per mouse per day (for four day treatment: 800 µl/mouse). As shown in Table 7.1, LF was weighed out and dissolved in solution to obtain a final concentration calculated according to the average weight of the mice in the treatment group.

Table 7.1: Dose calculation for LF in reference formulation. *Calculated for an average mouse weight of 25 g

Dose (mg/kg)	*Final concentration (mg/ml)	Mass of LF (mg)	Total volume of dosing solution (ml)
10	1.25	7.5	6
5	0.625	3.75	6
1	0.125	0.75	6

The positive control group received CQ dissolved in water at a dose concentration of 10 mg/kg. The negative control group was administered the diluent or solution that the compound is dissolved in. For the reference formulation the negative control group received DMSO:water (1:9 v/v) solution, and for the Pheroid[™] formulation they received a Pro-Pheroid[™] solution, containing no active drug.

The Pheroid[™] treatment group received LF in Pro-Pheroid[™] formulation prepared by Dr L Du Plessis (University of North West, Potchefstroom). As detailed in Table 7.2, the Pro-Pheroid[™] formulated LF was prepared at a 5 mg/ml stock solution and was diluted using a drug free pro-pheroid solution to obtain exact dosage concentrations based on the average weight of the mice in the treatment group.

Table 7.2: Dose calculation for LF in Pheroid™ formulation. *Calculated for an average mouse weight of 25g

Dose (mg/kg)	*Final concentration (mg/ml)	Pheroid™ Diluent volume (µl)	5µg/ml stock spiked volume (µl)	Total volume of dosing solution (ml)
10	1.25	4500	1500	6
5	0.625	5250	750	6
1	0.125	5850	150	6

P. berghei rodent malaria 4-day suppressive test

The experimental animals used for this study, 8-10 week old, male C57/BL6 mice, were obtained from the University of Cape Town's Medical School, Animal Unit. The mice were housed at the Animal Laboratory Unit, Groote Schuur Hospital, OMB (K floor) and kept in ventilated cages with food and water available *ad libitum*. All animals were treated humanely and the *in vivo* experiments were planned based on the guidelines for the ethical use of animals in research (Austin *et al.*, 2004).

To evaluate the blood schizontocidal activity of the formulations, the modified Peters' 4-day suppressive test was performed in mice infected with *P. berghei*, ANKA strain (CQ sensitive) parasites as per protocol, approved by UCT Animal Ethics Committee, ethics clearance no. 010/027 (Peters, 1975). The weight of the mice was used as an indication of health and monitored continuously throughout the experimental period. As per protocol, the mice were euthanized if a 20% loss in initial body weight was observed. Chloroquine (CQ) was used as the standard drug and the positive control group was dosed at 10 mg/kg (non-curative dose) via oral gavage. To generate statistically reliable results each treatment and control group consisted of 5 mice.

The experiment was performed on two separate occasions as it would have been difficult to efficiently dose the required amount of test mice. The first test compared the reference formulation to CQ and the second compared the Pheroid™ formulation to CQ. The procedure for each experiment was identical and is detailed in Figure 7.1.

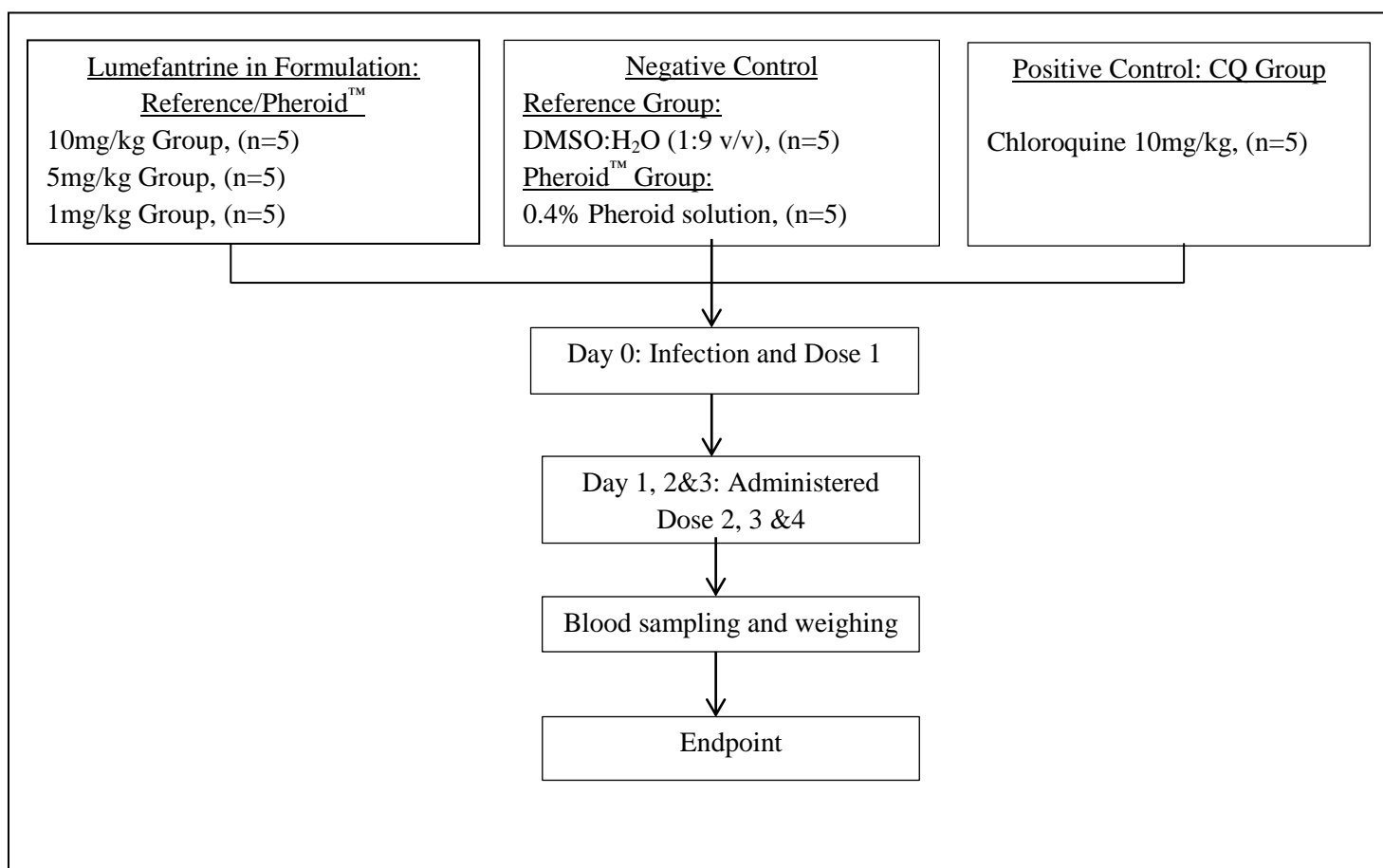


Figure 7.1: Schematic detailing the experimental procedure for the *in vivo* 4-day suppressive test.

Test Procedure

This efficacy study required ‘donor’ mice, to maintain parasitemia passage as the experimental mice had to be inoculated with parasitized red blood cells. The *P. berghei* parasite stock was stored in liquid nitrogen, thawed and used to infect the donor mouse. Once the donor mouse had developed the *P. berghei* infection, at approximately 30% parasitemia, blood samples were collected and the parasitized RBCs were diluted using sterile phosphate buffered saline (PBS). A 0.2 ml aliquot of this solution, containing 1×10^6 parasitized erythrocytes, was used to inoculate the experimental mice via intraperitoneal (IP) injection. The first treatment dose was administered 2 hours after inoculation. The test formulations were administered, by oral gavage, to the *P. berghei* infected mice as described by Peters *et al.*, and were evaluated according to the reduction in parasitemia and survival time of the experimental mice compared to the positive control group (Peters, 1975, Tona *et al.*, 2001). Each formulation was tested at three different concentrations; 10, 5, and 1 mg/kg, to obtain a preliminary indication of an effective dose range. LF in reference or Pheroid™ formulation

was administered daily for 4 consecutive days after the mice were infected. Similarly, the positive control group received CQ and the negative control groups the diluent or DMSO solution.

The level of parasitemia was determined, for all experimental mice, at specified time points. For the LF in reference formulation experiment, parasitemia was determined on days 1, 3, 8, 11 and 15. For the LF in Pheroid™ formulation experiment, parasitemia was determined on days 2, 4, 8, 12, 16 and 23.

For the determination of parasitemia: The tail is nicked and a small drop of blood is smeared on a glass slide, the smear is fixed onto the slide using 100% methanol and rinsed off using tap water. The slide is then stained using a Giemsa stain solution prepared using distilled water (1:9, v/v), the stained blood slide is then rinsed and dried. As depicted in Figure 7.2, the stained slide is viewed using a light microscope, under oil immersion with a 100 x 1.4 objective. The parasitemia was determined by counting four fields of approximately 100 RBCs per field, making note of the total number of infected and uninfected RBCs (Fidock *et al.*, 2004). The parasitemia is calculated using the following formula:

$$\text{Parasitemia} = \text{No. of Infected RBC} / \text{Total RBC}$$

Where total RBC is equal to the number of infected + uninfected RBCs.



Figure 7.2: Images depicting the morphology of *P. berghei* using light microscopy, the different stages of parasite development shown here are: a. ring-form, b. trophozoite and c. shizont.

For this experiment, the parasitemia values were calculated without distinguishing between the different stages of parasite development.

Survival Analysis

Survival analysis was performed on the data using Stata® 11.0 statistical software package. Cox proportional hazards regression model was used for the analysis and Kaplan-Meier survival estimates to plot the data.

7.3 Results

7.3.1 LF in reference formulation

Throughout the duration of the Peters' 4-day suppressive test, the level of parasitemia was determined for all treatment and control groups. Each group consisted of 5 mice and the average parasitemia values are presented in Table 7.3. For LF in reference formulation the treatment groups survived as long as the CQ group and almost twice as long as the negative control group. As shown in Figure 7.3, all the mice in the 1 mg/kg succumbed to infection by day 11 while the 5 and 10 mg/kg groups fared comparably to the CQ group, surviving to day 15. The mice in the negative control group survived for an average of eight days after infection.

Table 7.3: Average parasitemia (%) values for the LF in reference formulation group at each treatment dose including the controls

		%Parasitemia				
Treatment groups		D1	D3	D8	D11	D15
10 mg/kg	Average	1	1	1	4.2	29
	STDEV	0	0	0	4.44	0
5 mg/kg	Average	1	1	1	1	37.5
	STDEV	0	0	0	0	17.7
1 mg/kg	Average	1	1	27	45	
	STDEV	0	0	3.08	11.2	
CQ <i>positive control</i>	Average	1	1	1	3	25
	STDEV	0	0	0	0	0
DMSO <i>negative control</i>	Average	1	30.7	50		
	STDEV	0	8.91	0		

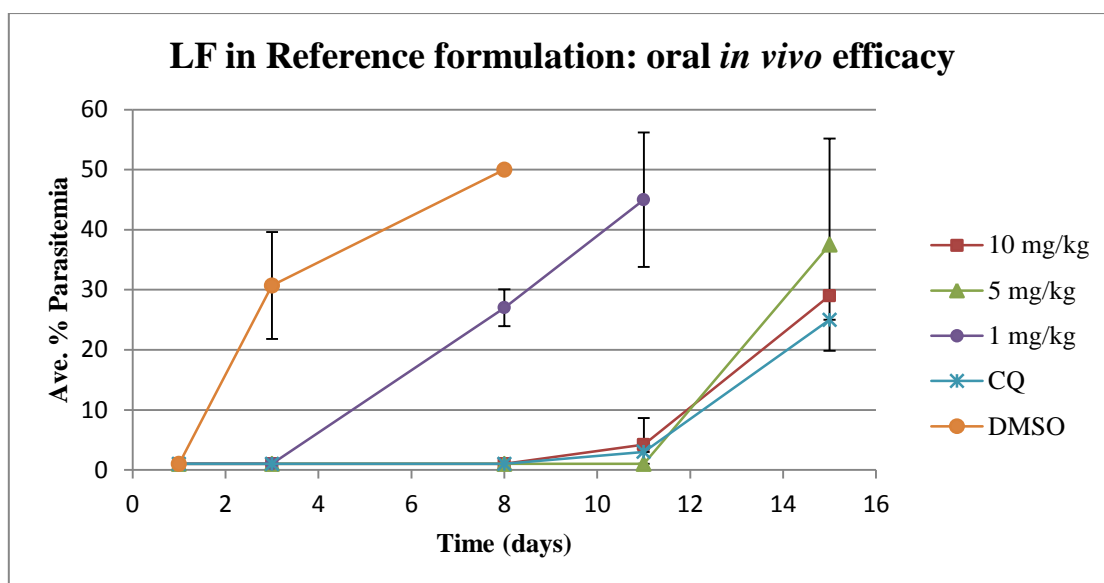


Figure 7.3: Average % parasitemia vs. time graph for the LF in Reference formulation treatment groups at concentrations of 10, 5 and 1 mg/kg as well as the control groups; CQ (positive control) and DMSO (negative control). The error bars represent the standard deviation in the data.

The percentage chemosuppression was calculated using the following formula: $[(A-B)/A] \times 100$, where A is the average parasitemia for the negative control group and B is the average parasitemia for the test group. Chemosuppression is usually determined using the parasitemia values calculated on day 5 but due to the low parasitemia values observed, it was decided to determine activity on day 8 for the reference group and day 12 for the Pheroid™ group. The infection rate was slower when testing the Pheroid™ group compared to the reference group therefore activity was calculated on different days.

The level of chemosuppression was determined for all treatment dose concentrations for the reference group on day 8 after infection and the results are detailed in Table 7.4. The 5 and 10 mg/kg group had a 98% chemosuppression on day 8 after infection, comparable to CQ, but the CQ group had lower parasitemia values throughout the experiment. However as seen in Figure 7.4, a higher proportion of mice in the 5 and 10 mg/kg group survived to day 15 than the CQ group. None of the treatment groups were able to cure the infection in the experimental mice

Table 7.4: *In vivo* antimalarial activity (chemosuppression) of LF in reference formulation on day 8 post infection. S.D; standard deviation

Treatment	Dose (mg/kg)	Ave. %Parasitemia (S.D)	Chemosuppression (%)
LF in Ref formulation	10	1	98
	5	1	98
	1	27 (3.08)	46
CQ (positvie control)	10	1	98
DMSO (negative control)	n/a	50	0

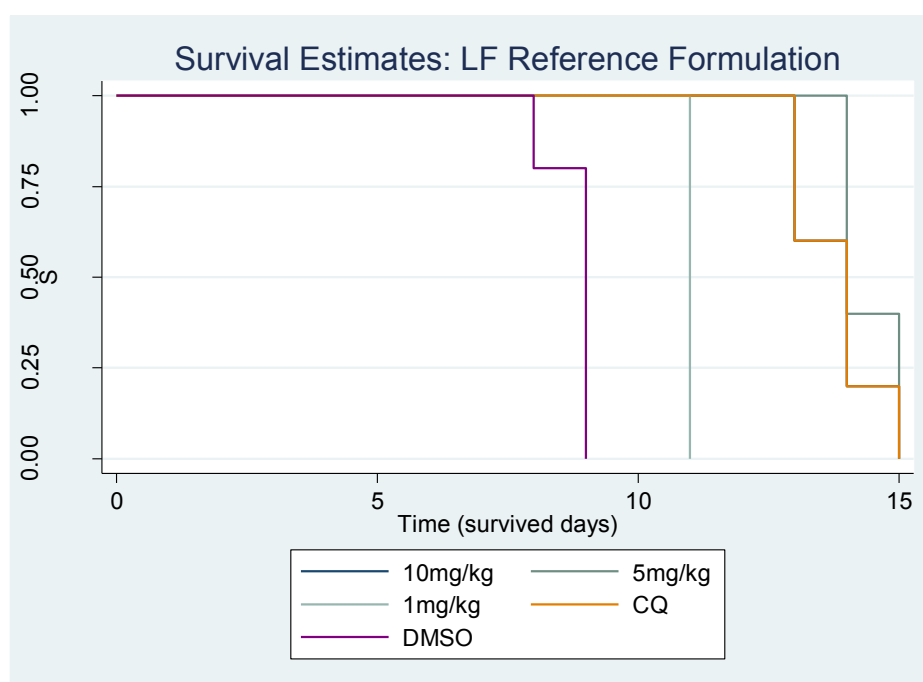


Figure 7.4: Kaplan-Meier survival estimate: Proportion surviving (S) vs. Time (days) plot for the LF in reference formulation treatment groups at 10, 5 and 1 mg/kg as well as the control groups. The survival plot for 10 mg/kg dose is identical to the 5 mg/kg plot. CQ; chloroquine, DMSO; 10% DMSO in water solution

A Cox regression was performed to establish if LF in reference formulation at the 10 mg/kg treatment dose was able to prolong the survival of the infected mice when compared to the CQ treated group. The statistical term hazard ratio in survival analysis relates the rate that an event (e.g. death from malaria infection) may occur in one group compared to the rate that the same event occurs in the other group. A hazard ratio of 1 means there is no difference between the two groups. Results from the regression yielded a hazard ratio of 0.826 (95% confidence interval [CI] 0.31, 2.21; $p = 0.704$), which indicated no significant difference

between the survival efficacy of the LF in reference formulation, at the highest tested dose, and CQ in treating the infected mice.

7.3.2 LF in Pheroid™ formulation

A similar result to the reference formulation was seen in the experiment comparing the LF in Pheroid™ formulation to CQ treatment. The infected mice in this experiment survived for a longer period of time than in the reference experiment. The parasitemia values for the LF in Pheroid™ treatment and control groups are detailed in Table 7.5 and graphically shown in Figure 7.5. As expected the 10 mg/kg treatment group performed better than the 5 and 1 mg/kg groups in suppressing the level of parasitemia.

Table 7.5: Average % parasitemia values for the LF in Pheroid™ formulation group at each treatment dose including the controls

		%Parasitemia					
Treatment groups		D2	D4	D8	D12	D16	D23
10 mg/kg	Average	1	1	1	2	24.4	50
	STDEV	0	0	0	0	6.95	0
5 mg/kg	Average	1	1	12.3	29.5	50	
	STDEV	0	0	6.34	0.707	0	
1 mg/kg	Average	1	1	31.2	43.3	50	
	STDEV	0	0	4.92	5.77	0	
CQ <i>positive control</i>	Average	1	1	1	5.32	36.7	50
	STDEV	0	0	0	6.36	15.3	0
DMSO <i>negative control</i>	Average	1	2.8	20.6	50		
	STDEV	0	0.837	16.1	0		

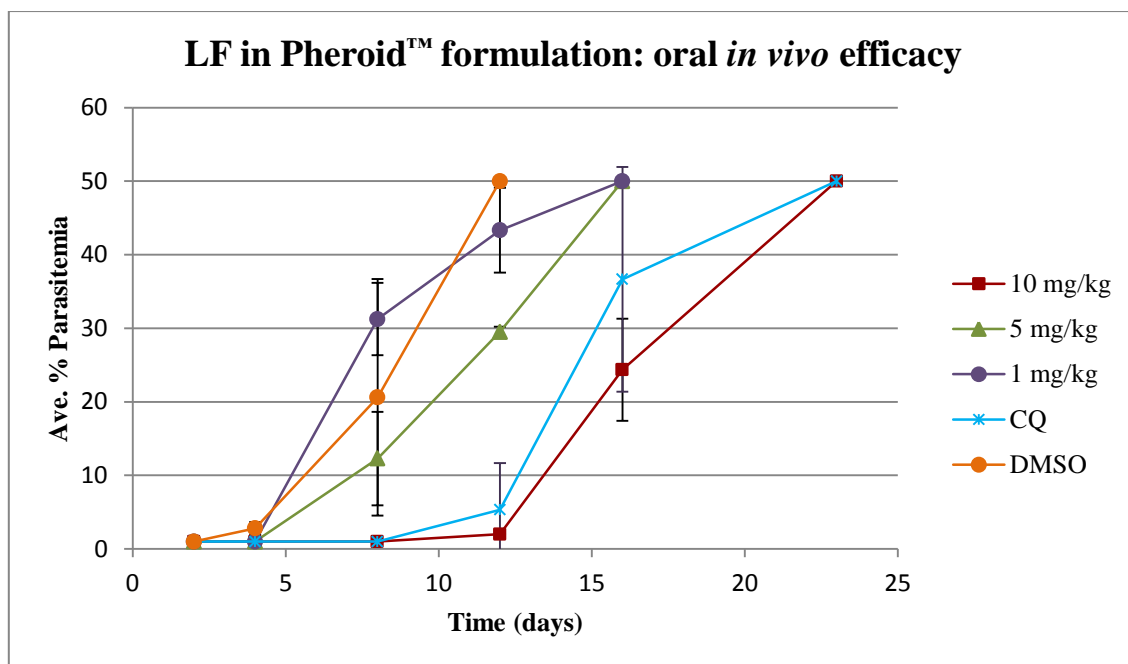


Figure 7.5: Average % parasitemia vs. time graph for the LF in Pheroid™ formulation treatment groups at concentrations of 10, 5 and 1 mg/kg as well as the control groups; CQ (positive control) and DMSO (negative control).

As seen in Figure 7.5, for LF, the higher the dose the better the suppression of parasitemia. The 10 mg/kg and CQ treated groups survived till day 23 (Figure 7.6), however as demonstrated in Figure 7.5 it may be deduced that the 10 mg/kg treatment was more effective than CQ in suppressing the parasitemia. The activity (chemosuppression) of the treatment groups and CQ was calculated on day 12 of the experiment and the results are presented in Table 7.6. LF in Pheroid™ formulation at 10 mg/kg demonstrated a chemosuppression of 96% which was higher than CQ's 89.4% chemosuppression. Figure 7.6 demonstrates the proportion of surviving mice, for each treatment and control group, for the duration of the experiment.

Table 7.6: *In vivo* antimalarial activity (chemosuppression) of LF in Pheroid™ formulation on day 12 post infection.

Treatment	Dose (mg/kg)	Ave. %Parasitemia (S.D)	Chemosuppression (%)
LF in Pheroid™ formulation	10	2	96
	5	29.5 (0.71)	41
	1	43.3 (5.8)	13.4
CQ (positvie control)	10	5.32 (6.4)	89.4
DMSO (negative control)	n/a	50	0

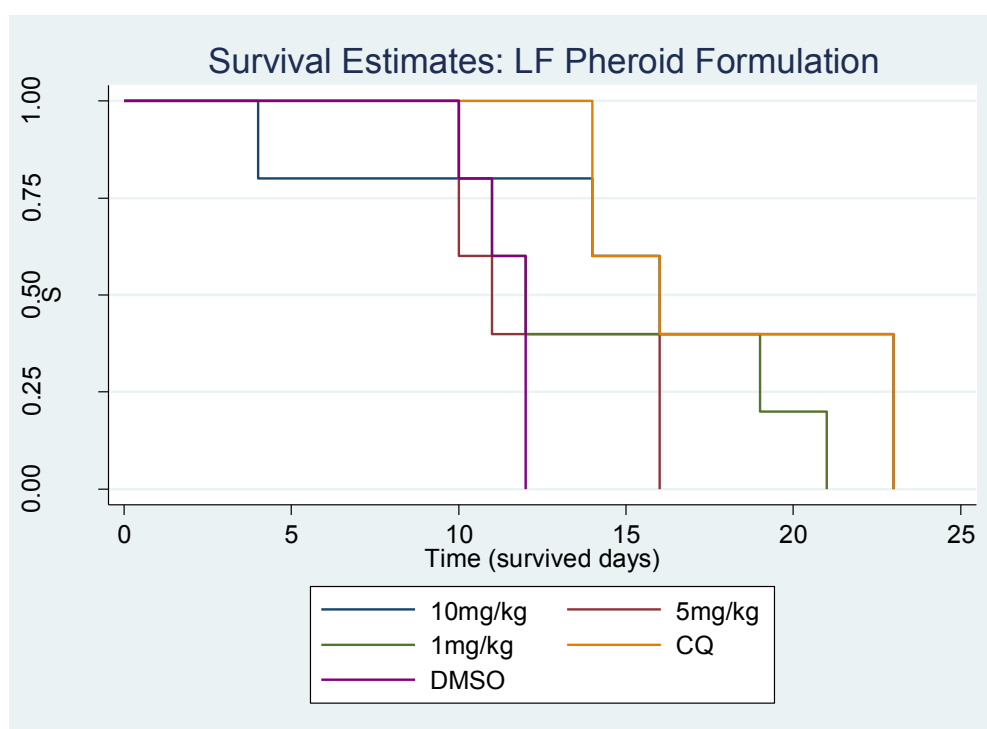


Figure 7.6: Kaplan-Meier survival estimate: Proportion surviving (S) vs. Time (days) plot for the LF in Pheroid™ formulation treatment groups at 10, 5 and 1 mg/kg as well as the control groups. The survival plot for the 10 mg/kg group and CQ are indiscernible after day 15. CQ; chloroquine, DMSO; 10% DMSO in water solution

One of the mice in the 10 mg/kg treatment group died on day 4 for unexplained reasons. Toxicity has been ruled out as an explanation as previous bioavailability experiments have been performed in mice which were administered higher doses of LF (results not shown). One mouse in the 1 mg/kg group survived till day 21 despite high parasitemia and performed much better than the mice in the 5 mg/kg group which only survived till day 16. The mice in the 10 mg/kg group survived just as long as the CQ group.

A Cox regression was performed to establish if LF in Pheroid™ formulation at the 10 mg/kg treatment dose was able to significantly prolong the survival of the infected mice when compared to the CQ treated group. Results from the regression yielded a hazard ratio of 0.935 (95% confidence interval [CI] 0.27, 3.23; $p = 0.916$), and a p value of 0.916 indicating that there was no significant difference between the survival efficacy of the LF in Pheroid™ formulation, at the highest tested dose, and CQ in treating the infected mice.

7.4 Discussion

The results from the modified Peters' 4-day suppressive test indicate that LF in the reference and Pheroid™ formulations, at 10 mg/kg, perform comparably to CQ in reducing parasitemia. This experiment was preliminary and higher dosing concentrations will have to be tested to determine an effective dose of LF in Pheroid™ formulation. The treatment doses used in this study were conservative as primary *in vivo* experiments are usually performed at dosing concentration of 50 or 100 mg/kg (Fidock *et al.*, 2004, Kalra *et al.*, 2006). As mentioned earlier Kiboi *et al.* reported an EC₉₀ of 3.93 mg/kg for LF also using *P. berghei* ANKA strain however the mice were not cured in this experiment, even with a treatment dose of 10 mg/kg (Kiboi *et al.*, 2009).

The LF in reference formulation at 5 and 10 mg/kg performed similarly with respect to chemosuppression and duration of survival. This may be due to the variable bioavailability observed with the reference formulation as one would expect the higher concentration dose to perform more effectively. However this deduction is merely speculative as blood samples for analysis were not collected and the plasma concentration of LF was not determined when the level of parasitemia was determined. Throughout the experiment CQ performed better at suppressing the parasitemia than the LF in reference formulation at all the dose concentrations.

The LF in Pheroid™ formulation treatment group showed good suppression of parasitemia and duration of survival, at the 10 mg/kg dose. Also the LF in Pheroid™ formulation at the 10 mg/kg dose demonstrated a higher reduction in parasitemia on day 12 than CQ. However none of the treatment formulations, at the tested concentrations, were able to cure the infection. Results from the Cox regression indicate that both the LF in reference formulation and LF in Pheroid™ formulation treatment groups were unsuccessful in significantly prolonging the survival of the infected mice when compared to the positive control, CQ.

Further efficacy studies, should be done to determine the lowest effective dose and determine conclusively if the LF in Pheroid™ formulation would be more efficacious than the reference solution. Also if blood samples were collected for the determination of drug plasma levels as well as for the determination of parasitemia then one would be able to relate LF bioavailability to its efficacy or pharmacodynamic effect, more accurately.

As reported by Ezzet *et al.*, the effect of LF when co-administered with artemether is to remove residual parasites, cure infection and prevent recrudescence (Ezzet *et al.*, 1998). The '*P. berghei* onset of action and recrudescence test' would be a more relevant *in vivo*

antimalarial experiment for the testing of LF in Pheroid™ formulation compared to a reference formulation. The test procedure includes administering a single dose, three days after infection followed by daily monitoring and determining parasitemia levels. This test allows for the establishment of onset of activity, time to onset of recrudescence and survival time (Fidock *et al.*, 2004).

This study was primarily a proof of concept study and optimization of the LF in Pheroid™ formulation and further *in vivo* testing may be warranted to establish improved antimalarial efficacy.

University of Cape Town

References

1. Austin JC, du Toit D, Fraser N, Lloyd P, Mansfield D, Macleod A, Odendaal JSJ and Seier J Guidelines on Ethics for Medical Research: Use of Animals in Research and Training *South African Medical Research Council* (2004)
2. Carter R. and Diggs C.L. Plasmodia of rodents. In: Parasitic Protozoa Vol.3 (1977) 359-465
3. Clark T.G., Bradburn M.J., Love S.B. and Altman D.G. Survival analysis part 1: basic concepts and first analyses. *British Journal of Cancer*, 89 (2003) 232-238
4. Ezzet F., Mull R. and Karbwang J. Population pharmacokinetics and therapeutic response of CGP 56697 (artemether + benflumetol) in malaria patients. *British Journal of Clinical Pharmacology*, 48(1998) 553-561
5. Fidock D.A., Rosenthal P.J., Croft S.L., Brun R. and Nwaka S. Antimalarial drug discovery: Efficacy models for compound screening. *Nature Reviews*, 3 (2004) 509-520
6. Kalra B.S., Chawla S., Gupta P. and Valecha N. Screening of antimalarial drugs: An overview. *Indian Journal of Pharmacology*, 38;1 (2006) 5-12
7. Kiboi D.M., Irungu B.N., Langat B., Wittlin S., Brun R., Chollet J., Abiodun O., Nganga J.K., Nyanbati V.C.S., Rukunga G.M., Bell A. and Nzila A. *Plasmodium berghei* ANKA: Selection of resistance to piperazine and lumefantrine in a mouse model. *Experimental Parasitology*, 122 (2009) 196-202
8. Peters W. The chemotherapy of rodent malaria XXII: the value of drug-resistant strains of *P. berghei* in screening for blood schizonticidal activity. *Annals of Tropical Medicine and Parasitology*, 69;2 (1975) 151-171
9. Peters, W. et al. The chemotherapy of rodent malaria. XXVII. Studies on mefloquine (WR 142,490). *Annals of Tropical Medicine and Parasitology*, 71 (1977) 407-418.
10. Peters, W., Robinson, B. L. and Ellis, D. S. The chemotherapy of rodent malaria. XLII. Halofantrine and halofantrine resistance. *Annals of Tropical Medicine and Parasitology*, 81 (1987) 639-646.
11. Pink R., Hudson A., Mouries M.A. and Bendig M. Opportunities and challenges in antiparasitic drug discovery. *Nature Reviews: Drug Discovery*, 4 (2005) 727-740
12. Posner G.H., Oh C.H., Webster K., Ager A.L., Ager J.R. and Rossan N. New antimalarial tricyclic 1,2,4-trioxanes: evaluations in mice and monkeys. *American Journal of Tropical Medicine and Hygiene*, 50;4 (1994) 522-526
13. Posner G.H., Paik I.H., Sur S., McRiner A.J., Borstnik K., Xie S. and Shapiro T.A. Orally active, antimalarial, anticancer, artemisinin-derived trioxane dimers with high stability and efficacy. *The Journal of Medicinal Chemistry*, 46 (2003) 1060-1065
14. Tona L, Mesia K, Ngimbi N.P, Chrimwami B, Okond'ahoka, Cimanga K, De Bruyne T, Apers S, Hermans N, Totte J, Pieters L and Vlietinck A.J. In vivo antimalarial activity of *Cassia occidentalis*, *Morinda morinoides* and *Phyllanthus niruri*. *Annals of Tropical Medicine & Parasitology*, 95;1 (2001) 47-57

Chapter 8

Conclusion

Drug discovery and development is a time consuming and costly process and without sufficient financial support for scientific research, 'neglected diseases' such as malaria will continue to claim lives in some of the poorest countries in the world. Malaria is a particularly devastating disease in Africa, with children and pregnant women being the most vulnerable to infection, disease complication and mortality. Currently, drug treatment strategies are challenged by the emergence of antimalarial drug resistant parasites therefore necessitating drug combination therapy to safeguard the longevity of clinically effective antimalarials. Continual efforts are being made to discover or synthesize novel antimalarial compounds with unique modes of action.

LF was synthesized in the 1970's and is currently partnered with artemether as a fixed dose ACT for the treatment of uncomplicated malaria. As is the case with many 'old' drugs, extensive pre-clinical investigation was not performed before clinical use, however, LF is still effective and well tolerated despite its poor aqueous solubility and variable bioavailability. The aim of this study was to improve the bioavailability of LF. It was hypothesized that by improving the solubility of LF with the application of Pheroid™ technology we could produce a LF formulation with enhanced bioavailability and efficacy as well as predictable pharmacokinetics.

The *in silico* tools predicted that LF had low solubility and good (Caco-2 cell membrane) permeability. Computational predictive models are usually used to explain experimental results or predict pharmacokinetic properties of new drug compounds. The low aqueous solubility of LF would result in inadequate dissolution and explain the slow, erratic absorption of LF. The fat in ingested food would facilitate the solubilisation and therefore improving the absorption of LF. It is thus relevant to describe the physicochemical factors of a test compound that may influence drug pharmacokinetics and efficacy.

With the advantage of mass spectrometric detection, sensitive and selective LC-MS/MS methods were developed and validated for the quantitation of LF in mouse whole blood and plasma. Due to the short analytical run time and sensitivity of mass spectrometric detection, the developed methods are suitable for high throughput analysis using a 20 µl sample volume. LF was quantitated in WB and plasma to determine if there was a difference between

the two biological matrices and using the PPK model no substantial differences were found in the PK parameters. Blood-plasma ratio testing should be included into pre-clinical drug testing and when validating new quantitative LC-MS/MS methods, the validation should be performed in the same matrix as the test samples to minimize the risk of matrix effects and ensure accurate analysis.

The bioavailability of LF with the application of Pheroid™ technology as a drug delivery system was 3.2 times higher when compared to LF in a reference (aqueous) solution in the starved state. LF dissolves completely in canola oil, results from the bioavailability study prove, and reiterates clinical findings, that the absorption of LF in the GI tract is limited by drug dissolution as LF in canola oil and Pheroid™ formulation produced similar bioavailability values. The concentration-time profiles for LF in canola oil and Pheroid™ formulation differ, when in the Pheroid™ formulation WB/plasma levels of LF remain at a higher concentration for a longer period of time, suggesting that the Pheroid™ has a more complicated functionality than just improving the solubility of the lipophilic drug. This may be a valuable characteristic of the formulation as LF (when co-formulated with artemether) functions to remove residual parasites and cure malarial infection. Using Pheroid™ technology, LF could be maintained at a therapeutic blood level for longer, minimising the risk of recrudescence infections.

When dissolved and administered in the reference formulation, the bioavailability of LF was 2.7 times higher in the fed compared to the fasted state. LF in Pheroid™ formulation is not associated with a positive food effect and produced similar bioavailability values in the fed and fasted state with reduced between-subject variability. Previous clinical studies found that very little dietary fat (1.6 g) is required to achieve optimum LF plasma levels and that the normal African diet contained sufficient quantities of fat to ensure optimum absorption of LF, yet LF is still associated with variable pharmacokinetics. Food did improve the absorption of LF in the reference formulation however the between subject variability was still high when compared to LF in Pheroid™ formulation. Unpredictable pharmacokinetics may favour the development of parasite drug resistance and undermine the efficacy of drug dosage regimens.

The *in vitro* efficacy of LF in reference solution and Pheroid™ formulation was tested against a chloroquine sensitive (D10) strain of *P. falciparum*. The results indicated that LF in Pheroid™ formulation improved *in vitro* antimalarial efficacy by 46% when compared to LF in reference solution, however the variance in the data was too high to draw reliable

conclusions. The mean IC₅₀ values for LF in reference and Pheroid™ formulation were 50.9 and 27.1 nM respectively. This improvement of antimalarial efficacy *in vitro* was not seen *in vivo*. Despite the enhancement in bioavailability of LF with the application of Pheroid™ formulation, no significant improvement in antimalarial efficacy was seen *in vivo*.

The *in vivo* efficacy experiment performed was a modified Peter's four day suppressive test; the test animals were inoculated with parasitized erythrocytes (*P. berghei*, ANKA strain) to induce an infection and were then treated with LF in reference solution or Pheroid™ formulation for four consecutive days where after parasitemia levels were monitored until the experimental end point. The antimalarial efficacy of LF in both formulations was tested at 10, 5 and 1 mg/kg dosage concentrations. None of the test or control animals survived the infection and LF in reference solution and Pheroid™ formulation performed comparably to CQ (positive control). Also the effective dose of LF, in reference and Pheroid™ formulation, was not determined. If the experiment was done testing LF at higher concentrations, investigating both formulations in the same experiment and if blood samples were collected for LF quantitation as well as for the determination of parasitemia, one would be able to make more conclusive deductions, relating the systemic concentration of LF to the antimalarial action rendered by LF in the Pheroid™ formulation compared to the reference formulation.

It can be concluded that the primary experimental aims and objectives were achieved during this study. This study was intended as a 'proof of concept' study, and it has been proven that Pheroid™ technology may be used to enhance the bioavailability of lipophilic drugs such as LF as well as reduce variability in bioavailability. With the application of Pheroid™ technology, the bioavailability of oral administrated LF was not affected by food. This would be an important implication, especially for severely ill malaria patients as LF in Pheroid™ formulation will be able to achieve optimum bioavailability irrespective of fed or fasted state.

The LF in Pheroid™ formulation used in this study was preliminary and further optimization of the formulation should be performed. Future studies may involve an extensive pharmacokinetic evaluation of optimized LF in Pheroid™ formulation to determine the effect of the Pheroid™ on LF PK parameters such as volume of distribution, drug clearance and elimination half-life. Further pre-clinical efficacy studies should be performed to confirm that the Pheroid™ formulation improves the efficacy of LF more so than the reference formulation or canola oil. It would be advantageous to determine if LF in Pheroid™ formulation is more

effective than LF in canola oil and thereby indicating that the PheroidTM functions in improving LF solubility as well as delivering the drug to the target site.